DOE/PC/888T1-T2
G/C--2782-2
SRI-ENV--91-471-6715-T2
(DE92018702)
Distribution Category UC-105

SCALEUP TESTS AND SUPPORTING RESEARCH FOR THE DEVELOPMENT OF DUCT INJECTION TECHNOLOGY

Topical Report No. 2
Task 3.1: Evaluation of System Performance
Contract DE-AC22-88PC88851

DOE/PC/88851--T2

DE92 018702

Duct Injection Test Facility
Muskingum River Power Plant
Beverly, Ohio

Prepared by

Larry G. Felix
Edward B. Dismukes
John P. Gooch
of
Southern Research Institute

and

Michael G. Klett
Atef G. Demian
of
Gilbert/Commonwealth, Inc.

Submitted by

Southern Research Institute
Post Office Box 55305
Birmingham, AL 35255

and

Gilbert/Commonwealth, Inc.
Post Office Box 1498
Reading, PA 19603

April 20, 1992
SRI-ENV-91-471-6715-T2

TABLE OF CONTENTS

	Page
1.0 ABSTRACT	1-1
2.0 INTRODUCTION	2-1
3.0 RESEARCH FACILITY	3-1
3.1 Description of the Duct Injection Test Facility (DITF)	3-1
3.1.1 System Description	3-1
3.2 Description of the Process Control System	3-4
3.2.1 Hardware/Equipment	3-7
3.2.2 Operation/Controls	3-7
3.2.3 COMPAQ System Support Computer	3-8
3.3 Description of the Gas Sampling System (GSS)	3-8
3.3.1 System Requirements	3-8
3.3.2 Evolution of GSS to the Present Form	3-9
3.3.3 QA/QC Concerns	3-11
3.4 Description of the Data Acquisition System (DAS)	3-13
3.4.1 System Requirements	3-13
3.4.2 Evolution of the DAS to the Present Form	3-13
3.5 Methods to Measure Sorbent Utilization	3-14
3.5.1 Gas Sampling	3-14
3.5.2 Solids Samples	3-15
3.5.2.1 ESP Hopper Samples	3-15
3.5.2.2 Quench Probe Samples	3-15
4.0 INITIAL SYSTEM PERFORMANCE	4-1
4.1 Gas Concentrations	4-1
4.2 Coal and Ash Properties	4-1
4.2.1 Chemistry of the Coal and Ash	4-1
4.2.2 Electrical Resistivity of the Fly Ash	4-1
4.3 ESP Performance	4-4
4.3.1 Performance Data	4-4
4.3.2 ESP Electrical Data	4-4
4.3.3 ESP Modeling	4-4
5.0 NOZZLE TESTS	5-1
5.1 Nozzle Testing to Minimize Wall Wetting	5-1
5.2 Droplet Size Measurements	5-16
5.2.1 Description of Measurement Methodology	5-16
5.2.2 Sampling Strategy and Data Analysis Methods	5-18
5.2.3 Test Results	5-20
5.2.3.1 Droplet Size Distributions	5-20
5.2.3.2 Concentration versus Downstream Distance	5-20

Page

6.0 SULFUR DIOXIDE REMOVAL EXPERIMENTS 6-1
6.1 Introduction 6-1
6.2 Dry Sorbent Injection 6-1
6.3 Slurry Injection 6-7
6.3.1 Experiments with Slurry Injection Before Outage 6-7
6.3.2 Experiments with Slurry Injection After Outage 6-10
6.3.2.1 Summary of Data 6-10
6.3.2.2 Influence of Ca/S Ratio and Approach to Saturation on SO_2 Removal 6-14
6.3.2.3 Influence of Inlet SO_2 Concentration on SO_2 Removal 6-14
6.3.2.4 Indications of Sorbent Utilization from Gas-Phase and Solids Analyses 6-26
6.3.2.5 Contribution of ESP to SO_2 Removal 6-31
6.3.2.6 Calculations of Heat Balance 6-38
6.3.2.7 Comparison with Data from Other Sources 6-43
6.4 Electrostatic Precipitator Performance with Sorbent Injection 6-46

7.0 MAJOR OPERATIONS AND MAINTENANCE EXPERIENCE 7-1
7.1 Major Milestones of Operations 7-1
7.2 Hydrated Lime and Slurry Preparatory Systems 7-1
7.3 Dry and Slurry Sorbent Injection System 7-2
7.3.1 Dry Injection System 7-2
7.3.2 Slurry Injection System 7-2
7.4 Duct Cleaning System 7-3
7.5 ESP Performance 7-3
7.6 Ash Collection System 7-3
7.7 Recycle/Slurry Mixing 7-3
7.8 Control System 7-3

APPENDIX A
DETAILS OF TEST RESULTS OF DROPLET SIZE MEASUREMENTS A-1

APPENDIX B
WEEKLY TEST SCHEDULE B-1

LIST OF FIGURES

Number		Page
1-1	Upper and lower limits of SO_2 removal at the ESP inlet based on gas-phase and solids analyses	1-4
3-1	Schematic of Duct Injection Test Facility	3-3
3-2	Simplified process flow diagram	3-5
3-3	Process control system configuration	3-6
3-4	Probe for extracting solids-free stream for gas analysis	3-10
3-5	System for conveying filtered gas sample to analyzers	3-12
3-6	System for withdrawing a gas sample through a quench probe and recovering the entrained solids on a filter	3-16
3-7	Quench probe for extracting a solids sample	3-17
4-1	ESP air load V-I curves	4-6
4-2	ESP V-I curves after several days of operation on flue gas	4-7
4-3	ESP V-I curves after 1 week of operation on flue gas	4-8
5-1	Location of duct wall thermocouples in the horizontal duct of the DITF	5-2
5-2	Arrangements of nozzles and lances at the DITF	5-3
6-1	Dry hydrate injection with water spray from Lechler and Parker-Hannifin nozzles	6-6
6-2	SO_2 removal with slurry injection	6-9
6-3	Percent of SO_2 removed at the ESP inlet as measured by the gas sampling system. Summary of all test data at all approach temperatures	6-15
6-4	Percent of SO_2 removed at the ESP inlet as measured by the gas sampling system. Summary of test data for approach temperatures from 20 to 30° F	6-16
6-5	Percent of SO_2 removed at the ESP inlet as measured by the gas sampling system. Summary of test data for approach temperatures from 30 to 40° F	6-17

Number		Page
6-6	Percent of SO_2 removed at the ESP inlet as measured by the gas sampling system. Summary of test data for approach temperatures from 40 to 50°F	6-18
6-7	Percent of SO_2 removed at the ESP inlet as measured by the gas sampling system. Summary of test data for approach temperatures from 50 to 55°F	6-19
6-8	Percent of SO_2 removed at the ESP outlet as measured by the gas sampling system. Summary of all test data	6-20
6-9	Percent of SO_2 removed at the ESP outlet as measured by the gas sampling system. Summary of test data for approach temperatures from 20 to 30°F	6-21
6-10	Percent of SO_2 removed at the ESP outlet as measured by the gas sampling system. Summary of test data for approach temperatures from 30 to 40°F	6-22
6-11	Percent of SO_2 removed at the ESP outlet as measured by the gas sampling system. Summary of test data for approach temperatures from 40 to 50°F	
6-12	Percent of SO_2 removed at the ESP outlet as measured by the gas sampling system. Summary of test data for approach temperatures from 50 to 55°F	6-24
6-13	Percent of sorbent utilized at the ESP inlet as determined by the gas sampling system and chemical analyses of quench probe samples and ESP inlet hopper samples. Summary of test data for approach temperatures from 20 to 30°F	6-27
6-14	Percent of sorbent utilized at the ESP inlet as determined by the gas sampling system and chemical analyses of quench probe samples and ESP inlet hopper samples. Summary of test data for approach temperatures from 30 to 40°F	6-28
6-15	Percent of sorbent utilized at the ESP inlet as determined by the gas sampling system and chemical analyses of quench probe samples and ESP inlet hopper samples. Summary of test data for approach temperatures from 40 to 50°F	6-29

Number		Page
6-16	Percent of sorbent utilized at the ESP inlet as determined by the gas sampling system and chemical analyses of quench probe samples and ESP inlet hopper samples. Summary of test data for approach temperatures from 50 to 55°F	6-30
6-17	Upper and lower limits of SO_2 removal at the ESP inlet based on gas-phase and solids analyses	6-33
6-18	Percent of sorbent utilized at the ESP inlet and outlet as determined by the gas sampling system. Summary of test data for approach temperatures from 20 to 30°F	6-34
6-19	Percent of sorbent utilized at the ESP inlet and outlet as determined by the gas sampling system. Summary of test data for approach temperatures from 30 to 40°F	6-35
6-20	Percent of sorbent utilized at the ESP inlet and outlet as determined by the gas sampling system. Summary of test data for approach temperatures from 40 to 50°F	6-36
6-21	Percent of sorbent utilized at the ESP inlet and outlet as determined by the gas sampling system. Summary of test data for approach temperatures from 50 to 55°F	6-37
6-22	Data from Bechtel, GE, and the present investigators	6-44
6-23	Current density as a function of applied ESP voltage	6-48

LIST OF TABLES

Number		Page
4-1	Coal Composition	4-2
4-2	Coal Ash Composition	4-3
4-3	Fly Ash Resistivity	4-3
4-4	ESP Performance Data	4-5
4-5	ESP Model Results	4-5
5-1	Results of Lechler Nozzle Tests, Part 1 (May)	5-4
5-2	Results of Lechler Nozzle Tests, Part 2 (May)	5-5
5-3	Results of Lechler Nozzle Tests, Part 3 Insert Installed in Atomizer Port (May)	5-6
5-4	Results of Nozzle Tests, Parker-Hannifin Nozzles (May)	5-7
5-5	Velocity and Temperature Measurements made in the Horizontal Duct at the DITF	5-10
5-6	Results of Lechler Nozzle Tests, Part 1 (June)	5-12
5-7	Results of Lechler Nozzle Tests, Part 2 (June)	5-13
5-8	Results of Parker-Hannifin Nozzle Tests, Part 1 (June)	5-14
5-9	Results of Parker-Hannifin Nozzle Tests, Part 2 (June)	5-15
5-10	Results of Single Point and Traverse Measurements. Parker-Hannifin Nozzles in Port 2, VDA Only	5-19
5-11	Results of Size Distribution Measurements for Parker-Hannifin Nozzles, Combined VDA and PCSV Data Taken at the Center of the Top Port, 5 ft downstream	5-21
5-12	Results of Size Distribution Measurements for Parker-Hannifin Nozzles, VDA Only Data Taken at the Center of the Top Port, 5 ft Downstream	5-21
5-13	Results of Size Distribution Measurements for Lechler Supersonic Nozzles, Combined VDA and PCSV Data Taken at the Center of the Top Port, 5 ft Downstream	5-22

Number		Page
5-14	Results of Size Distribution Measurements for Lechler Supersonic Nozzles, VDA Only Data Taken at the Center of the Top Port, 5 ft Downstream	5-22
5-15	Results of Size Distribution Measurements for Parker-Hannifin Nozzles, VDA Traverse Data Taken at Port Sets 2, 3, and 4	5-23
5-16	Results of Size Distribution Measurements for Lechler Supersonic Nozzles, VDA Traverse Data Taken at Port Sets 2, 3, and 4	5-23
6-1	Properties of Hydrated Lime	6-2
6-2	Non-Scavenging Mode Test Results	6-4
6-3	Scavenging Mode Test Results	6-5
6-4	Properties of Pebble Lime	6-8
6-5	Comparison of SO_2 Removals by Dry Sorbent and Slurry Injection Materials	6-11
6-6	Results of Slurry Tests, Part 1 & 2	6-12&13
6-7	Summary of Post-Outage Data on SO_2 Removal with Slurry	6-25
6-8	Utilization Measured Across the ESP for Test 29-SL-01	6-32
6-9	Results of Heat Balance Calculations, Parts 1-4	6-39/6-42
6-10	ESP Parametric Test Summary	6-49
6-11	DITF ESP Average Operating Points during Mass Train Tests	6-50

1.0 ABSTRACT

This Topical Report [illegible] is an interim report on the Duct Injection Test Facility being operated for the Department o[illegible]ergy at Beverly, Ohio. Either dry calcium hydroxide or an aqueous slurry of calcium hydroxide (prepared by slaking quicklime) is injected into a slipstream of flue gas to achieve partial removal of SO_2 from a coal-burning power station. Water injected with the slurry or injected separately from the dry sorbent cools the flue gas and increases the water vapor content of the gas. The addition of water, either in the slurry or in a separate spray, makes the extent of reaction between the sorbent and the SO_2 more complete; the presumption is that water is effective in the liquid state, when it is able to wet the sorbent particles physically, and not especially effective in the vapor state. An electrostatic precipitator collects the combination of suspended solids (fly ash from the boiler and sorbent from the duct injection process). All of the operations are being carried out on the scale of approximately 50,000 acfm of flue gas.

This report discusses the initial experimental work, which was conducted between April 30, 1990, and February 4, 1991. During that period of time, the effort was devoted to Task 3.1, Characterization of System Performance. This initial phase of experimental work was completed during the period reported. The principal results from the work are described in the following paragraphs.

Characterization of the ESP without lime injection. The test facility includes an electrostatic precipitator that removes suspended particulate matter from the gas stream, with or without sorbent injection. Initially, the ESP was evaluated with only fly ash as the suspended material, at a temperature near 300° F and a specific collecting area of 329 ft^2/1000 acfm. The ESP was found to be highly efficient in removing fly ash alone. The high efficiency of the ESP thus observed was in accord with the ash electrical resistivity at a value of the order of 2×10^9 ohm-cm. This low resistivity is in turn consistent with observed concentrations of SO_3 in the flue gas around 30 ppm.

Avoidance of wall wetting by the spray nozzles. Wall wetting by the spray nozzles is an operating problem that may prevent satisfactory overall performance by the duct injection system, but it can be minimized and made to exist at a tolerable level by the proper selection of operating parameters. Nozzle operating parameters that were studied in connection with wall wetting were the type of nozzle (Lechler or Parker-Hannifin), the array of nozzles in the duct (number and alignment with respect to the duct walls), water throughput, and atomizing air pressure. One of the more satisfactory arrangements of nozzles, which was used in the sorbent testing summarized below, was as follows:

> an array of six Lechler nozzles arranged as three nozzles on each of two lances at different elevations between the top and bottom of the duct;
>
> the upper three nozzles depressed 1.25° from the horizontal and the lower nozzles elevated 5° to avoid wetting the top and bottom of the duct, and the outer four nozzles canted inward 5° to avoid wetting the sides of the duct;
>
> water flow rate of 10 gal/min (83 lb/min) at an atomizing pressure of 90 psig (providing 104 lb/min of air flow). During this test series, emphasis was placed on operability, and it is believed the apparent need for the high air/water ratio (1.25 vs a design value of 0.5) is due to changes in the

trajectory of the nozzle jets with increasing air/water ratio and the operating constraints imposed by the small duct size rather than changes in droplet size. Additional work with the objective of minimizing the air/water ratio will be performed in subsequent portions of the test program.

Sizes of droplets from the spray nozzles. The sizes of droplets from the spray nozzles were reported in terms of the Sauter mean diameter. The sizes measured only with plain water being atomized were found to depend upon the type of nozzle, the rate of atomization of water, the atomization pressure, and the distance down the duct from the point of origin. At the nearest point to the origin where measurements could be made satisfactorily (about 1.6 m downstream), the Parker-Hannifin nozzles produced droplets with SMDs ranging from about 20 μm at high atomization pressures and low liquid flow rates to 45 μm at low pressures and high liquid flows. At this same location, the Lechler nozzles gave SMDs ranging from about 25 to 40 μm with the same change in operating conditions. With increasing distance from the point of origin, the SMDs increased slightly, owing to the faster evaporation of the smaller droplets. The concentrations of water still present as droplets at downstream locations indicated that only about one-third of the original volume had not evaporated after a transit time of 0.5 s.

Removal of SO_2 with dry sorbent. When dry hydrated lime was injected, the flue gas was humidified and cooled with a spray of plain water. The nozzles for the water sprays were located either upstream or downstream from the point of lime addition. When water was injected at the upstream location, the droplets evaporated before they reached the point of lime addition, and the humidification mode was called non-scavenging, meaning that no interception and physical wetting of sorbent particles by water droplets occurred. When water was injected at the downstream location, on the other hand, some fraction of the sorbent particles and water droplets collided, and the operating mode was termed scavenging.

The principal factors influencing SO_2 removal were the operating mode (scavenging or non-scavenging), the relative quantity of lime added (indicated by the Ca/S mole ratio), and the degree of cooling (reported as the difference between the temperature reached and the temperature of adiabatic saturation, or "approach"). The scavenging mode produced substantially higher results; the limited quantity of data obtained, however, make it difficult to say quantitatively how the two humidification modes differed. Among all the tests performed with dry sorbent, the most successful test removed 42% of the SO_2 at the ESP inlet and 53% at the ESP outlet; this was a test with the scavenging mode producing an approach of approximately 25°F at Ca/S = 2.5.

Removal of SO_2 with slurry. Lime injected in slurry form produced significantly greater SO_2 removal than lime injected in dry form with a separate humidification process. This conclusion is illustrated by the following data:

	Dry sorbent	Slurry
Ca/S ratio	2.5	1.5
Approach, °F	26	43
Removal, %		
at ESP inlet	42	50
at ESP outlet	53	56

The differences in removals shown here are not large, but they show that the slurry process was superior in that higher SO_2 removal was achieved with a lower Ca/S ratio and at a higher approach temperature.

As with dry injection, increases in the Ca/S ratio and decreases in the approach were the primary factors influencing SO_2 removal with slurry injection. The tests performed covered the range of SO_2 inlet concentrations from 1200 to 2800 ppm but showed no important effect of this variable on the percent removal. The ESP, on the other hand, made a significant contribution to removal, as indicated by the data tabulated below.

During the studies with slurry injection, extensive work was done to determine whether the extent of SO_2 removal found routinely by direct measurements of SO_2 was reliable. This work consisted of:

1. Performance of "spike tests" in which SO_2 was injected ahead of the heated filters of the probes that sampled gases for the gas sampling system, and

2. Single-point collection of solid sorbent samples in a probe designed to quench SO_2-sorbent reactions, followed by determinations of the utilization of calcium in the collected samples.

The spike tests indicated satisfactory performance of the gas sampling system, but the quench probe samples consistently indicted lower calcium utilizations at the ESP inlet than those obtained from the gas-phase results. Figure 1-1 shows SO_2 removal as a function of Ca/S ratio as a region, with the lower bounds of the included area determined by the quench probe solids samples. Two possible reasons for the disagreement between gas and solids results are: 1) wall effects, and 2) under-representation of reentrained agglomerates of more highly utilized sorbent in the single-point solids samples. We expect that this ambiguity will be resolved in long-term tests which will be conducted later in the project. For the present, however, a conservative approach is to estimate removal in a full scale plant at the ESP inlet from the solids samples in view of the higher surface to volume ratio in the DITF compared with a full-scale plant.

The SO_2 removal in the ESP in the pilot-scale facility should, on the other hand, be duplicated in an ESP of the same relative size (in terms of specific collecting area). To reach a conservative estimate, then, of SO_2 removal in a full-scale installation, it is reasonable to add the ESP removal based on gas-phase data to the duct removal based on solids analysis. The result for approaches in the 20-30°F range are as follows:

	SO_2 removal, %		
	Duct	ESP	Total
Ca/S = 1.0	35	15	50
Ca/S = 2.0	53	16	69
Ca/S = 2.5	60	17	77

Performance of the ESP during sorbent injection. The performance of the ESP was determined occasionally during the work with slurry injection. The performance was satisfactory unless there was

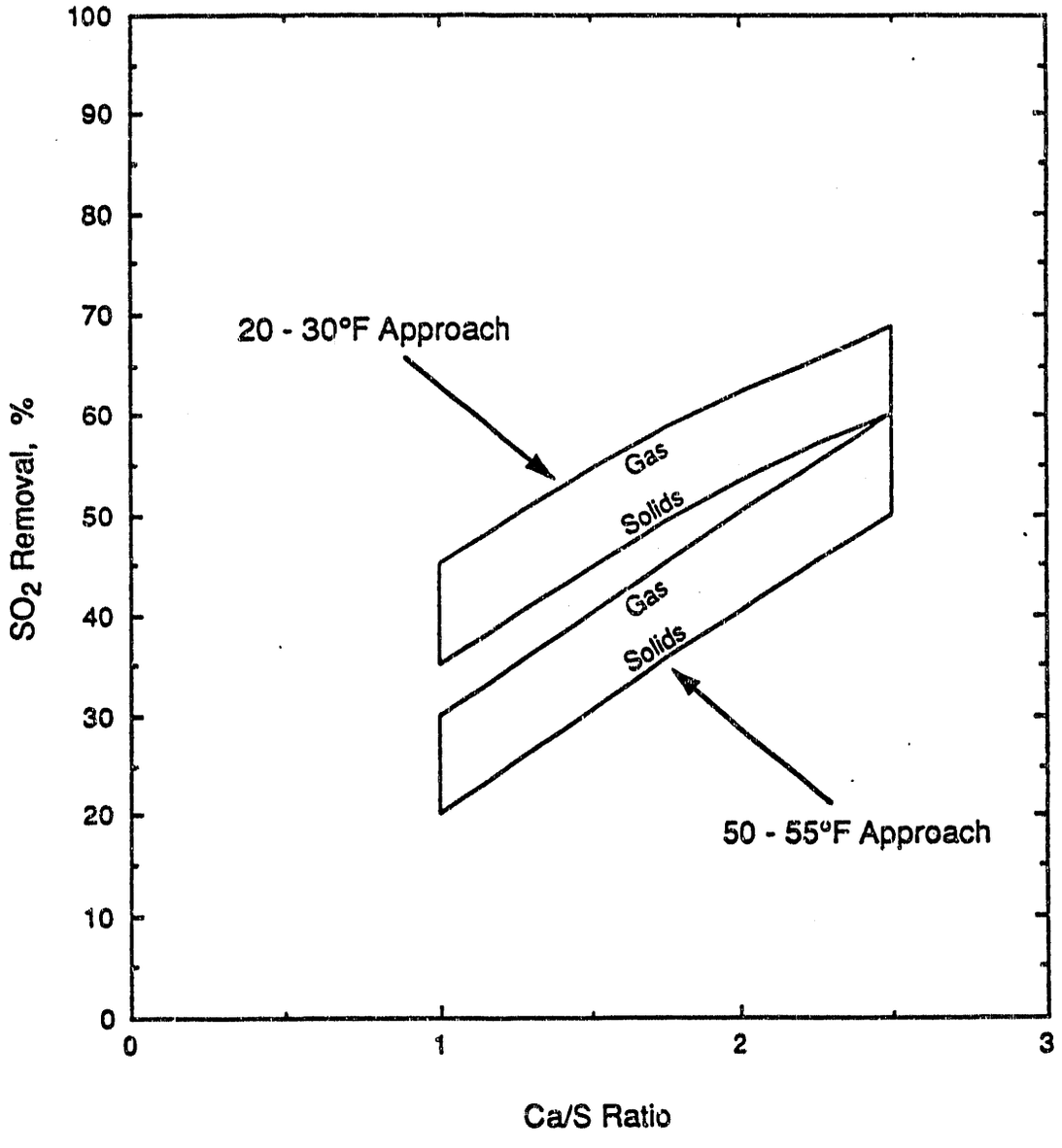

Figure 1-1. Upper and lower limits of SO_2 removal at the ESP inlet based on gas-phase and solids analyses.

an obvious problem caused by electrode deposits. A mass efficiency of the order of 99.9% appeared to be typical at the usual specific collecting area of 400 ft^2/1000 acfm. There was no evidence of the massive reentrainment of sorbent particles at low approaches as was observed in the tests of E-SO_X in the EPA program.

System operation and maintenance. The most crucial issue anticipated in advance and experienced in actual practice is how system operation is handicapped by the buildup of deposits in the duct, which seriously impede gas flow. Injection of dry lime leads to difficulty of this type more rapidly than injection of slurry. Injection of dilute slurries -- 10% solids, for example (to achieve a given approach at a low Ca/S ratio) -- leads to difficulty more rapidly than injection of concentrated slurries -- 25% solids. There has been no attempt at operation for several days or weeks at fixed conditions, but it seems reasonable to expect that operation for several days without interruption will be possible with a slurry having 25% solids at an approach of 25°F.

Controlling deposits at the test facility can be difficult due to the relatively small size of the duct which results in a high wall to gas volume ratio. It is expected that, for larger sized ducts, the control of deposits will be easier.

Although this is an interim report representing preliminary conclusions, the following observations can be made:

1. The program goal of 50% SO_2 removal can be obtained without difficulty with slurry injection at a 20-30°F approach to saturation. Slurry injection is superior to dry hydrate injection in both ease of operation (control of deposits) and in degree of SO_2 removal. The SO_2 removal obtained with slurry injection at the DITF is comparable to that obtained by other investigators.

2. Calcium utilization needs to be increased to improve the economics of the process. Recycle and additives will be investigated later in the project as a means of accomplishing this objective.

3. Although the Lechler nozzles performed well with respect to operability, a higher-than acceptable value of air to water appeared to be necessary to avoid contact of the slurry droplets with the wall in the relatively small duct at the DITF. The use of a single nozzle and other operational changes will be investigated in an effort to reduce the air requirements.

2.0 INTRODUCTION

Duct injection of calcium hydroxide is being investigated under the auspices of the U. S. Department of Energy as a low-cost, retrofit technology for controlling SO_2 emissions from coal-burning electric power stations. This report describes the results of one study of this technology that is being conducted by Gilbert/Commonwealth, Inc., and Southern Research Institute. This study is being performed at the Duct Injection Test Facility (DITF), which is located at Unit 5 of the Muskingum River power station of Ohio Power Company at Beverly, Ohio.

This report describes the initial phase of the experimental work, performed under Contract DE-AC22-88PC88851, which was started on April 30, 1990, and completed on February 4, 1991. The report covers in entirety the research performed under Task 3.1, Evaluation of System Performance.

The contents of the report are as follows:

- A description of the test facility (Section 3.0).
- A discussion of initial work prior to the injection of calcium hydroxide for controlling the emission of SO_2 (Section 4.0).
- A description of the work performed with nozzles for injecting either plain water or a slurry of calcium hydroxide in the duct, where primary removal of SO_2 occurs (Section 5.0). Plain water is sprayed into the duct for increasing the humidity level and lowering the temperature of the flue gas when dry calcium hydroxide is added. Slurry is sprayed into the duct when humidification, cooling, and sorbent addition are accomplished in one step. (The data in Section 5.0 were all obtained with plain water rather than slurry.)
- A detailed presentation of the results on SO_2 removal in three operating modes (Section 6.0):

  Injection of dry calcium hydroxide accompanied by injection of plain water at an upstream location. This is referred to as the non-scavenging mode, which means that the water droplets evaporate before they reach the plane of sorbent injection and thus do not undergo particle-to-particle collisions with the sorbent.

  Injection of dry calcium hydroxide accompanied by injection of plain water at a downstream location. This is the scavenging mode, which means that collisions occur between sorbent particles and water droplets before the droplets evaporate.

Injection of a slurry of calcium hydroxide, in which the water for humidifying and cooling are combined with the sorbent.

- A review of operating experience with the test facility (Section 7.0).

3.0 RESEARCH FACILITY

3.1 Description of the Duct Injection Test Facility (DITF)

The Duct Injection Test Facility of the Department of Energy (DOE), located in Beverly, Ohio, at the Muskingum River power plant of Ohio Power Company, has been converted to test alternative duct injection technologies. The technologies tested include slurry sorbent injection of slaked pebble lime with dual fluid nozzles and pneumatic injection of dry hydrated lime with flue gas humidification before or after sorbent injection. The test facility was modified to test a range of flue gas SO_2 concentrations and a range of flue gas temperatures in vertical and horizontal duct test sections. This test program is part of a larger DOE program to fully characterize low cost, retrofittable dry SO_2 removal technologies for application to existing power plants.

Two types of duct injection technologies are being tested: (1) slurry sorbent injection of slaked pebble lime, using dual fluid nozzles; and (2) pneumatic injection of dry hydrated lime, with flue gas humidification before and after sorbent injection. A wide range of flue gas SO_2 concentrations and temperatures is being utilized for testing.

A two-year test program is now being implemented for the facility. The purpose of the test program is to:

- Obtain scale-up engineering design data for both slurry and dry sorbent injection.
- Provide scale-up data for humidification and ESP performance.
- Develop and test process-control systems.
- Validate the first and second generation process models developed under other parts of the DOE program.

3.1.1 System Description

The DITF operates as a 12 MWe, 50,000 ACFM "slipstream" system on Ohio Power Company, Muskingum River Unit No. 5, in Beverly, Ohio. The boiler is a B & W dry-bottom pulverized coal, front and rear wall-fired unit, rated at 585 MW (net).

The unit is base-loaded but it can drop to half load during summer months, usually between midnight and morning. Currently, the plant burns local coal with an as-received sulfur content of about 4.2%. The nominal flue gas conditions at the exit of the air preheater (feeding the test facility) are as follows:

N_2	75.6%
CO_2	11.9%
H_2O	7.5%
O_2	4.6% (30% excess air)
SO_2	3200 ppm
Ash	3.4 gr/acf
Molecular Weight	29.46
Temperature	325° F

The slipstream is taken from the existing air preheater discharge, through ductwork with three test stations to the DITF precipitator, then to an induced draft fan, and back to the existing precipitator inlet. A provision also exists to bypass the pilot precipitator and allow gas to flow through a high-efficiency cyclone. Figure 3-1 is a schematic drawing of the DITF.

The DITF precipitator is a weighted-wire design, consistent with the majority of older units for which the sorbent duct injection technology is intended. The precipitator has four independent electrical fields and is designed for an SCA of 360 ft^2/1000 acfm at a system inlet flow rate of 40,000 acfm at 190° F. Although this design is somewhat larger than most units that are candidates for duct injection technology, it will provide additional flexibility for the test program.

The test facility was originally designed to deliver slaked pebble lime slurry to a rotary atomizer in one of three duct locations--one in a vertical duct and two in a horizontal duct. New equipment was designed and installed to test two different types of duct injection technologies: (1) Slurry sorbent injection of slaked pebble lime, using dual fluid nozzles, and (2) Pneumatic injection of hydrated lime, with flue gas humidification before or after sorbent injection. The new equipment consists of:

- Flue gas dilution air heater to vary SO_2 content and temperature of the incoming gas.
- Flue gas steam humidifier.
- Slurry sorbent injection pumps and nozzles.
- Hydrated lime silo and blowers.
- Flue gas humidification nozzles and water pump.
- Ash recycle system.
- Compressed air system.
- Duct hoppers and cleaning systems.
- Waste ash silo.
- State-of-the-art programmable logic controller and data acquisition system.

A great deal of flexibility was designed into the facility to provide the capability of testing over a wide range of process conditions. These capabilities include the following:

- Flue gas velocity of 20-60 ft/s which corresponds to a gas flow of 16,700-50,000 acfm at the inlet conditions.
- Inlet gas temperature 275-320° F.
- Inlet gas SO_2 concentration of 1100-3200 ppmv.
- Sorbent addition at a Ca/S ratio of 1.0-2.0 (nominal limits).

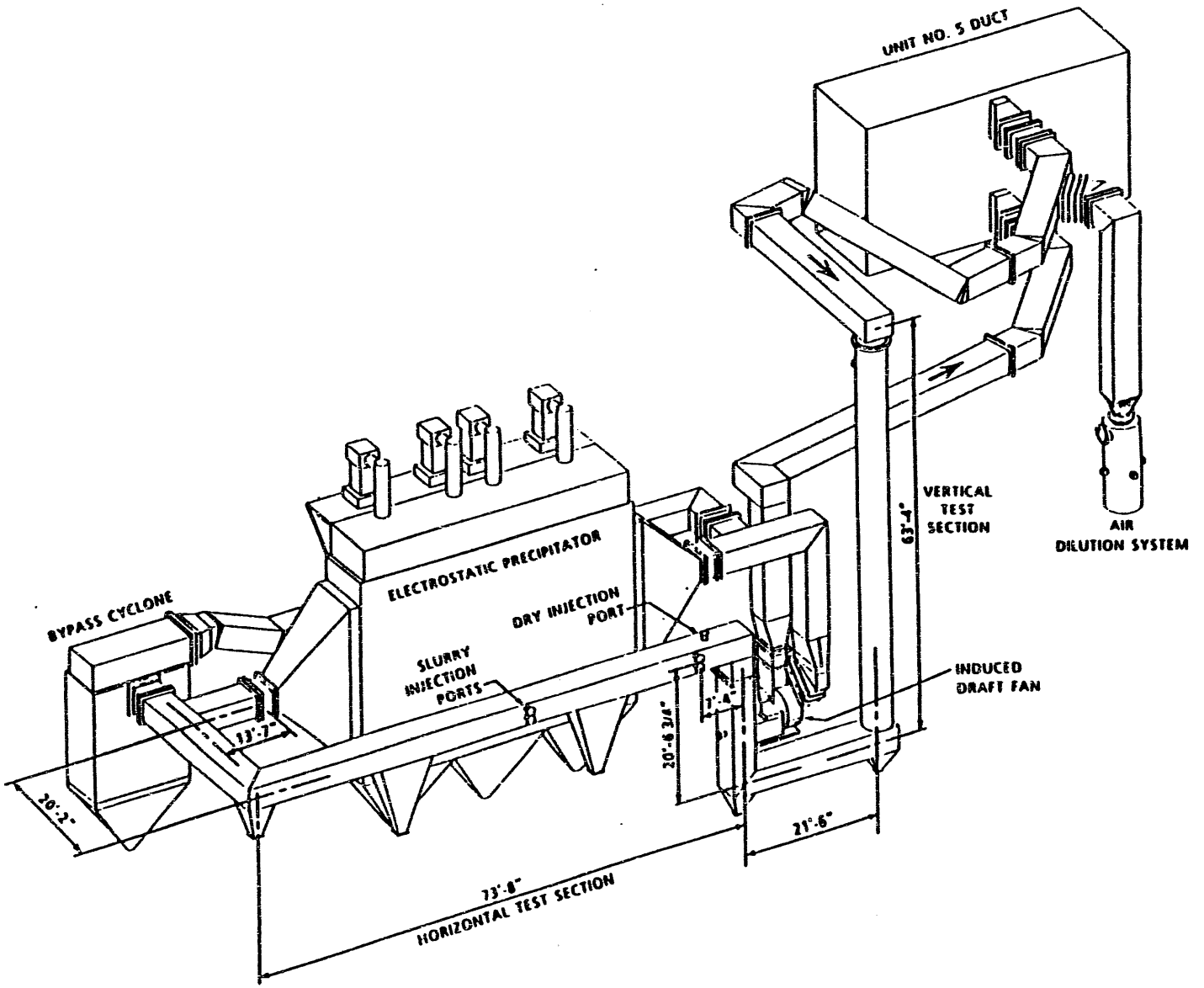

Figure 3-1. Schematic of Duct Injection Test Facility.

- Duct residence time of 0.5-3.0 s.
- Approach to adiabatic saturation temperature of 20-80° F.
- Recycle of spent sorbent for either slurry or dry sorbent injection.

Figure 3-2 shows a simplified process flow diagram of the facility. Construction was completed in May 1990 and the first test series, Evaluation of System Performance, has been completed.

3.2 Description of the Process Control System

The DITF instrument and control system was developed from a mixture of existing equipment hardware and software and a new Allen-Bradley Programmable Logic Controller (PLC) 5/25 control system. All of the process and equipment control is assigned to the new PLC system while the existing Data Acquisition System (DAS) was strictly limited to data acquisition. Figure 3-3 shows a schematic of the PLC and DAS systems.

All new equipment start and stop functions are performed via a work station in the control room. The work station consists of a keyboard and CRT and has the capability of displaying the various process loops in real-time. The control scheme for slurry injection is based on setting the slurry feed rate to maintain a desired Ca/S ratio, while slurry concentration is adjusted by dilution water to maintain exit gas approach temperature. For dry sorbent injection, both lime addition and exit gas temperature can be controlled independently. In addition, the capability is present to test the use of SO_2 removal efficiency as the control point by automatically adjusting the lime or slurry feed rate. The PLC system is able to respond to fluctuations in the inlet SO_2 concentration, gas temperature, gas flow rate, and allow the process or equipment upset conditions to be detected and corrected without process shutdown.

Process control relative to flue gas dilution and temperature is designed to produce a flue gas stream with a specified or test SO_2 concentration, inlet gas temperature, and inlet gas volumetric flow rate. In order to minimize changes to other flue gas parameters, particularly the adiabatic saturation temperature, when diluting the extracted flue gas from Unit 5, the water concentration of the diluting gas must match those of the extracted flue gas from Unit 5. The dilution air is controlled by the desired SO_2 concentration, the duct burner firing by the desired test temperature, and the moisture addition by an algorithm which calculates the required humidity from the coal analysis and the measured excess air and ambient humidity. Moisture is added by a controlled steam flow based on dilution air flow rate.

Associated with the process control/additions and changes are the changes to the ash handling system as presently configured. With the addition of mechanical equipment there is the incorporation of both monitoring and control instrumentation for equipment and personnel safety.

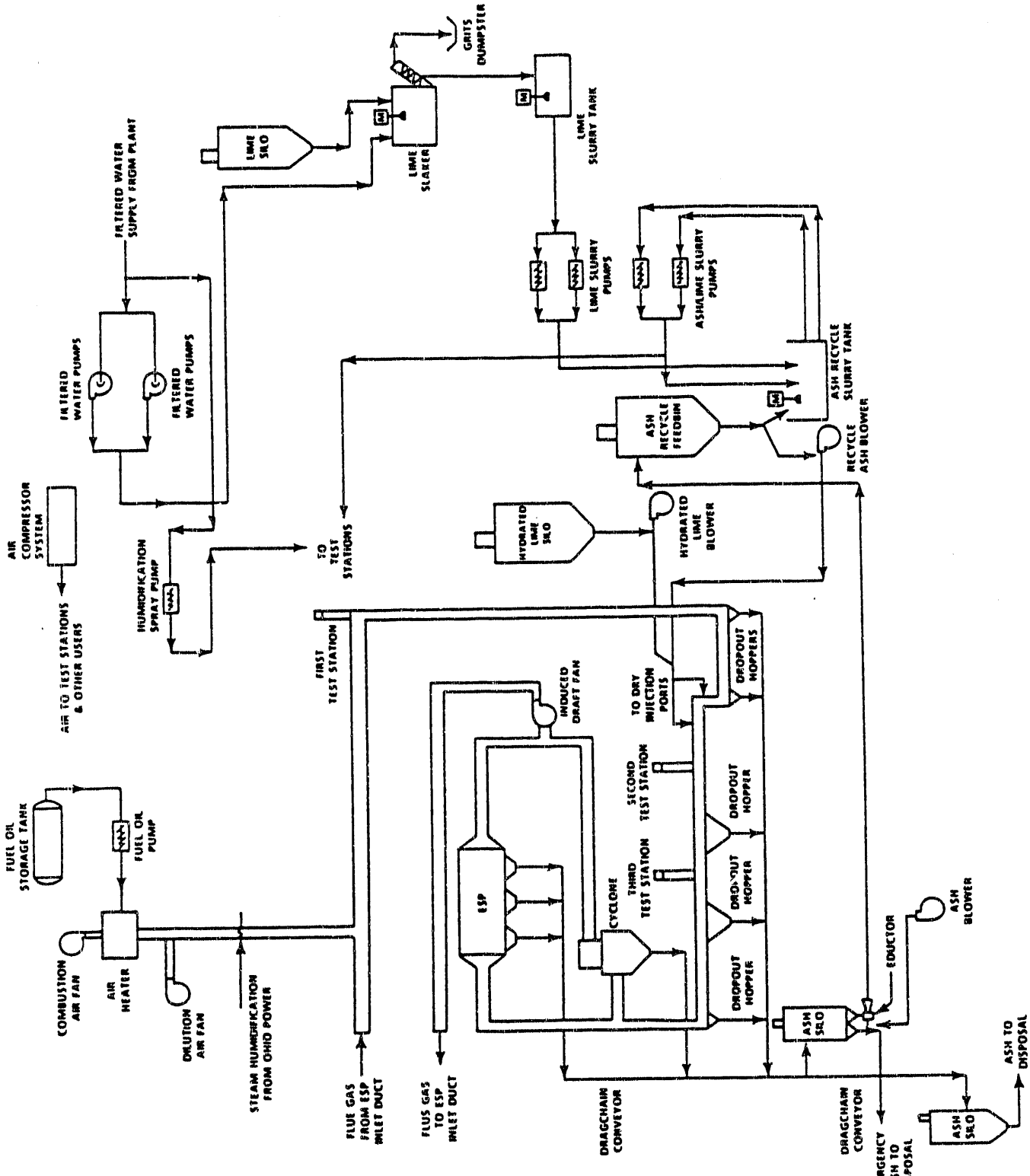

Figure 3-2. Simplified process flow diagram.

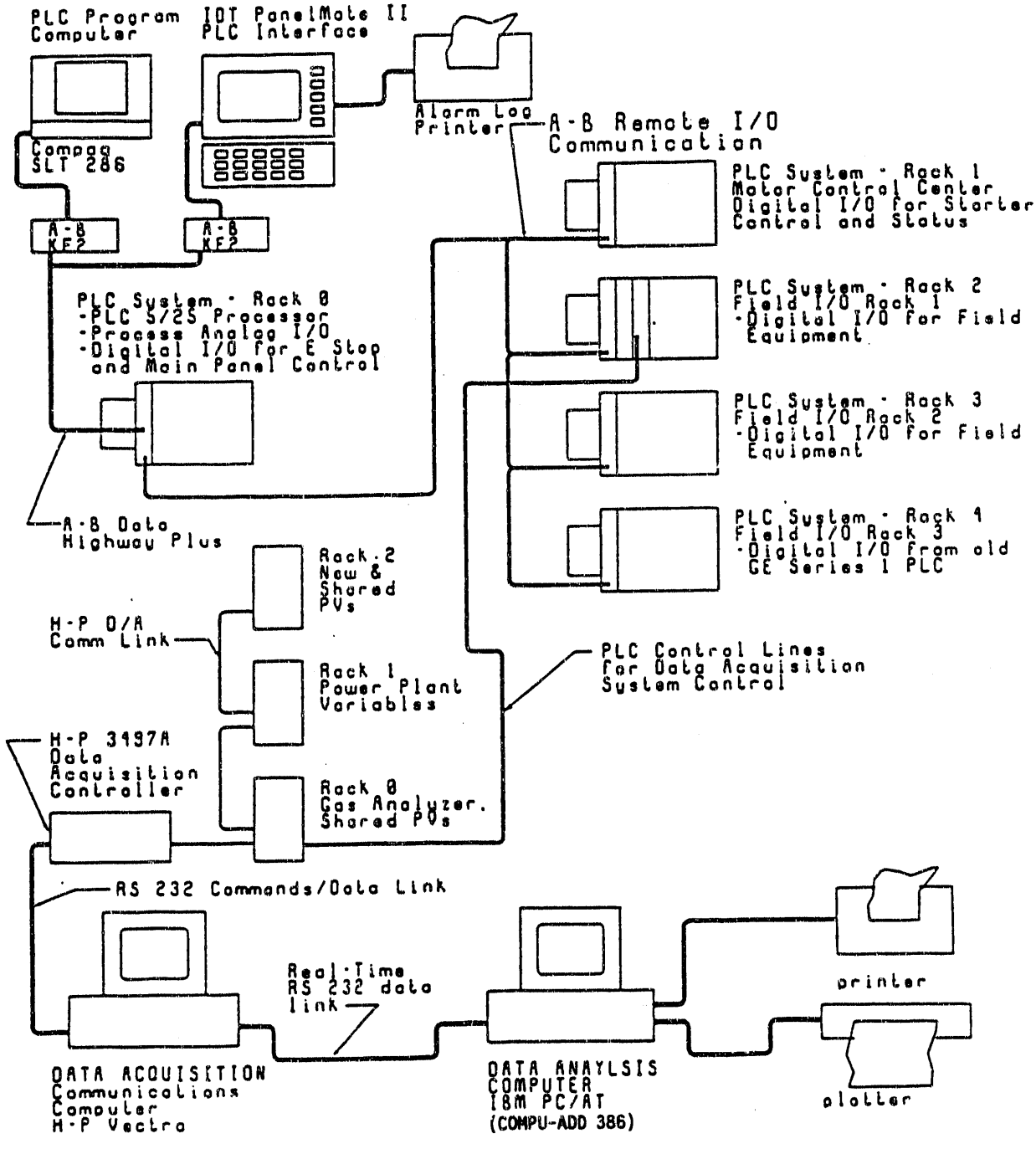

Figure 3-3. Process control system configuration.

3.2.1 Hardware/Equipment

Allen-Bradley PLC 5/25 System

5 Rack Configuration

2 - Main Control Panel (CP003 and CP004)
2 - Motor Control Center (MCC)
1 - Existing Control Panel (CP-001)
1 - Dilution Air Variable Frequency Drive (VFD)

20 K Word Processor RAM Memory (approximately 16 K used)

A-B 1770-KF2 Data Highway Plus Communications Interfaces for (1) Programming and (2) PanelMate

COMPAQ SLT 286 with ICOM PLC 5 Programming and Documentation software (purchased as part of the PCSV Particle Measurement system)

IDT PanelMate II Operator Interface - 16 Screen Capacity

3.2.2 Operation/Controls

With the exception of the Air Compressor system, the two Lime Slurry Pumps, the Lime Slurry Agitator, the Air Heater Burner Ignition which are controlled from the Main Control Panel, and the existing motors controlled at the existing MCC, all of the equipment in the Test Facility is controlled using the PanelMate which is located on the Main Control Panel. Nearly all of the equipment is set up to have a "Hand" and an "Auto" mode of operation. In the "Hand" mode, the selected device will operate on command, taking into account any safety interlocks. In the "Auto" mode, the device is "enabled" and will operate when called upon by the logic of the operation.

- PanelMate Control Screens

  All of the "Hand-Off-Auto" controls for a specific area are located on one or two screens of "Legend Displays". These PanelMate displays show the status of each device. In addition, any equipment fault is shown on this display. Selecting one of these "Legend Displays" from the 15-key panel displays the associated control function, such as "Start - Auto", "Start - Hand" or "Stop".

  Any alarm condition detected by the PanelMate/PLC system causes the central alarm system light and horn to be activated. The alarm condition is displayed on the PanelMate and logged on the alarm printer. The alarm system may be "Acknowledged" with the pushbutton on the Main Control Panel or the "Silence Alarm" key pad on the PanelMate. The "Acknowledge" is also logged.

- PanelMate System Status Screens

  For each process loop there is a graphic screen showing the process flow and equipment status for the process. There is normally no operator control on this screen. However, the state of the devices shown on the control screens is indicated by the color of the device.

  Also shown on this screen are process alarm conditions such as high or low hopper or silo levels.

- PanelMate Process Control Screens

  To set the process parameters, there are several Process Control Screens. These screens contain two types of displays: a controller on which the Process Variable, Setpoint, and Alarm Limits are shown in a format very similar to the classic stand-alone controller and a variable display format which simply indicates the current value of the Process Variable and Setpoint.

For either of these displays, the numbers in the white legend block can be modified by the operator to alter the setpoint as needed.

3.2.3 COMPAQ System Support Computer

In addition to being used for gas particle size measurements, the INSITEC computer provides the PLC/DAS System Support. For this purpose, it has been loaded and configured to perform the support operations listed below.

- PLC 5/25 Programming and Documentation
- Equipment Data Base
- Reports - IDT PanelMate Support

3.3 Description of the Gas Sampling System (GSS)

3.3.1 System Requirements

In order to measure the effectiveness of duct injection for the removal of SO_2 and NO_x and to control the level of SO_2 at the inlet to the DITF, it is necessary to know the constituency of the flue gas at a number of points. Before the DITF was configured to study the duct injection process, it was operated by General Electric Environmental Services, Inc., (GEESI) for a previous DOE project. As part of that earlier project GEESI contracted with Pace Environmental to design and install a "multiple point" flue gas sampling system (GSS) that could measure flue gas concentrations of SO_2, O_2, CO_2, and NO_x at up to five locations throughout the facility. This existing system has been modified and updated by SRI. In addition to this multiple point GSS, a "single point" GSS has been installed to provide continuous SO_2 and O_2 information at the system inlet (after dilution). Data from the single point GSS is used by the Allen-Bradley Programmable Logic Controller (PLC) that

controls DITF operation to set the amount of dilution required to maintain a constant SO_2 level at the system inlet.

3.3.2 Evolution of GSS to the Present Form

As installed, the GEESI/Pace GSS took a gas sample from one of five probes inserted into the DITF ductwork, transported the gas sample through heated sample hoses to a heated switching network that, in turn, routed the gas sample to a dilution system (with a dilution ratio of 10:1) and a gas permeation dryer, and finally sent the diluted gas sample to a bank of gas analyzers. Motor-driven mechanical relays in the GSS control circuitry then activated a bank of motorized ball valves to sample through the next port in the gas sampling sequence. After all ports were sampled, each sample line was purged with high pressure air to clean the sample probes. The sample probes were made of a fritted stainless steel filter that was inserted midway into the duct, enclosed in a semi-circular protective shell. The advantage of this system was that no sample conditioning was required to remove water vapor. The major disadvantage of this system was that because of low sample flow rates about 3 min could elapse from the time a sample was withdrawn from a sample probe to the time that a measurement of flue gas concentration was made. This time was usually doubled because measurements were made with wet diluted flue gas (by bypassing the permeation dryer) and with dry diluted flue gas to obtain an estimate of water vapor concentration at a given sample port. Indeed, a considerable time could elapse from the time a gas sample from the DITF inlet (port 1) was analyzed to the time a gas sample from the outlet of the ESP (port 5) was analyzed. Thus, changes in system operation that occurred between the time the inlet and outlet samples were analyzed could affect the results of a particular test in an unpredictable manner.

Before the DITF was brought on line the GEESI/Pace GSS was inspected and cleaned. It was found that the permeation dryer was inoperable; most of the stainless steel sampling lines, valves, and solenoids were internally corroded; and many of the flue gas analyzers required maintenance or repair. It was decided to rebuild the GSS completely. As part of this rebuild, a "double bypass" design was adopted with an integral refrigerated sample conditioning system for water removal. Heated sampling probes were also designed and installed at each sample port. The GSS was also integrated into the PLC control system for the DITF so that control of the GSS is no longer governed by a set of motor-driven mechanical relays. Currently, sample ports are located at the inlet to the system, at the inlet to the horizontal test duct (before sorbent injection or humidification), at the end of the horizontal duct (1.0 s residence time), at the ESP inlet (1.5 s residence time), and at the ESP outlet (ESP residence time is approximately 10 s).

The heated probes were designed and installed because no provision was made in the GEESI/Pace system to prevent the reaction of sorbent caught on the surface of the in stack filter with flue gas as it passed through the layer of sorbent. Figure 3-4 shows how these probes are designed. The probes are made of 316 stainless steel. The reaction of flue gas with sorbent caught on the fritted stainless steel filter in the probe is quenched by heat. The interior of the probe is maintained at 350° F or above so that the surface of the in stack filter is heated to a point where no reaction can take place with fresh sorbent caught on the surface of the filter. Each probe is also fitted with a stainless steel line through which span or zero gas can be bled into the probe. This probe design has been tested by introducing SO_2 span gas to the interior of the filter which was coated with a thick layer of unreacted $Ca(OH)_2$ sorbent. In each test, 98% or more of the span gas was recovered downstream of the probe.

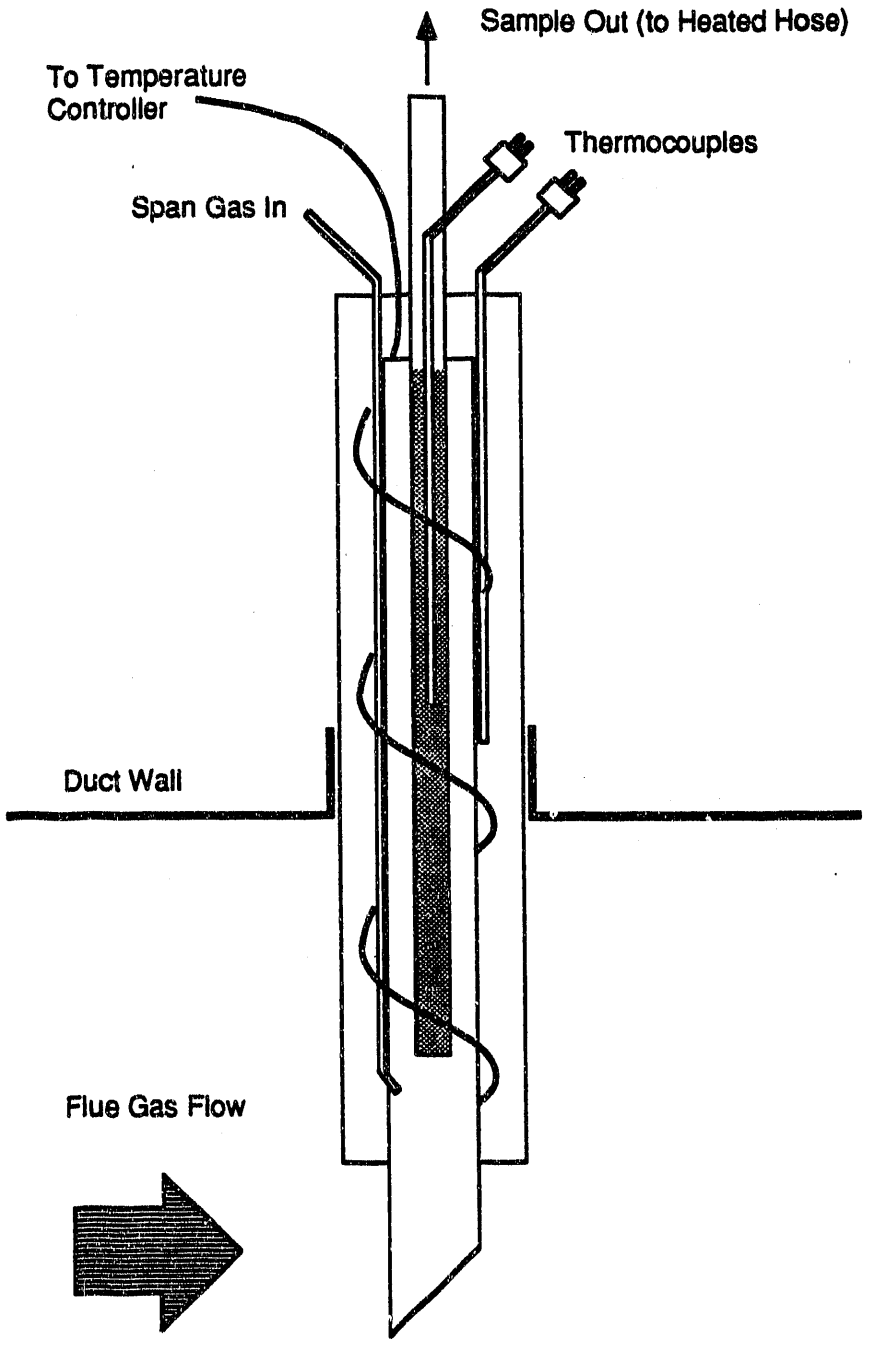

Figure 3-4. Probe for extracting solids-free stream for gas analysis.

As Figure 3-5 shows, flue gas is drawn through each heated probe and is conveyed through a heated sampling line to a heated oven where the stream passes through a motorized ball valve, filter, and solenoid valve that either routes all of the sample flow to the main bypass pump through a sampling manifold that is shared by all of the sample lines or diverts the sample flow to two sets of condenser coils in a refrigerated bath maintained at 33°F. Condensed water is removed with a double-headed peristaltic pump. A second sample pump is located between the two sets of condenser coils, providing sample flow to an array of gas analyzers located downstream of the refrigerated cooler. The gas analyzers are each equipped with an appropriate sample pump. The second sample pump is sized so that it delivers more sample flow than is required for the gas analyzers. Extra sample flow is vented. This sample conditioning system serves a Western Research Model 721-AT SO_2 analyzer, a Servomex Model 540A oxygen analyzer, an Automated Custom Systems Model 3300 CO_2 analyzer, and a Thermoelectron Model 10 NOx analyzer.

A separate heated line is connected to the gas sample coming from port 1 at a point after the filter but before the solenoid valve. This line supplies a gas sample from the inlet of the DITF to the single point GSS. This system is constructed in much the same manner as the multi-point GSS. The gas sample passes through a refrigerated cooler and passes to a Fuji Model ZRC/760 SO_2 analyzer and a Servomex Model 540A oxygen analyzer. Water is removed from the refrigerated cooler with a single-headed peristaltic pump. As with the multi-point GSS, the single point GSS is controlled by the PLC that is used to run the DITF.

Recently a Servomex PSA 402 water analyzer was added to the multi-point GSS. This analyzer takes a sample from the heated line that passes a gas sample to the refrigerated cooler, passes it through a heated head pump and filter, and conveys the gas sample to the water analyzer through a heated sample hose. The measurement cell of the water analyzer is maintained at 150°C. The water analyzer measures absorption of light energy by water vapor at a wavelength of 6.01 μm. This wavelength was chosen by the manufacturer because none of the components of the flue gas exhibit significant absorption at this wavelength. The water analyzer is calibrated with a "mimic" gas, propylene, that strongly absorbs light energy at 6.01 μm. Initial results with the water analyzer are promising; however, much more experience needs to be gained with this analyzer before it can be recommended as a water vapor monitor.

As indicated above, the multi-point GSS and the single point GSS are controlled by the Allen-Bradley PLC system that is used to control the DITF. Currently, each gas sampling line is purged with compressed air immediately after the PLC switches the GSS to the next sample line. When a line is selected for sampling by the PLC, approximately 90 s elapses before any measurements are accepted from the gas analyzers. This is to ensure that the previous gas sample is completely flushed from the refrigerated cooler and analyzers before any measurement is made. The PLC can select any number of ports or combination of ports to sample. If only one port is selected for sampling, that port is not purged until the port is deselected.

3.3.3 QA/QC Concerns

To make sure that the GSS functions properly, frequent checks are made of system integrity. Each gas analyzer is calibrated on a daily basis, and a log is kept of zero and span adjustments as well as any maintenance that has been performed on components of either GSS. Calibrations are not based on meter response but are based on instrument output to the DITF data acquisition system (DAS). Filters in the GSS are changed on a regular basis, and the single point and multi-point GSS systems

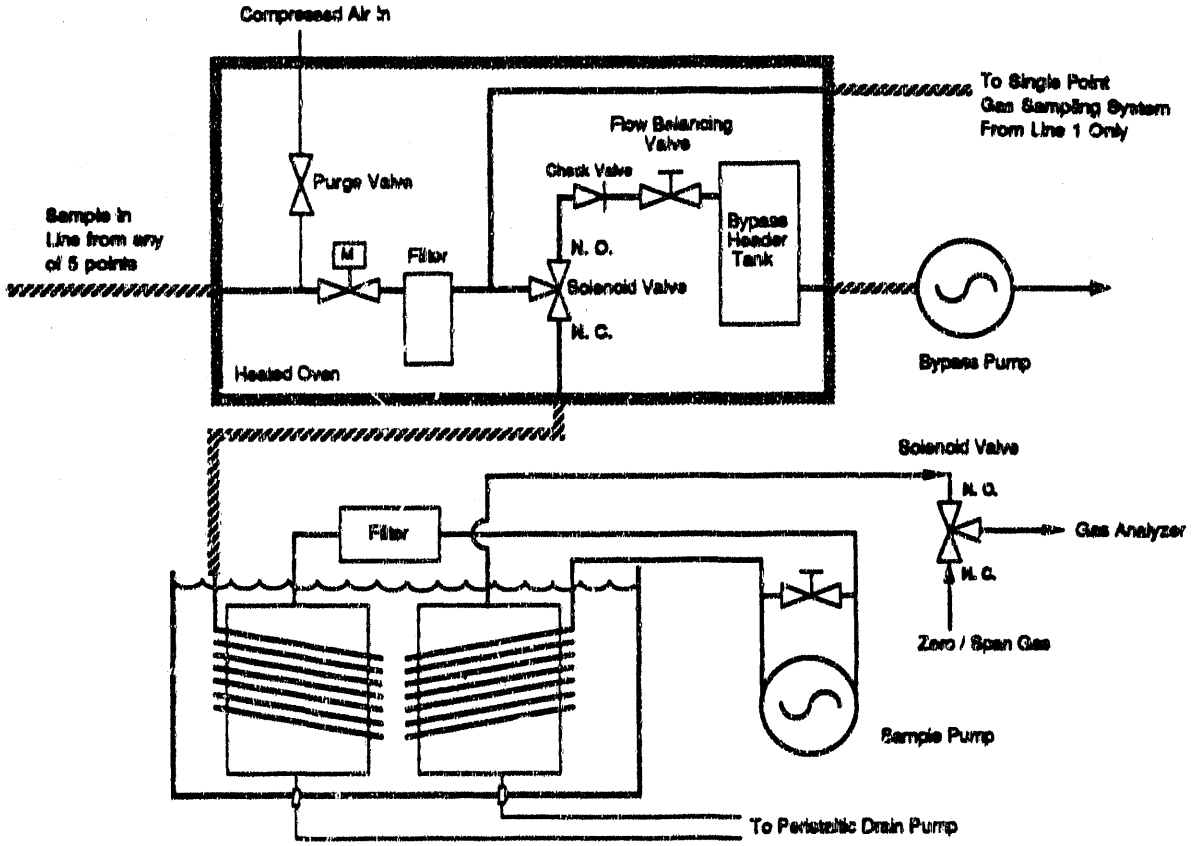

Figure 3-5. System for conveying filtered gas sample to analyzers.

are monitored to assure that both systems agree. On a weekly basis, each heated sample probe is checked to be sure it is operating properly, and span gas is introduced into each probe in the duct. Slight losses in sample recovery usually are caused by small leaks that are corrected before proceeding to the next probe. Although this process is time-consuming, it assures the integrity of the GSS. Results of these checks are kept in the GSS maintenance and calibration log.

3.4 Description of the Data Acquisition System (DAS)

3.4.1 System Requirements

The DAS must fulfil several major requirements. First, it must produce a permanent record of test activity carried out at the DITF to permit subsequent analysis of process data. Second, the DOE requires that all data must be logged in Lotus 123™ format files on floppy disks that are transmitted to the DOE on a regular basis. This second requirement generates a back-up of all data and provides process data to other individuals interested in results obtained at the DITF. Third, in addition to producing permanent records of process data, the DAS must provide real-time information for ongoing experiments at the DITF. Ideally, this real-time information should be available for any process parameter over the duration of the most recent test.

3.4.2 Evolution of the DAS to the Present Form

When the DITF was first brought on line, DAS hardware consisted of a Hewlett Packard (HP) Model 3497A data logger connected to an HP Vectra PC/AT computer, which was also connected to an AST 286 PC/AT computer. Custom software was written in Microsoft QuickBasic™ to interface the HP Vectra computer with the HP datalogger, to allow on-line analysis of process data from the DITF, and store each data scan in an archival file. The AST computer was primarily intended for data analysis although it could be used to monitor raw data as it was echoed to the HP Vectra computer.

Before a decision was made to write site specific software to automate data collection and retrieval, commercial software packages were investigated. However, with the amount of information to be stored (in excess of 300 channels of data and calculations per scan) any commercial package that could handle the stream of data (approximately one scan every 90 s) was either very expensive, required a considerable investment in training to configure, or both.

Initially, data scans were stored on the HP Vectra in an ASCII format and these files were transformed into a Lotus-compatible file format on the AST computer. This process was time consuming and inefficient. In addition, while process data were displayed for each scan, it was difficult to view earlier data acquired during a test without stopping data collection to copy a data file or performing frequent screen dumps to a printer attached to the HP Vectra. Because it is very desirable to be able to view recent process data and compare it with current system behavior, it was decided to modify the DAS. A major requirement was that this modification could not disrupt the ongoing program of experimentation during its development, testing, and installation.

As indicated above, the QuickBasic program that polls the HP datalogger also echoes process data and calculations to the AST computer. This ability to echo data to a second computer is the key to the new data analysis system. In order to provide on-line analysis of recent as well as current process data, it was decided to replace the AST 286 PC with the 386-based PC and utilize the

multi-processing capabilities of this type of microprocessor to log the data received from the HP Vectra and provide a display of any process parameter or parameters desired within the last 1200 data scans (approximately the last 30 hours of data). This display can be up-dated as required.

The expanded data analysis system consists of a 386-based PC, a serial data communications buffer, a multi-tasking operating system called Deskview™, custom software written in Borland's Turbo Pascal™, and an Iomega Bernoulli™ removable cartridge drive. The 386 platform and Deskview are necessary to allow the computer to perform two simultaneous tasks. The serial buffer is used to allow the 386 computer to go off line for up to several hours and not lose process data relayed from the HP Vectra. Hourly and daily process data are logged on removable 44MB Bernoulli cartridges. Data continues to be logged on the HP Vectra as it was in the past. Data files from the HP Vectra are now being archived on the Bernoulli cartridges.

The custom software performs several tasks: it accepts data from the HP Vectra, checks for communication errors, writes the process data to compact binary files, prints historical data to a line printer or to a file, plots process data to the screen or to an HP plotter file, and converts hourly data files to Lotus 123 compatible spreadsheets for subsequent data manipulation. The software written to produce Lotus 123 compatible spreadsheets from the process data files will convert a day's worth of process data into worksheets in 10 to 15 min.

One important addition to the expanded data analysis system is the ability to view graphical images of process data in essentially real time while data logging continues. A file containing all of the data from the last 1200 scans is maintained on the fixed disk in the 386 computer and is echoed to a 2.8 MB ramdrive. Through a series of menus, predefined sets of data or operator selected data can be viewed to monitor a test in progress or view the results of recent testing. Data are stored in a ramdrive to minimize access time.

The ability to write typed files of binary numbers yields a large saving in disk space: one hour's data in ASCII format requires 420 KB of disk space, while the same file in a typed binary file format requires only 60 KB of disk space. One disadvantage of typed files is that the data cannot be viewed directly from DOS.

3.5 Methods to Measure Sorbent Utilization

Central to the evaluation of a SO_2 removal technology is measurement of sorbent utilization. Sorbent reacts with SO_2 in the flue gas and if $Ca(OH)_2$ is the sorbent material $CaSO_3$ is formed by the reaction. The sorbent never reacts completely, however, and thus is never fully "utilized". Utilization can be determined from gas-phase measurements or from analyses of solids.

3.5.1 Gas Sampling

Sorbent utilization is calculated from gas phase measurements by dividing the percent of SO_2 removal by the Ca/S ratio. Because the Ca/S ratio is a molar ratio, this calculation really determines the ratio of the number of moles of sulfur to the number of moles of calcium present (as sorbent). Sources of error that can affect this method of determining sorbent utilization are an inaccurate determination of the Ca/S ratio--through an incorrect measurement of slurry flow, inlet SO_2 concentration, or the physical parameters of the slurry (% $Ca(OH)_2$, density, or % solids) and an inaccurate measurement of SO_2 concentration downstream of the point where sorbent is introduced into the system. This

measurement can also be affected by accumulations of moist sorbent in the duct (for example, as duct wall deposits) that tend to remove SO_2. In this case sorbent utilization as determined from gas-phase measurements will be higher than utilizations determined from solids analyses.

3.5.2 Solids Samples

Sorbent utilization can also be determined from chemical analysis of ash/sorbent samples obtained downstream from the point where sorbent was introduced into the system. In the case of the DITF, these samples are most immediately available from the ESP hoppers but are also available from mass train catches. However, samples of solids obtained with particle sampling devices can also become over utilized (compared to suspended solids in the flue gas) because they remain in contact with flue gas for the duration of sampling.

3.5.2.1 ESP Hopper Samples

The ESP of the DITF has three hoppers, and the ash conveying system has been modified to permit samples of ash to be obtained from each ESP hopper. However, most of the ESP hopper samples analyzed during the period covered by this report were obtained from the inlet hopper only. Sorbent utilization determined from chemical analyses of ESP inlet hopper samples was always somewhat higher than utilization determined from gas phase measurements.

3.5.2.2 Quench Probe Samples

To obtain samples of solids that are not over-utilized either by extended contact with flue gas on the collection plates of an ESP or in a particle collection device, a specialized sampling probe was designed and built. This "quench probe" is designed to capture an isokinetic sample of a flue gas aerosol, immediately dilute the aerosol sample with hot filtered air, and convey the sample to a heated filter where it is retained for subsequent analysis. Figures 3-6 and 3-7 show the basic elements of the design of this device. In contrast to the gas sampling probes where the sorbent-SO_2 reaction is quenched by heating, this device quenches the sorbent-SO_2 reaction by dilution with heated air. At the tip of the probe heated air is injected into the sample stream through a section of porous sample line. Thus, contact between sorbent and a solid surface is prevented until the sample stream has been heated by mixing with heated dilution air.

This probe was first tested with unreacted sorbent on the filter. The probe was spiked with SO_2 span gas that was diluted by a known amount of fresh air that passed through the porous section at the end of the probe. Little (<2%) uptake of SO_2 by the sorbent was observed. Subsequently, in comparisons of sorbent utilization determined from gas phase measurements and from chemical analyses of solids samples obtained with the quench probe, utilizations measured with the quench probe have always been less than utilizations determined from gas phase measurements. This is in the direction that should be expected if the quench probe operates properly because gas-phase utilization determinations can be increased by deposits of active sorbent inside the duct reacting with SO_2 in the flue gas.

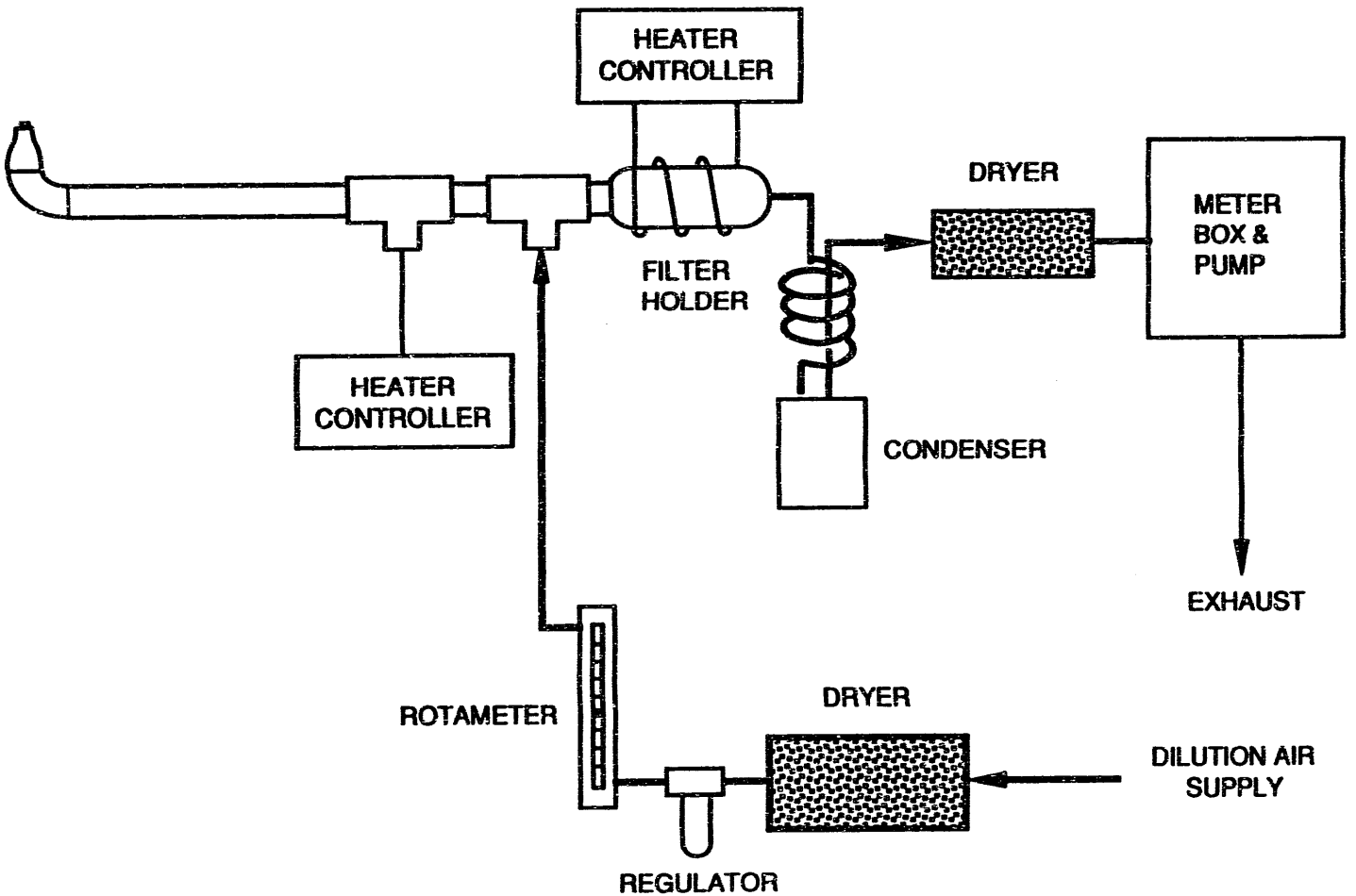

Figure 3-6. System for withdrawing a gas sample through a quench probe and recovering the entrained solids on a filter.

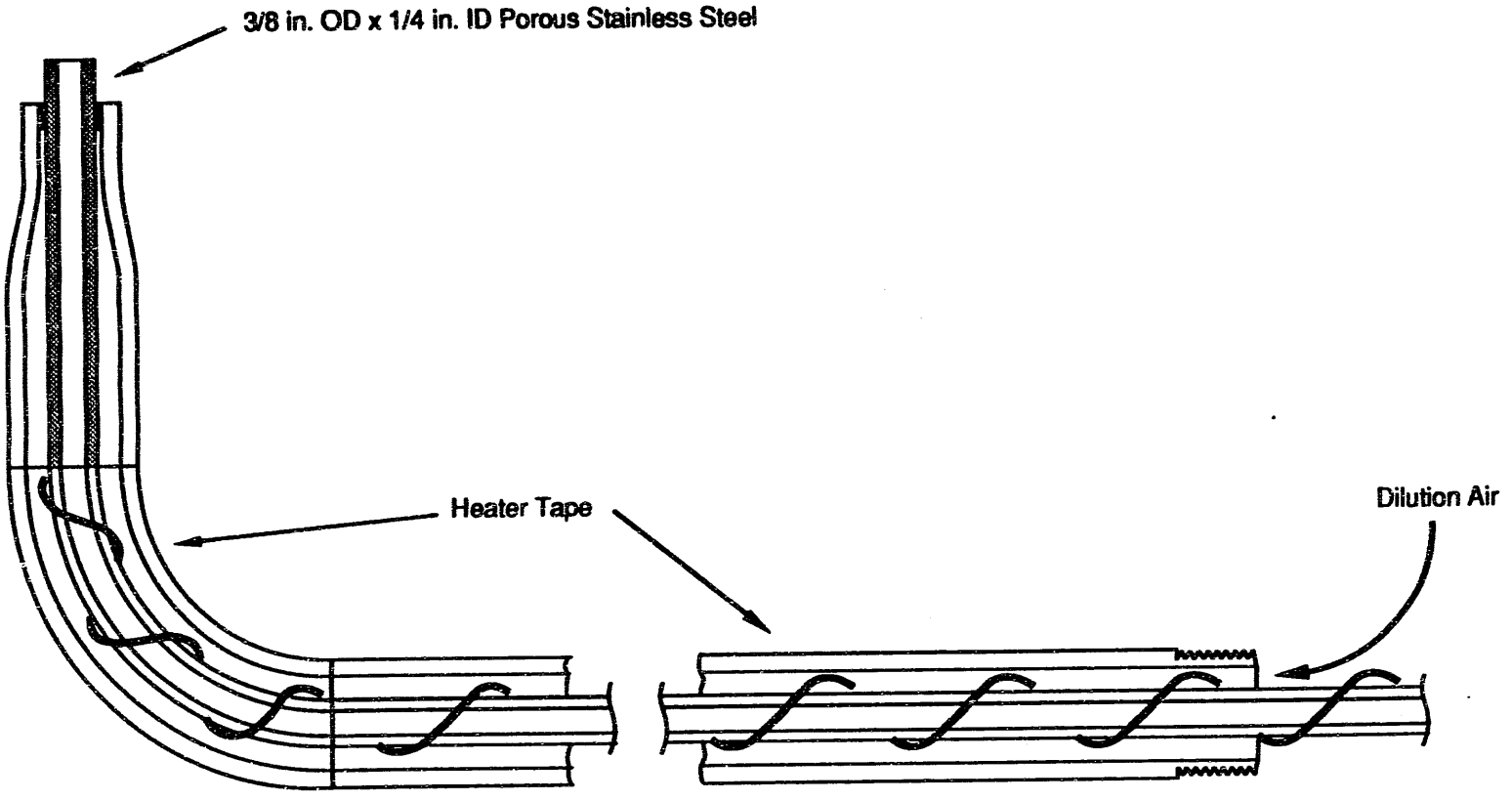

Figure 3-7. Quench probe for extracting a solids sample.

4.0 INITIAL SYSTEM PERFORMANCE

During the period April 30-May 3, 1990, the DITF was continuously operated on flue gas without the addition of sorbent or water. During this week, preliminary measurements of concentrations of certain flue gases, mass concentrations of suspended fly ash, electrical resistivity of fly ash, and performance of the ESP were conducted. The results of these measurements are described in the following paragraphs.

4.1 Gas Concentrations

Measurements of the concentrations of SO_2 and SO_3 (actually, sulfuric acid vapor) were made with a Cheney-Homolya controlled condensation apparatus at the inlet to the ESP on May 1 and 2. Measurements of HCl were made with another sampling device, which collects HCl in a bubbler containing NaOH. At an average flue gas temperature of 315°F, the results of eight separate determinations gave an average SO_2 concentration of 3204 ± 66 ppm and an average SO_3 level of 30 ± 3 ppm. Four measurements of the concentration of HCl gave an average result of 36.5 ± 1.3 ppm.

4.2 Coal and Ash Properties

4.2.1 Chemistry of the Coal and Ash

The coal burned at Unit 5 of the Muskingum River power plant is reputedly highly consistent in composition. No coal samples were initially available for analysis, but samples accumulated over a period of several months later were analyzed. The results of those analyses are given in Table 4-1. They confirm that the variability of the coal composition is within narrow limits.

The result of an analysis of the ash produced by igniting one sample of coal in the laboratory at 750°C is given in Table 4-2. A key feature of this analysis is the low percentage of CaO. This makes the determination of CaO in an ash-sorbent mixture a fairly good indicator of the total amount of sorbent present.

4.2.2 Electrical Resistivity of the Fly Ash

The electrical resistivity of the fly ash entering the ESP was measured in situ with a point-plane resistivity probe. The data were obtained with the so-called spark method, in which current density is measured at the electrical field causing electrical breakdown of the ash layer; the results are given in Table 4-3. The values are in the range (2 to 3) x 10^9 ohm-cm. They are consistent with the chemical composition of the dust and the measured values of the SO_3 concentration. The dust resistivity is sufficiently low that the electrical conditions of the ESP will not be limited by the collected solid matter as long as the dust consists of fly ash alone. The resistivity may be even lower when sorbent is also present in an environment of lower temperature and increased water vapor concentrations.

Table 4-1. Coal Composition

	Date of Sample				
	11/20/90	12/04/90	01/08/91	02/06/91	03/05/91
% Moisture	7.52	10.52	6.46	6.07	8.87
% Ash	12.33	11.67	12.84	12.26	11.73
% Volatile	37.16	36.09	37.42	38.17	36.10
% Fixed Carbon	42.99	41.72	43.28	43.50	43.30
Btu/lb	11497	11238	11588	11802	11532
% Carbon	63.60	61.74	64.13	64.53	64.35
% Hydrogen	4.34	4.21	4.27	4.33	4.09
% Nitrogen	1.06	1.01	0.99	1.05	1.01
% Sulfur	4.50	4.07	4.11	4.24	3.97
% Oxygen	6.55	6.78	7.20	7.52	5.98
% Chlorine	0.04	0.04	0.05	0.05	0.02

Table 4-2. Coal Ash Composition

% Li_2O	0.05
% Na_2O	0.60
% K_2O	1.9
% MgO	1.2
% CaO	1.9
% Fe_2O_3	18.8
% Al_2O_3	23.1
% SiO_2	47.7
% TiO_2	1.2
% P_2O_5	0.23
% SO_3	1.8

Table 4-3. Fly Ash Resistivity

Date	Gas Temperature, °F	Layer Thickness, cm	Electric Field, kV/cm	Dust Resistivity, ohm-cm
5/1/90	312	0.141	11.7	2.5×10^9
5/2/90	314	0.102	17.2	2.2×10^9

4.3 ESP Performance

4.3.1 Performance Data

The results of determinations of the concentrations of suspended fly ash by EPA Method 17 are shown in Table 4-4. Two determinations were made at the ESP inlet, and one determination was made at the ESP outlet. The average inlet mass loading value of 3.96 gr/scf is consistent with the coal ash content typical of this fuel (12-13%). The flue gas volume flow rate was close to the intended value of 50,000 acfm. Inlet and outlet dry standard gas volumes were within 1% of each other and indicated that very low air inleakage occurred in the ESP.

The value of outlet mass loading (0.0005 gr/acf) and ESP collection efficiency (99.998%) should be used with caution. The total filter and nozzle weight gain from the 72-min run was only 0.18 mg. This sample catch is one to two orders of magnitude lower than desired for accurate determinations. The loss of filter fibers on the filter holder O-ring could easily produce errors larger than the total catch. However, even if the measured value were low by one order of magnitude, the performance of the ESP would still be excellent.

4.3.2 ESP Electrical Data

Voltage-current curves measured at the ESP with calibrated voltage dividers are shown in Figures 4-1, 4-2, and 4-3. Figure 4-1 shows data collected under air-load conditions (with clean electrodes) before start-up. The air-load V-I curves indicate good electrical and mechanical conditions in the ESP.

Figures 4-2 and 4-3 show the V-I curves measured after periods of several days and one week on-line, respectively. All of the curves were terminated upon reaching the current-limit or voltage-limit of the T-R set and not because of sparking. The curves are consistent with the low measured values of dust resistivity, with 40-80 nA/cm^2 in all fields. They show no evidence of back corona. Very little change can be observed in the V-I characteristics due to the additional time on-line, indicating the ESP may be close to electrical equilibrium, providing that deposits on the discharge electrode do not become a problem.

4.3.3 ESP Modeling

Revision 3 of the EPA/SRI Mathematical Model of ESP performance was used to simulate the ESP under the measured conditions. A particle size distribution typical for PC boilers burning bituminous coal (mmd = 16.3 μm, σ_g = 3.4) was assumed. The results of the model run are shown in Table 4-5. Since the dust layers in the outlet field are not likely to have reached equilibrium in the short period this ESP had been on-line, the particle emissions caused by plate rapping reentrainment are probably lower than expected. Therefore, the results of the model calculations both including and excluding the rapping adjustment are shown in the table. The actual performance is probably somewhere between these two extremes.

Two sets of non-ideal conditions were used in modeling of the ESP. The results for each set of non-ideal conditions are shown in the table. The non-ideal parameters describe the fraction of gas sneakage per section and the normalized standard deviation of the gas velocity distribution (σ_g) in the ESP. The conditions of s = 0 and σ_g = 0 describe ideal behavior, while the values of s = 0.05 and σ_g = 0.15 generally correspond to operation observed in modern ESPs in good condition. Values

Table 4-4. ESP Performance Data

ESP INLET MEASUREMENTS

Date	Mass Loading gr/acf	gr/scf	Gas Flow acfm	dscfm	SCA ft^2/kacfm	Temp °F	Water %	Isokin %
5/1/90	2.07	3.34	52292	32291		313	7.2	100.1
5/2/90	2.84	4.57	52696	32784		313	7.3	98.0
Average ±	2.46	3.96	52494	32538		313	7.3	99.1
1 SD	0.38	0.62	202	247		0	0.0	1.0
C.O.V.	0.16	0.16	0.00	0.01		0.00	0.01	0.01

ESP OUTLET MEASUREMENTS

5/2/90	0.0005	0.0008	50493	32337	329	310	6.6	96.7

Table 4-5. ESP Model Results

Non-Ideal Parameters s	σ_g	Without Rapping Efficiency, %	Penetration, %	With Rapping Efficiency, %	Penetration, %
0.05	0.05	99.991	0.009	99.980	0.020
0.05	0.15	99.958	0.043	99.929	0.072
0.10	0.25	99.829	0.172	99.758	0.242

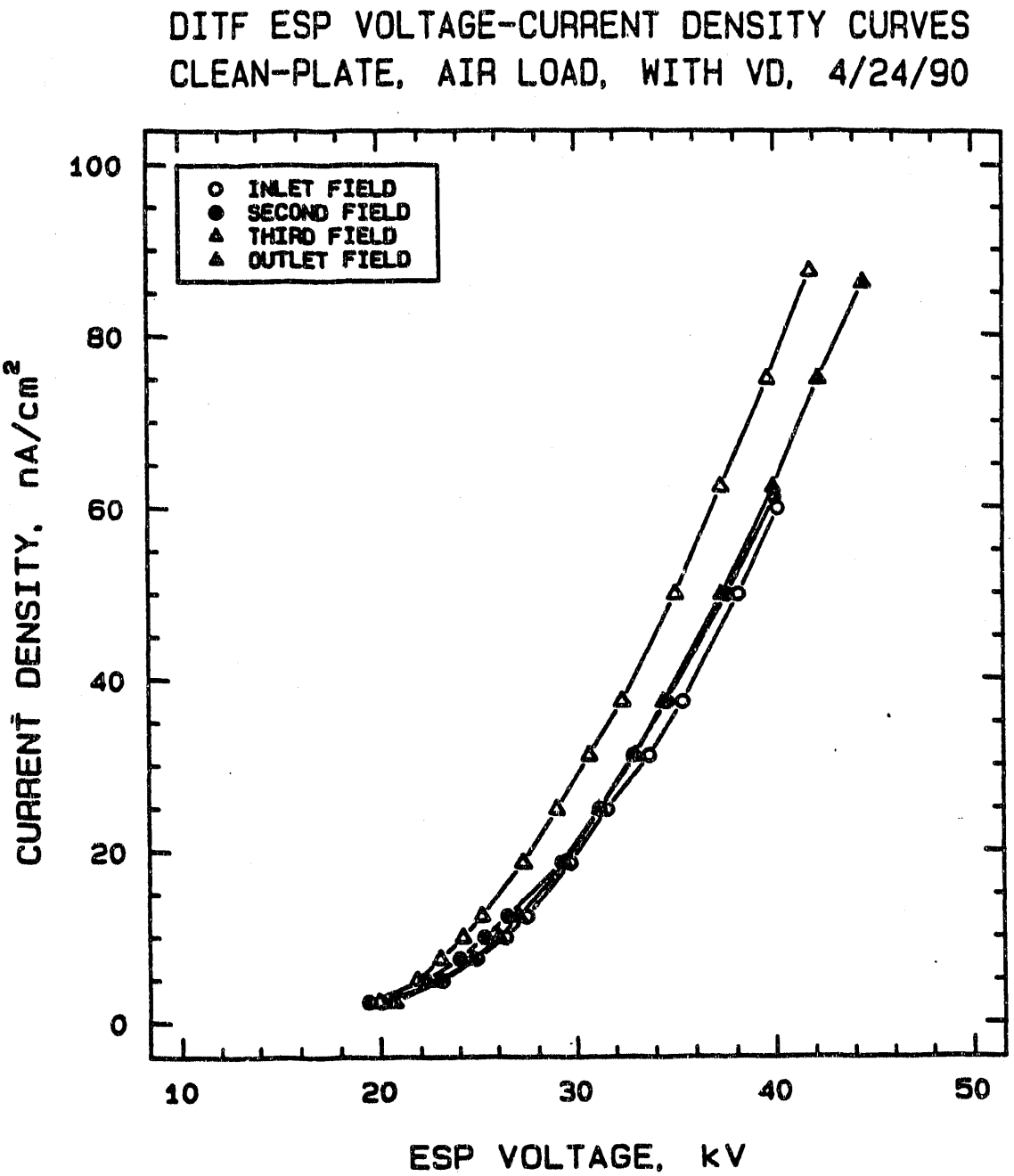

Figure 4-1. ESP air load V-I curves.

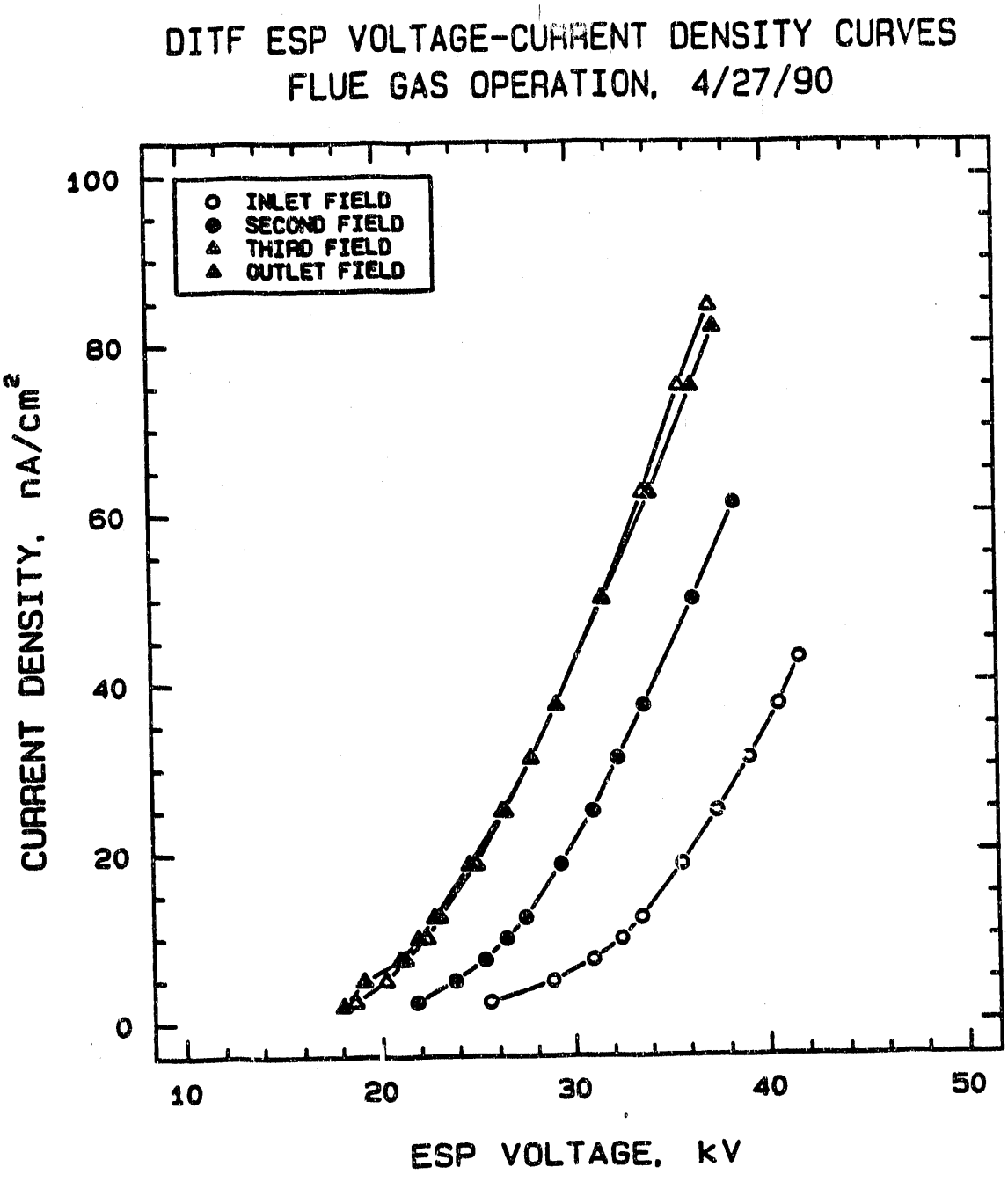

Figure 4-2. ESP V-I curves after several days of operation on flue gas.

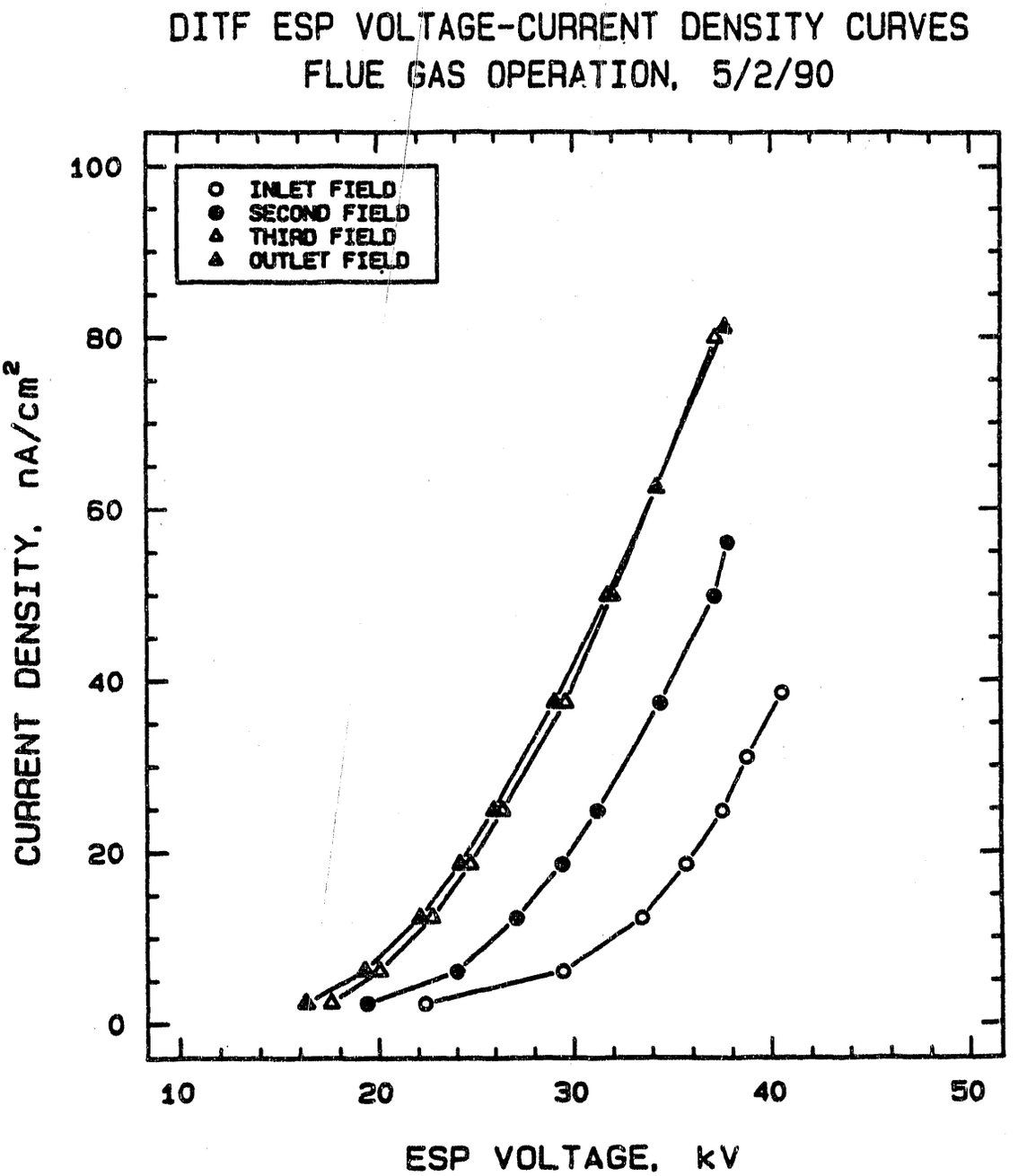

Figure 4-3. ESP V-I curves after 1 week of operation on flue gas.

of $s = 0.10$ and $\sigma_g = 0.25$ have been related to performance of older ESPs in questionable condition. The measured performance previously indicated by Table 4-4 (which includes the effect of rapping) is better than the performance under any of these modeled conditions.

5.0 NOZZLE TESTS

5.1 Nozzle Testing to Minimize Wall Wetting

A series of nozzle tests were performed to characterize the behavior of the Lechler and Parker-Hannifin nozzles for a variety of nozzle configurations, air flow rates, water flow rates, and flue gas velocities. The nozzle tests were carried out with spray injection in the horizontal test section of the DITF, always with just plain water rather than sorbent slurry. The primary purpose of the nozzle tests were to determine which operating conditions affected wall wetting by the water spray.

A total of 48 separate nozzle tests were conducted in the first test series. Figure 5-1 shows the location of the duct wall thermocouples that were used to monitor wall wetting as well as the location of the thermocouple used to measure the approximate adiabatic saturation temperature within the duct. Figure 5-2 shows how the nozzles and nozzle holders (lances) could be arranged within the duct.

Data from the nozzle tests are presented in Tables 5-1 through 5-4. Tables 5-1 through 5-3 show the results of tests conducted with the Lechler nozzles; Table 5-4 gives the results of tests conducted with the Parker-Hannifin nozzles. The tests summarized in Table 5-3 were performed after a large port in the horizontal duct (previous used by GE to install an atomizer) was plugged with an insert. It had been speculated that some of the wall wetting along the top of the duct was caused by turbulence induced by the port cavity.

The data in the four tables are arranged according to the placement and orientation of the nozzles. Within each table, the test results are listed in order of increasing approach to adiabatic saturation (that is, in order of diminishing approach temperature). Temperatures that are near the adiabatic saturation temperature (134°F or lower) are shaded for emphasis. Unfortunately, data from all 48 tests could not be reported because the data acquisition system (DAS) malfunctioned during some of these tests or because the instruments used to measure water flow rate or flue gas flow rate were temporarily inoperable or incorrectly calibrated.

The data in Tables 5-1 through 5-4 should be interpreted with care. In particular, the approach to adiabatic saturation temperature is subject to uncertainty; it was estimated by taking the difference between the temperature at the inlet to the ESP and the adiabatic saturation temperature as measured by a thermocouple located in the middle of the duct, 10 ft downstream from the nozzle array, which was inevitably wet from the impaction of spray droplets. (The temperature at the inlet to the ESP is measured by averaging the temperature reported by three thermocouples located across the duct immediately upstream of the inlet to the ESP; the temperature indicating the saturation temperature is, as indicated, shown by a single thermocouple). A further basis for caution is the possibility that temperatures reported in Tables 5-1 through 5-4 may be somewhat in error, because these data were taken when software compensation rather than hardware compensation was used in the conversion of thermocouple output to temperature. Hardware compensation was installed subsequently. Specifically, Test 3 should be disregarded. The adiabatic approach temperature is not consistent with a water flow rate of 10 gal/min.

Lechler nozzles. Six nozzles were used for all of these tests, with three nozzles per lance, located at positions 2, 3, and 4 on each lance (for nozzle location, refer to Figure 5-2). Table 5-1 shows the

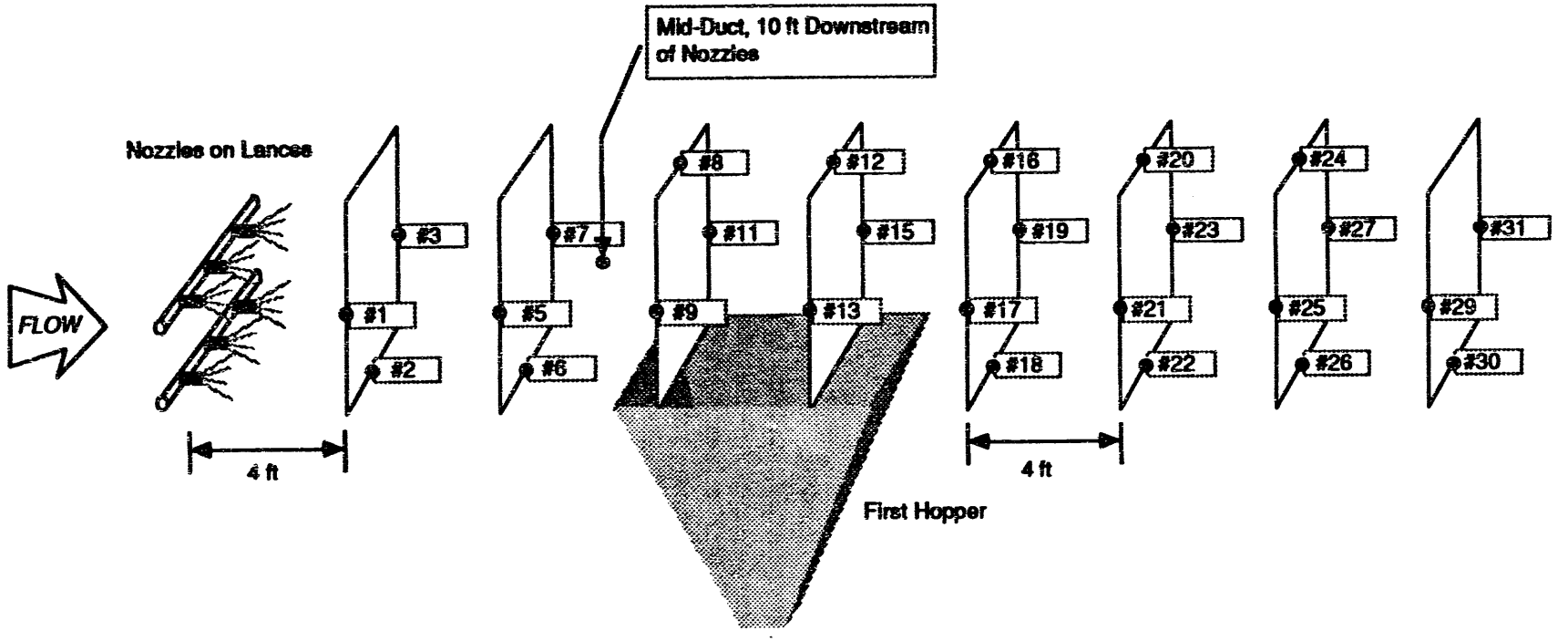

Figure 5-1. Location of Duct Wall Thermocouples in the Horizontal Duct of the DITF.

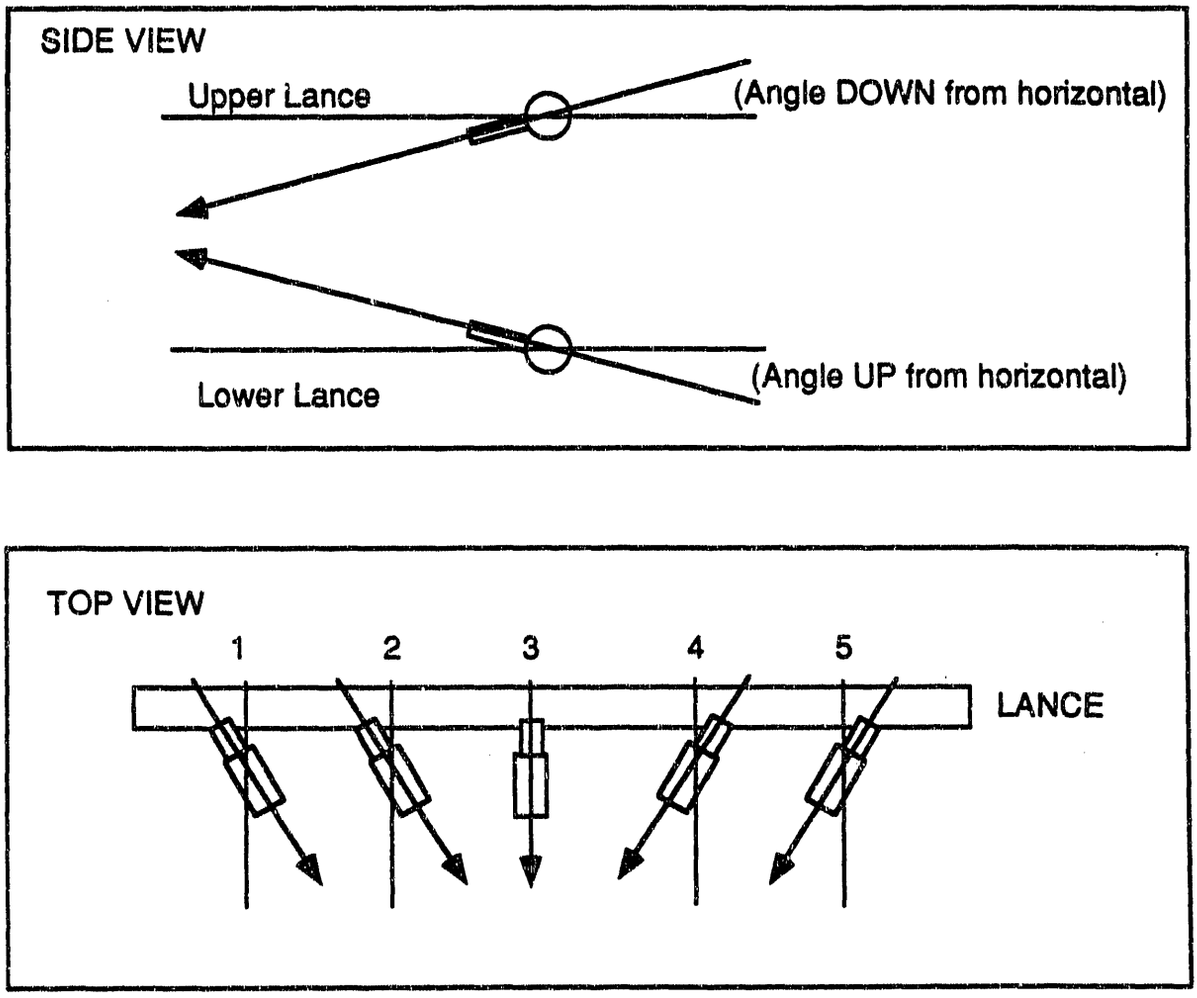

Figure 5-2. Arrangements of Nozzles and Lances at the DITF.

Table 5-1. Results of Lechler Nozzle Tests, Part 1 (May)

TEST PARAMETERS										
Test Number	5	1	6	2	3	9	10	10A	8	4
Nozzle Type	Lechler	Lechler	Lechler	Lechler	Lechler	Lechler	Lechler	Lechler	Lechler	Lechler
No. of Lances	2	2	2	2	2	2	2	2	2	2
Upper Lance Position (° Down)	5	5	5	5	5	0	0	0	5	5
Lower Lance Position (° Up)	2.5	2.5	2.5	2.5	2.5	0	0	0	2.5	2.5
No. of Nozzles per Lance (Top/Bottom)	3/3	3/3	3/3	3/3	3/3	3/3	3/3	3/3	3/3	3/3
Upper Lance, Outside Nozzle Position (° In)	0	0	0	0	0	0	0	0	0	0
Lower Lance, Outside Nozzle Position (° In)	0	0	0	0	0	0	0	0	0	0
Humidification Water Flow (gpm)	5.9	6.4	7.9	8.0	10.0	8.0	8.0	8.0	4.9	12.0
Nozzle Atomizing Air Supply Press. (psig)	80.3	80.4	50.0	80.4	79.9	80.4	86.3	100.2	50.5	80.2
Flue Gas Flow (acfm)	51670	51743	51573	50792	51092	50390	50469	50297	25357	47283
Flue Gas Flow (scfm)	37675	36140	38806	36934	38346	37598	38022	37464	20287	37207
Temperatures (°F)										
Test Section Inlet Temperature	332	335	330	334	331	330	329	330	310	334
Saturation Temperature	129	127	127	126	127	127	126	126	124	128
ESP Inlet Temperature	229	217	203	202	196	197	196	196	159	140
Approach to Saturation	100	89	76	76	69	70	70	70	35	12
Wall Thermocouple # 1	320	321	318	320	317	314	314	316	227	320
Wall Thermocouple # 2	307	310	307	307	301	299	299	297	156	301
Wall Thermocouple # 3	316	316	316	316	312	207	214	235	253	315
Wall Thermocouple # 5	287	277	229	268	262	268	274	283	165	189
Wall Thermocouple # 6	267	260	277	245	253	202	208	215	127	221
Wall Thermocouple # 7	274	247	266	234	250	246	248	249	124	193
Wall Thermocouple # 8	203	156	130	137	135	126	126	125	128	126
Wall Thermocouple # 9	261	229	179	216	213	225	224	235	163	131
Wall Thermocouple # 11	198	159	148	144	145	145	153	182	123	129
Wall Thermocouple # 12	200	137	126	126	126	126	126	126	126	127
Wall Thermocouple # 13	253	229	139	212	208	210	211	225	143	130
Wall Thermocouple # 15	185	148	145	131	135	144	152	164	125	129
Wall Thermocouple # 16	201	175	129	145	148	132	127	126	137	128
Wall Thermocouple # 17	249	224	154	206	205	203	204	217	150	130
Wall Thermocouple # 18	222	210	226	184	182	183	182	187	129	134
Wall Thermocouple # 19	182	154	134	139	136	157	154	161	125	129
Wall Thermocouple # 20	199	174	130	159	140	142	144	163	142	128
Wall Thermocouple # 21	245	223	155	203	201	203	194	212	149	130
Wall Thermocouple # 22	221	212	219	184	181	201	201	205	131	133
Wall Thermocouple # 23	191	196	140	166	159	171	159	158	125	129
Wall Thermocouple # 24	206	183	131	159	156	146	147	169	147	129
Wall Thermocouple # 25	238	222	173	202	199	188	198	207	152	131
Wall Thermocouple # 26	218	206	207	180	180	180	180	163	133	137
Wall Thermocouple # 27	195	171	134	148	154	151	147	151	129	129
Wall Thermocouple # 29	237	218	159	198	196	187	194	204	151	131
Wall Thermocouple # 30	215	208	168	186	180	195	189	193	137	130
Wall Thermocouple # 31	205	187	138	161	163	162	157	164	139	129

Table 5-2. Results of Lechler Nozzle Tests, Part 2 (May)

TEST PARAMETERS									
Test Number	22	23	24	30	29	26	25	27	28
Nozzle Type	Lechler	Lechler	Lechler	Lechler	Lechler	Lechler	Lechler	Lechler	Lechler
No. of Lances	2	2	2	2	2	2	2	2	2
Upper Lance Position (° Down)	0	0	0	5	5	5	5	5	5
Lower Lance Position (° Up)	10	10	10	10	10	10	10	10	10
No. of Nozzles per Lance (Top/Bottom)	3/3	3/3	3/3	3/3	3/3	3/3	3/3	3/3	3/3
Upper Lance, Outside Nozzle Position (° In)	5	5	5	5	5	5	5	5	5
Lower Lance, Outside Nozzle Position (° In)	5	5	5	5	5	5	5	5	5
Humidification Water Flow (gpm)	8.1	10.0	12.0	8.0	7.9	10.1	10.0	10.1	11.0
Nozzle Atomizing Air Supply Press. (psig)	80.0	80.0	79.7	79.6	99.9	60.6	79.5	99.5	99.7
Flue Gas Flow (acfm)	46851	49903	49113	49143	48927	48458	48535	48959	49357
Flue Gas Flow (scfm)	36107	38221	38454	36067	37470	37271	37562	37691	39089
Temperatures (°F)									
Test Section Inlet Temperature	330	329	326	328	327	325	326	326	327
Saturation Temperature	127	126	125	125	124	125	125	125	124
ESP Inlet Temperature	191	167	139	193	189	167	165	165	156
Approach to Saturation	64	41	14	68	65	42	40	40	32
Wall Thermocouple # 1	316	315	313	315	316	314	313	314	315
Wall Thermocouple # 2	292	293	292	301	297	294	292	293	295
Wall Thermocouple # 3	308	302	304	305	308	308	305	306	306
Wall Thermocouple # 5	292	293	291	295	300	287	292	298	299
Wall Thermocouple # 6	201	213	216	234	227	223	220	225	225
Wall Thermocouple # 7	196	202	205	234	225	213	209	218	222
Wall Thermocouple # 8	127	126	125	125	125	125	125	124	124
Wall Thermocouple # 9	231	204	171	224	202	166	160	175	183
Wall Thermocouple # 11	230	229	223	257	248	234	215	243	242
Wall Thermocouple # 12	127	126	125	125	124	125	125	124	125
Wall Thermocouple # 13	203	168	140	186	162	145	150	150	152
Wall Thermocouple # 15	219	212	203	236	219	216	209	217	209
Wall Thermocouple # 16	127	126	126	126	126	126	126	125	125
Wall Thermocouple # 17	205	173	134	173	152	139	151	147	144
Wall Thermocouple # 18	165	168	169	189	173	177	173	177	171
Wall Thermocouple # 19	193	168	180	203	182	182	178	183	176
Wall Thermocouple # 20	136	127	126	128	127	126	126	126	126
Wall Thermocouple # 21	196	137	126	159	160	127	128	127	126
Wall Thermocouple # 22	177	182	180	190	175	182	181	179	172
Wall Thermocouple # 23	156	147	127	175	150	136	134	137	134
Wall Thermocouple # 24	171	128	127	142	147	126	126	126	126
Wall Thermocouple # 25	196	146	129	166	146	129	133	136	129
Wall Thermocouple # 26	153	152	150	162	148	150	150	151	147
Wall Thermocouple # 27	184	173	138	179	156	139	139	145	141
Wall Thermocouple # 29	197	147	130	171	153	135	136	143	136
Wall Thermocouple # 30	172	169	163	171	157	159	160	159	154
Wall Thermocouple # 31	211	187	149	192	161	137	137	145	143

Table 5-3. Results of Lechler Nozzle Tests, Part 3, Insert Installed in Atomizer Port (May)

TEST PARAMETERS							
Test Number	42	46	43	47	44	48	45
Nozzle Type	Lechler	Lechler	Lechler	Lechler	Lechler	Lechler	Lechler
No. of Lances	2	2	2	2	2	2	2
Upper Lance Position (° Down)	5	5	5	5	5	5	5
Lower Lance Position (° Up)	0	0	0	0	0	0	0
No. of Nozzles per Lance (Top/Bottom)	3	3	3	3	3	3	3
Upper Lance, Outside Nozzle Position (° In)	5	5	5	5	5	5	5
Lower Lance, Outside Nozzle Position (° In)	5	5	5	5	5	5	5
Humidification Water Flow (gpm)	5.9	5.9	8.1	8.0	10.1	10.2	12.2
Nozzle Atomizing Air Supply Press. (psig)	79.6	100.2	80.6	99.1	39.8	100.3	79.5
Flue Gas Flow (acfm)	50942	51874	51552	51631	51465	51624	51709
Flue Gas Flow (scfm)	36877	37526	38493	38843	38557	39675	38911
Temperatures (°F)							
Test Section Inlet Temperature	327	326	327	330	328	329	329
Saturation Temperature (Estimated)	126	126	127	126	127	126	126
ESP Inlet Temperature	223	215	198	196	179	173	149
Approach to Saturation	97	89	71	70	52	47	23
Wall Thermocouple # 1	314	314	316	317	317	317	317
Wall Thermocouple # 2	299	303	302	305	306	305	305
Wall Thermocouple # 3 (failed)							
Wall Thermocouple # 5	300	307	300	311	299	310	304
Wall Thermocouple # 6	278	275	274	273	289	266	270
Wall Thermocouple # 7	295	289	296	290	299	289	300
Wall Thermocouple # 8	140	168	129	131	129	127	127
Wall Thermocouple # 9	258	258	235	253	174	232	210
Wall Thermocouple # 11	251	241	241	228	260	210	213
Wall Thermocouple # 12	136	170	128	128	127	126	126
Wall Thermocouple # 13	233	232	199	210	138	174	141
Wall Thermocouple # 15	231	225	210	205	200	173	145
Wall Thermocouple # 16	190	193	136	144	129	129	126
Wall Thermocouple # 17	228	226	186	206	130	172	130
Wall Thermocouple # 18	222	208	187	190	177	151	131
Wall Thermocouple # 19	224	218	196	197	164	150	133
Wall Thermocouple # 20	184	187	132	138	128	128	127
Wall Thermocouple # 21	224	220	181	196	132	157	130
Wall Thermocouple # 22	219	210	180	191	163	160	132
Wall Thermocouple # 23	220	209	197	187	185	159	141
Wall Thermocouple # 24	195	201	154	163	132	133	127
Wall Thermocouple # 25	222	216	181	195	133	161	130
Wall Thermocouple # 26	214	205	178	191	169	170	138
Wall Thermocouple # 27	217	210	180	188	138	154	129
Wall Thermocouple # 29	222	215	183	193	131	152	128
Wall Thermocouple # 30	219	209	181	192	153	165	134
Wall Thermocouple # 31	220	213	185	190	147	154	131

Table 5-4. Results of Nozzle Tests, Parker-Hannifin Nozzles (May)

TEST PARAMETERS									
Test Number	17	19	11	14	20	12	16	21	13
Nozzle Type	P-H	P-H	P-H	P-H	P-H	P-H	P-H	P-H	P-H
No. of Lances	2	2	2	2	2	2	2	2	2
Upper Lance Position (° Down)	0	5	0	0	5	0	0	5	0
Lower Lance Position (° Up)	0	0	0	0	0	0	0	0	0
No. of Nozzles per Lance (Top/Bottom)	3/3	3/3	3/3	3/3	3/3	3/3	3/3	3/3	3/3
Upper Lance, Outside Nozzle Position (° In)	0	0	0	0	0	0	0	0	0
Lower Lance, Outside Nozzle Position (° In)	0	0	0	0	0	0	0	0	0
Humidification Water Flow (gpm)	6.0	6.0	8.0	8.0	6.0	10.0	12.0	9.9	12.0
Nozzle Atomizing Air Supply Press. (psig)	99.9	100.0	80.8	99.8	99.7	80.0	99.8	100.3	79.2
Flue Gas Flow (acfm)	49792	49699	50294	50131	49741	48748	49685	49941	49582
Flue Gas Flow (scfm)	36251	36439	36791	37173	37406	36686	38579	36072	38545
Temperatures (°F)									
Test Section Inlet Temperature	328	328	329	329	330	327	331	327	329
Saturation Temperature	128	127	126	127	127	127	127	126	126
ESP Inlet Temperature	215	208	190	189	188	170	165	164	159
Approach to Saturation	87	81	64	62	61	44	38	38	32
Wall Thermocouple # 1	315	314	314	315	315	310	316	312	311
Wall Thermocouple # 2	305	305	304	303	306	303	305	301	304
Wall Thermocouple # 3	305	303	304	303	305	301	305	301	300
Wall Thermocouple # 5	253	239	199	246	226	182	213	209	148
Wall Thermocouple # 6	225	227	232	227	225	231	219	218	229
Wall Thermocouple # 7	147	160	225	166	162	208	141	161	136
Wall Thermocouple # 8	142	143	126	126	127	126	126	125	126
Wall Thermocouple # 9	172	209	163	183	190	151	159	175	142
Wall Thermocouple # 11	168	179	158	170	174	148	145	166	134
Wall Thermocouple # 12	168	166	126	127	127	126	127	126	126
Wall Thermocouple # 13	203	208	145	176	185	138	145	163	132
Wall Thermocouple # 15	164	183	166	161	186	154	153	187	138
Wall Thermocouple # 16	190	187	131	138	156	130	131	137	128
Wall Thermocouple # 17	201	209	148	181	188	140	145	171	152
Wall Thermocouple # 18	184	188	204	188	185	195	176	180	183
Wall Thermocouple # 19	162	183	195	159	182	167	156	181	149
Wall Thermocouple # 20	169	206	172	186	193	150	150	182	141
Wall Thermocouple # 21	211	212	162	190	190	142	149	174	135
Wall Thermocouple # 22	203	206	225	207	201	213	191	196	199
Wall Thermocouple # 23	149	154	178	152	154	165	144	154	147
Wall Thermocouple # 24	180	200	160	181	184	143	147	172	138
Wall Thermocouple # 25	200	208	192	192	192	164	171	184	142
Wall Thermocouple # 26	174	176	198	179	173	189	166	170	174
Wall Thermocouple # 27	152	163	184	151	165	169	146	169	142
Wall Thermocouple # 29	206	209	196	193	193	173	171	185	145
Wall Thermocouple # 30	176	185	203	169	178	182	161	170	160
Wall Thermocouple # 31	196	203	195	179	193	180	172	186	156

results of Tests 1-10A, Table 5-2 shows the results of Tests 22-30, and Table 5-3 shows the results of Tests 42-48. For Tests 1-8, the upper nozzle lance was pointed downward by 2.5° while the lower nozzle lance was pointed upward by 5°. For Tests 9-10A, both the upper and lower lances were level. For Tests 22-24, the lower lance was elevated by 10°, the upper lance was kept horizontal, and the outer nozzles on each lance were pointed inward by 5°. The 10° elevation of the lower nozzle lance was not intended. Because of operator error, the lances were elevated instead of being kept horizontal. For Tests 25-30, the upper nozzle lance was depressed by 5°; otherwise, the nozzles were located as in Tests 22-24. For Tests 42-48, the nozzles were oriented as for Tests 25-30, but the lower lance kept horizontal, as was originally intended for Tests 22-30.

It is apparent from these tests that, if wall wetting is identified with temperatures of 134°F or less, then wetting did not occur at water flow rates below 6.4 gal/min (at an approach of approximately 90°F). (A temperature of 134°F or less was initially chosen to indicate an indication of wetting or near wetting since it is significantly below the planned average temperature for the gas.) On the other hand, at water flow rates of 8 gal/min or greater, some wall wetting was always present. When wall wetting occurred, it occurred first at the top of the duct, usually no closer to the nozzles than 12 ft (Thermocouple 8 is 12 ft downstream of the nozzles, at the top of the duct). The data also suggest that Lechler nozzles should not be operated at 50 psig or less (60 psig is recommended by the manufacturer). Angling the nozzles away from the top and bottom of the duct may reduce wall wetting. Test 9, with the nozzles pointed straight ahead, appeared to produce wall wetting closer to the nozzles than did Test 2, where the nozzles were angled away from the top and bottom of the duct.

At 8 gal/min of water flow, pointing the nozzles inward by 5° and elevating the lower lance by 10° (Test 22) did not appear to reduce wall wetting, compared to Test 9. Angling the upper lance down by 5° (Test 30) appeared to cause more wall wetting. Tests 43 and 47 suggested that keeping the lower lance horizontal while the upper lance was lowered (with the outer nozzles pointed inward by 5°) reduced wall wetting. Surprisingly, increasing the air pressure to 100 psig further reduced wall wetting in Test 47.

At 10 gal/min of water flow, all of the useful test results were obtained with the outer nozzles pointed inward by 5°. With 80 psig of air pressure (Tests 23 and 25), lowering the upper lance caused more wall wetting.

Increasing the air pressure to 100 psig reduced wall wetting (Tests 27 and 48). At 100 psig of air pressure, depressing the lower lance to the horizontal slightly reduced wall wetting.

At 11 gal/min and 100 psig of air pressure (Test 28), a 32°F approach to adiabatic saturation was obtained with wall wetting mainly in the top of the duct by pointing the outer nozzles inward, depressing the upper nozzle lance by 5°, and by raising the lower nozzle lance by 10°. At 12 gal/min and 80 psig of air pressure (Test 24), much less wall wetting was also observed (compared to Tests 4 and 45) when the outside nozzles were pointed inward and when the lower lance was pointed upward by 10°.

A four-nozzle array of Lechler nozzles was investigated in still other tests not listed in Tables 5-1 through 5-3, but the data from these tests were lost due to a malfunction in the DAS. A discussion of these tests is nevertheless appropriate even though the data were lost. Velocity traverses were made in three test ports located approximately 5 ft downstream of the nozzle array while the nozzles

were operated at 20 or 80 psig of air pressure to look for flow disturbances that may have been caused by a large existing atomizer port, located in the top of the duct, just ahead of the test ports. There was concern that such a flow disturbance might have been responsible for the wall wetting in the top of the duct. Another concern was that the flue gas passing by the nozzle lances was stratified because of the lances being located immediately downstream of a 90° bend in the ductwork.

Table 5-5 shows the results of the velocity traverses. Inspection of this table reveals that the atomizer test port is not responsible for any stratification in the velocity distribution in the horizontal duct, because the results of velocity traverses made with and without an insert that fills the atomizer test port are essentially the same (with air flow through the nozzles at a nominal air pressure of 20 psig to keep the air lines supplying the nozzles cooled). What may be responsible for wetting of the top of the duct by the water spray is seen in the results of the velocity traverse made with the nozzles operated at an air flow of 80 psig. Here the velocity of the flue gas in the middle of the duct as measured at the middle and top test ports was found to be approximately 150 ft/s (far higher than the nominal average of 60 ft/s). This high velocity appears to be due to the position of the upper nozzle lance, relative to the top of the duct. The upper nozzle lance is located only 8 in. from the top of the duct, while the lower nozzle lance is located 15 in. from the bottom of the duct. The upper nozzle lance was subsequently modified to lower it to a position approximately 15 in. from the top of the duct.

Parker-Hannifin nozzles. Table 5-4 contains the results of tests conducted with the Parker-Hannifin nozzles. These tests were conducted with six nozzles mounted on the lances in the same locations as those used for the Lechler nozzles. No tests were conducted with the lower nozzle lance elevated beyond the horizontal or with the outer nozzles pointed toward the center of the duct. However, tests were performed with the upper nozzle lance held horizontal (Tests 11-13, 14-16) or depressed 5° (Tests 19-21).

Because the Parker-Hannifin nozzles were found to have a spray pattern that was much broader than the spray pattern for the Lechler nozzles, it was assumed initially that they would not perform as well as the Lechler nozzles. This was not the case. Like the Lechler nozzles, these nozzles were observed to wet the duct walls, starting 12 ft down the duct at the top. However, at high water flow rates, these nozzles did not appear to wet the walls as far down the duct as the Lechler nozzles did. Also, the Parker-Hannifin nozzles appeared to perform more satisfactorily at an atomizing air pressure of 100 psig than at a lower pressure.

A second series of nozzle tests were conducted during which two modifications were made. First, the upper lance was lowered from a position 8.5 in. from the top of the duct to a position 15 in. from the top of the duct (so that the upper and lower lances were both 15 in. from the upper and lower duct walls, respectively). The upper nozzle lance was lowered because the results of earlier nozzle tests indicated that when areas on the top of the duct tended to be wet the bottom of the duct remained dry. Second, a perforated plate was installed at the inlet to the horizontal duct. The perforated plate was investigated to determine whether it would improve the uniformity of gas flow. The velocity distribution immediately downstream of the nozzle lances was not severely skewed, however, and was not improved by insertion of the perforated plate. The perforated plate reduced the maximum flue gas flow rate to below 50,000 acfm and made it impossible to inject dry $Ca(OH)_2$ or slurry upstream of the plate. Therefore, since it gave no offsetting advantage, the perforated plate was removed.

Table 5-5. Velocity and Temperature Measurements made in the Horizontal Duct at the DITF

Flow is as if it is going INTO the paper, all measurements made 5 ft downstream of the nozzle lances. Velocities are in ft/s and temperatures are in °F.

1. 4 Lechler nozzles in a cluster, 20 psig air pressure, no water, insert NOT installed in atomizer port. Kurtz array indicates 50 ft/s average velocity.

Port 1	V	**67.5**	**69.7**	**71.1**	**58.1**	Avg.	V	**66.6**
	T	314	314	312	314		T	314
Port 2	V	**61.8**	**73.7**	**70.0**	**58.1**	Avg.	V	**65.9**
	T	313	306	307	313		T	310
Port 3	V	**61.1**	**48.9**	**49.9**	**54.3**	Avg.	V	**53.5**
	T	313	313	311	312		T	312

2. Same as 1, but nozzles at 80 psig, but insert INSTALLED in the atomizer test port.

Port 1	V	**50.6**	**153.**	**144.6**	**32.6**	Avg.	V	**95.2**
	T	313	298	297	309		T	304
Port 2	V	**41.3**	**151.0**	**154.1**	**36.3**	Avg.	V	**95.7**
	T	313	297	294	310		T	304
Port 3	V	**43.4**	**31.3**	**52.2**	**43.8**	Avg.	V	**42.7**
	T	314	312	310	310		T	312

3. Same as 2, but nozzles at 20 psig.

Port 1	V	**69.2**	**68.6**	**68.7**	**63.4**	Avg.	V	**67.5**
	T	314	314	310	314		T	313
Port 2	V	**67.6**	**67.0**	**66.9**	**62.6**	Avg.	V	**66.0**
	T	307	307	304	312		T	308
Port 3	V	**65.7**	**49.3**	**58.7**	**56.9**	Avg.	V	**57.7**
	T	314	313	310	312		T	312

As described earlier, thermocouples attached to the inside walls of the horizontal duct were used to detect wall wetting. Previously, a duct wall temperature of 134°F was presumed to be close enough to the adiabatic saturation temperature (approximately 126-128°F) to justify the belief that at or below 134°F the duct wall was indeed wet. However, at a nozzle review meeting at PETC in May, various investigators indicated that a more likely temperature for wall wetting was about 130°F rather than 134°F. Therefore, in the analysis that follows, only duct wall temperatures of 130°F or less were presumed to indicate wall wetting. In Tables 5-6 through 5-9 which record the results of these tests, temperatures at or below 130°F are printed in bold face type and are enclosed in a box. Temperatures from 131°F to 134°F are printed in boldface type, to signify sufficient proximity to the adiabatic saturation temperature to cause concern.

Two other comments need to be made about the data presented in Tables 5-6 - 5-9. First, it was determined that water flow to the nozzles was not being measured properly because air entrained in the water line would migrate to the pressure transducer and produce false readings. This problem was corrected only after these tests were completed. Thus, for these tests, the water flow rate was estimated by calculating the amount of water necessary to lower the temperature of the incoming flue gas to the temperature measured at the inlet of the ESP. In Tables 5-6 - 5-9, this value is listed as "CALCULATED Humidification Water Flow." Second, the approach to saturation was estimated in two ways. In Tables 5-6 - 5-9, the "Estimated Approach to Saturation" was determined by subtracting a presumed adiabatic saturation temperature of 128°F from the temperature at the ESP inlet. The approach to saturation was also determined by subtracting a calculated adiabatic saturation temperature from the temperature at the ESP inlet and a presumed 7% (volume) water content in the flue gas. The adiabatic saturation temperature was calculated from the following relation:

$$T_s = 83.03 + 0.08505T_g + 240.0X_w$$

where T_s is the adiabatic saturation temperature in degrees Fahrenheit, T_g is the temperature of the flue gas at the system inlet in degrees Fahrenheit (before humidification), and X_w is the volume fraction of water content in the flue gas. This relationship was determined by making a curve fit to a rigorous calculation of T_s as the simultaneous solution of the equation that expresses the adjusted temperature of the flue gas due to the evaporation of water and another equation that expresses the maximum vapor concentration of water vapor as a function of temperature. T_s is not actually a linear function of either T_g or X_w, although linearity of both is assumed in the above equation. However, in the range of $0.05 < X_w < 0.09$, the equation provides a close estimate of T_s. At values of X_w between 0.07 and 0.08, the curve fit was configured to give almost exact agreement. In generating this relationship, a value of 7.492 cal/(mole-°C) was used for the heat capacity of the flue gas.

Nozzle configurations. Two basic nozzle configurations were tested with both Lechler and Parker-Hannifin nozzles. The first configuration was a six-nozzle cluster with three nozzles per lance, with nozzles located at positions 2, 3, and 4, as illustrated in Figure 5-2, except that the outer nozzles were canted inward by 5°. The second configuration was a four-nozzle cluster, with two nozzles per lance. In this configuration, the nozzles were located 16 in. from the vertical duct walls and were canted inward by 5°. The horizontal location of the upper and lower lances was not changed from that used when three nozzles were attached to each lance. For each of the two basic configurations for each type of nozzle (six nozzles and four nozzles), tests were conducted with the lances set so that the nozzles were either horizontal or arranged with the upper lance depressed by 2.5° and the lower lance elevated by 2.5°.

Table 5-6. Results of Lechler Nozzle Tests, Part 1 (June)

Test Numbers	49	49A	58	58A	59	61	60	50	52	51
Date	6/12/90	6/12/90	6/18/90	6/18/90	6/18/90	6/18/90	6/18/90	6/12/90	6/12/90	6/12/90
Time	1158	1334	1423	1543	1520	1744	1648	1408	1559	1443
Nozzle Type	Lechler	Lechler	Lechler	Lechler	Lechler	Lechler	Lechler	Lechler	Lechler	Lechler
No. of Lances	2	2	2	2	2	2	2	2	2	2
Upper Lance Position (° Down)	0	0	2.5	2.5	2.5	0	0	0	0	0
Lower Lance Position (° Up)	0	0	2.5	2.5	2.5	0	0	0	0	0
No. of Nozzles per Lance (Top/Bottom)	3	3	3	3	3	3	3	3	3	3
Upper Lance, Outside Nozzle Position (° In)	5	5	5	5	5	5	5	5	5	5
Lower Lance, Outside Nozzle Position (° In)	5	5	5	5	5	5	5	5	5	5
INDICATED Humidification Water Flow (gpm)	10.0	9.9	10.6	11.0	11.2	12.3	12.3	11.0	9.9	10.1
CALCULATED Humidification Water Flow (gpm)	8.8	9.2	10.2	9.9	10.1	10.1	10.3	11.0	11.3	11.7
Nozzle Atomizing Air Flow (acfm)	1310.2	1072.4	1111.3	1074.5	828.4	812.2	1060.4	1075.5	1312.2	1085.2
Nozzle Atomizing Air Supply Press. (psig)	92.0	99.9	80.5	79.8	60.2	59.9	79.5	100.3	99.9	80.1
Air to Water Ratio	0.610	0.713	0.613	0.587	0.359	0.350	0.577	0.716	0.872	0.596
Flue Gas Flow (acfm)	47310	47593	46225	46626	45728	46129	46386	47213	46848	46645
Flue Gas Flow (scfm)	35584	35797	36164	35281	35467	35364	35834	36832	37052	36656
Temperatures (°F)										
Test Section Inlet Temp.	322	321	335	334	333	330	331	319	319	319
Station # 2 Outlet Temp., Array 2, Mid-Duct	124	121	114	112	113	111	111	119	117	119
Mid-Duct, 1 sec. Downstream	185	177	152	128	116	113	145	156	150	131
ESP Inlet Temp.	167	162	170	170	169	168	167	162	159	151
Estimated Approach to Saturation (Ts=128°F)	59	54	42	42	41	40	39	34	31	23
Calculated Approach to Saturation (7% Water)	61	56	43	43	42	42	40	37	34	26
Array 1: Top, (Wall T/C #10)	199	207	163	179	155	138	150	206	205	206
Right, (Wall T/C # 1)	305	306	318	319	320	314	313	304	303	303
Bottom, (Wall T/C # 2)	305	306	307	314	313	311	312	305	304	304
Left, (Wall T/C # 3)	174	171	158	160	161	156	154	167	168	205
Array 2, Right, (Wall T/C # 5)	266	262	126	137	137	136	142	254	251	262
Bottom, (Wall T/C # 6)	176	172	259	273	253	230	256	154	146	126
Left, (Wall T/C # 7)	241	234	152	158	148	158	157	222	219	242
Array 3: Top, (Wall T/C # 8,)	167	155	198	194	191	180	167	127	127	123
Right, (Wall T/C # 9)	200	194	203	211	208	208	208	164	153	131
Left, (Wall T/C # 11)	182	167	124	128	124	136	134	131	130	127
Array 4: Top, (Wall T/C # 12)	150	144	156	140	142	152	153	123	122	121
Right, (Wall T/C # 4)	184	174	292	292	248	246	277	137	134	125
Left, (Wall T/C # 15)	172	156	124	130	124	132	138	127	128	125
Array 5: Top, (Wall T/C # 16)	179	170	121	134	123	133	134	134	133	127
Right, (Wall T/C # 17)	181	166	153	140	143	150	144	136	137	125
Bottom, (Wall T/C # 18)	167	152	121	125	127	125	124	125	128	123
Left, (Wall T/C # 19)	176	162	152	134	141	150	139	128	130	125
Array 6: Top, (Wall T/C # 20)	183	172	122	136	124	135	145	138	133	123
Right, (Wall T/C # 21)	185	175	154	141	144	155	150	141	145	124
Bottom, (Wall T/C # 22)	182	167	152	132	142	133	131	134	136	123
Left, (Wall T/C # 23)	190	181	138	131	132	138	137	151	146	137
Array 7: Top, (Wall T/C # 24)	188	179	134	144	133	140	154	148	146	128
Right, (Wall T/C # 25)	188	180	148	142	140	147	148	149	147	128
Bottom, (Wall T/C # 26)	186	175	125	117	119	120	118	140	142	127
Left, (Wall T/C # 27)	188	180	154	152	152	154	150	151	147	134
Array 8: Right, (Wall T/C # 29)	188	180	145	149	140	140	149	153	148	129
Bottom, (Wall T/C # 30)	188	178	148	152	150	158	161	147	151	129
Left, (Wall T/C # 31)	186	178	155	158	151	154	159	152	147	129

Table 5-7. Results of Lechler Nozzle Tests, Part 2 (June)

Test Numbers	63A	63	62A	62
Date	6/19/90	6/19/90	6/19/90	6/19/90
Time	1436	1359	1231	1132
Nozzle Type	Lechler	Lechler	Lechler	Lechler
No. of Lances	2	2	2	2
Upper Lance Position (° Down)	2.5	2.5	0	0
Lower Lance Position (° Up)	2.5	2.5	0	0
No. of Nozzles per Lance (Top/Bottom)	2	2	2	2
Upper Lance, Outside Nozzle Position (° in)	5	5	5	5
Lower Lance, Outside Nozzle Position (° in)	5	5	5	5
INDICATED Humidification Water Flow (gpm)	10.7	10.7	10.9	11.5
CALCULATED Humidification Water Flow (gpm)	9.9	9.8	10.2	10.2
Nozzle Atomizing Air Flow (acfm)	722.4	546.8	782.1	553.4
Nozzle Atomizing Air Supply Press. (psig)	79.8	59.8	80.2	60.0
Air to Water Ratio	0.395	0.236	0.429	0.239
Flue Gas Flow (acfm)	45824	46064	45602	45455
Flue Gas Flow (scfm)	35244	34527	35726	35409
Temperatures (°F)				
Test Section Inlet Temp.	327	328	327	328
Station # 2 Outlet Temp., Array 2, Mid-Duct	123	124	125	125
Mid-Duct, 1 sec. Downstream	137	127	147	128
ESP Inlet Temp.	170	169	169	167
Estimated Approach to Saturation (Ts=128°F)	42	41	41	39
Calculated Approach to Saturation (7% Water)	44	43	42	40
Array 1: Top, (Wall T/C #10)	196	211	190	216
Right, (Wall T/C # 1)	318	318	317	316
Bottom, (Wall T/C # 2)	311	307	310	310
Left, (Wall T/C # 3)	310	306	308	302
Array 2, Right, (Wall T/C # 5)	165	165	140	119
Bottom, (Wall T/C # 6)	285	288	274	277
Left, (Wall T/C # 7)	136	144	129	132
Array 3: Top, (Wall T/C # 8,)	234	233	229	235
Right, (Wall T/C # 9)	195	194	194	190
Left, (Wall T/C # 11)	125	126	126	126
Array 4: Top, (Wall T/C # 12)	184	212	186	187
Right, (Wall T/C # 4)	302	296	295	298
Left, (Wall T/C # 15)	148	166	151	163
Array 5: Top, (Wall T/C # 16)	126	127	128	127
Right, (Wall T/C # 17)	171	191	170	173
Bottom, (Wall T/C # 18)	129	130	116	102
Left, (Wall T/C # 19)	157	176	157	158
Array 6: Top, (Wall T/C # 20)	127	135	131	130
Right, (Wall T/C # 21)	172	191	170	173
Bottom, (Wall T/C # 22)	151	158	142	135
Left, (Wall T/C # 23)	135	150	132	134
Array 7: Top, (Wall T/C # 24)	135	136	134	132
Right, (Wall T/C # 25)	161	173	160	160
Bottom, (Wall T/C # 26)	125	128	117	113
Left, (Wall T/C # 27)	159	173	154	157
Array 8: Right, (Wall T/C # 29)	168	176	169	168
Bottom, (Wall T/C # 30)	163	172	148	141
Left, (Wall T/C # 31)		180	165	167

Table 5-8. Results of Parker-Hannifin Nozzle Tests, Part 1 (June)

Test Number	57	56	54A	55	54-110	54-100	54-115	53
Date	6/14/90	6/14/90	6/14/90	6/14/90	6/12/90	6/12/90	6/12/90	6/12/90
Time	1827	1752	2115	2203	2211	2153	2222	2103
Nozzle Type	P-H	P-H	P-H	P-H	P-H	P-H	P-H	P-H
No. of Lances	2	2	2	2	2	2	2	2
Upper Lance Position (° Down)	2.5	2.5	0	0	0	0	0	0
Lower Lance Position (° Up)	2.5	2.5	0	0	0	0	0	0
No. of Nozzles per Lance (Top/Bottom)	3	3	3	3	3	3	3	3
Upper Lance, Outside Nozzle Position (° In)	5	5	5	5	5	5	5	5
Lower Lance, Outside Nozzle Position (° In)	5	5	5	5	5	5	5	5
INDICATED Humidification Water Flow (gpm)	10.8	10.7	10.0	10.0	9.4	9.4	9.5	10.0
CALCULATED Humidification Water Flow (gpm)	9.7	9.9	9.8	10.0	11.0	10.9	11.2	12.0
Nozzle Atomizing Air Flow (acfm)	788.5	958.1	965.8	773.5	1019.8	937.6	1062.5	942.5
Nozzle Atomizing Air Supply Press. (psig)	79.8	100.1	100.1	80.3	109.7	100.1	115.1	100.0
Air to Water Ratio	0.431	0.637	0.643	0.426	0.736	0.624	0.801	0.627
Flue Gas Flow (scfm)	45373	45527	46222	45930	45952	46364	45966	45072
Flue Gas Flow (acfm)	35084	35550	35510	35452	36493	35586	36770	36149
Temperatures (°F)								
Test Section Inlet Temp.	333	332	329	327	320	317	320	311
Station # 2 Outlet Temp., Array 2, Mid-Duct	111	113	115	116	121	121	122	119
Mid-Duct, 1 sec. Downstream	144	147	140	134	155	149	153	125
ESP Inlet Temp.	172	172	172	170	160	156	158	145
Estimated Approach to Saturation (Te=128°F)	44	44	44	42	32	30	30	17
Calculated Approach to Saturation (7% Water)	46	45	46	44	35	33	33	20
Array 1: Top, (Wall T/C #10)	213	215	210	208	208	203	208	187
Right, (Wall T/C # 1)	281	282	302	292	295	293	293	282
Bottom, (Wall T/C # 2)	295	300	299	289	298	292	298	272
Left, (Wall T/C # 9)	231	298	145	142	137	136	136	131
Array 2, Right, (Wall T/C # 5)	174	197	201	187	205	189	203	176
Bottom, (Wall T/C # 6)	118	118	128	124	134	145	132	134
Left, (Wall T/C # 7)	128	128	136	151	140	142	139	133
Array 3: Top, (Wall T/C # 8,)	185	186	140	143	139	152	137	144
Right, (Wall T/C # 9)	181	182	150	153	156	153	156	130
Left, (Wall T/C # 11)	118	118	129	127	128	125	126	123
Array 4: Top, (Wall T/C # 12)	141	141	127	131	133	136	133	129
Right, (Wall T/C # 4)	165	152	131	135	151	170	147	145
Left, (Wall T/C # 15)	127	127	127	134	133	140	132	133
Array 5: Top, (Wall T/C # 16)	154	154	150	145	146	159	144	141
Right, (Wall T/C # 17)	163	156	144	151	153	163	150	143
Bottom, (Wall T/C # 18)	134	141	131	130	133	146	130	135
Left, (Wall T/C # 19)	124	124	124	128	134	147	133	133
Array 6: Top, (Wall T/C # 20)	139	136	134	131	130	131	130	125
Right, (Wall T/C # 21)	162	157	152	158	155	160	153	136
Bottom, (Wall T/C # 22)	128	130	128	131	135	148	133	132
Left, (Wall T/C # 23)	127	127	146	146	148	164	143	147
Array 7: Top, (Wall T/C # 24)	157	161	162	162	150	158	148	134
Right, (Wall T/C # 25)	155	152	154	154	153	157	151	133
Bottom, (Wall T/C # 26)	120	123	124	128	135	145	134	131
Left, (Wall T/C # 27)	141	140	138	146	142	156	139	139
Array 8: Right, (Wall T/C # 29)	153	153	143	143	155	153	152	132
Bottom, (Wall T/C # 30)	146	146	129	135	138	152	136	132
Left, (Wall T/C # 31)	148	145	149	150	148	149	147	126

Table 5-9. Results of Parker-Hannifin Nozzle Tests, Part 2 (June)

Test Numbers	64	64A	65	65B
Date	6/19/90	6/19/90	6/19/90	6/19/90
Time	1829	1930	2012	2146
Nozzle Type	P-H	P-H	P-H	P-H
No. of Lances	2	2	2	2
Upper Lance Position (° Down)	2.5	2.5	0	0
Lower Lance Position (° Up)	2.5	2.5	0	0
No. of Nozzles per Lance (Top/Bottom)	2	2	2	2
Upper Lance, Outside Nozzle Position (" In)	5	5	5	5
Lower Lance, Outside Nozzle Position (" In)	5	5	5	5
INDICATED Humidification Water Flow (gpm)	9.5	9.9	9.5	9.6
CALCULATED Humidification Water Flow (gpm)	9.9	9.9	9.9	10.0
Nozzle Atomizing Air Flow (acfm)	642.0	541.0	657.3	552.5
Nozzle Atomizing Air Supply Press. (psig)	100.0	79.7	99.9	80.6
Air to Water Ratio	0.427	0.296	0.437	0.305
Flue Gas Flow (acfm)	46103	45880	45845	45568
Flue Gas Flow (scfm)	34922	34504	34594	34609
Temperatures (°F)				
Test Section Inlet Temp.	325	326	325	327
Station # 2 Outlet Temp., Array 2, Mid-Duct	121	121	121	122
Mid-Duct, 1 sec. Downstream	127	124	125	124
ESP Inlet Temp.	169	168	168	167
Estimated Approach to Saturation (Ts=128°F)	41	40	40	39
Calculated Approach to Saturation (7% Water)	43	42	42	41
Array 1: Top, (Wall T/C #10)	176	176	203	205
Right, (Wall T/C # 1)	314	312	314	314
Bottom, (Wall T/C # 2)	305	304	303	278
Left, (Wall T/C # 3)	172	165	166	168
Array 2, Right, (Wall T/C # 5)	169	183	183	173
Bottom, (Wall T/C # 6)	265	251	274	255
Left, (Wall T/C # 7)	147	139	132	124
Array 3: Top, (Wall T/C # 8,)	193	169	188	179
Right, (Wall T/C # 9)	181	169	179	169
Left, (Wall T/C # 11)	123	123	123	123
Array 4: Top, (Wall T/C # 12)	198	184	183	182
Right, (Wall T/C # 4)	267	230	269	242
Left, (Wall T/C # 15)	176	166	158	160
Array 5: Top, (Wall T/C # 16)	126	127	128	125
Right, (Wall T/C # 17)	182	152	171	168
Bottom, (Wall T/C # 18)	123	127	129	130
Left, (Wall T/C # 19)	162	169	166	163
Array 6: Top, (Wall T/C # 20)	129	131	134	132
Right, (Wall T/C # 21)	184	187	179	175
Bottom, (Wall T/C # 22)	151	157	155	152
Left, (Wall T/C # 23)	141	143	141	139
Array 7: Top, (Wall T/C # 24)	145	129	135	133
Right, (Wall T/C # 25)	170	172	167	162
Bottom, (Wall T/C # 26)	118	122	123	124
Left, (Wall T/C # 27)	168	170	167	163
Array 8: Right, (Wall T/C # 29)	173	177	172	174
Bottom, (Wall T/C # 30)	165	171	168	163
Left, (Wall T/C # 31)	178	183	179	180

Tables 5-6 and 5-8 give results for nozzle tests conducted with three Lechler nozzles per lance and three Parker-Hannifin nozzles per lance, respectively. Tables 5-7 and 5-9 give results for nozzle tests conducted with two Lechler nozzles per lance and two Parker-Hannifin nozzles per lance, respectively.

Results for Lechler nozzles. Although the intent was to operate at humidification water flow rates from 10 to 12 gal/min, the actual water flow rates ranged from 8.8 to 11.7 gal/min, corresponding to calculated approach temperatures at the ESP inlet from 61 to 26°F. The atomizing air pressure was also varied for these tests, and values from 60 to 100 psig were used. The purpose of investigating the effect of changing the atomizing air pressure was that the Lechler nozzles should reach choked (sonic) flow at 60 psig of air pressure. Thus, operation at higher air pressures should be unnecessary if choked flow occurs at an air pressure of 60 psig.

Depressing the nozzles in the upper lance and elevating the nozzles in the lower lance did not appear to reduce wall wetting for three nozzles per lance (compare Tests 59 and 61 or Tests 58 and 60), but may help with two nozzles per lance (compare Tests 63 and 63A with Tests 62 and 62A). However, less wall wetting was observed with three nozzles per lance than with two nozzles per lance regardless of how the lances were set. With respect to air pressure, it appears that higher air pressures may help with high water flow rates (compare Tests 51 and 52).

Lowering the upper lance by 6.5 in. to a distance of 15 in. from the top of the duct does not appear to reduce wall wetting in the third, fourth, or fifth thermocouple array (see Figure 5-1) as compared to earlier data from the tests during May (Test 52 compared to Test 28). However, in Test 28, wall wetting was observed past the sixth array. Overall, for the Lechler nozzles, a slight improvement in nozzle performance was realized by lowering the upper lance. The four-nozzle cluster did not perform well (compare Tests 62 with Test 61).

Results for Parker-Hannifin nozzles. Results appear to be less clear-cut for these nozzles than for the Lechler nozzles. What can be said is that at lower approach temperatures, three nozzles per lance appear to wet the duct walls less than two nozzles per lance. Tests 54-100, 54-110, and 54-115 were consecutive tests run with increasing air pressure to determine if air pressures above 100 psig reduced wall wetting. While the results recorded for Test 54-115 appear to suggest that operation at 115 psig leads to wall wetting, compared to operation at 100 psig, the difference is only that of time. Data for the test at 115 psig were taken approximately one-half hour after that for Test 54-100. It is unclear from these data that air pressures above 80 psig reduce wall wetting.

It is not clear that lowering the upper lance reduces wall wetting because earlier tests with the Parker-Hannifin nozzles were conducted with the outer nozzles pointing straight ahead and these tests were conducted with the outer nozzles pointed inward by 5°.

5.2 Droplet Size Measurements

5.2.1 Description of Measurement Methodology

In-situ measurements of droplet size distributions of water sprays (no slurries) were made at the DOE Beverly, Ohio, Duct Injection Test Facility (DITF) during May and July 1990. All measurements were made in the horizontal duct downstream of Station 2. Measurements were made of sprays produced by both Parker-Hannifin and Lechler nozzles. Tests were performed with each nozzle type

operating over a range of air pressures and water flow rates. The tests were all made with normal flue gas flows in the duct. Two measurement devices were used in taking the data: the SRI Video Droplet Analyzer (VDA) and an Insitec in-situ optical particle sizing device, described by Insitec as a Particle Concentration Size and Velocity Probe (PCSV-P or PCSV). Appendix A contains tables that provide a summary of each nozzle test as well as graphs that show the cumulative mass and differential mass size distribution determined from each test. A total of twenty-five tests were run.

SRI VDA. The SRI VDA is an imaging system that provides on-line droplet diameter measurement based on real-time measurement of the height (diameter) of droplet images obtained by a synchronized high speed strobe illuminator/video camera combination. The camera and illuminator are mounted in a probe which can be inserted through a 4-inch or larger diameter port, making it possible to make in-situ measurements in a flowing gas stream. A combination of shrouds and purge air are used to keep the optical windows clean and dry. The purge air also provides limited cooling of the camera, lenses, and illuminator electronics but the system is not capable of prolonged operation in hot gas streams. However, at the DITF, the sprays being measured provided sufficient external cooling of the probe that continuous operation was possible.

The VDA was configured to provide data over the size range of 3 to 450 μm for the DITF nozzle tests. However, because of the high gas velocities in the duct, blur from particle motion was about 10 μm which resulted in a loss of data at the small end of the VDA's nominal sizing range. Consequently reliable data were obtained with the VDA over the more restricted range of 25 to 450 μm rather than the full range for which it was configured.

PCSV-P. The Insitec PCSV-P is a dual range in-situ optical single particle counting device that provides data on particle sizes, concentration, and velocity in either or each of its two ranges. The small particle configuration is set up to provide data over a nominal size span of 0.5 to 2.5 μm while the large particle configuration is setup to provide data over a nominal range of 3 to 40 μm. Data can be taken in only one of the two modes at any one time, but mode switching is automated and fast so data can be taken sequentially in the two modes in a fairly short period of time. As with the VDA, a combination of purge air and shrouds is used to keep the optical windows clean and dry. Cooling provided by an external water jacketed sheath permits use of the instrument at temperatures far greater than that of normal flue gases. The instrument response is sensitive to the refractive index and shape of the particles being measured; consequently, the indicated sizes can differ somewhat from the true sizes. Provision is made in data analysis to account for the difference between absorbing and transparent particles in instrument response. This takes care of the major effect of refractive index.

In order for the PCSV-P to work properly only one particle can be in the sensing zone at any one time. For most aerosols the number concentrations fall off as size increases. Thus, if the concentrations in a size range are high this requirement can be met only by increasing the lower detection threshold for that range. Thus, data can be taken at high concentrations, but only by restricting the range of measurement, losing the ability to obtain data for the smaller sizes in the design range for the affected configuration. The concentrations produced by the nozzles in these tests were high enough to restrict the range of the large particle mode to about 13 to 40 μm. Insitec's data analysis algorithm uses an interpolation scheme to fill in for missing data between the upper sizing limit of the small particle mode and the lower limit of the large particle mode. The accuracy of the interpolation in matching the true distribution is open to question.

5.2.2 Sampling Strategy and Data Analysis Methods

Two major series of tests were conducted with each of the two types of nozzles. In the first, single point measurements were made at a fixed location downstream of the plane of the nozzles. Sequential data sets were obtained with the VDA and PCSV at each of a number of combinations of operating air pressures and water flow rates for each nozzle type during these tests. Before performing this test series some preliminary traverses were made to provide comparative data from the single point sampling location and that obtained by a full traverse of the duct. The results of these measurements are given in Table 5-10. These comparisons show that the single point data could be expected to be representative in-so-far as droplet size distribution measurement was concerned.

In order to minimize changes in the measured distribution from that actually produced by the nozzles we wished to make the measurements as close to the nozzles as possible. Attempts were made to obtain data at a location about 0.55 m downstream of the plane of the nozzles but the concentrations at that distance were too high for either the VDA or the PCSV systems to cope with. Satisfactory conditions appeared to be found at the next sampling plane downstream of the nozzles (about 1.6 m) and the variable pressure and water flow tests were made at that plane. The sampling point used was horizontally centered at very nearly the height of the nozzle mounted at the center of the upper lance. Data from the PCSV and VDA were combined to construct overall size distributions for each test condition.

The PCSV data were used up to about 23 μm and the VDA data for sizes greater than 23 μm. The results from the two techniques compared quite well in the overlap range from about 20 to 40 μm. Below 20 μm the VDA data tended to be systematically low as compared to the PCSV as would be expected because of the effect of blur from the high particle velocities. The PCSV data analysis algorithms produce values for sizes much greater than 40 μm but any such values are not valid because the instrument sensitivity with respect to size becomes quite limited above about 40 μm.

The second series of tests conducted with each type of nozzle was intended to provide more quantitative data regarding liquid water concentrations versus distance downstream of the plane of the nozzles. For these tests traverses of the duct were made at downstream distances of 1.6, 2.6, and 8 m using only the VDA. Limits to the movement of the PCSV probe were set by the length of the cooling water supply line and the probe umbilical which, coupled with time constraints, made it impractical to perform similar traverses with the PCSV. The size range covered by the VDA appeared to cover the range in which the bulk of the spray was to be found.

All tests were run in a gas stream composed of 100% flue gas. This resulted in a high fly ash background which had the effect of reducing the light transmission for the instruments and contributing a background particulate concentration. The tests were to have been conducted with the dilution air burner in operation to alleviate this problem but the burner failed just before the start of the measurement period and remained out of service throughout the tests.

The fly ash background was measured with both the PCSV and the VDA, although the VDA data were limited because the probe could not withstand prolonged exposure to high temperatures. The fly ash backgrounds were subtracted from the data as reported here. However, the sprays collect fly ash to some unknown extent; consequently, these data may be somewhat overcorrected. In a few

Table 5-10. Results of Single Point and Traverse Measurements. Parker-Hannifin Nozzles in Port 2, VDA Only.*

Port #2 Traverse Location	DITF System Flow, acfm	Sauter Mean Diameter, μm	Calculated Water Flow, gpm
Top	42000	36.8	2.9
Middle	42000	35.5	3.3
Bottom	42000	37.5	3.4
Average		36.8	3.2
Top, Center	25000	41.6	7.0
Top, Center	42000	36.0	5.0
Top, Center	56000	34.7	3.9

* All measurements in Port 2, 5 ft downstream of nozzles, 8 gpm water flow, and 80 psig air pressure

instances this was almost certainly the case as the background values were greater than the values measured with the spray on. This resulted in negative values in the corrected results.

5.2.3 Test Results

5.2.3.1 Droplet Size Distributions

Parker-Hannifin Nozzles. Results of the combined size distribution measurements for the Parker-Hannifin nozzles are given in Table 5-11. Results from the VDA measurements only are given in Table 5-12. The test matrix included measurements at water flow rates of 6, 8, 10, and 11 gpm and air pressures of 80, 100, and 110 psig. Measured Sauter Mean Diameters (SMD) based on the combined VDA and PCSV data ranged from about 20 μm when the nozzles were operated at high (110 psig) air pressure and low (6 gpm) water flow to about 45 μm at low (80 psig) air pressure and high (11 gpm) water flow.

Non-uniform duct coverage was indicated by transport rates that, if projected from the single point measurements to the whole duct, were often greater than the actual water flow rate. The estimated transport rates decreased with increasing air pressure at any given water flow. This might reflect higher evaporation rates because of smaller droplet sizes and/or an increase in spray cone angle. In general, SMD increased with increasing water flow and decreased with increasing air pressure as would be expected. Log-normal fits to the mass size distributions showed Mass Median Diameters (MMD's) ranging from about 25 to 50 μm with geometric standard deviations of about 1.7 to 2.0.

Lechler Nozzles. Results of the combined size distribution measurements for the Lechler nozzles are given in Table 5-13. Results from the VDA data only are given in Table 5-14. The test matrix included measurements at water flow rates of 6, 8, 10, and 11 gpm and air pressures of 60 and 80 psig. Measured SMD, based on the combined VDA and PCSV data, ranged from about 25 μm when the nozzles were operated at high (80 psig) air pressure and low (6 gpm) water flow to about 40 μm at low (60 psig) air pressure and high (11 gpm) water flow.

As was the case with the Parker-Hannifin nozzles, non-uniform duct coverage was indicated by transport rates that, if projected from the single point measurements to the whole duct, were generally greater than the actual feed rate. The discrepancies were greater with the Lechler nozzles than with the Parker-Hannifin nozzles, probably because of the narrower cone angles produced by the Lechler nozzles. The estimated transport rates decreased markedly with increasing air pressure at any given water flow. This might reflect higher evaporation rates because of smaller droplet sizes and/or an increase in spray cone angle with the latter probably being the more important. In general, SMD increased with increasing water flow and decreased with increasing air pressure as would be expected. In two cases no useful data were obtained from the PCSV, once because of negative values after background correction and the second because of fouling of the optical window of the probe. Log-normal fits to the mass size distributions showed MMD's ranging from about 30 to 50 μm with geometric standard deviations of about 1.8 to 2.0.

5.2.3.2 Concentration versus Downstream Distance

Parker-Hannifin Nozzles. The results of the (VDA only) traverse measurements for tests conducted with Parker-Hannifin nozzles are shown in Table 5-15. Tests were conducted at two water flow rates (6 and 10 gpm) and a single air pressure (100 psig). The data indicate that the SMD tended to

Table 5-11. Results of Size Distribution Measurements for Parker-Hannifin Nozzles, Combined VDA and PCSV Data Taken at the Center of the Top Port, 5 ft downstream.

Water Flow, gpm	6	8	10	11
Air Pressure, psig		Sauter Mean Diameter, μm		
80	31.1	38.8	40.8	44.5
100	23.5	28.9	33.4	38.1
110	19.1	27.0	28.1	28.1
		Calculated Water Flow*, gpm		
80	6.0	7.9	11.0	13.8
100	4.7	6.9	9.4	10.1
110	4.1	5.7	5.7	7.2

* From single point size distribution and velocity measurements.

Table 5-12. Results of Size Distribution Measurements for Parker-Hannifin Nozzles, VDA Only Data Taken at the Center of the Top Port, 5 ft Downsteam.

Water Flow, gpm	6	8	10	11
Air Pressure, psig		Sauter Mean Diameter, μm		
80	36.9	39.9	43.9	47.5
100	32.9	35.7	39.2	40.5
110	31.5	32.0	32.9	35.2
		Calculated Water Flow*, gpm		
80	5.5	8.0	10.8	13.5
100	3.4	5.8	8.4	9.6
110	2.5	3.8	4.1	5.0

* From single point size distribution and velocity measurements.

Table 5-13. Results of Size Distribution Measurements for Lechler Nozzles, Combined VDA and PCSV Data Taken at the Center of the Top Port, 5 ft Downstream.

Water Flow, gpm	6	8	10	11
Air Pressure, psig		Sauter Mean Diameter, μm		
60	---	37.5	35.0	---
80	26.3	28.1	27.2	29.2
		Calculated Water Flow*, gpm		
60	---	13.2	15.7	---
80	6.9	8.2	9.1	9.1

* From single point size distribution and velocity measurements.

Table 5-14. Results of Size Distribution Measurements for Lechler Nozzles, VDA Only Data Taken at the Center of the Top Port, 5 ft Downstream.

Water Flow, gpm	6	8	10	11
Air Pressure, psig		Sauter Mean Diameter, μm		
60	39.2	40.5	42.4	43.3
80	34.8	34.7	36.4	35.8
		Calculated Water Flow*, gpm		
60	9.1	11.7	14.4	15.0
80	5.6	6.8	8.3	8.1

* From single point size distribution and velocity measurements.

Table 5-15. Results of Size Distribution Measurements for Parker-Hannifin Nozzles, VDA Traverse Data Taken at Port Sets 2, 3, and 4.*

Water Flow, gpm			6	10
----------Downstream ----------				
Port Set #	Distance (ft)	Time of Flight (sec)	Sauter Mean Diameter, μm (Air Pressure = 100 psig)	
2	5	0.11	35.2	39.2
3	8	0.17	34.6	40.3
4	24	0.54	38.5	46.7
			Calculated Water Flow*, gpm	
2	5	0.11	3.8	6.2
3	8	0.17	3.0	4.8
4	24	0.54	2.0	3.5

* Data taken in top and bottom ports, 2 points per port.

Table 5-16. Results of Size Distribution Measurements for Lechler Nozzles, VDA Traverse Data Taken at Port Sets 2, 3, and 4.*

Water Flow, gpm		6			10		
------- Downstream -------		Sauter Mean Diameter, μm (Air Pressure = 80 psig)					
Port Set, #	Distance, ft	---- Background Correction** ---			---- Background Correction** ---		
		None	Average	Highest	None	Average	Highest
2	5	31	32	34	36	37	38
3	8	37	40	44	35	38	41
4	24	33	36	42	44	48	56
		Calculated Water Flow*, gpm					
2	5	2.6	2.4	1.9	4.7	4.7	4.0
3	8	2.9	3.2	2.6	3.4	3.9	3.3
4	24	2.1	2.1	1.5	3.2	3.6	3.0

* Data taken in top and bottom ports, 2 points per port.
** See text for explanation of background correction procedure.

increase with downstream distance while the liquid water concentration decreased. This behavior is consistent with evaporative losses which would be more rapid for small droplets than for larger droplets, resulting in a shift toward larger mean droplet sizes--at least in the initial phases of the evaporative process.

Under the conditions of the tests the sampling planes represented evaporation times of 0.10, 0.17, and 0.54 s. These results indicate that about one-third of the water sprayed was still liquid after about 0.5 s of evaporation time. The indicated mean diameters at the planes closest to the nozzles may be too large and the water transport rates too low because of the lack of data for small droplet sizes. This lack of data for small sizes should not be as serious at the farthest sampling plane since, in any case, the smaller size droplets must have been highly depleted at that location.

Lechler Nozzles. The results of the (VDA only) traverse measurements for the Lechler nozzles are given in Table 5-16. Tests were conducted at two water spray rates (6 and 10 gpm) and a single air pressure (80 psig). These data indicate that the SMD tended to increase with downstream distance at the higher water flow rate but first increased and then fell at the lower flow rate. Regardless of water flow rate, the concentration of liquid water was observed to decrease with distance. This behavior is consistent with evaporative losses which would be more rapid for small droplets than for larger droplets, resulting in a shift toward larger mean droplet sizes--at least in the initial phases of the evaporative process. The final indication of a decreasing mean size at large downstream distances at the lower spray test condition might be the result of the inevitable droplet shrinkage that must take place in warm flue gas.

Under the conditions of these tests the sampling planes represented evaporation times of 0.1, 0.17, and 0.54 s. The background particle size distribution data were not altogether consistent for this test so the results were reported in three ways: first in raw (uncorrected) form, second using a mean value from all background measurements, and third using the set which showed the highest background concentrations. Similar trends were found in all three treatments but the details changed somewhat.

These data indicate that about one-fourth to one-third of the water sprayed was still liquid after about 0.5 s of evaporation time. Indicated SMD at the planes closest to the nozzles may be too large and the water transport rates may be too low because of the lack of data for small droplet sizes. As in the case of the Parker-Hannifin results, this lack of data for small SMD should not be regarded as a serious loss at the farthest sampling plane because these data indicate that the smaller size droplets must have been highly depleted at that location.

The results presented in the preceding paragraphs are useful for relative nozzle performance evaluations. However, no information is presently available concerning the performance of the nozzles with slurries of varying concentration and composition. If time and budget constraints permit, the VDA and Insitec instruments will be used to measure slurry droplet size distributions at a later point in the program.

The performance of the nozzles was generally within the specifications of 30 SMD, but it should be noted that the manufacturers and B&W use a Malvern system to measure droplet size distributions. Significant difference in results due to differences in measurement techniques may occur with respect to the Insitec/VDA data vs the Malvern. Comparisons between these methods are planned later in

the project. The principal utility of these in situ measurements, however, is to assist in the development of process models.

6.0 SULFUR DIOXIDE REMOVAL EXPERIMENTS

6.1 Introduction

Pilot plant experimental studies of SO_2 removal with sorbent injection were conducted in three segments during the time period covered by this report (see the test plan schedule given in Appendix B):

1. Injection of dry hydrated lime during Test Weeks 9 through 16.
2. Slurry injection during the two-week period immediately preceding a scheduled three-month outage of Unit 5 (Test Weeks 16 & 17).
3. Slurry injection during Test Weeks 18 through 28 (Nov. 19, 1990 through Feb. 4, 1991).

The period available prior to the Unit 5 outage for tests to determine the effectiveness of sorbent injection for removing SO_2 from the flue gas was approximately from July 1 to August 22. Testing was resumed on November 19 when the unit was brought back into service after the outage.

6.2 Dry Sorbent Injection

Dry sorbent refers to the powdered hydrate of lime--that is, calcium hydroxide, $Ca(OH)_2$. This material was injected in three types of tests, as summarized in the following paragraphs. Key properties of the hydrated lime used during this test period are summarized in Table 6-1.

In one type of test, dry hydrate was injected without any simultaneous attempt to humidify the flue gas. The purpose was to determine the degree of SO_2 removal that was possible in the absence of humidification. The powder was injected pneumatically into the horizontal duct with a background water vapor concentration of 5.6% by volume and an SO_2 concentration in the range 1300-1400 ppm by volume. The rate of sorbent injection achieved a Ca/S mole ratio of approximately 2.3. In this initial test of this type, the degrees of removal of SO_2 at various locations downstream from the point of sorbent injection were determined from photometric determinations of the SO_2 concentration, with correction for changes due to inleakage of air. The total removal of SO_2, based on system inlet and ESP outlet SO_2 concentrations, was 17.8%; of this amount, the removal in the ESP alone was 4.9%. In a repetition of the test, the total removal was close to the original value. The removal in the repetition was 17.0%, of which 5.3% occurred in the ESP. The removal up to the ESP inlet, 11.7%, corresponds to a sorbent utilization of 5.1% (% utilization = % SO_2 removal/ [Ca/S]).

To validate the results from the second test described above, samples of entrained solids were removed from the gas stream at the ESP inlet and analyzed in the laboratory. To remove the solids in the same chemical state as that existing in the suspended state, the sample stream was both heated and diluted with air using the previously described quench probe. Thus, the reaction between suspended solids and SO_2 in the gas duct was quenched during the sampling step. The ratio of sulfite to calcium found in the laboratory analyses indicated that the utilization of the sorbent was 5.0% versus the 5.1% indicated by the gas analysis system.

This result is considered to be in excellent agreement with the utilization calculated from the change in SO_2 gas-phase concentration and lends confidence in SO_2 concentration data as a reliable indicator of the degree of SO_2 removal. The dry hydrate test without humidification is considered to be an

Table 6-1. Properties of Hydrated Lime

BET surface area	21.9 - 23.1 m^2/g[1]
Loss on ignition (750°C)	24.5%[2]
Chemical composition[3]	

Oxide	Wt %
Li_2O	<0.01
Na_2O	0.16
K_2O	0.04
MgO	0.75
CaO	95.4
Fe_2O_3	0.14
Al_2O_3	0.43
SiO_2	0.69
TiO_2	<0.1
P_2O_5	0.07
SO_3	<0.1

1. Range for eight samples.
2. Calculated for $Ca(OH)_2$, 23.5%.
3. Determined for ignited residue.

appropriate means of comparing gas analysis systems results with solids analyses because reactive deposits in the duct are not a factor in the comparison.

In the second type of test of dry hydrate injection, the sorbent was injected downstream from the water spray nozzles. This type of process is best referred to as the non-scavenging mode, in distinction from the scavenging mode described below. That is, the water droplets are evaporated before they can reach the location of the dry sorbent injection nozzles and thus no interception of sorbent particles by water droplets can occur. For this type of test, the flue gas was humidified with a water spray at the top of the vertical duct (using four Parker-Hannifin nozzles), and dry hydrate was injected in the horizontal duct. The inlet SO_2 level was maintained at 1900-2000 ppm and the inlet flue gas temperature was maintained at 300°F. Table 6-2 summarizes the results of these tests. Under the most favorable conditions -- a Ca/S ratio of 3.15 and an ESP inlet temperature of 170°F (equivalent to an approach temperature of 40°F) -- the apparent total removal of SO_2, based on measurements of SO_2 at the ESP outlet, was 37%.

In the third type of test, dry hydrate was injected upstream from the water spray nozzles in the horizontal duct (scavenging mode). As the sorbent particles and water droplets moved together down the duct, collisions occurred until ultimately the water was totally evaporated. The scavenging mode was expected to be more efficient for removing SO_2, since the physically wet sorbent particles were expected to react more completely than the dry particles. Table 6-3 summarizes the results of three series of tests of the scavenging mode, which involved both the Parker-Hannifin and Lechler nozzles. The highest SO_2 removal achieved, with an inlet SO_2 concentration of 1900 ppm, was 53% during a 4-hour test with a Ca/S ratio of 2.5, a water rate of 11 gal/min from Lechler nozzles, and approximately a 26°F approach to adiabatic saturation at the ESP inlet.

From the results with the different types of nozzles, it is apparent that, under the same conditions, higher SO_2 removal efficiencies could be achieved with the Parker-Hannifin nozzles than with the Lechler nozzles. Data obtained with the two types of nozzles are shown in Figure 6-1 for two system inlet temperatures, 285°F and 330°F. The approximate approach temperatures for these data sets at the 10 GPM water rate are 30°F for an initial temperature of 285°F and 50°F for an initial temperature of 330°F.

Some cautionary notes are appropriate with regard to the data in Figure 6-1. Quench probe samples are not available for these tests, so the effect of nozzle type on suspended phase solids utilizations is not known. The gas analysis system records the total SO_2 removal, a portion of which may be caused by reactive deposits of moist calcium hydroxide in the duct. The Parker-Hannifin nozzles have a broader spray pattern than the Lechler nozzles, so it is conceivable that the additional SO_2 removal observed with the Parker-Hannifin's may be due to both more sorbent-water interception and more deposit formation. Additional testing is required to resolve this question.

Testing of the scavenging mode was also performed for extended periods on two occasions (that is, for 1 to 2 days, rather than for just a few hours). All tests were conducted with three Lechler nozzles on each of the two lances installed in the horizontal test duct. The upper lance was depressed 1.25° and the lower lance was elevated by 5°. The outer nozzles on each lance were canted inward by 5°F. For these tests, the inlet SO_2 concentration was controlled to 1300 ppm and the Ca/S ratio was intended to be 2.0, with approximately a 40°F approach (ESP inlet temperature of 170°F). The first of these extended tests had to be terminated after 57 hours because a large deposit of ash and sorbent formed on the top of the ductwork above a hopper in the horizontal duct (12 ft downstream

Table 6-2

Non-Scavenging Mode Test Results

Ca/S Ratio	Inlet SO_2, ppm	ESP Inlet Temp. °F[1]	Water Flow (gpm)	Cumulative SO_2 Removal, %[2] A	B	C
1.0	1900	181	8	3	7	14
2.1	1900	176	9	0	5	14
2.6	1900	178	9	4	8	22
3.0	2000	177	9	14	25	36
3.2	1900	170	10	18	27	37

1. The approximate temperature for adiabatic saturation was 125°F. Thus, the approaches to saturation ranged from about 45 to 56°F. (The inlet temperature was typically 300° F.)

2. Locations: A = outlet of horizontal duct.
   B = inlet of ESP
   C = outlet of system

Table 6-3. Scavenging Mode Test Results

Nozzle type[1]	Ca/S ratio	Inlet SO_2, ppm	ESP inlet temp, °F[2]	Water flow, gpm	Cumulative SO_2 removal,%[3] A	B	C
P-H	1.1	3000	190	8	12	14	17
	1.2	2800	170	10	20	21	26
	1.4	3400	195	8	16	19	21
	1.5	3400	167	10	22	28	33
	1.5	3100	156	10	29	35	40
L	1.5	2800	194	6	16	19	23
	1.5	3000	173	8	20	19	22
	1.5	2900	160	10	21	22	25
L	1.0	1900	164	8	12	11	17
	1.0	1900	145	10	22	22	27
	1.0	1900	149	10	21	20	25
	2.0	1900	152	10	27	28	37
	2.5	1900	155	10	31	34	42
	2.5	1900	154	11	41	42	53

1. P-H = Parker-Hannifin; L = Lechler

2. In the first series of tests, the inlet temperature was 320°F and the saturation temperature about 128°F, making the approaches 28 to 67°F. In the latter two series, the inlet temperature was 285°F and the saturation temperature around 124°F, making the approaches 30 to 70°F.

3. Locations: A = outlet of horizontal duct
   B = inlet of ESP
   C = outlet of system

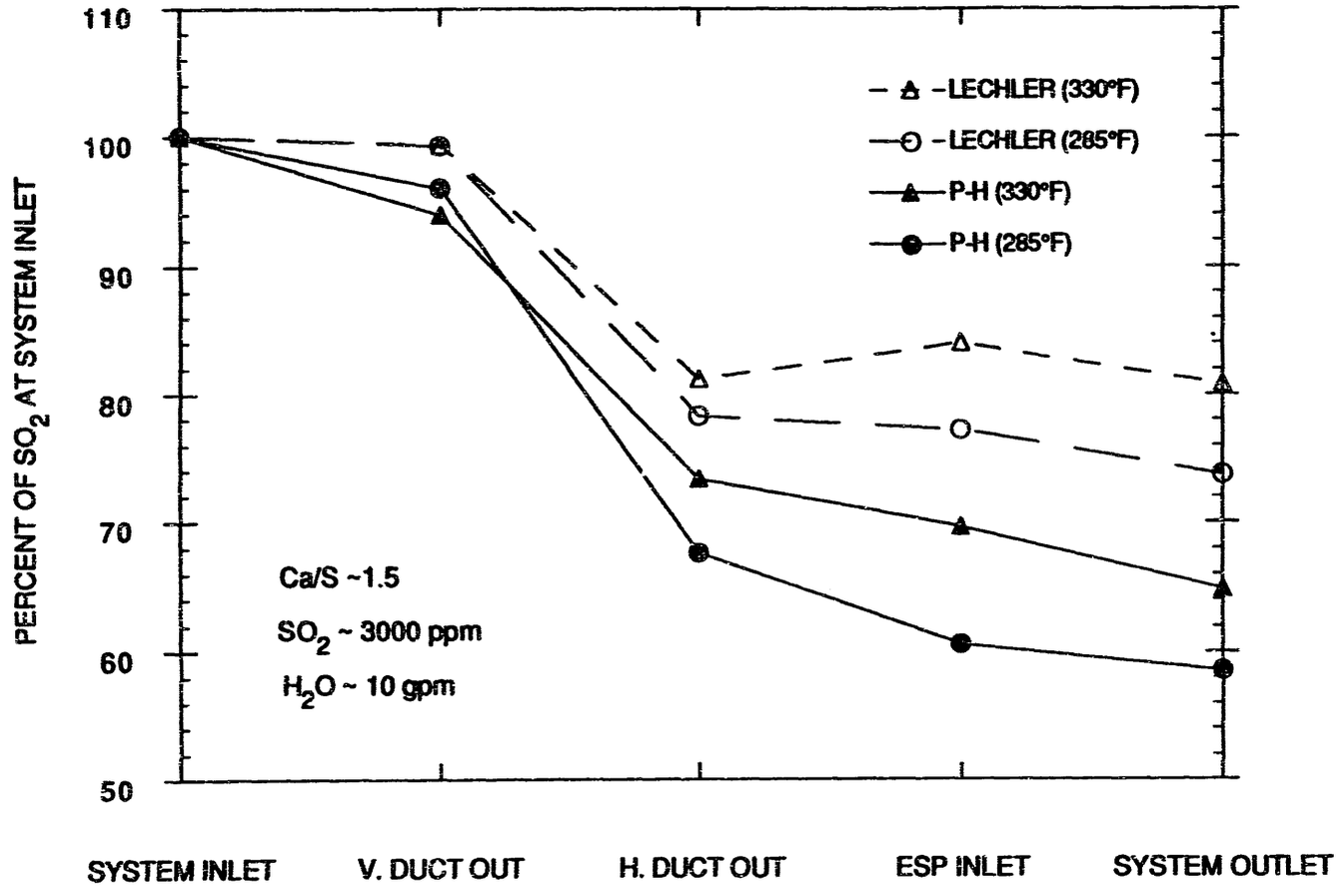

Figure 6-1. Dry hydrate injection with water spray from Lechler and Parker-Hannifin nozzles.

from the spray nozzles). The deposit extended to the bottom of the duct, bridged the hopper, and blocked approximately 80% of the duct.

When the test was repeated, the upper spray lance was positioned down 1.25° from the horizontal. This eliminated the formation of a solid deposit at the top of the duct. This test was terminated after 19 hours when the supply of dry hydrate was exhausted. Inspection of the duct at the end of testing showed no deposit on the top of the duct. A small deposit had formed, however, on the trailing lip of the hopper mentioned above. It is not known how this deposit would have grown with time.

During the 57-hour run, quench probe samples of solids entrained at the ESP inlet were obtained to compare sorbent utilization as determined directly on the solids with the values calculated from the gas-phase analyses. While the quench probe samples were being collected, measurements from the gas analysis system indicated that 30.3% SO_2 removal occurred across the entire system while 24.4% SO_2 removal occurred up to the ESP inlet. The Ca/S ratio was determined to be 1.83 during that period. The calculated sorbent utilization at the ESP inlet was thus 13.3%; this was higher than the utilization of 10.4% based on solids analyses. During the second extended run that lasted 19 hours, the dry sorbent feed rate was not stable for long periods; however, during one stable period of several hours, the gas analysis system measured an overall system SO_2 removal of about 28%, with about 22% SO_2 removal at the ESP inlet.

6.3 Slurry Injection

6.3.1 Experiments with Slurry Injection Before Outage

Two tests were conducted with slurry injection. Because there was a strong possibility the Unit 5 outage would occur earlier than scheduled (which did happen), all dry hydrate testing was suspended to make sure that the slurry system functioned properly before the outage began. As with the dry hydrate tests, the slurry tests were conducted with spray injection in the horizontal duct with the Lechler nozzles arranged as described above in connection with the dry sorbent tests. Slurry was prepared on site using a Portec M15 Slaker with pebble lime (with a typical composition as given in Table 6-4 as feed. Preparation of a slurry of the desired composition on a continuous basis requires water addition in two stages because it is necessary to maintain a temperature range of 160-180° F in the slaker vessel.

The inlet SO_2 concentration for these initial slurry injection tests was 1300 ppm; the slurry solids content was intended to be 20% by weight. The first of these tests was terminated after 29 hours after a stirrer shaft in the slurry tank sheared midway through the test. This test was beneficial, however, because at the conclusion of this test the duct was inspected and virtually no deposits were found.

After the stirrer shaft was repaired and a new supply of pebble lime was obtained, the last test before the Unit 5 outage was started. The plan was to continue this test until Unit 5 was brought off line, 2 days later. Unfortunately, the test was cut short when the unit was brought down on the first evening because of a tube leak. This test was intended to be run at a Ca/S ratio of 2.0 (solids content of 20%) and a 40° F approach to adiabatic saturation at the ESP inlet. Figure 6-2 shows that high values of SO_2 removal were measured by the gas analysis system during this last test. At the time when quench probe samples were being collected, an SO_2 removal of 48.4% was measured at the ESP inlet (after 1.5 s of residence time) and an SO_2 removal of 56.6% was measured at the

Table 6-4. Properties of Pebble Lime

Loss on ignition (750°C)	2.8%

Chemical composition[1]

Oxide	Wt. %
Li_2O	0.01
Na_2O	0.17
K_2O	0.06
MgO	1.8
CaO	94.2
Fe_2O_3	0.6
Al_2O_3	0.7
SiO_2	0.7
TiO_2	0.2
P_2O_5	0.02
SO_3	<0.1

1. Determined for ignited residue.

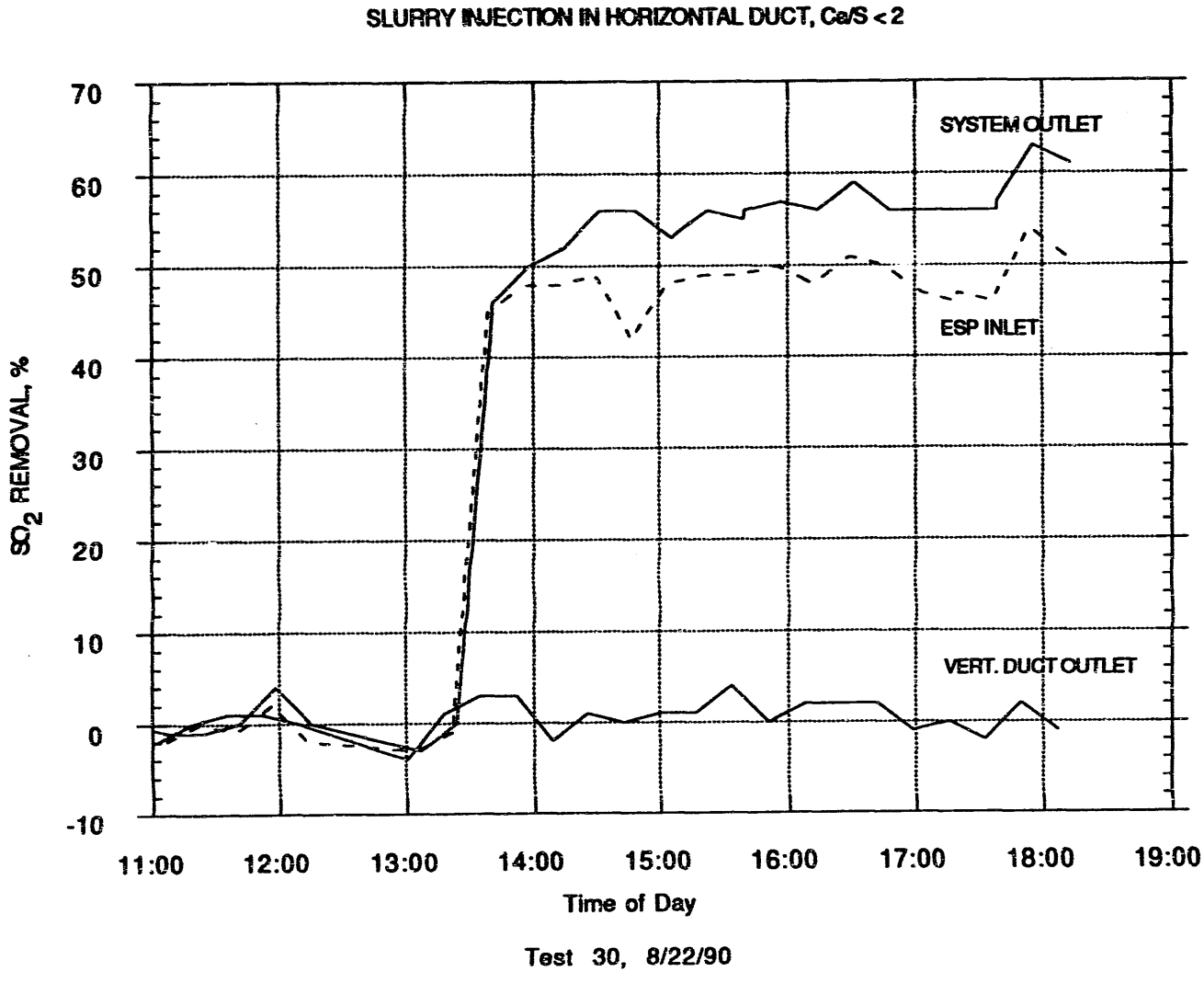

Figure 6-2. SO_2 removal with slurry injection.

system outlet. Sorbent utilizations based on the gas phase data were made uncertain because two slurry samples taken during the test had different solids concentrations (13.5% and 15.6%), which corresponded to Ca/S ratios of 1.42 and 1.72, respectively); the sorbent utilization value thus apparently fell between 28 and 34%. The average sorbent utilization based on the analyses of quench probe samples was 22.3%.

Although there was significant discrepancy between sorbent utilization values based on data from the two slurry tests described above, there is no doubt that slurry injection produced superior sorbent utilization and SO_2 removal compared with dry hydrate injection in the scavenging mode at similar approach temperatures. This conclusion is illustrated by the data presented in Table 6-5. There are not data available for tests of the two sorbent modes that are matched in all of the relevant parameters. The parameters in the two data sets given in Table 6-5, however, that are most important -- Ca/S ratio, ESP inlet temperature, and water addition rate -- favor the dry mode over the slurry mode. Hence, the better SO_2 removal with the slurry mode is even more significant than the direct comparison with SO_2 removal with dry sorbent suggests.

At the conclusion of the latter slurry test, the horizontal duct was inspected. No deposits of slurry solids were found. Hopper 1 was empty, and Hopper 2 was less than one-third full of ash. The first hopper of the ESP was quite full. All of the ash was soft and dry, and no hopper evacuation problems were encountered. The results of this test in terms of system operability are quite encouraging; the results in terms of SO_2 removal are also encouraging. A decision was therefore made to concentrate the experimental efforts on slurry injection following the conclusion of the Unit 5 outage.

6.3.2 Experiments with Slurry Injection After Outage

6.3.2.1 Summary of Data

Slurry injection experiments were resumed following the outage on November 19 and were continued under Task 3.1 until February 4, 1991, at which time the Task 3.1 Test Series (Evaluation of System Performance) was concluded. Testing has continued under Task 3.2 (Scale-up Tests) and 3.3 (Advanced Concepts). This latter work will be covered in a subsequent topical report.

Table 6-6 contains most of the essential data from post-outage slurry testing; it includes information on the following parameters:

- Approach to saturation. The values listed for this parameter were calculated by subtracting the estimated temperature of adiabatic saturation from the observed temperature at the inlet to the ESP. The estimated saturation temperature was usually 124 or 125°F; it was based upon the customary temperature at the system inlet (very close to 300°F in all experiments) and the measured water vapor concentration at the system inlet (usually about 6% by volume).

- Inlet SO_2 concentration. This parameter was adjusted by controlling the proportions of flue gas from Unit 3 and dilution gas from the dilution burner. Although a superficial inspection of the table indicates that the concentration of SO_2 varied indiscriminately, the concentrations actually were clustered about three averages with only moderately large standard deviations: 1191 ± 51, 1793 ± 56, and 2763 ± 23.

Table 6-5

Comparison of SO_2 Removals by
Dry Sorbent and Slurry Injection Materials[1]
(Summary of data prior to outage)

	Dry Sorbent			
	Without water	Non-scavenging	Scavenging	Slurry
Ca/S ratio	2.3	3.2	2.5	1.5
Inlet SO_2, ppm	1350	1900	1900	1300
ESP inlet temp., °F	--	--	154	171
Water flow, gpm	--	--	11	10
Cumulative SO_2 removal				
End of horizontal duct	--	18	41	50
ESP inlet	12	27	42	50
System outlet	17	37	53	56

1. Lechler nozzles used either for the water to humidify the dry hydrate or for the slurry.

Table 6-6. Results of Slurry Tests, Part 1

Test Week #	Date	Test Number	Approach (°F)	Inlet SO2 (ppm)	Ca/S Ratio	ESP Inlet ΔSO2 (%)	ESP Inlet Util. (%)	ESP Outlet ΔSO2 (%)	ESP Outlet Util. (%)	% Utilization from Analysis of Quench Probe Samples	% Utilization from Analysis of ESP Hopper #1 Samples
20	12/04/90	20-SL-01	38	1186	2.32	51.0	22.0	60.1	25.9		
	12/05/90	20-SL-02	43	1213	2.43	49.7	20.5	59.1	24.3	20.2	22.6
			48	1271	2.29	46.7	20.4	56.8	24.8	20.1	
	12/06/90	20-SL-03	38	1205	2.20	49.3	22.4	56.4	25.6	20.2	22.3
	12/07/90	20-SL-05	42	1216	2.23	50.6	22.7	61.0	27.4		22.2
21	12/10/90	21-SL-01	48	1252	1.98	50.2	25.4	62.4	31.5	18.7	24.2
			52	1227	2.01	47.8	23.8	59.8	29.8	18.5	
	12/12/90	21-SL-01	51	1137	2.29	54.6	23.6	65.7	28.7	19.5	
		21-SL-01	56	1159	2.22	51.9	23.4	61.6	27.7	19.1	
22	12/16/90	21-SL-01	55	1200	2.08	NO GAS SAMPLING DATA				14.7	22.3
			55	1200	2.08	NO GAS SAMPLING DATA				14.9	20.4
			55	1201	2.08	48.4	23.3	61.1	29.4	14.1	20.4
	12/17/90	21-SL-01	51	1129	2.17	50.3	23.2	62.3	28.7	19.0	19.5
			53	1151	2.15	48.7	22.7	62.5	29.1	18.1	23.0
			53	1247	2.00	45.1	22.6	60.3	30.2	17.5	
	12/18/90	21-SL-01	47	1064	2.34	48.5	20.7	62.1	26.5	19.7	
24	01/03/91	24-SL-01	39	1253	2.88	56.2	19.5	67.7	23.5		
	01/04/91	24-SL-02	32	1167	2.86	60.1	21.0	74.5	26.0		
			35	1788	1.95	54.4	27.9	67.5	34.6		
25	01/08/91	25-SL-01	43	1770	1.83	49.2	26.9	62.9	34.4	22.2	26.7
		25-SL-02	21	1156	3.27	78.4	24.0	89.9	27.5	20.2	23.4
	01/09/91	25-SL-03	37	2146	1.45	46.2	33.2	62.5	43.1		
		25-SL-04	28	2764	1.45	52.1	35.9	70.8	48.8	28.6	30.2
			30	2734	1.44	49.8	34.6	71.3	49.5	28.1	32.8
	01/10/91	25-SL-05	40	2764	1.27	44.0	34.6	58.2	45.8		
	01/11/91	25-SL-06	56	2790	1.30	36.3	27.9	44.0	33.8	24.8	27.1
26	01/14/91	26-SL-01	50	1771	1.52	35.5	23.4	42.0	27.6		
	01/16/91	26-SL-02	46	1794	1.75	45.3	25.9	55.3	31.6	23.3	27.7
	01/18/91	26-SL-03	56	1804	1.64	41.1	25.1	46.9	28.6	24.0	26.6
27	01/25/91	27-SL-01	43	1692	2.15	48.6	22.6	61.4	28.6	21.0	22.6
			45	1679	2.15	47.1	21.9	59.7	27.8		
	01/26/91	27-SL-02	38	1738	2.09	53.4	25.6	66.8	32.0	23.0	25.9
			35	1675	1.93	55.1	28.5	65.9	34.1		

Table 6-6. Results of Slurry Tests, Part 2

Test Week #	Date	Test Number	Approach (°F)	Inlet SO2 (ppm)	Ca/S Ratio	ESP Inlet ΔSO2 (%)	ESP Inlet Util. (%)	ESP Outlet ΔSO2 (%)	ESP Outlet Util. (%)	% Utilization from Analysis of Quench Probe Samples	% Utilization from Analysis of ESP Hopper #1 Samples
28	01/27/91	28-SL-01	28	1700	2.15	60.4	28.1	78.6	36.6	25.4	28.2
			27	1775	2.10	61.9	29.5	79.5	37.9		
		28-SL-02	35	1804	1.49	45.1	30.3	56.0	37.6	24.4	27.7
			35	1788	1.51	45.6	30.2	58.8	38.9		
	01/28/91	28-SL-03	35	1873	1.49	48.9	32.8	59.2	39.7	27.4	32.3
			35	1869	1.49	51.8	34.8	61.4	41.2		
	01/29/91	28-SL-04	25	1805	1.54	55.5	36.0	67.4	43.8	30.1	35.0
			25	1909	1.43	54.0	37.7	64.4	45.0		
			24	1780	1.60	57.4	35.9	70.4	44.0		
			23	1773	1.60	58.3	36.4	70.1	43.8	32.3	36.1
	01/31/91	28-SL-05	44	1790	1.05	37.4	35.6	41.5	39.5	26.6	29.0
			43	1803	1.04	36.5	35.1	41.3	39.7		
			43	1780	1.05	35.9	34.2	40.4	38.5		
	02/01/91	28-SL-06	35	1875	0.99	42.6	43.0	50.9	51.4	29.6	33.6
			35	1799	1.03	43.7	42.4	50.1	48.6		
			35	1702	1.07	43.5	40.7	52.2	48.8		
	02/02/91	28-SL-07	27	1781	1.01	44.9	44.5	51.1	50.6	34.2	38.0
			25	1790	1.03	45.8	44.5	52.2	50.7		
			28	1852	0.98	45.0	45.9	50.3	51.3		
29	02/03/91	29-SL-01	47	1836	1.91	49.5	25.9	60.5	31.7	20.6	22.5
			43	≈1850	1.94	NO GAS SAMPLING DATA					
			49	1878	1.85	47.3	25.6	55.4	29.9		
	02/04/91	29-SL-02	38	1766	1.97	52.7	26.8	61.4	31.2	24.0	27.4
			37	1773	2.02	55.8	27.6	67.3	33.3		
			37	1752	2.06	54.8	26.6	65.9	32.0		

- Ca/S mole ratio. This ratio was calculated from the feed rate of slurry, the $Ca(OH)_2$ concentration in the slurry, the SO_2 inlet concentration, and the inlet gas flow rate.

- Percent removal at the ESP inlet and outlet, and apparent utilization of the sorbent. Percent removal was calculated from measured SO_2 concentrations with correction to constant O_2 concentration. Apparent utilization was the percent SO_2 removal divided by the Ca/S ratio.

- Percent sorbent utilization based on solids collected at two locations: a quench probe inserted into the horizontal near the ESP inlet, and the first or inlet hopper of the ESP. Both types of solids were analyzed for water-soluble Ca^{+2} and SO_3^{-2}. Control experiments have shown that essentially all of the calcium from the sorbent is extracted in a large excess of water under the conditions used, and a negligible amount of calcium is extracted from the fly ash in the ash-sorbent mixture. These experiments similarly have indicated that essentially all of the sorbent in the form of $CaSO_3$, due to the reaction of sorbent with SO_2, is also recovered by the water extraction. Utilization is calculated as the mole ratio SO_3^{-2}/Ca^{+2}.

6.3.2.2 Influence of Ca/S Ratio and Approach to Saturation on SO_2 Removal

One set of figures summarizes the data on SO_2 removal at the ESP inlet as a function of the two parameters having the greatest influence on removal -- Ca/S ratio and approach to saturation:

Figure 6-3 shows SO_2 removal versus Ca/S ratio for all tests, without regard to approach.

Figures 6-4, -5, -6, and -7 show SO_2 removal versus Ca/S ratio for approaches in selected ranges of temperature.

The second set of figures summarizes the data on SO_2 removal at the ESP outlet rather than the inlet:

Figure 6-8 for all conditions.

Figures 6-9, -10, -11, and -12 for selected approach intervals.

The data in these figures have been interpolated and summarized with the results shown by Table 6-7. The optimum conditions for SO_2 removal that are shown in this table are an approach of 20-30°F and a Ca/S ratio of 2.5. These conditions appear to afford a removal of 70% of the SO_2 at the ESP inlet and 85% at the ESP outlet. As will be explained momentarily, the SO_2 removals in this table represent the upper limits of results to be expected, on the basis of the available data, for the conditions listed.

6.3.2.3 Influence of Inlet SO_2 Concentration on SO_2 Removal

As stated above, the inlet concentrations of SO_2 fell within narrow ranges around three average concentrations: approximately 1200, 1800, and 2800 ppm. Other investigations of sorbent injection

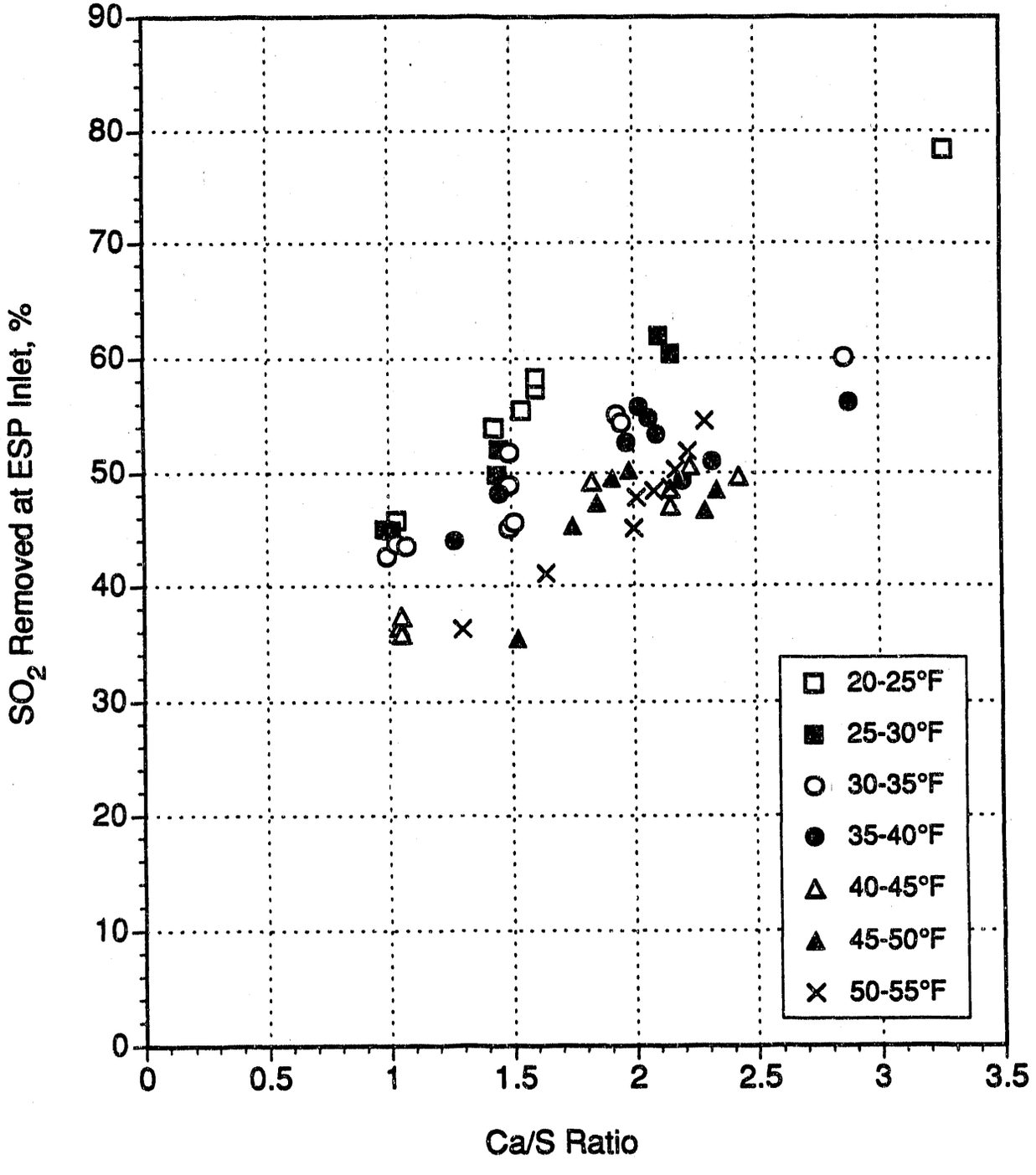

Figure 6-3. Percent of SO_2 removed at the ESP inlet as measured by the gas sampling system. Summary of all test data at all approach temperatures.

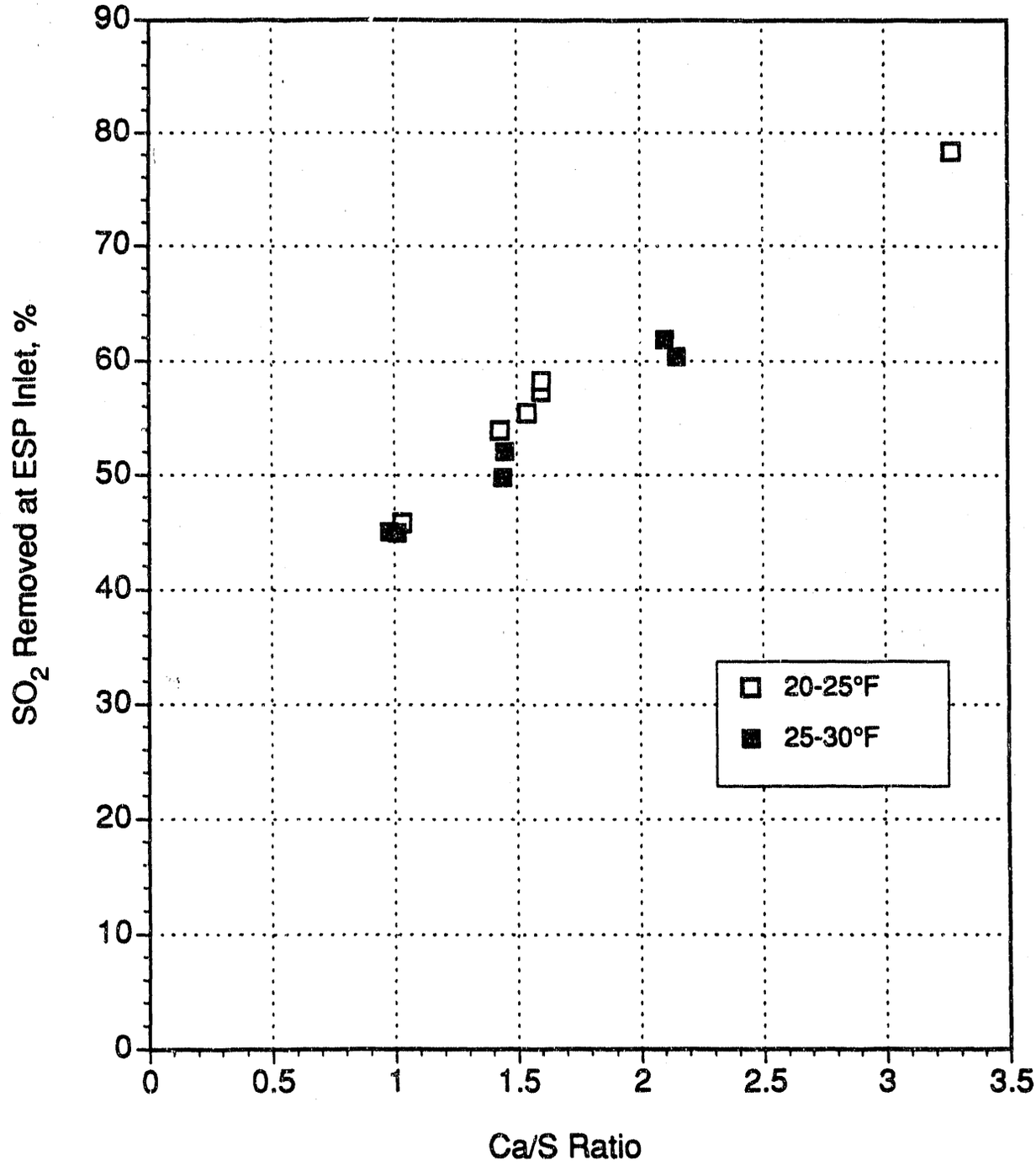

Figure 6-4. Percent of SO_2 removed at the ESP inlet as measured by the gas sampling system. Summary of test data for approach temperatures from 20 to 30° F.

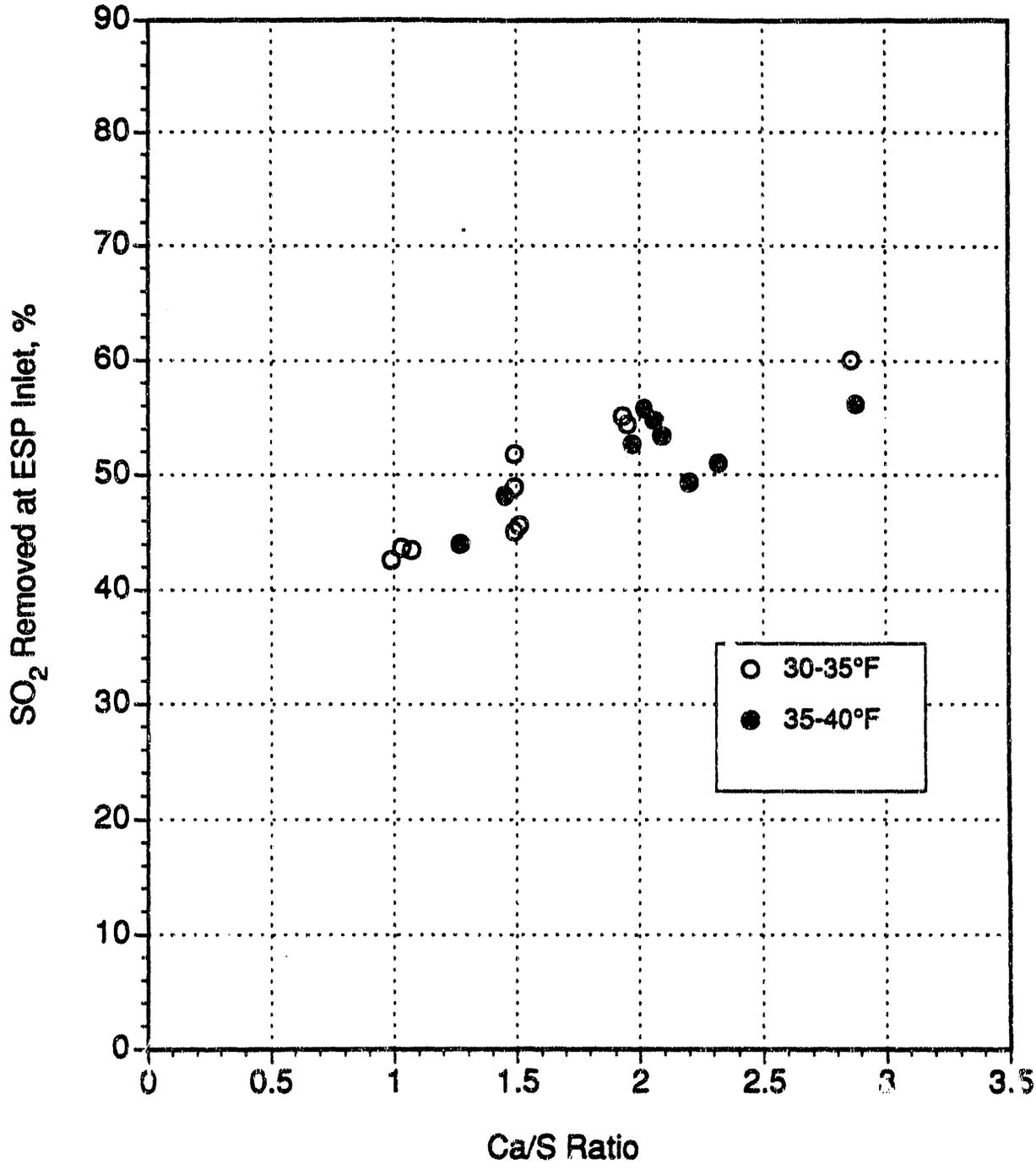

Figure 6-5. Percent of SO_2 removed at the ESP inlet as measured by the gas sampling system. Summary of test data for approach temperatures from 30 to 40° F.

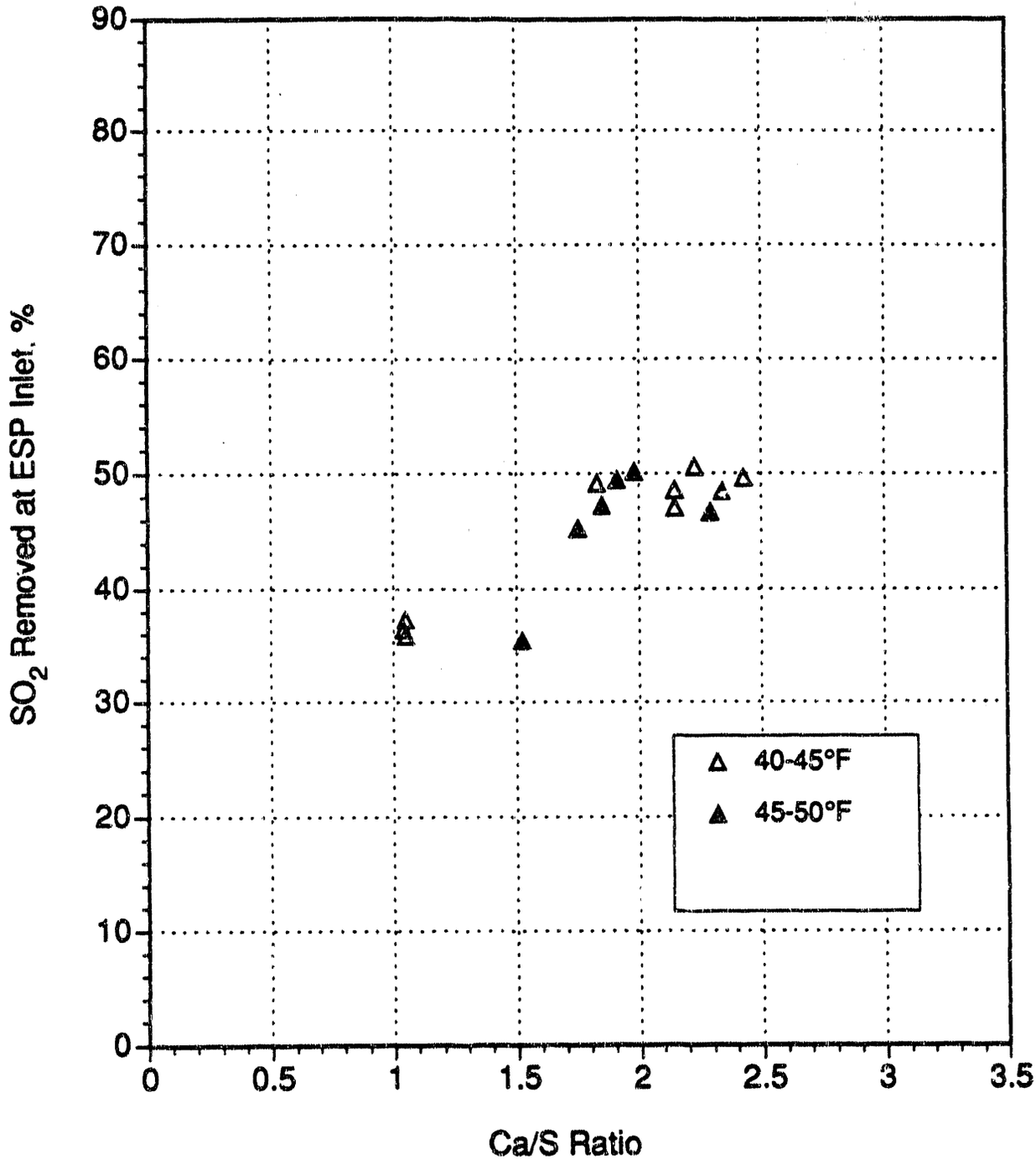

Figure 6-6. Percent of SO_2 removed at the ESP inlet as measured by the gas sampling system. Summary of test data for approach temperatures from 40 to 50° F.

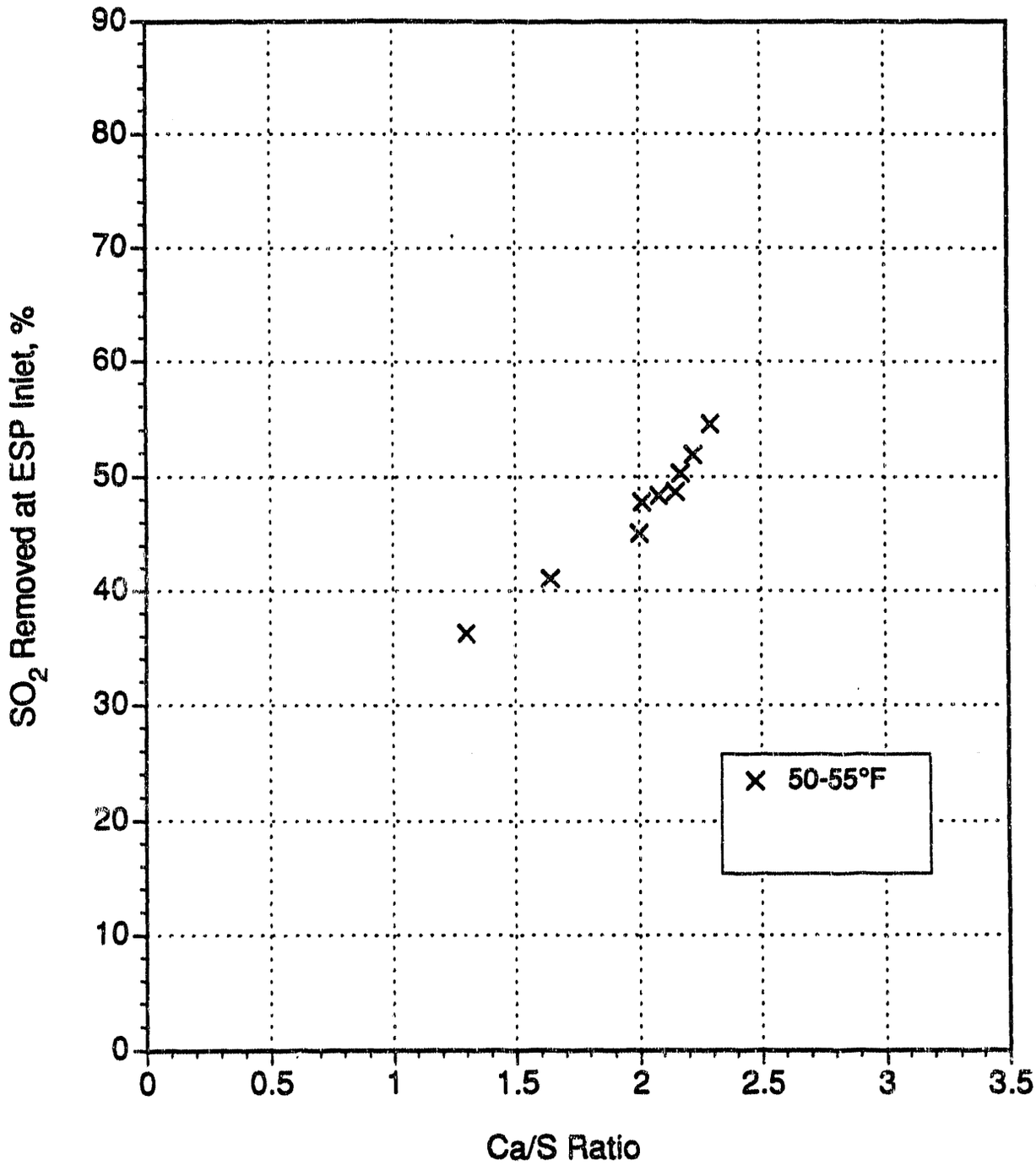

Figure 6-7. Percent of SO_2 removed at the ESP inlet as measured by the gas sampling system. Summary of test data for approach temperatures from 50 to 55°F.

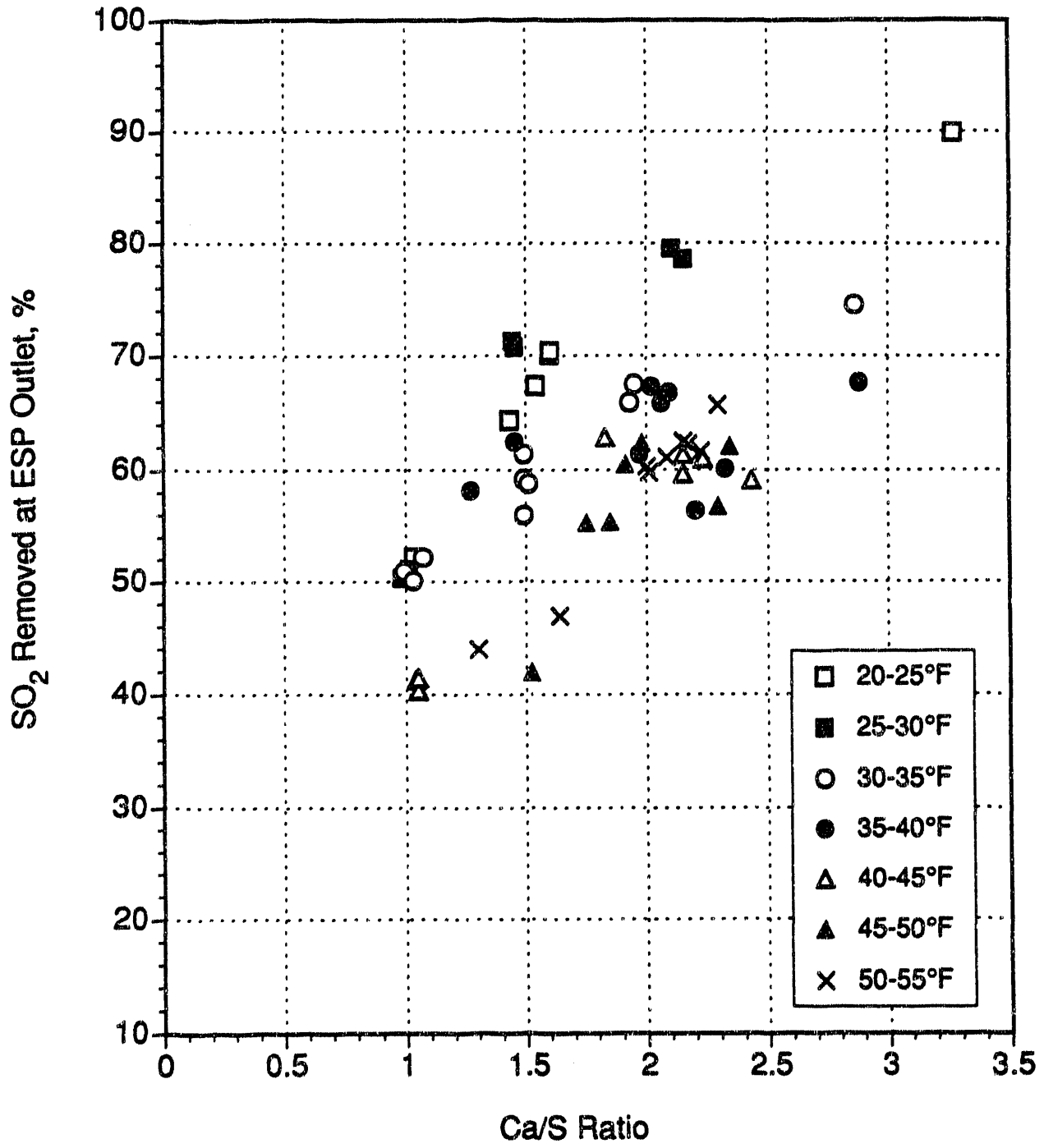

Figure 6-8. Percent of SO_2 removed at the ESP outlet as measured by the gas sampling system. Summary of all test data.

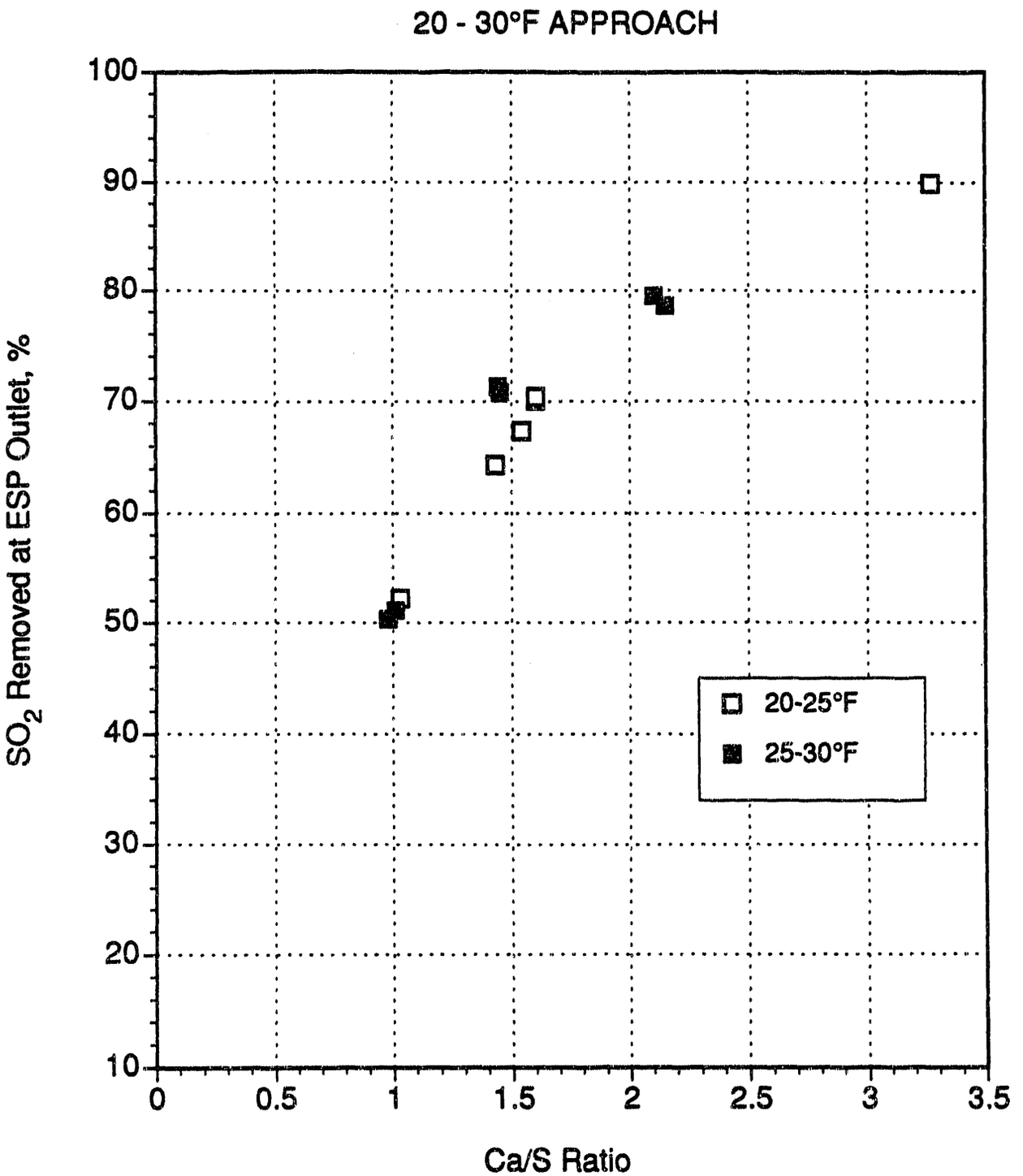

Figure 6-9. Percent of SO_2 removed at the ESP outlet as measured by the gas sampling system. Summary of test data for approach temperatures from 20 to 30° F.

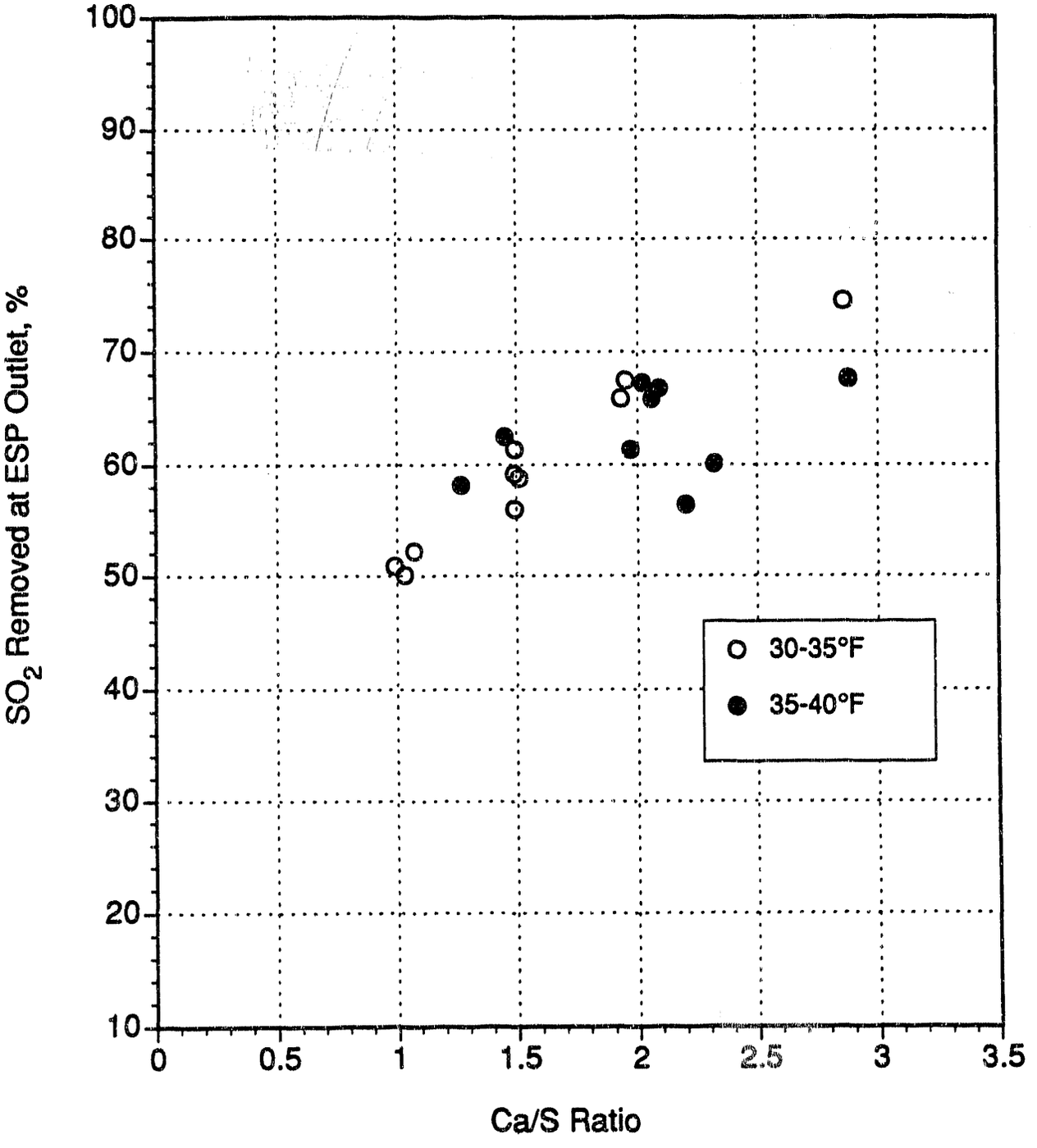

Figure 6-10. Percent of SO_2 removed at the ESP outlet as measured by the gas sampling system. Summary of test data for approach temperatures from 30 to 40° F.

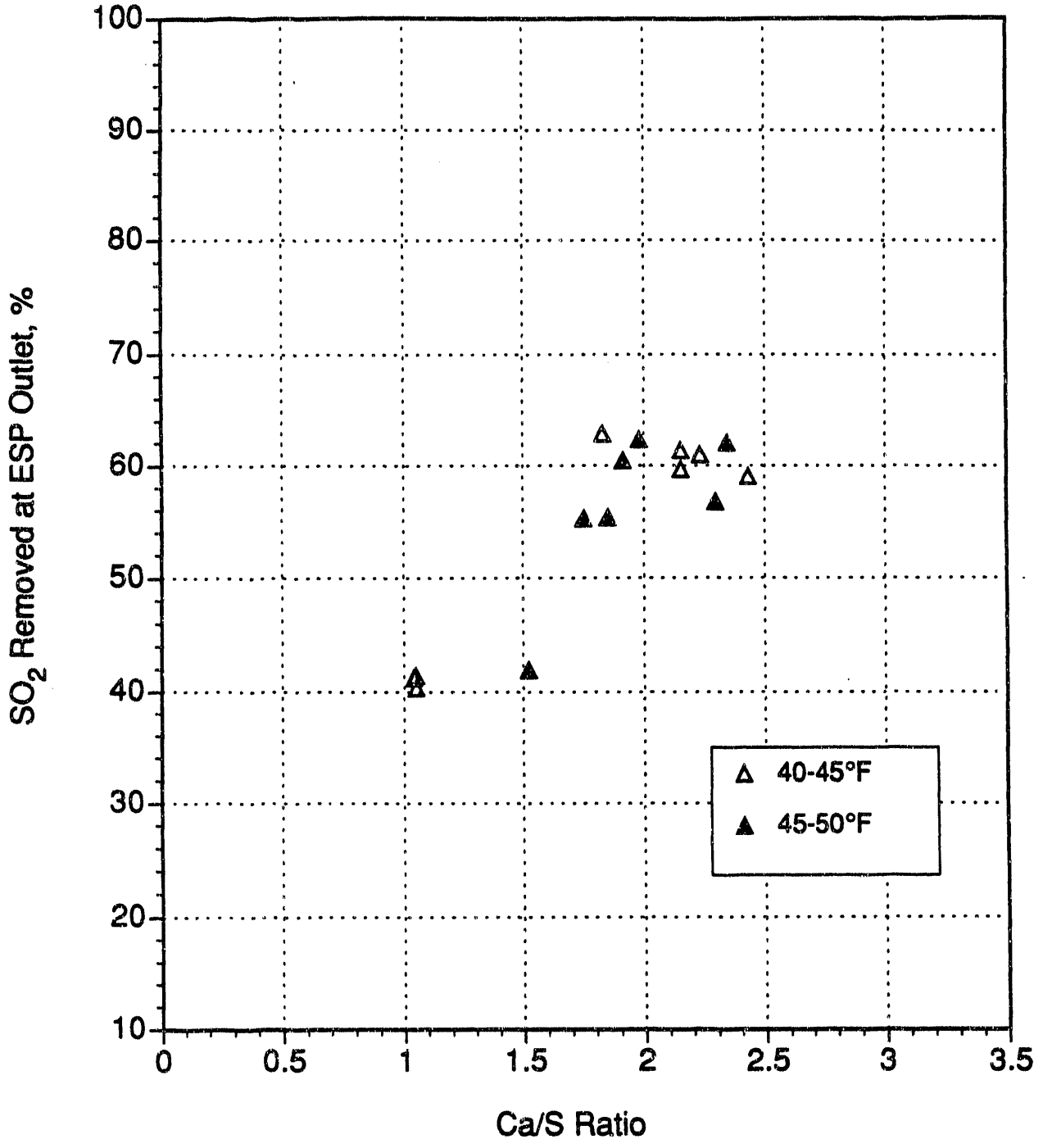

Figure 6-11. Percent of SO_2 removed at the ESP outlet as measured by the gas sampling system. Summary of test data for approach temperatures from 40 to 50°F.

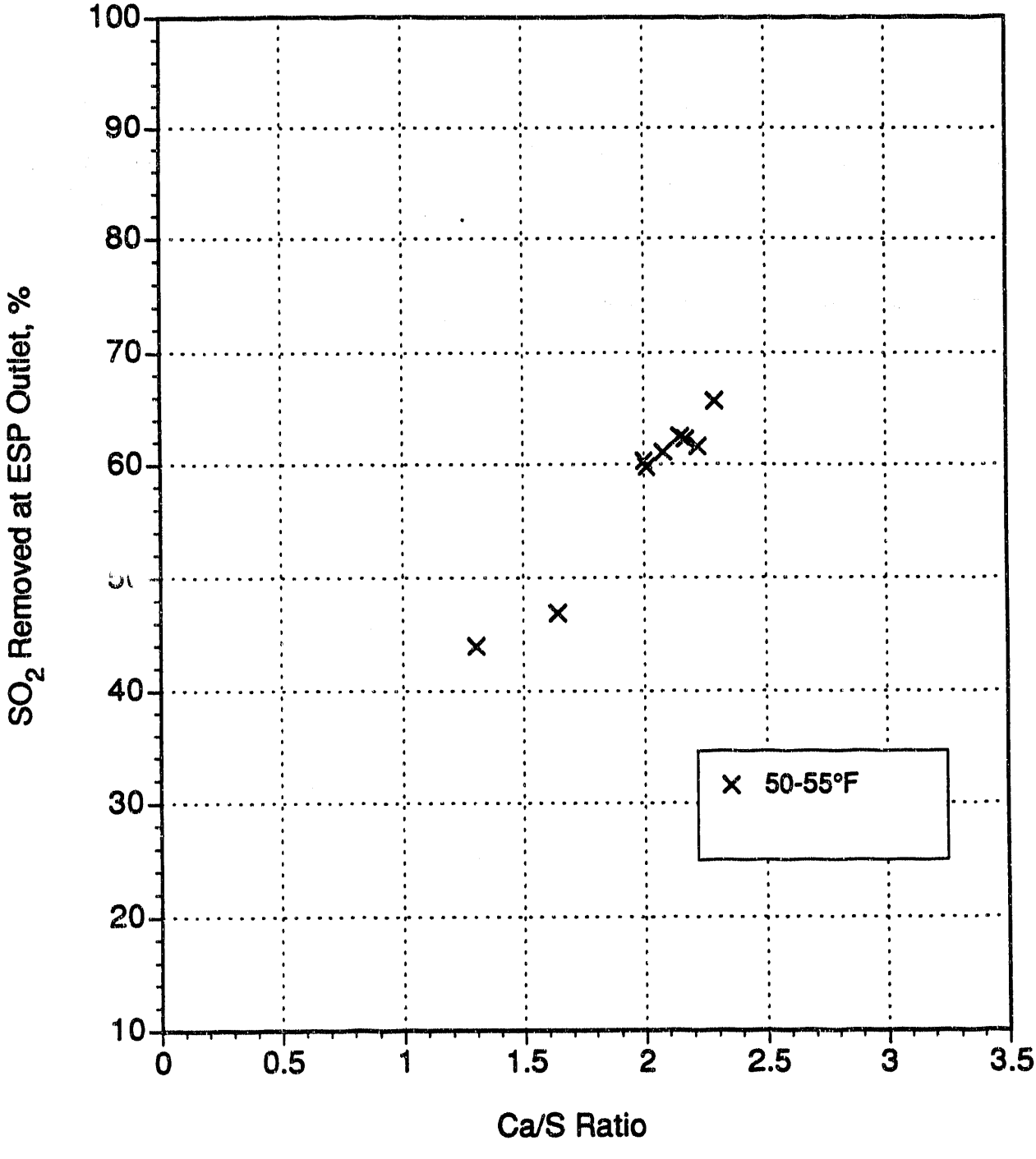

Figure 6-12. Percent of SO_2 removed at the ESP outlet as measured by the gas sampling system. Summary of test data for approach temperatures from 50 to 55°F.

Table 6-7. Summary of Post-Outage Data on SO_2 Removal with Slurry

Approach, °F	Ca/S ratio	SO_2 removal, %	
		ESP inlet	ESP outlet
20-30	1.0	45	50
	2.0	60	75
	2.5	70	85
50-55	1.0	30	40
	2.0	50	60
	2.5	60	70

processes for SO_2 control--one example is HYPAS--have found that the inlet concentration has an effect on the extent of SO_2 removal. In this study, however, this seems not to have been the case. Data in plots of SO_2 removal as a function of Ca/S ratio at selected approach intervals were prepared with different symbols indicating the three representative inlet concentrations. The locations of the data points appeared to be random insofar as the inlet SO_2 concentration was concerned.

6.3.2.4 Indications of Sorbent Utilization from Gas-Phase and Solids Analyses

Figures 6-13, -14, -15, and -16 present data on sorbent utilization at locations near the ESP inlet. In each figure one set of data points shows apparent utilizations calculated from the SO_2 removals. Another set is based on analyses of quench probe solids, and a third is based on analyses of ESP inlet hopper samples. On occasions when utilizations were calculated from all three data sources, the utilizations inevitably ranked in the following order: highest, based on gas analyses; second highest, based on ESP samples, and lowest, based on quench probe samples. Conceptually, the utilization based on a quench probe sample should be the most accurate indicator of the extent of reaction between SO_2 and sorbent at the point of collection; whether this is correct cannot, unfortunately, be stated definitively. The reason for this ambiguity is that the quench probe sample is obtained at a single point which may not be completely representative of the sorbent across the entire duct at the plane of the sampling point.

A higher utilization of sorbent in the ESP is a reasonable result, inasmuch as solids collected in the ESP remain in contact with the gas phase a longer time before they undergo separation. An even higher apparent utilization based on gas-phase data is also plausible if SO_2 reacts with sorbent deposited on the duct walls as well as in the suspended state. Indeed, concern about the reaction with wall deposits and the need to set a more dependable, conservative value on the extent of reaction than the SO_2 data affords is the reason for collecting and analyzing the solids. A realistic scale-up of pilot data must ignore the contribution of wall effects, since the relative contribution of wall effects at full scale will be substantially less than the contribution at the high surface-to-volume ratio at pilot scale.

It should be emphasized that the difference between the single-point quench probe samples and the gas sampling system results was not associated with the presence of large moist deposits of sorbent in the duct at the higher Ca/S ratios. Relatively long-term experiments were conducted without the need to shut down and remove deposits. The term "wall deposits" in the context of this discussion means, in effect, any sorbent particles which contacted duct surfaces or turning vanes, remained there for some time period greater than the mean gas residence time, and then reentrained in the gas stream. Such reentrained material is unlikely to be uniformly distributed, and therefore may be missed by the quench probe. We expect that the discrepancy between solids analyses and gas system results will be more definitively resolved by long-term experiments which will be conducted later in the project.

Some of the data points in Figures 6-13, -14, -15, and -16 indicate the difference between utilizations based on gas and solids analyses is greater at low Ca/S ratios. Later work was put forth to examine this possibility and to find a possible explanation. Even now, the available data do not resolve the issue definitively. If the difference does in fact exist, however, it may be explained by the occurrence of sorbent at lower slurry concentrations in tests at lower Ca/S ratios. If a given approach to saturation is to be maintained while the Ca/S ratio is lowered, the sorbent concentration in the slurry obviously must be lowered. Such a change increases the likelihood of forming wall deposits of wet

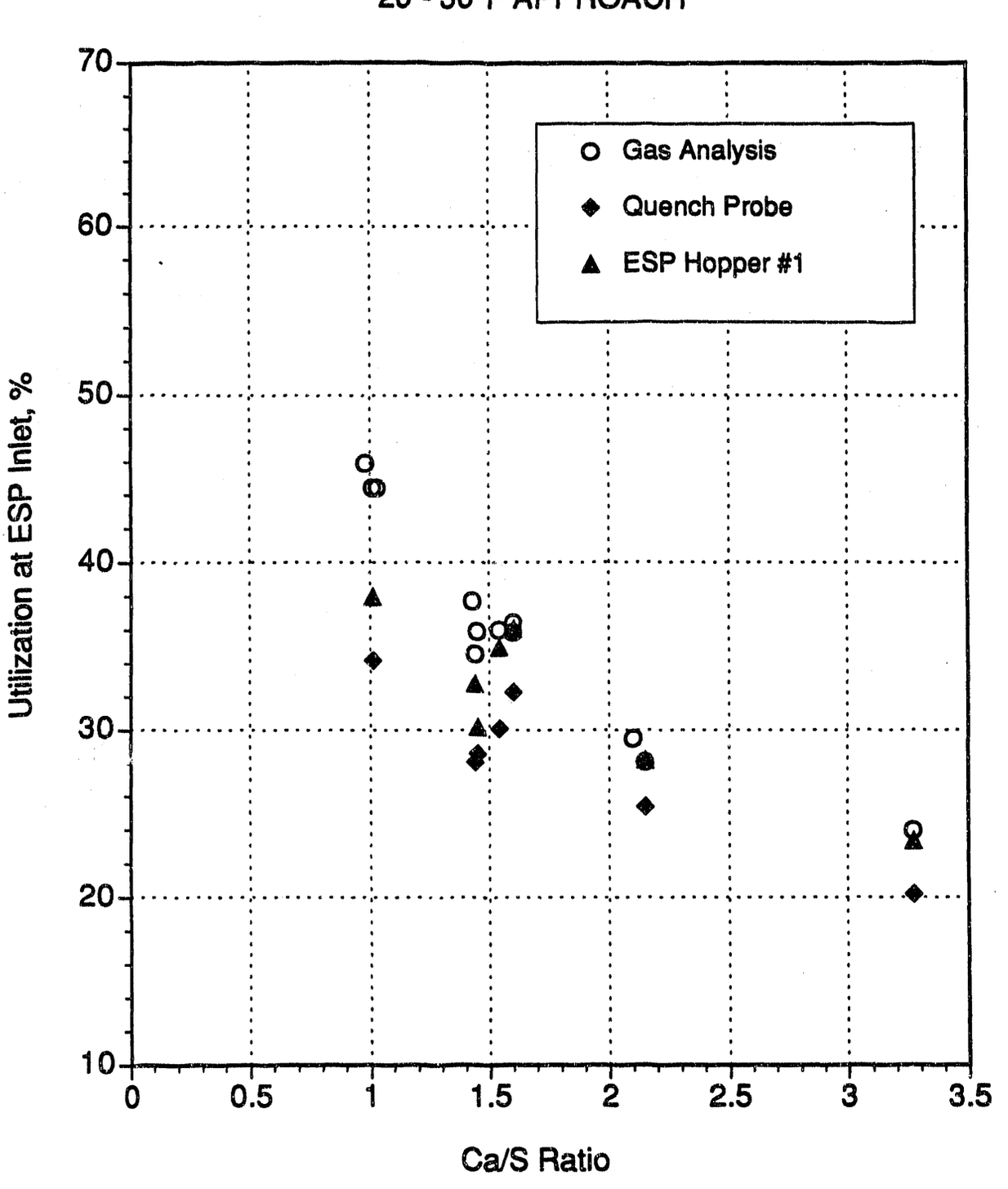

Figure 6-13. Percent of sorbent utilized at the ESP inlet as determined by the gas sampling system and chemical analyses of quench probe samples and ESP inlet hopper samples. Summary of test data for approach temperatures from 20 to 30° F.

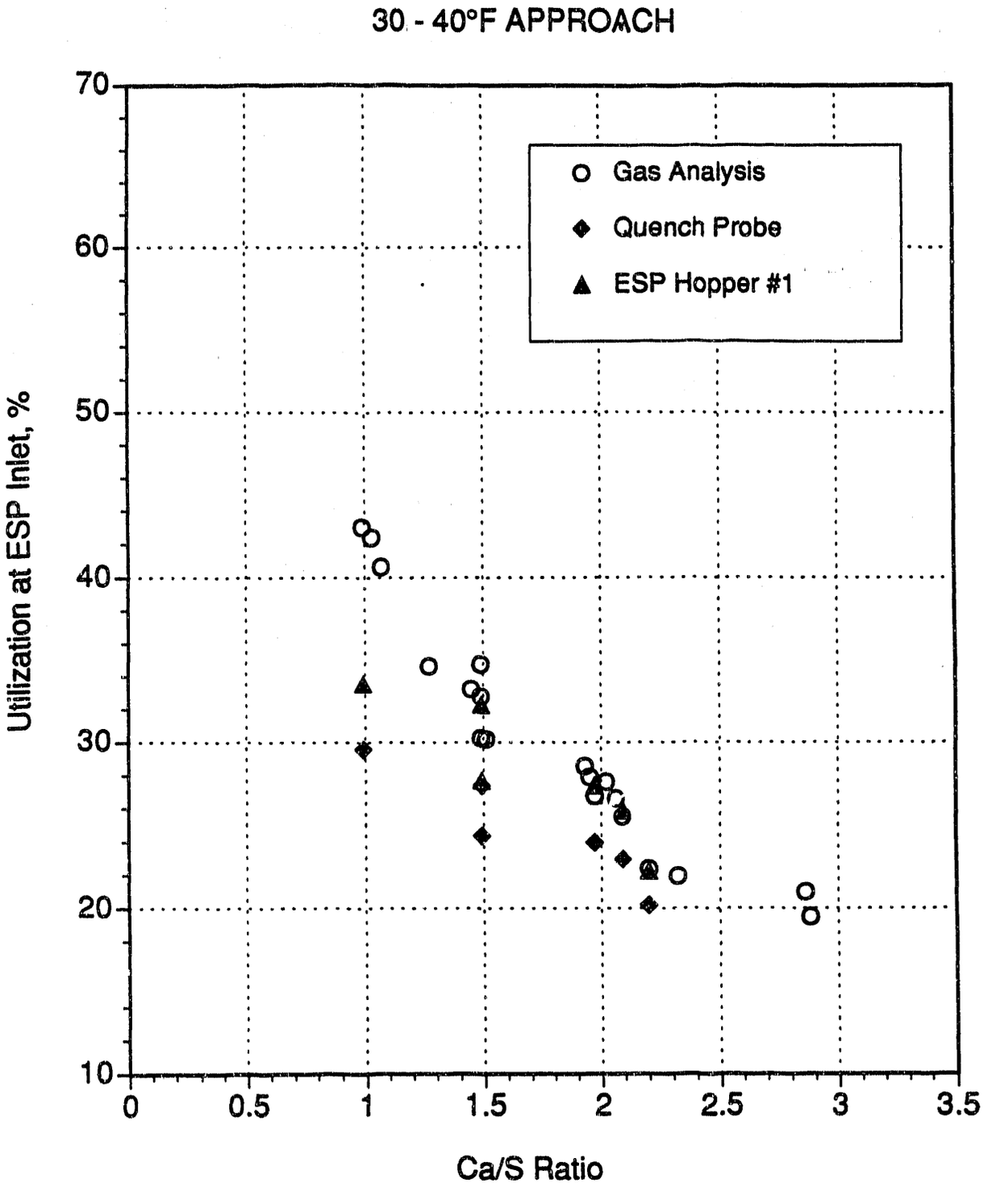

Figure 6-14. Percent of sorbent utilized at the ESP inlet as determined by the gas sampling system and chemical analyses of quench probe samples and ESP inlet hopper samples. Summary of test data for approach temperatures from 30 to 40°F.

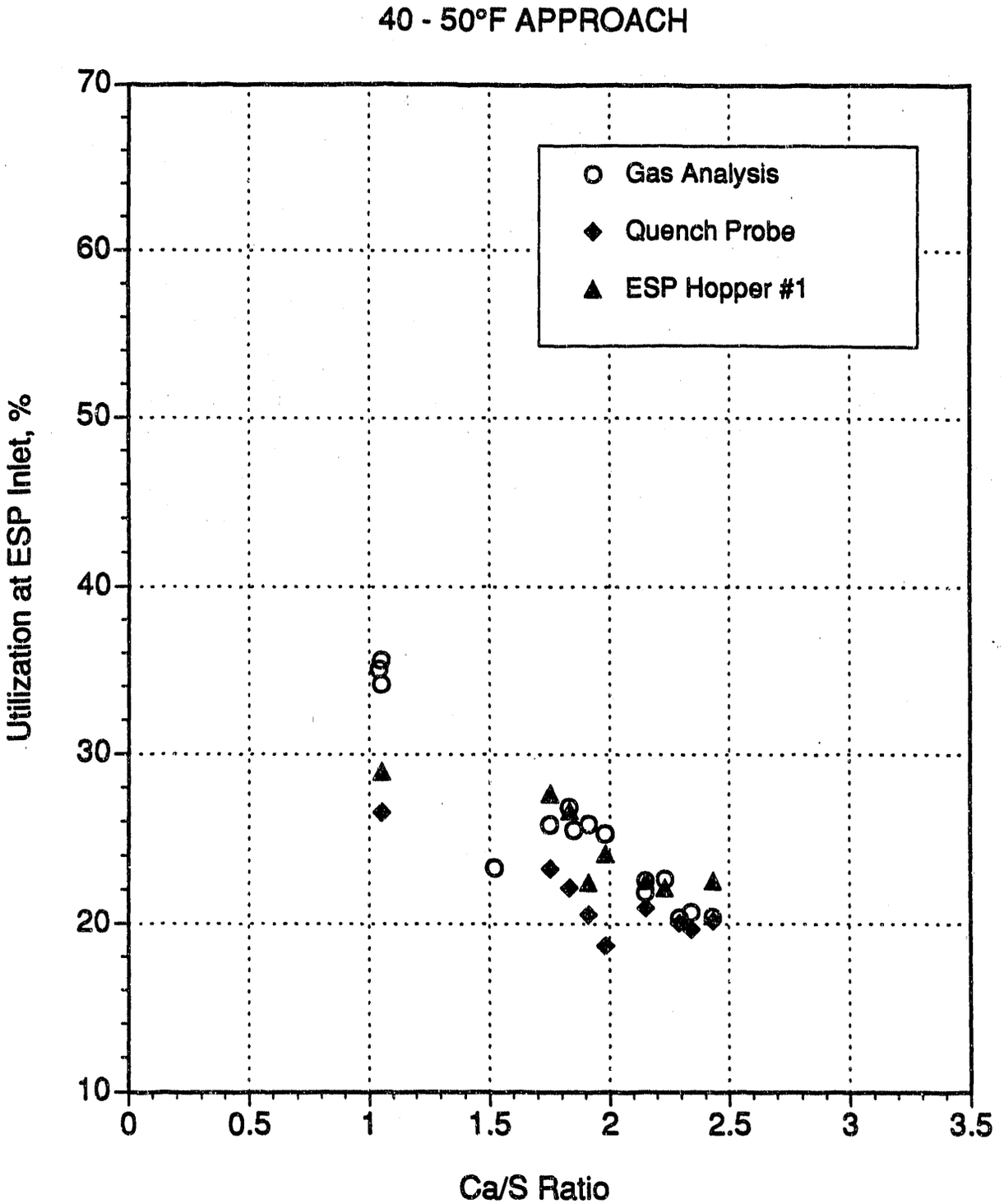

Figure 6-15. Percent of sorbent utilized at the ESP inlet as determined by the gas sampling system and chemical analyses of quench probe samples and ESP inlet hopper samples. Summary of test data for approach temperatures from 40 to 50°F.

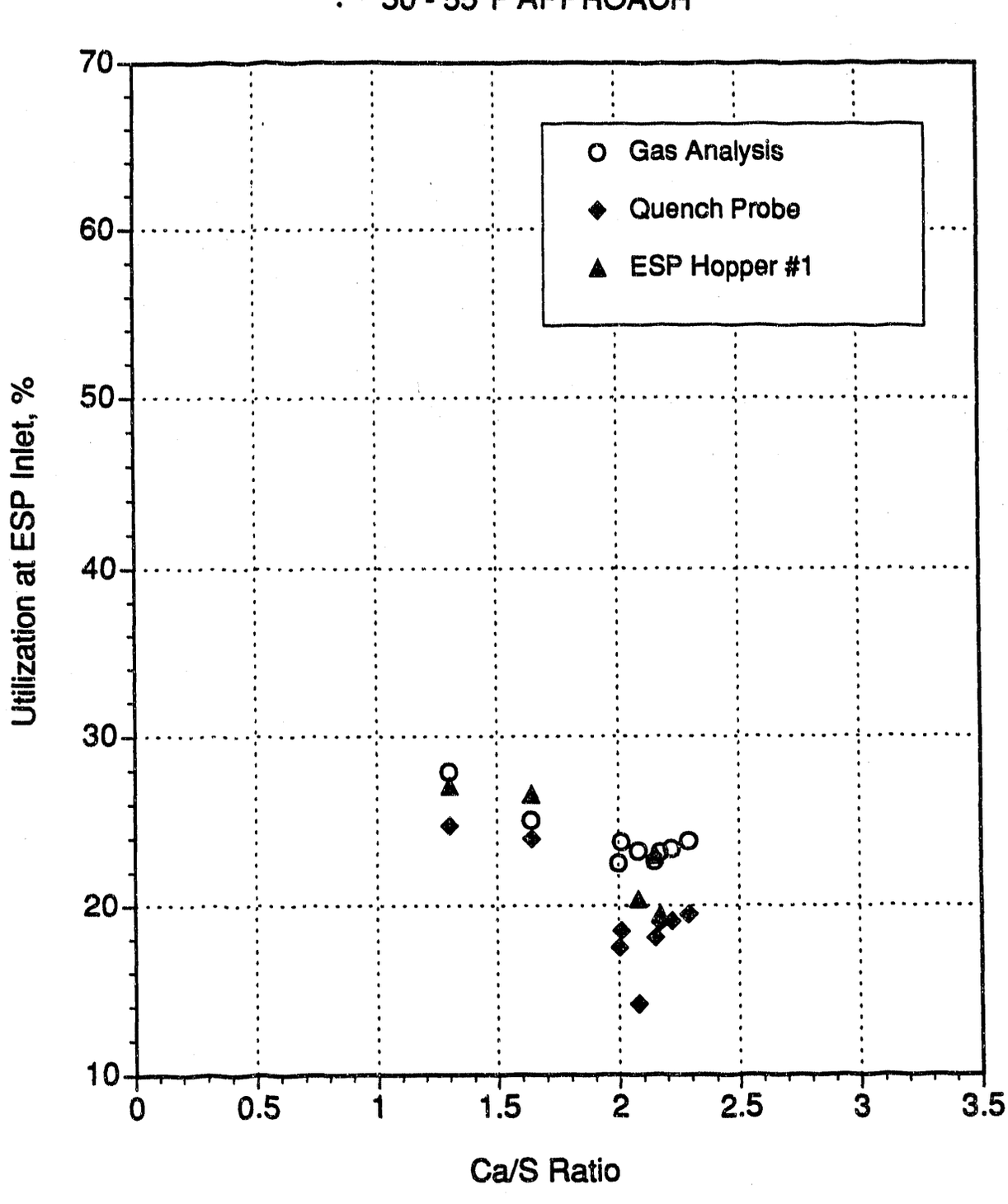

Figure 6-16. Percent of sorbent utilized at the ESP inlet as determined by the gas sampling system and chemical analyses of quench probe samples and ESP inlet hopper samples. Summary of test data for approach temperatures from 50 to 55°F.

and thus more reactive sorbent, which can give misleading high indications of the extent of reaction in the suspended state.

On one occasion, a broader set of solids samples was collected and analyzed for calculations of sorbent utilization. The data for this set of samples are given in Table 6-8. There are sorbent utilization values for samples from the second and third hoppers of the ESP as well as the quench probe sample and first hopper sample. There is also a utilization value for a sample collected in a mass train at the system outlet. Because of the high ESP efficiency for collecting solids, the quantities of solids in the second and third hoppers is limited, and the outlet concentration of suspended solids is very low. The data show that the utilization based on either SO_2 concentration or solids composition increased as the location of the sample was moved downward through the system. This, of course, was expected because of increased reaction time and, for the solids, decreased concentration in the suspended state and thus increased utilization for a given amount of SO_2 removal. The higher utilization of the solids is also expected to be due in part to the finer particle size toward the outlet of the system and a higher exposure of the sorbent to the gas phase.

The upper limits of SO_2 removal that can be reported from the available data have been previously summarized in Table 6-7. The lower limits would be based on the analyses of the quench probe solids. The comparison of these upper and lower limits of SO_2 removal are depicted in Figure 6-17. This figure indicates that there is approximately a 10% difference in SO_2 capture based on analyses of gas and solids. If this constant difference does exist, then, from purely mathematical considerations, utilizations based on the two analyses must converge as Ca/S increases, as shown in Figures 6-13, -14, -15, and -16.

6.3.2.5 Contribution of ESP to SO_2 Removal

Figures 6-18, -19, -20, and -21 compare apparent sorbent utilizations, based on gas-phase data, at the ESP inlet and the ESP outlet. These graphs indicated that the differences in utilizations may be as high as 10% at Ca/S = 1 and as high as 7-8% at Ca/S = 2.5. The corresponding differences in SO_2 removals would be around 10 to 15%, as previously indicated in Table 6-7.

To make a conservative estimate of the extent of SO_2 removal in a full-scale system, it is appropriate to take the utilization based upon solids analysis as the true indicator of reaction in the suspended state preceding the ESP and add the increment in utilization based on solids at the ESP inlet and gas at the ESP outlet. The rationale for scale-up of the duct reaction on this basis has already been set forth. The rationale for scale-up of the ESP effect as indicated is as follows: for an ESP with a given specific collecting area (400 ft^2/1000 acfm at Beverly with the gas temperature lowered) the SO_2 removal process will be affected to the same degree by reaction of electrode deposits at the full scale as at the pilot scale. Following the rule of addition set forth in the first sentence of this paragraph gives the following estimates of SO_2 removal at full scale, assuming an approach of 20-30°F and with an ESP of the size at Beverly:

Table 6-8. Utilization Measured Across the ESP For Test 29-SL-01[1]

LOCATION	% UTILIZATION AS DETERMINED BY:	
	GAS SAMPLING	SOLIDS ANALYSES
ESP INLET	25.9	20.6
ESP HOPPER # 1		22.5
HOPPER # 2		52.3
HOPPER # 3		46.5
ESP OUTLET	31.7	
SYSTEM OUTLET[2]		47.4

---

1. Conditions: Ca/S Ratio = 1.91
   Approach = 47°F
   SO_2 at Inlet = 1836 ppm
2. No sampling ports exist at the ESP exit. The outlet test station is located approximately 100 ft downstream of the ESP, past the system fan.

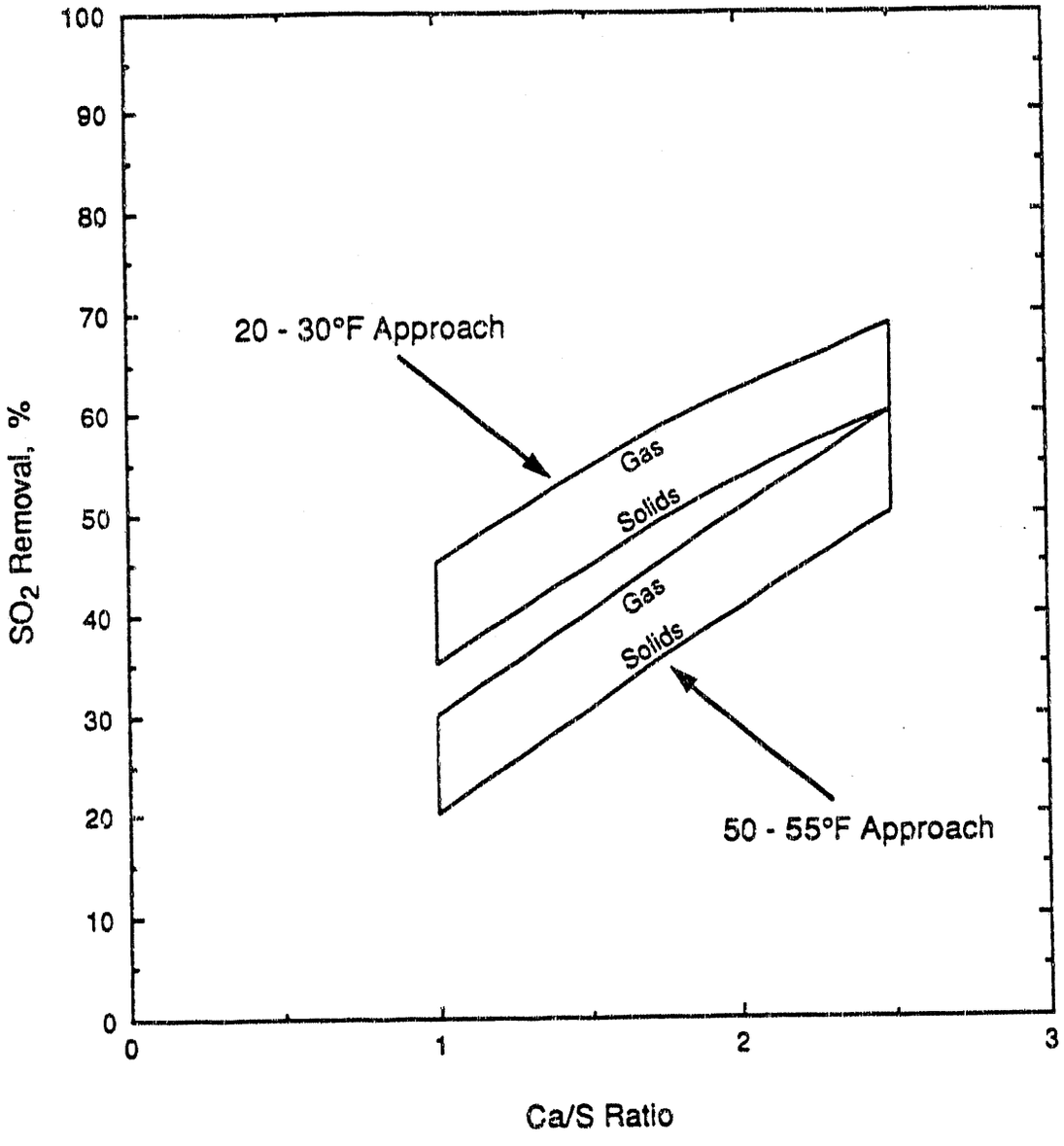

Figure 6-17. Upper and lower limits of SO_2 removal at the ESP inlet based on gas-phase and solids analyses.

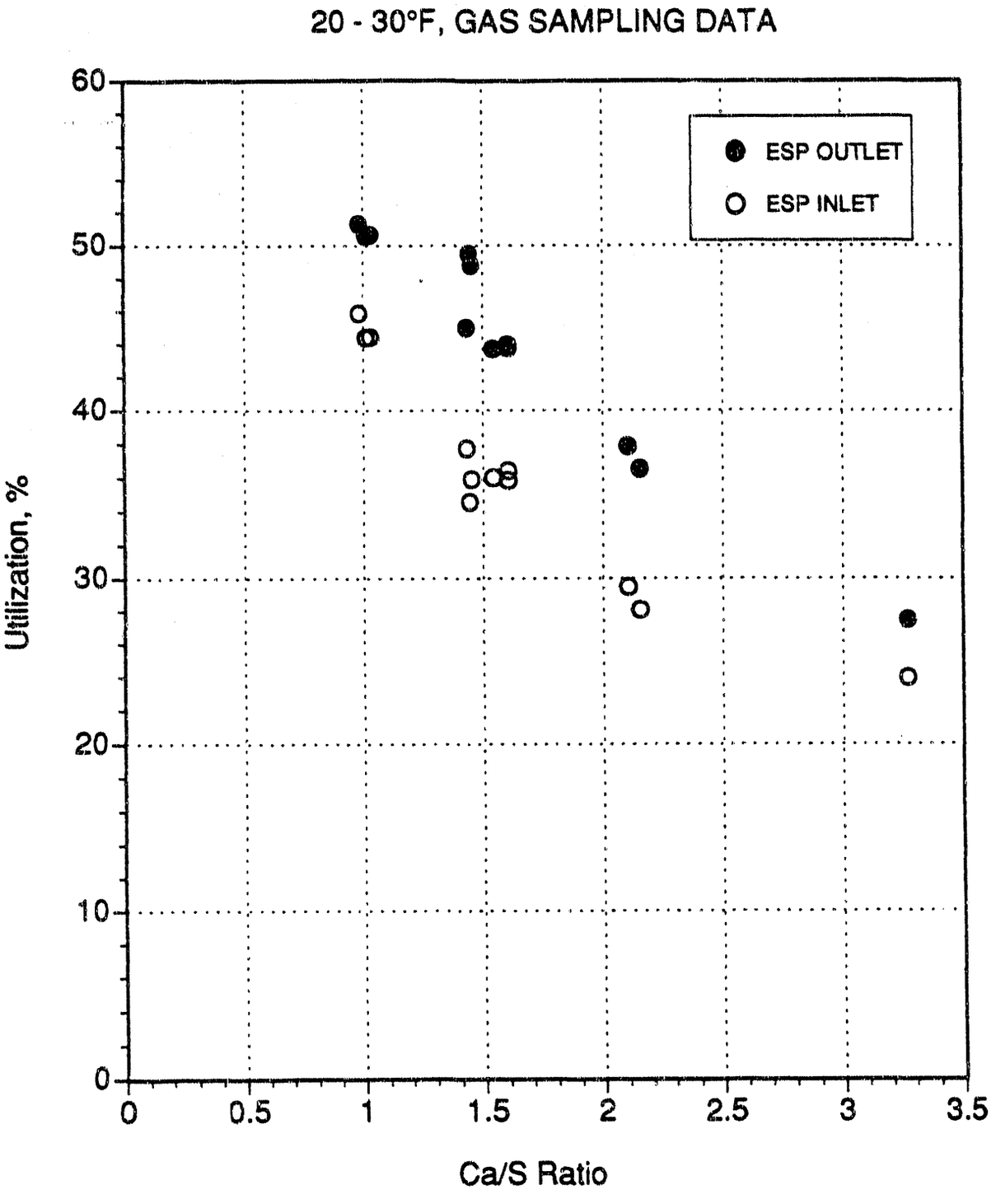

Figure 6-18. Percent of sorbent utilized at the ESP inlet and outlet as determined by the gas sampling system. Summary of test data for approach temperatures from 20 to 30° F.

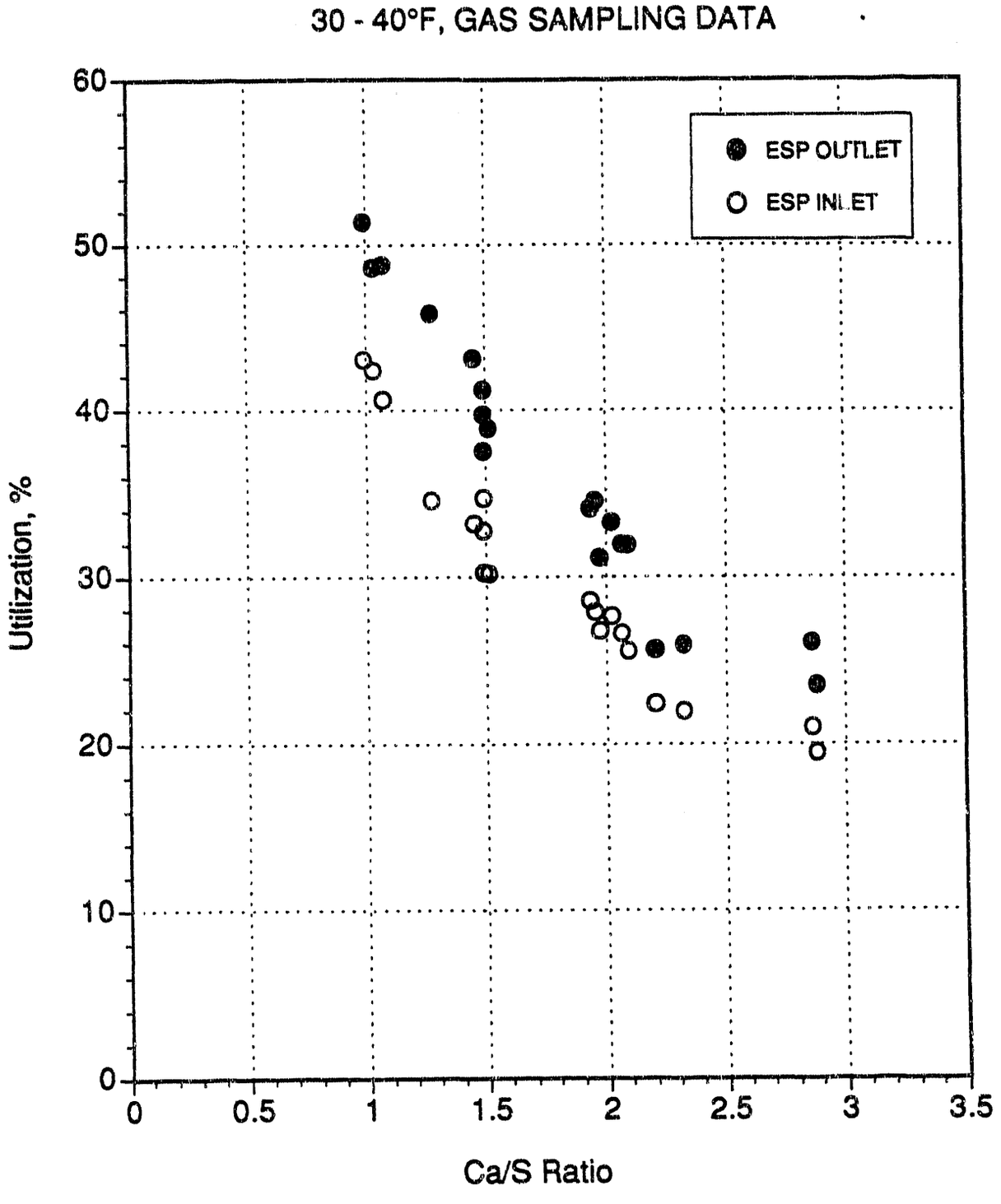

Figure 6-19. Percent of sorbent utilized at the ESP inlet and outlet as determined by the gas sampling system. Summary of test data for approach temperatures from 30 to 40°F.

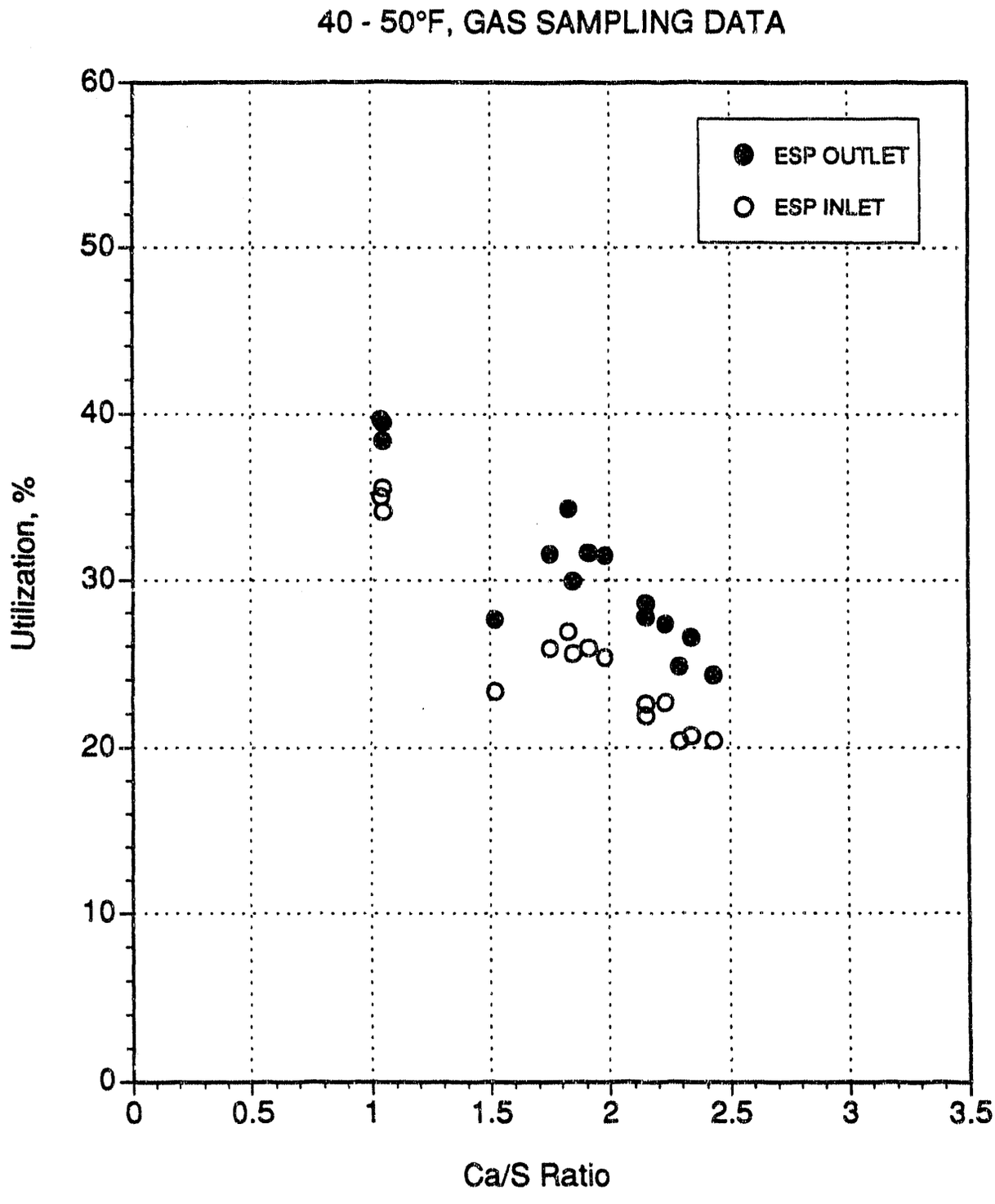

Figure 6-20. Percent of sorbent utilized at the ESP inlet and outlet as determined by the gas sampling system. Summary of test data for approach temperatures from 40 to 50°F.

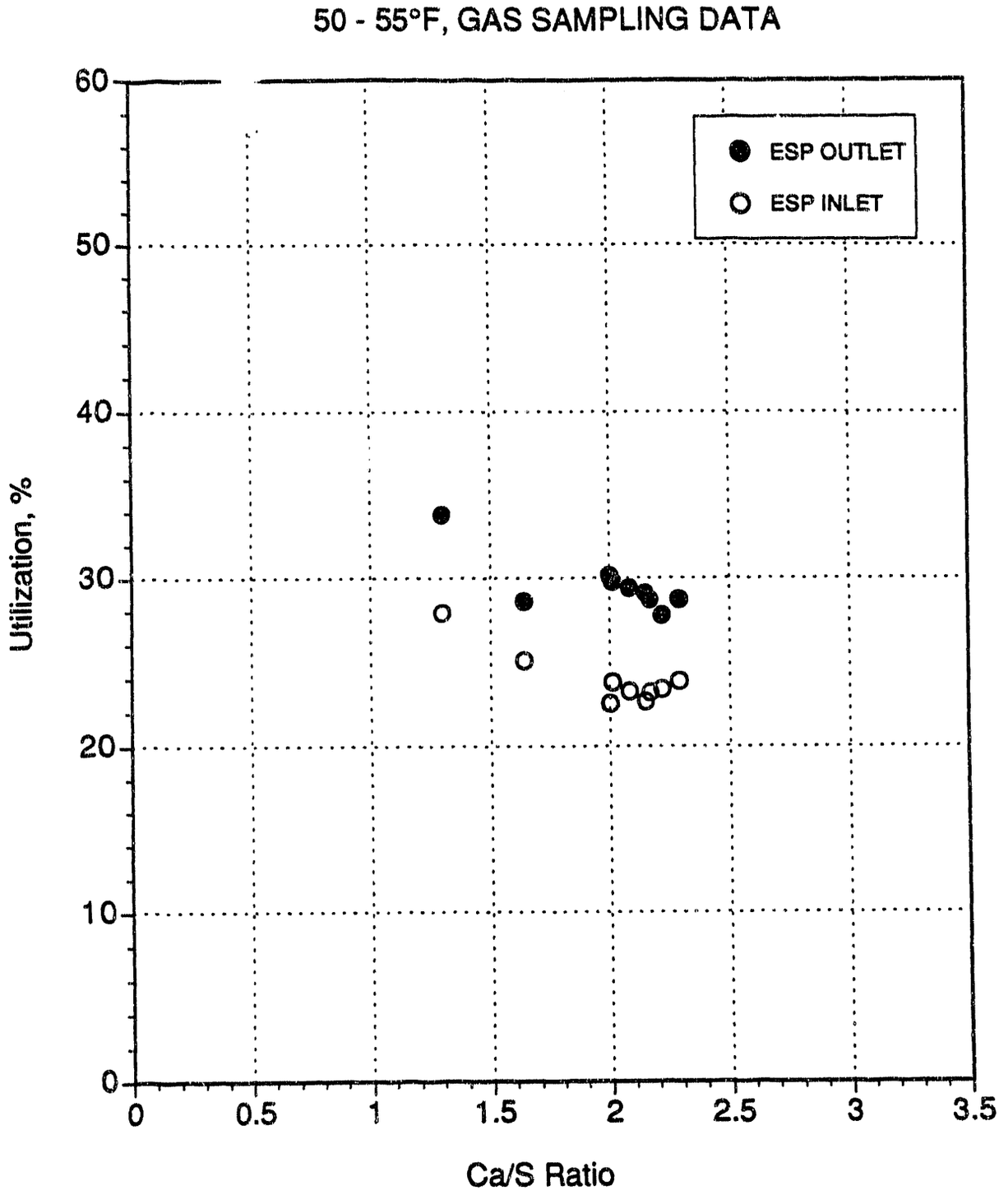

Figure 6-21. Percent of sorbent utilized at the ESP inlet and outlet as determined by the gas sampling system. Summary of test data for approach temperatures from 50 to 55°F.

Ca/S	Removal of SO_2, %		
	Duct	ESP	Total
1.0	35	15	50
2.0	53	16	69
2.5	60	17	77

6.3.2.6 Calculations of Heat Balance

Heat balance calculations were made for 22 periods of testing that spanned a time period from January 27, 1991, to February 4, 1991. The results of these calculations are shown in Tables 6-9A through 6-9D. For the purposes of these calculations heat balance was based on a comparison of the enthalpy (referenced to 25° C) of each component of the system at the system inlet (Enthalpy In) and at the ESP inlet (Enthalpy Out). Heat closure is defined by:

$$\% \text{ Closure} = [100 \bullet (\text{Enthalpy Out/Enthalpy In}] - 100.$$

Thus, if every source of heat loss and heat gain is accounted for, the % Closure will be zero. Positive values of heat balance closure indicate that more energy was accounted for at the system outlet than at the system inlet (a net energy gain). Likewise, negative values of heat balance closure indicate that more energy was accounted for at the system inlet that at the system outlet (a net energy loss).

For the purposes of our calculations of enthalpy at the system inlet, sources of heat energy were considered to be the incoming flue gas, the incoming ash, air that was injected with the slurry through the nozzles, the solids in the slurry, and heat from the reaction of SO_2 with $Ca(OH)_2$. At the ESP inlet, heat energy had been expended to vaporize and heat water (both slurry and humidification water), slurry solids, and the compressed air that entered through the nozzles. Likewise, the heating and vaporization of water cooled the flue gas that entered the system to the ESP inlet temperature.

For these calculations, molar heat capacities were determined by integrating polynomial curve fits for the heat capacity of each component in flue gas (O_2, N_2, CO_2, H_2O), and by assuming the specific heat capacity of $Ca(OH)_2$ was the same as that of fly ash. Molar heat capacities were determined at the system inlet and at the ESP inlet. The molar heat capacity was also determined for air at the temperature of injection into the lances. If the incoming air was less than 25° C (77° F) then a negative enthalpy could be calculated. This did occur frequently because ambient temperatures at the DITF in January averaged much lower than 77° F.

It is unrealistic to interpret heat closure calculations in terms of a percentage (even though such results are given in Table 6-9) since neither the enthalpy entering the system nor the enthalpy leaving the system can be assigned an absolute value. Enthalpy must always be thought of as a difference from the value in some reference state. In Table 6-9, the reference state was taken to be 25 °C. If, however, the reference state had been assumed to be 0 K, the enthalpy values would have been larger and the differences as "% closure" would have been smaller.

Thus, in addition to values of % closure, values of "equivalent ΔT" were calculated as well. This parameter does not imply that the observed change in temperature was incorrect. Instead, it represents the cooling observed that was in excess of that expected from the recorded amount of

Table 6-9A. Results of Heat Balance Calculations, Part 1

TEST:		28-SL-02	28-SL-02	28-SL-03	28-SL-03	28-SL-04	28-SL-04
DATE:		1/27/91	1/27/91	1/28/91	1/28/91	1/29/91	1/29/91
	Units						
Ca/S Ratio	–	1.51	1.53	1.50	1.50	1.58	1.47
Approach	(°F)	45.3	46.6	36.2	35.6	25.6	25.7
SO_2 Removal at ESP	(%)	45.1	45.6	48.8	51.8	55.6	53.9
GAS IN							
Flue Gas Flow	(acfm)	50321	50370	49871	49844	49857	49952
Flue Gas Temp	(°F)	314.4	314.4	309.6	309.5	309.4	309.4
SO_2	(ppm)	1804	1788	1873	1870	1805	1909
O_2	(%)	11.63	11.71	11.39	11.42	11.53	11.32
CO_2	(%)	9.0	9.0	9.0	9.0	9.0	9.0
H_2O	(%)	4.9	4.9	5.0	5.0	6.1	6.1
SLURRY/AIR IN							
Slurry Flow	(gpm)	7.82	7.88	7.95	7.94	7.78	7.67
Solids	(%)	24.07	24.07	24.58	24.58	25.18	25.18
$Ca(OH)_2$	(%)	22.9	22.9	23.1	23.1	23.55	23.55
Density	(gm/cc)	1.1444	1.1444	1.1484	1.1484	1.1527	1.1527
Air in Flow	(scfm)	1181	1180	1172	1167	1174	1166
Air/Slurry Temp	(°F)	71.3	71.3	75.4	77.3	70.3	73.7
HUMID. WATER							
Measured Flow	(gpm)	2.52	2.55	3.60	4.04	4.60	4.70
Expected Flow with No Heat Loss	(gpm)	4.12	3.98	4.43	4.50	5.32	5.44
ESP INLET							
SO_2	(ppm)	968	957	941	871	789	873
O_2	(%)	11.84	11.86	11.56	11.73	11.68	11.4
CO_2	(%)	8.5	8.5	8.5	8.5	8.5	8.5
H_2O	(%)	9.4	9.4	8.94	8.9	10.44	10.44
Flue Gas Temp	(°F)	166.6	167.9	157.3	156.7	149.2	149.3
Adiabatic Saturation	(°F)	121.3	121.3	121.1	121.1	123.6	123.6
ENTHALPY IN							
Flue Gas In	(KCal/min)	38730.2	38768.7	37831.6	37799.8	37865.7	37935.8
Ash In	(KCal/min)	193.9	192.4	195.5	195.0	188.2	199.4
Air In	(KCal/min)	-25.4	-25.2	-7.0	1.3	-29.5	-14.4
Slurry Solids In	(KCal/min)	-7.3	-7.3	-2.1	0.4	-9.0	-4.4
Reaction	(KCal/min)	1175.4	1178.8	1318.1	1396.4	1445.3	1484.9
ENTHALPY OUT							
Heated Air	(KCal/min)	476.3	482.8	423.8	418.8	381.5	379.5
Htd. Slurry Solids	(KCal/min)	187.7	190.8	174.4	172.9	155.2	157.6
Vap. & Htg. of Water	(KCal/min)	21288.9	21488.6	23922.9	24925.0	25649.9	25707.4
Flue Gas	(KCal/min)	14442.9	14668.6	12899.6	12797.4	11610.4	11648.2
TOTAL IN	(KCal/min)	40067	40107	39336	39393	39461	39601
TOTAL OUT	(KCal/min)	36396	36831	37421	38314	37797	37893
Difference	(KCal/min)	3671	3277	1915	1079	1664	1709
HEAT BALANCE							
% Closure	(%)	-9.2	-8.2	-4.9	-2.7	-4.2	-4.3
Equivalent ΔT	°F	20.7	18.4	10.8	6.1	9.3	9.5

Table 6-9B. Results of Heat Balance Calculations, Part 2

TEST:		28-SL-04	28-SL-04	28-SL-05	28-SL-05	28-SL-05	28-SL-06
DATE:		1/29/91	1/29/91	1/31/91	1/31/91	1/31/91	2/1/91
	Units						
Ca/S Ratio	–	1.64	1.64	1.08	1.07	1.08	1.02
Approach	(°F)	25.3	24.4	44.5	43.4	43.1	36.0
SO_2 Removal at ESP	(%)	56.4	58.3	37.4	36.8	35.9	40.6
GAS IN							
Flue Gas Flow	(acfm)	49822	49849	49792	49856	49863	49905
Flue Gas Temp	(°F)	309.4	309.4	309.44	309.56	309.41	309.5
SO_2	(ppm)	1780	1773	1790	1803	1780	1876
O_2	(%)	11.78	11.73	12.04	12.00	12.12	11.54
CO_2	(%)	9.0	9.0	9.0	9.0	9.0	9.0
H_2O	(%)	6.1	6.1	6.5	6.5	6.5	6.5
SLURRY/AIR IN							
Slurry Flow	(gpm)	7.96	7.96	5.42	5.4	5.39	5.39
Solids	(%)	25.18	25.18	24.41	24.41	24.41	24.04
$Ca(OH)_2$	(%)	23.55	23.55	22.99	22.99	22.99	22.8
Density	(gm/cc)	1.1527	1.1527	1.1473	1.1473	1.1473	1.1461
Air In Flow	(acfm)	1151	1147	1199	1199	1194	1182
Air/Slurry Temp	(°F)	81.0	81.0	46.0	37.7	43.9	65.8
HUMID. WATER							
Measured Flow	(gpm)	4.79	5.00	5.42	3.76	3.81	5.19
Expected Flow with No Heat Loss	(gpm)	5.15	5.24	5.64	5.79	5.78	6.35
ESP INLET							
SO_2	(ppm)	758	728	1075	1089	1112	1077
O_2	(%)	12	11.87	12.4	12.4	12.34	11.86
CO_2	(%)	8.5	8.5	8.5	8.5	8.5	8.5
H_2O	(%)	10.57	10.82	9.39	9.27	9.55	9.98
Flue Gas Temp	(°F)	148.9	148	169	167.9	167.6	160.5
Adiabatic Saturation	(°F)	123.6	123.6	124.5	124.5	124.5	124.5
ENTHALPY IN							
Flue Gas In	(KCal/min)	37841.6	37861.6	37850.2	37912.5	37901.5	37938.2
Ash In	(KCal/min)	185.4	184.8	186.4	188.1	185.6	195.8
Air In	(KCal/min)	17.3	17.2	-139.1	-176.2	-147.9	-49.6
Slurry Solids In	(KCal/min)	5.5	5.5	-27.9	-35.3	-29.7	-9.9
Reaction	(KCal/min)	1444.5	1489.1	963.2	954.7	921.4	1097.2
ENTHALPY OUT							
Heated Air	(KCal/min)	372.8	366.8	495.7	489.5	486.0	444.1
Htd. Slurry Solids	(KCal/min)	156.0	153.8	156.7	155.1	153.5	143.9
Vap. & Htg. of Water	(KCal/min)	26575.0	27043.8	22854.7	18976.4	19128.1	22485.7
Flue Gas	(KCal/min)	11554.3	11414.9	14809.4	14647.4	14604.0	13459.7
TOTAL IN	(KCal/min)	39494	39558	38833	38844	38831	39172
TOTAL OUT	(KCal/min)	38658	38979	38316	34268	34372	36514
Difference	(KCal/min)	836	579	516	4575	4459	2658
HEAT BALANCE							
% Closure	(%)	-2.1	-1.5	-1.3	-11.8	-11.5	-6.8
Equivalent ΔT	°F	4.7	3.2	2.9	26.0	25.3	15.0

Table 6-9C. Results of Heat Balance Calculations, Part 3

TEST:		28-SL-06	28-SL-06	28-SL-07	28-SL-07	28-SL-07	29-SL-01
DATE:		2/1/91	2/1/91	2/2/91	2/2/91	2/2/91	2/3/91
	Units						
Ca/S Ratio	–	1.06	1.11	1.03	1.06	1.00	1.95
Approach	(°F)	35.8	36.0	28.0	26.0	29.4	47.7
SO_2 Removal at ESP	(%)	41.1	41.5	44.9	45.8	45.0	49.5
GAS IN							
Flue Gas Flow	(acfm)	49798	49895	49862	49901	49897	49934
Flue Gas Temp	(°F)	309.6	309.5	309.5	309.5	309.5	309.3
SO_2	(ppm)	1799	1702	1781	1790	1855	1836
O_2	(%)	11.91	12.14	11.51	11.50	11.52	11.56
CO_2	(%)	9.0	9.0	9.0	9.0	9.0	9.0
H_2O	(%)	6.5	6.5	6.0	6.0	6.0	6.0
SLURRY/AIR IN							
Slurry Flow	(gpm)	5.39	5.32	5.33	5.49	5.38	10.5
Solids	(%)	24.04	24.04	23.68	23.68	23.68	23.44
$Ca(OH)_2$	(%)	22.8	22.8	22.27	22.27	22.27	22.14
Density	(gm/cc)	1.1461	1.1461	1.1486	1.1486	1.1486	1.1473
Air In Flow	(scfm)	1180	1177	1185	1175	1167	1159.3
Air/Slurry Temp	(°F)	73.1	78.0	74.8	79.0	83.3	73.1
HUMID. WATER							
Measured Flow	(gpm)	5.18	5.40	6.29	6.26	6.45	0.00
Expected Flow with No Heat Loss	(gpm)	6.31	6.33	7.06	7.08	6.91	1.03
ESP INLET							
SO_2	(ppm)	1013	962	945	931	976	900
O_2	(%)	12.31	12.44	11.85	11.88	11.93	11.84
CO_2	(%)	8.5	8.5	8.5	8.5	8.5	8.7
H_2O	(%)	9.99	10.11	10.04	10.13	10.15	9.44
Flue Gas Temp	(°F)	160.3	160.5	151.4	149.4	152.8	171
Adiabatic Saturation	(°F)	124.5	124.5	123.4	123.4	123.4	123.3
ENTHALPY IN							
Flue Gas In	(KCal/min)	37872.2	37936.5	37874.9	37904.4	37901.6	37906.7
Ash In	(KCal/min)	187.5	177.6	185.8	186.9	193.6	191.6
Air In	(KCal/min)	-17.3	4.4	-9.8	8.8	27.6	-16.9
Slurry Solids In	(KCal/min)	-3.4	0.9	-1.9	1.8	5.5	-6.5
Reaction	(KCal/min)	1062.9	1017.7	1152.7	1182.0	1203.1	1310.4
ENTHALPY OUT							
Heated Air	(KCal/min)	442.5	442.6	397.0	383.1	398.5	490.6
Htd. Slurry Solids	(KCal/min)	140.6	136.4	123.5	122.3	129.0	235.1
Vap. & Htg. of Water	(KCal/min)	22525.1	22947.2	24941.9	25226.2	25531.0	21136.2
Flue Gas	(KCal/min)	13397.7	13458.6	11964.1	11649.6	12199.2	15166.6
TOTAL IN	(KCal/min)	39102	39137	39202	39284	39331	39385
TOTAL OUT	(KCal/min)	36506	36985	37426	37381	38258	37028
Difference	(KCal/min)	2596	2152	1775	1903	1074	2357
HEAT BALANCE							
% Closure	(%)	-6.6	-5.5	-4.5	-4.8	-2.7	-6.0
Equivalent ΔT	°F	14.7	12.1	10.0	10.7	6.0	13.3

Table 6-9D. Results of Heat Balance Calculations, Part 4

TEST:		29-SL-01	29-SL-02	29-SL-02	29-SL-02
DATE:		2/3/91	2/4/91	2/4/91	2/4/91
	Units				
Ca/S Ratio	–	1.89	2.02	2.07	2.11
Approach	(°F)	49.5	38.1	37.4	37.7
SO_2 Removal at ESP	(%)	47.2	52.7	55.8	54.8
GAS IN					
Flue Gas Flow	(acfm)	49936	49885	49822	49918
Flue Gas Temp	(°F)	308.4	309.5	309.5	309.3
SO_2	(ppm)	1878	1766	1773	1752
O_2	(%)	11.2	11.64	11.72	11.51
CO_2	(%)	9.0	9.0	9.0	9.0
H_2O	(%)	6.0	6.0	6.0	6.0
SLURRY/AIR IN					
Slurry Flow	(gpm)	10.43	10.79	11.1	11.18
Solids	(%)	23.44	22.96	22.96	22.96
$Ca(OH)_2$	(%)	22.14	21.48	21.48	21.48
Density	(gm/cc)	1.1473	1.1422	1.1422	1.1422
Air In Flow	(scfm)	1140.9	1168.1	1156.5	1140.7
Air/Slurry Temp	(°F)	86.9	70.1	74.2	87.0
HUMID. WATER					
Measured Flow	(gpm)	0.00	0.00	0.00	0.00
Expected Flow with No Heat Loss	(gpm)	0.85	1.52	1.32	1.19
ESP INLET					
SO_2	(ppm)	952	812	762	768
O_2	(%)	11.59	11.89	11.98	11.79
CO_2	(%)	8.7	8.7	8.7	8.7
H_2O	(%)	9.23	9.5	9.62	9.66
Flue Gas Temp	(°F)	172.8	161.5	160.8	161.0
Adiabatic Saturation	(°F)	123.3	123.4	123.4	123.3
ENTHALPY IN					
Flue Gas In	(KCal/min)	37799.4	37893.7	37846.6	37894.1
Ash In	(KCal/min)	195.3	184.3	184.8	182.8
Air In	(KCal/min)	42.4	-30.2	-12.1	42.8
Slurry Solids In	(KCal/min)	16.5	-11.6	-4.8	17.4
Reaction	(KCal/min)	1281.4	1342.6	1423.4	1385.6
ENTHALPY OUT					
Heated Air	(KCal/min)	492.5	444.3	436.3	431.8
Htd. Slurry Solids	(KCal/min)	240.3	208.9	211.4	212.3
Vap. & Htg. of Water	(KCal/min)	21158.0	21640.8	22302.8	22612.1
Flue Gas	(KCal/min)	15476.9	13606.3	13476.0	13537.4
TOTAL IN	(KCal/min)	39335	39379	39438	39523
TOTAL OUT	(KCal/min)	37368	35900	36426	36793
Difference	(KCal/min)	1967	3478	3011	2729
HEAT BALANCE					
% Closure	(%)	-5.0	-8.8	-7.6	-6.9
Equivalent ΔT	°F	11.1	19.6	16.9	15.3

water added. Part of the excess (we believe not much) was due to heat losses to the surroundings. Most of the excess cooling, on the other hand, seems attributable to inaccurate data on the rates of water supplied for evaporation. Specifically, we believe that the actual rate of water addition exceeded that recorded. The parameter "Expected Flow" is the rate of water addition that would have balanced inlet and outlet enthalpy rates in the absence of heat losses to the surroundings.

Each value of equivalent ΔT was determined by assuming that the difference between the enthalpy calculated at the system inlet and the enthalpy calculated at the ESP inlet could be set equal to the product of the mass at the ESP inlet (air, water, slurry, ash, and flue gas), an average specific heat capacity at the ESP inlet, and the equivalent ΔT. The average specific heat capacity was determined by taking the molar heat capacity of each component of the mass at the ESP inlet, determining a specific heat capacity for that component, and weighting that specific heat capacity by the percentage of total mass of that component. A weighted sum was then made to obtain this average specific heat capacity.

In general, the heat balances shown by % closure and equivalent ΔT in Table 6-9 are small. There are, however, a number of cases where % closure exceeds 9% or equivalent ΔT exceeds 20 °F. These results are higher than they should be, considering the effort expended to make the measurements that were used in making the calculations. As suggested above, however, the accuracy of measurements of water addition rates was somewhat doubtful, and conversations with DITF personnel made us convinced that errors in these measurements -- specifically, observed rates that were lower than the actual rates -- were the most likely cause of heat imbalances. The DITF personnel confirmed that the orifice plate that is used to monitor water flow (in the humidification line, not the slurry line) was sized for flow rates higher (about 20 gal/min) than those employed. They also said that at low rates the water flow is made unstable by two factors: insufficient fine adjustment in the flow controller, and back pressure from the slurry line into which the humidification water is fed. Our plans are to recalibrate the humidification water flow controller and meter in the future.

6.3.2.7 Comparison with Data from Other Sources

A comparison of the present results on slurry injection for the removal of SO_2 and the earlier results from previous investigations is given in Figure 6-22. The data in this figure are for an approach of 30-40° F and a range of Ca/S ratios up to 2.0. All three studies included the effects of an ESP. There is very good agreement between the results at Ca/S ratios that are common to all three studies. The principal difference evident in the figure is that the removal indicated by the present investigation rises less sharply as the Ca/S ratio increases above a value of 1.6. The difference at Ca/S ratios above this value, however, is more implied than real, since no data in this range were recorded in the previous studies. Further remarks on the background of the data compared in Figure 6-22 are given in the following paragraphs.

The data points representing results from the present investigation are based on the data in Figure 6-10. The assigned values of removal plotted in Figure 6-22 are as follows: Ca/S = 1.0, 50%; Ca/S = 1.5, 58%; and Ca/S = 2.0, 64%.

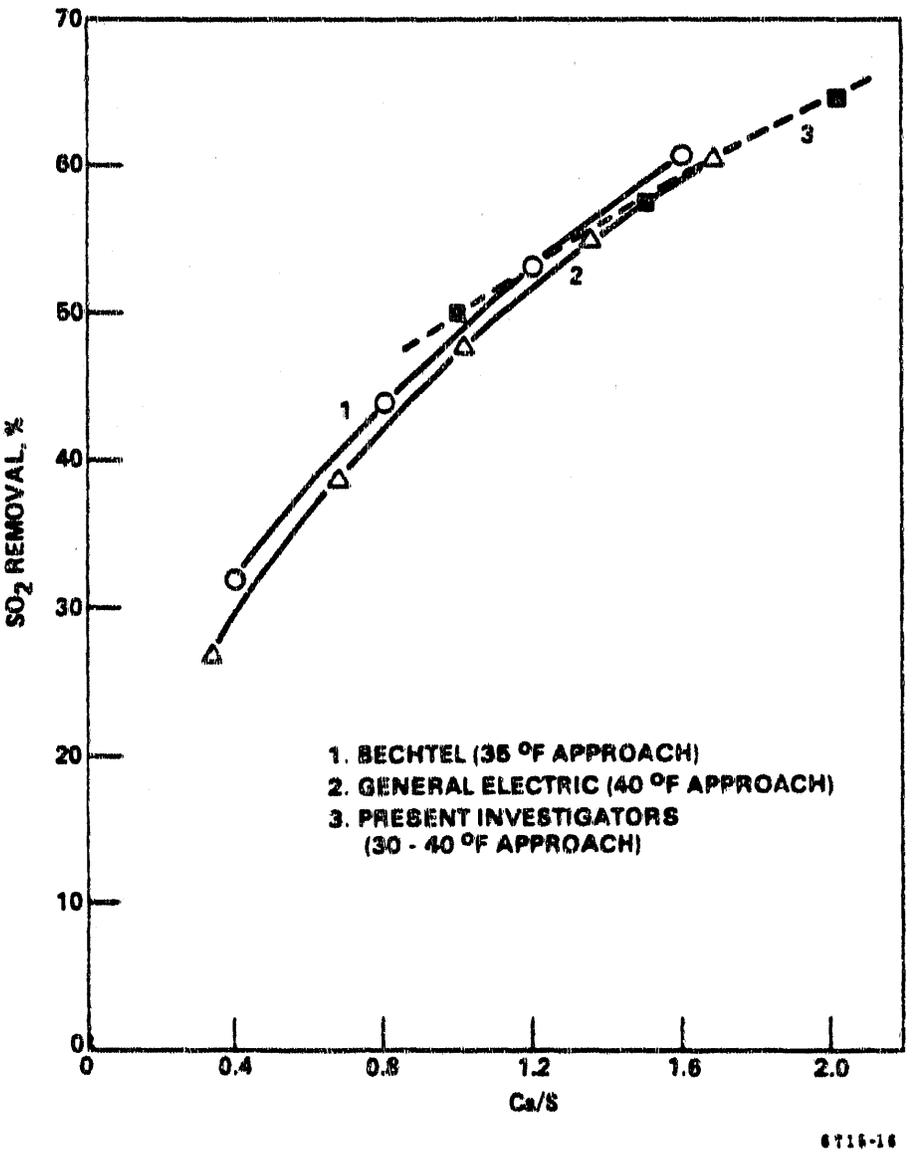

Figure 6-22. Data from Bechtel, GE, and the present investigators.

The other investigations represented in Figure 6-22 were conducted by Bechtel[1] and General Electric[2] under DOE auspices. Bechtel investigated the Confined-Zone Dispersion (CZD) process, in which the slurry is meant to be dispersed by a spray nozzle within a duct but isolated from the duct walls with a sheath of hot gas; Bechtel's investigations were conducted at Consumer Power's Campbell Station at the 7-MW scale and at Pennsylvania Electric Company's Seward Station at the 70-MW scale. General Electric's process was termed the In-Duct Scrubbing (IDS) process; the heart of the IDS process was a rotary atomizer for dispersing the $Ca(OH)_2$ slurry. The IDS process was investigated in the 12-MW pilot facility subsequently modified and now in use for the present investigation at Ohio Edison's Muskingum River Station.

Bechtel correlated SO_2 removal, expressed as a fraction of the inlet concentration, with key variables in equations of the form below:

$$\text{Fractional } SO_2 \text{ removal} = K(NWIR)0.65(Wt\%)0.45(\text{Avg } SO_2)\text{-}0.4(AST)\text{-}0.4$$

where K = coefficient for the selected sorbent type (calcitic or dolomitic lime)

NWIR = "normalized water injection rate", expressed as the ratio of water addition in gallons per minute to gas flow in thousands of standard cubic feet per minute

Wt% = sorbent concentration in the slurry

Avg SO_2 = average of inlet and outlet SO_2 concentrations in parts per million on the wet basis

AST = approach to adiabatic saturation in degrees Fahrenheit.

The Bechtel equation fundamentally deals with the effects of two key parameters: the degree of humidification and the Ca/S ratio. The equation does not, however, contain either parameter as an explicit term. The effects of humidification appear in two terms, NWIR and AST; the effects of these two terms obviously cannot be independent, however, because the rate of water addition is a major factor in determining approach to saturation. The effects of the Ca/S ratio appear through three terms -- NWIR and Wt%, which introduce the quantity of sorbent in the numerator, and Avg SO_2, which indirectly places the inlet concentration in the denominator but not in a simple form.

General Electric derived a theoretical equation relating the fractional removal of SO_2 within the evaporation zone to the degree of humidification and the Ca/S ratio, with the following form:

$$-\ln(1 - E) = a\, S \ln [(T_i - T_{as})/(T_f - T_{as})]$$

where E = fractional SO_2 removal

a = constant

---

[1]Bechtel National, Inc., "Desulfurization of Flue Gas by the Confined Zone Dispersion Method," Final Report to Department of Energy, Contract DE-AC22-85PC81009, April 1988 (draft).

[2]E. A. Samuel, K. R. Murphy, and A. Demian, "A 12-MW Pilot Study of In-Duct Scrubbing (IDS) Using a Rotary Atomizer," Final Report to Department of Energy, Contract DE-AC22-85PC81010, January 1989 (draft).

S = Ca/S ratio

T_i = initial gas temperature

T_f = final gas temperature

T_{as} = adiabatic saturation temperature (the difference $T_f - T_{as}$, then, is the approach to saturation).

Practical experience showed that the theoretical equation could be usefully modified by the empirical addition of an exponent:

$$-\ln(1 - E) = a X^b$$

where b = constant

$$X = S \ln[(T_i - T_{as})/(T_f - T_{as})]$$

With the empirical modification, the equation was used satisfactorily for correlating SO_2 removal with Ca/S and approach to saturation both within the evaporation zone and the total system, including an ESP.

The Bechtel report states that data were recorded as approaches to saturation ranging from 25 to 55°F; however, the report clearly shows that the majority of the data points were taken at AST = 35°F and SO_2 concentrations near 1500 ppm. The General Electric study, at SO_2 concentrations around 2000 ppm, was based on approaches to saturation not less than 40°F. Accordingly, the Bechtel and GE data shown in Figure 6-22 are designated as being for approaches of 35 and 40°F, respectively.

6.4 Electrostatic Precipitator Performance with Sorbent Injection

A reliable evaluation of electrostatic precipitator performance with sorbent injection requires several days of relatively stable process conditions. This time period is necessary to allow an equilibrium thickness of a dust layer with properties representative of the process condition under study to accumulate on the electrodes.

During this initial phase of experimental measurements, emphasis has been placed on parametric testing with relatively short-duration test periods. Although these conditions are not ideal for precipitator performance tests, some useful information has been obtained. Specifically, voltage-current relationships were obtained with dry sorbent injection, and electrical operating conditions and mass collection efficiencies were obtained with slurry injection.

Dry sorbent injection caused a significant degradation in the electrical operating conditions with both downstream (scavenging) and upstream (non-scavenging) humidification. The inlet field exhibited severe corona current suppression, to the point that corona onset and sparkover voltages were separated by only 2 kV. Mass collection efficiencies across the ESP were not determined during these initial tests.

With slurry injection, voltage-current relationships were usually normal, as would be expected with a low resistivity dust. Figure 6-23 contains a typical set of V-I curves for the four fields of the ESP during slurry injection at a Ca/S of 2 with a 25°F approach to saturation. Table 6-10 contains ESP performance data obtained during a series of parametric test from January 25 through February 4, 1991. Averaged electrical operating points obtained during this same test period are presented in Table 6-11. In general, operating points near the maximum points recorded for each TR set were achieved during the test period. Occasional problems were experienced with shorting due to build-ups of low resistivity dust which caused sparkover at low voltages. These problems were resolved during the parametric test program by power-off rapping or, in one case, by manual cleaning of dust build ups in the ESP prior to this test series.

The mass emission data in Table 6-10 were calculated on a $lb/10^6$ Btu basis using the following procedure: 1) the inlet loading of fly ash to the ESP was increased by an amount equal to the dilution of fly ash concentration resulting from the dilution burner operation, 2) the efficiency of the ESP was used with the adjusted inlet loading to calculate an outlet mass concentration for each condition shown in Table 6-10, and 3) the resulting outlet mass concentrations were converted to $lb/10^6$ Btu as if they were measured on a boiler with a flue gas oxygen content of 5.6%. This procedure is necessary because of the excess oxygen introduced by the DITF dilution burner. A precipitation rate parameter (omega-k) is shown in Table 6-10 to indicate relative performance. As points of reference, omega k values of full-scale ESPs collecting ash downstream of spray dryers have been reported to range from 27 to 62 cm/s. With the exception of one data point taken while a problem with build up in the horizontal duct was occurring, the ESP performance was acceptable. The data at 25°F approach show no indication of severe reentrainment problems as has been reported with the E-SO_X process.[3]

A recent DOE survey has indicated that most ESP installations for plants that may consider duct injection technology have SCA values less than 325 $ft^2/1000$ acfm. Therefore, future testing of ESP performance with sorbent injection will be conducted with one or two of the TR sets deenergized.

---

[3]Marchant, G. H., Jr., J. P. Gooch, M. G. Faulkner, "Effects of E-SO_X Technology on ESP Performance", presented at the Eighth Symposium on the Transfer and Utilization of Particulate Control Technology, San Diego, CA, March, 1990.

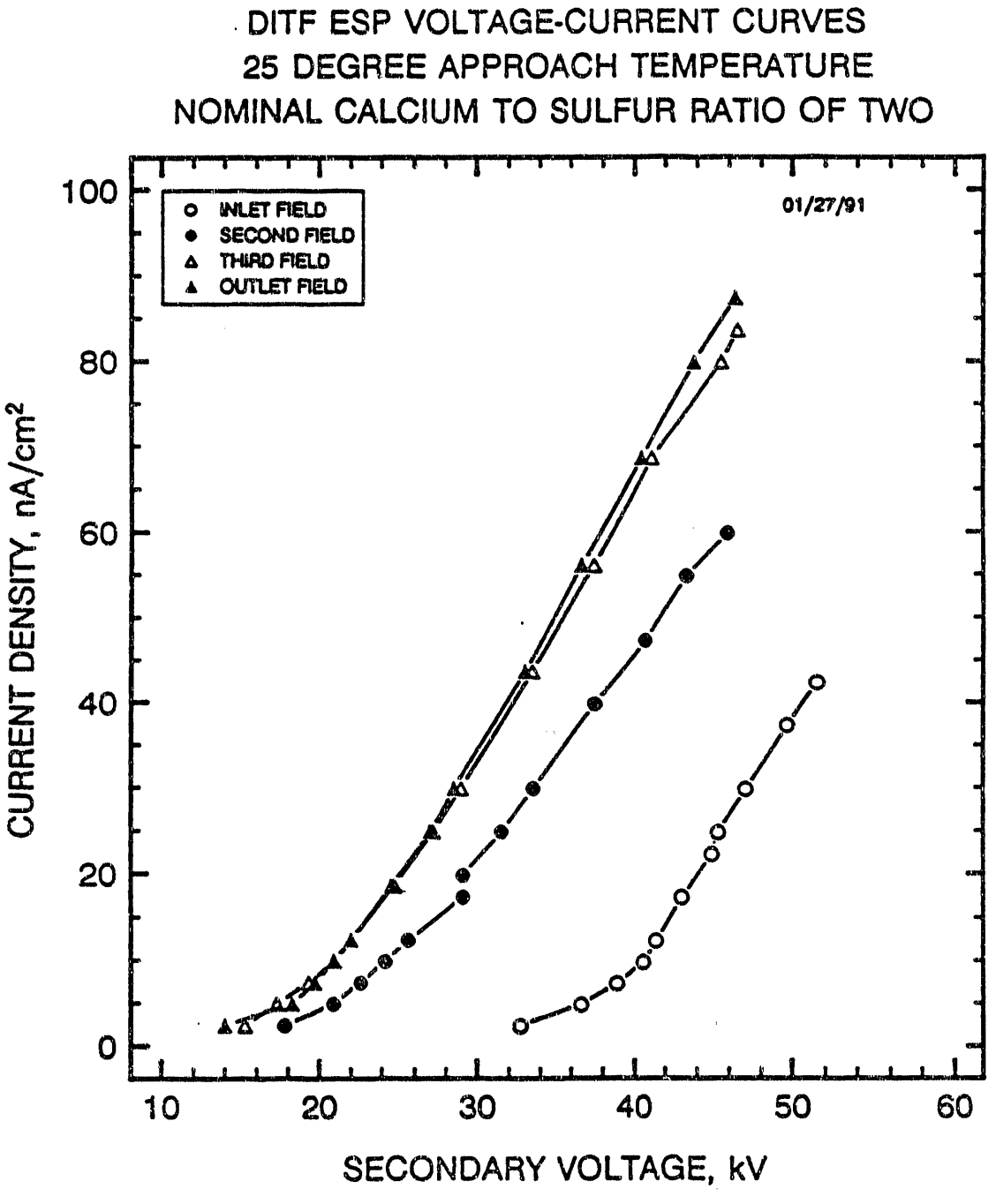

Figure 6-23. Current density as a function of applied ESP voltage.

Table 6-10. ESP PARAMETRIC TEST SUMMARY

Nominal Ca/S Ratio, Approach Temperature	Inlet grains/ dscf	Outlet		%, Efficiency	w_k, cm-sec	SCA	Inlet dscfm	Date
		gr/dscf	lb/10^6 Btu[B]					
2 Ca/S, 45°F	9.34	0.0043	0.008	99.95	72	417	31257	01/25/91
2 Ca/S, 45°F	8.22	0.0181	0.035	99.78	47	407	31171	02/03/91
2 Ca/S, 35°F	9.59	0.0044	0.008	99.95	75	402	31660	01/26/91
2 Ca/S, 35°F	9.68	0.0042	0.008	99.96	68	446	28787	02/04/91
2 Ca/S, 25°F	8.16	0.0070	0.013	99.91	60	425	30640	01/27/91
1.5 Ca/S, 45°F	7.22	0.0059	0.011	99.92	61	423	30048	01/27/91
1.5 Ca/S, 35°F	7.12	0.0602	0.115	99.16[A]	27	421	29954	01/28/91
1.5 Ca/S, 25°F	7.03	0.0066	0.013	99.91	58	424	30273	01/29/91
1 Ca/S, 45°F	6.39	0.0361	0.069	99.43	33	411	31237	01/31/91
1 Ca/S, 35°F	5.42	0.0331	0.064	99.39	33	401	32541	02/01/91
1 Ca/S, 25°F	4.74	0.0049	0.009	99.90	61	392	33466	02/02/91

[A]Significant build-up in horizontal duct during this test.
[B]Corrected for 5.6% O_2.

Table 6-11. DITF ESP AVERAGE OPERATING POINTS DURING MASS TRAIN TESTS

DATE	INLET FIELD kV	INLET FIELD nA/cm^2	SECOND FIELD kV	SECOND FIELD nA/cm^2	THIRD FIELD kV	THIRD FIELD nA/cm^2	OUTLET FIELD kV	OUTLET FIELD nA/cm^2
1-25	45.9	36	42.6	60	45.0	78	44.7	89
1-26	51.8	37	42.6	60	46.1	82	44.7	87
1-27[a]	46.7	38	50.1	59	47.2	78	47.0	85
1-28	49.8	37	45.9	57	47.6	74	46.1	80
1-29	52.8	39	40.8	59	46.6	83	45.9	85
1-31	39.2	30	38.3	57	41.4	83	40.3	84
2-1	46.5	36	44.5	60	46.1	76	44.7	82
2-2	54.7	38	42.4	61	45.9	77	44.7	81
2-3	43.2	36	42	63	44.6	80	43.4	84
2-4	51.4	38	41.4	61	45.4	81	44.0	86

[a]Operating point before VI curve (no data in DAS files during mass train run)

7.0 MAJOR OPERATIONS AND MAINTENANCE EXPERIENCE

The DITF is staffed to operate continuously, five days per week in three shifts. When required, seven day a week operations is accommodated by the use of overtime. Much of this test series, System Characterization, entailed short term (i.e., 2- to 4-hour) parametric tests. A two shift mode of operation is used for this type of testing with the facility shut down from 12 to 6 A.M. This allowed access to the duct for inspection and cleaning, if necessary.

7.1 Major Milestones of Operations

April 25, 1990--Hot flue gas sent through the duct and baseline ESP testing begun.

May 3, 1990--Nozzle testing with water begun.

June 1, 1990--Construction complete with the flue gas dilution system turned over to the operations staff.

June 20, 1990--Dry hydrated lime testing begun.

August 21, 1990--Lime slurry testing begun.

August 22, 1990--Ohio Power Company outage started.

November 19, 1990--Ohio Power Company outage ended.

February 1, 1991--Task 3.1 Evaluation of System Performance ended.

Total Test Hours (Through April 17, 1991)

Nozzle Testing	71 hours
Dry Hydrate Lime Testing	255 hours
Lime Slurry Testing	677 hours

7.2 Hydrated Lime and Slurry Preparatory Systems

During initial operation of the hydrated lime system, hydrated lime leaks were observed inside the hydrated lime building. The leaks were fixed by welding a plate beneath the belt feeder and repiping the vent system from the ends of the rotary airlock to the chute above the airlock. The belt feeder redundant slide gates were also removed since they were a source of leakage. A maximum of 1800 lbs/hr of hydrated lime, and 2000 lbs/hr of recycle have been run with no problems. Occasionally, the belt enclosure must be opened and cleaned.

The slurry is prepared by mixing Mid Ohio pebble lime with water at a ratio of 1:4 in a detention slaker. The system has run well since initiating the slurry injection testing in August 1990. There is some difficulty in preparing a slurry with a specified solids content since the pebble lime feeder

cannot be recalibrated in place. However, the slaker seems to maintain a solids concentration fairly well. Recent analyses showed a % solid variation from 19.5 to 21.0% within a 4-hour period. This variation would not have a major impact on the DITF overall SO_2 removal efficiency.

7.3 Dry and Slurry Sorbent Injection System

Humidification water for dry injection or slurry sorbent is injected through two spray lances mounted in the flue gas duct. Each lance is connected to three dual-fluid spray nozzles. The two spray lances are attached to flange connections which are slotted to allow rotation of the lance. The initial nozzle testing showed that the ability to rotate the lance and to aim the nozzles greatly reduced low thermocouple readings, an indication of wall wetting, on the duct walls.

The nozzle and lances were constructed from Hastelloy to protect against flue gas and corrosion. There has been no indication of corrosion on the lances and nozzles to date.

7.3.1 Dry Injection System

The dry duct injection nozzle is a single nozzle which directs the air and solids mixture into the duct. A 4-inch beveled pipe injects the dry sorbent into the center of the duct approximately 2 feet upstream of the spray humidification nozzles.

The system has run easily since eliminating the hydrated lime leakage problem. However, because of concerns about good lime mixing, the injection nozzle was extended so that the injection point is now in the same plane as the humidification nozzles. Co-planar injection will be demonstrated when the dry injection testing resumes.

7.3.2 Slurry Injection System

The Lechler nozzles have been used for slurry injection since slurry testing began in August 1990. The nozzles have required minimum maintenance. The key to maintaining nozzle performance has been keeping the nozzles clean by adequate flushing when shutting down, plus periodic inspection.

On one occasion, nozzle air passages became partially plugged as the evident result of significant duct deposits. The nozzles were cleaned in a dilute HCl solution, reinstalled in the duct, and appeared to function properly.

The internal-mix Lechler nozzles are designed with erosion-resistant silicon-carbide inserts. There has been no detectable wear to date on these inserts. During recycle testing, the nozzles will be monitored closely to detect any signs of erosion.

A major problem with slurry injection at the DITF occurs when dilute slurries are used (i.e., with less than 20% solids). When dilute slurries are run, significant deposits occur even at moderate approach temperatures. The duct deposit is minimized only when using concentrated slurries (20% solids or more). Extended tests of up to 120 hours and approaches as close as 25°F have been run with concentrated slurries without significant deposits.

In general, for similar test conditions, duct deposits appeared to be less significant with slurry injection than with dry injection. Co-planar dry injection could improve this performance.

7.4 Duct Cleaning System

The duct cleaning system consists of a sonic horn, three soot blowers, and duct hoppers 10 to 18 feet downstream of the slurry injection points. Since dry deposits are seldom found on the roof or sides of the duct, the performance of the sonic horn is not very clear.

The soot blowers appeared to function efficiently only when the duct deposits are dry. Since duct deposits initiate on the far end lip of the duct hopper, one of the soot blowers, which were located upstream of the duct hopper, was relocated downstream of the duct hopper blowing against the gas flow. This appeared to hinder the dust deposits on the hopper lip. Additional soot blowers will be installed between the duct hoppers to attempt to minimize duct deposits occurring in this area.

Deposits can be controlled by these systems at conditions that minimize deposition. However, at conditions which promote depositions, these systems do not control solids buildup in the duct. On these occasions, the DITF eventually must be shut down and cleaned out.

7.5 ESP Performance

In general, the ESP performed very well for approach to saturation temperatures ranging from 50 to 25°F. On one occasion, the collection efficiency degraded at the end of an extended test. An inspection of the ESP revealed that the seals had become detached, resulting in a heavy coating of ash in the penthouse. Further inspection also revealed that large pieces of deposits had bridged between some of the corona support frames and the collection plates. When the penthouse was cleaned, seals repaired, and deposits removed, the ESP collection efficiency returned to normal.

7.6 Ash Collection System

This system consists of four drag chain conveyors and rotary air locks. On several occasions, the collecting conveyor plugged during unloading of the duct hoppers because of wet fly ash/sorbent. The major problem with the ash collection system is unloading the duct hoppers continuously. The fly ash/sorbent collected in the hoppers is lumpy and the rotary airlocks are not capable of breaking it up. A delumper might be able to break the deposits if they are not too damp.

7.7 Recycle/Slurry Mixing

The recycle/slurry testing has been postponed because of recycle/slurry mixing problems. The mix appears to agglomerate and cause the strainers (located upstream the Moyno pump) to clog in less than a minute. It was also found that the recycle contains some particles larger than the 1/8" strainers. A short test was done with the strainers located downstream of the pump. The preliminary results indicated that the Moyno pump was capable of deagglomerating the mix, but the strainers still clogged every 20 minutes, because of the presence of large particles in the recycle. It is not practical to run long tests under these conditions. To eliminate this problem a pipeline delumper is being investigated. Slurry and recycle samples were sent to the manufacturer to test this concept.

7.8 Control System

The DITF instrument and control system was developed from a mixture of existing equipment hardware and software and a new Allen-Bradley Programmable Logic Controller (PLC) 5/25 control

system. All of the process and equipment control is assigned to the new PLC system while the existing Data Acquisition System (DAS) was strictly limited to data acquisition.

All new equipment start and stop functions are performed via a work station in the control room. The work station consists of a keyboard and CRT and has the capability of displaying the various process loops in real-time.

The PLC system is able to respond to fluctuations in the inlet SO_2 concentration, gas temperature, gas flow rate, and allow the process or equipment upset conditions to be detected and corrected without process shutdown.

For each process loop, there is a graphic screen on the Panelmate showing the process flow and equipment status. To set process parameters, there are several Process Control Screens containing two types of displays: a controller and a variable display format that indicates the current value of the Process Variable and Setpoint.

The automatic controls and operation of the Panelmate Operator station were easily understood and quickly learned by the operating staff. Several minor program changes have been made to help the operators better see and understand operational data. Reliability of the control system has been 100% barring human error (approximately 15 months of operation).

The portion of the PLC program which controls the sampling of the gas ports in the gas analyzer has been extensively revised. Also, an air flow computer was added to the atomizing air flow control loop so that more accurate air flow data could be recorded.

The algorithm used to calculate the steam humidification flow of the dilution air appears to have a problem resulting in too high a set point. This is being revised. The humidification spray water control is hard to maintain due to an oversized pump. The pressure to the flow control valve is not well regulated causing the PID loop to hunt for the set point. The PID loops that are cascaded to control ESP approach temperature, by humidity water flow, need further tuning. This is difficult to control because of the long period of time for the change in temperature to occur and the very small increments of flow needed to adjust the ESP approach temperature.

APPENDIX A

DETAILS OF TEST RESULTS OF DROPLET SIZE MEASUREMENTS

Tables A-1 and A-2 contain data summaries for each test performed with the Lechler supersonic and Parker-Hannifin nozzles, respectively. Besides listing the test number, air pressure, and water flow rate for each test, the tables also include the Sauter mean diameter, total mass concentration, mass mean diameter, σ_g (geometric standard deviation), percentage of mass greater than 106 micrometers, and percentage of mass greater than 138 micrometers for each test. These data were determined by combining size distribution data measured with the PCSV and VDA for each test condition. For Tests 23 and 24 of the Lechler supersonic nozzles, the windows of the PCSV were fouled and no PCSV data were obtained. Otherwise, PCSV and VDA data were obtained for each test condition. Tables A-3 and A-4 contain these results (with the exception of mass mean diameter and σ_g) for the measurements made with the VDA.

Following these tables are graphical representations of the cumulative mass size distribution and the differential mass size distribution measured for each test. In these graphs the cumulative mass size distribution was obtained by integrating the differential mass size distributions measured by the PCSV and VDA within their measurement range. The differential mass size distributions measured with each instrument, over their range of accurate measurement, are shown in each graph. The agreement is better than might be expected given the fact that each set of experimental conditions had to be set up twice: once for each instrument.

Table A-1. Lechler Nozzle Tests, Combined PCSV and VDA Data

Test #	Air Pressure psig	Water Flow Rate gpm	Sauter Mean Dia. µm	Mass Concentration g/m^3	Mass Mean Dia. µm	σ_g	%>106 µm	%>138 µm
15	80	6	26.3	22.5	31.1	1.90	3.0	0.6
16		8	28.1	25.9	31.6	1.83	1.6	0.0
17		10	27.2	28.9	34.3	2.04	3.6	1.1
18		11	29.2	29.0	33.5	1.89	2.2	0.4
19		8	28.2	29.2	31.0	1.79	1.0	0.0
20	60	6	43.1	27.5	41.3	1.73	2.3	0.0
21		8	32.9	42.4	37.7	1.91	4.1	1.6
22		10	35.0	50.2	41.1	1.96	4.3	0.4
23*		11	43.3	47.6	49.3	1.83	5.9	2.0
24*	80	8	35.9	22.4	37.5	1.71	1.5	0.0

* VDA data only. PCSV windows fouled.

Table A-2. Parker-Hannifin Nozzle Tests, Combined PCSV and VDA data

Test #	Air Pressure psig	Water Flow Rate gpm	Sauter Mean Dia. µm	Mass Concentration g/m^3	Mass Mean Dia. µm	σ_g	%>106 µm	%>138 µm
18	100	10	34.1	31.8	38.5	1.72	2.8	0.3
19		6	23.5	14.6	27.1	1.76	0.0	0.0
20		8	28.9	21.5	32.1	1.75	1.2	0.0
21		10	33.4	29.8	37.7	1.72	2.5	0.7
22		11	38.1	31.8	41.5	1.69	2.6	0.4
23	80	6	31.1	19.3	33.4	1.68	0.8	0.0
24		8	38.8	25.4	40.7	1.63	0.8	0.0
25		11	40.8	35.4	45.2	1.74	3.6	0.7
26		10	44.5	43.9	51.4	1.81	7.8	2.4
27	100	10	38.0	27.3	40.9	1.69	2.0	0.4
28	110	6	19.1	13.2	23.7	1.97	2.2	0.0
29		8	27.0	17.9	30.3	1.70	0.0	0.0
30		10	28.1	17.8	32.8	1.72	2.1	0.0
31		11	28.1	22.9	32.6	1.81	1.5	0.0
32	100	10	28.7	24.6	33.8	1.72	1.4	0.0

Table A-3. Lechler Nozzle Tests, VDA Data Only

Test #	Air Pressure psig	Water Flow Rate gpm	Sauter Mean Dia. µm	Mass Concentration g/m^3	%>106 µm	%>138 µm
15	80	6	34.8	17.9	3.8	0.8
16		8	34.7	21.7	1.9	0.0
17		10	36.4	26.3	4	1.3
18		11	35.9	25.8	2.3	0.4
19		8	35.5	24.1	1.2	0.0
20	60	6	39.3	28.6	2.3	0.0
21		8	40.7	37.3	4.6	1.6
22		10	42.4	45.7	4.7	0.5
23		11	43.3	47.6	5.9	2.0
24	80	8	35.9	22.4	1.5	0.0

Table A-4. Parker-Hannifin Nozzle Tests, VDA Data Only

Test #	Air Pressure psig	Water Flow Rate gpm	Sauter Mean Dia. µm	Mass Concentration g/m^3	% > 106 µm	%>138 µm
18	100	10	39.4	28.7	0.4	0.0
19		6	32.9	10.8	0.0	0.0
20		8	35.7	18.6	1.3	0.0
21		10	39.2	26.8	2.8	0.4
22		11	40.5	30.4	2.8	0.4
23	80	6	36.9	17.5	0.9	0.0
24		8	39.9	25.1	0.8	0.0
25		11	43.9	34.3	3.7	0.8
26		10	47.5	43.0	8.0	2.5
27	100	10	39.5	26.5	2.0	0.4
28	110	6	31.5	8.0	3.6	0.0
29		8	32.0	12.4	0.0	0.0
30		10	32.9	13.2	2.8	0.0
31		11	35.2	16.0	2.8	0.0
32	100	10	36.3	17.6	1.9	0.0

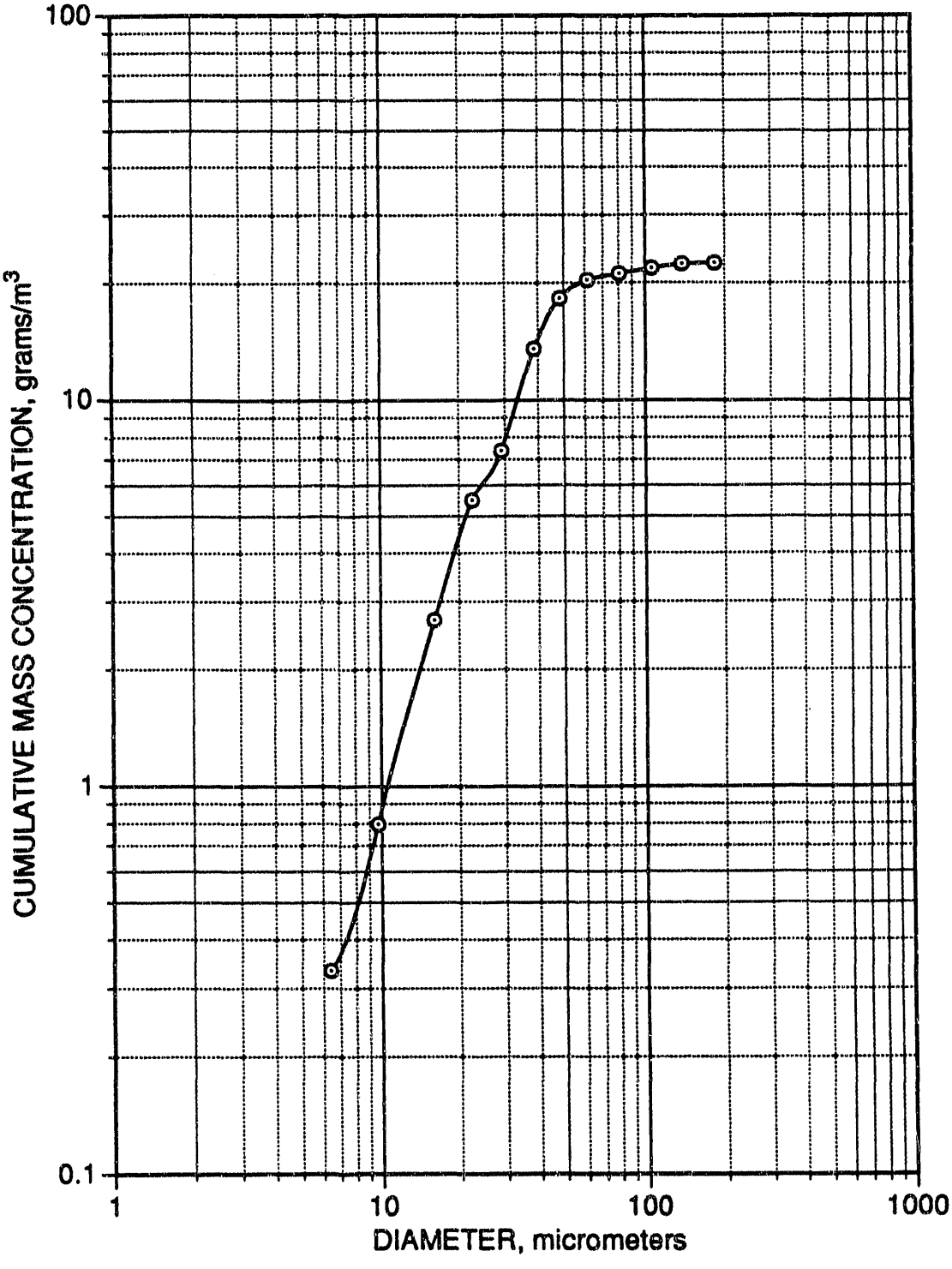

Figure A-1. Cumulative mass concentration versus particle size for Lechler nozzle test #15.

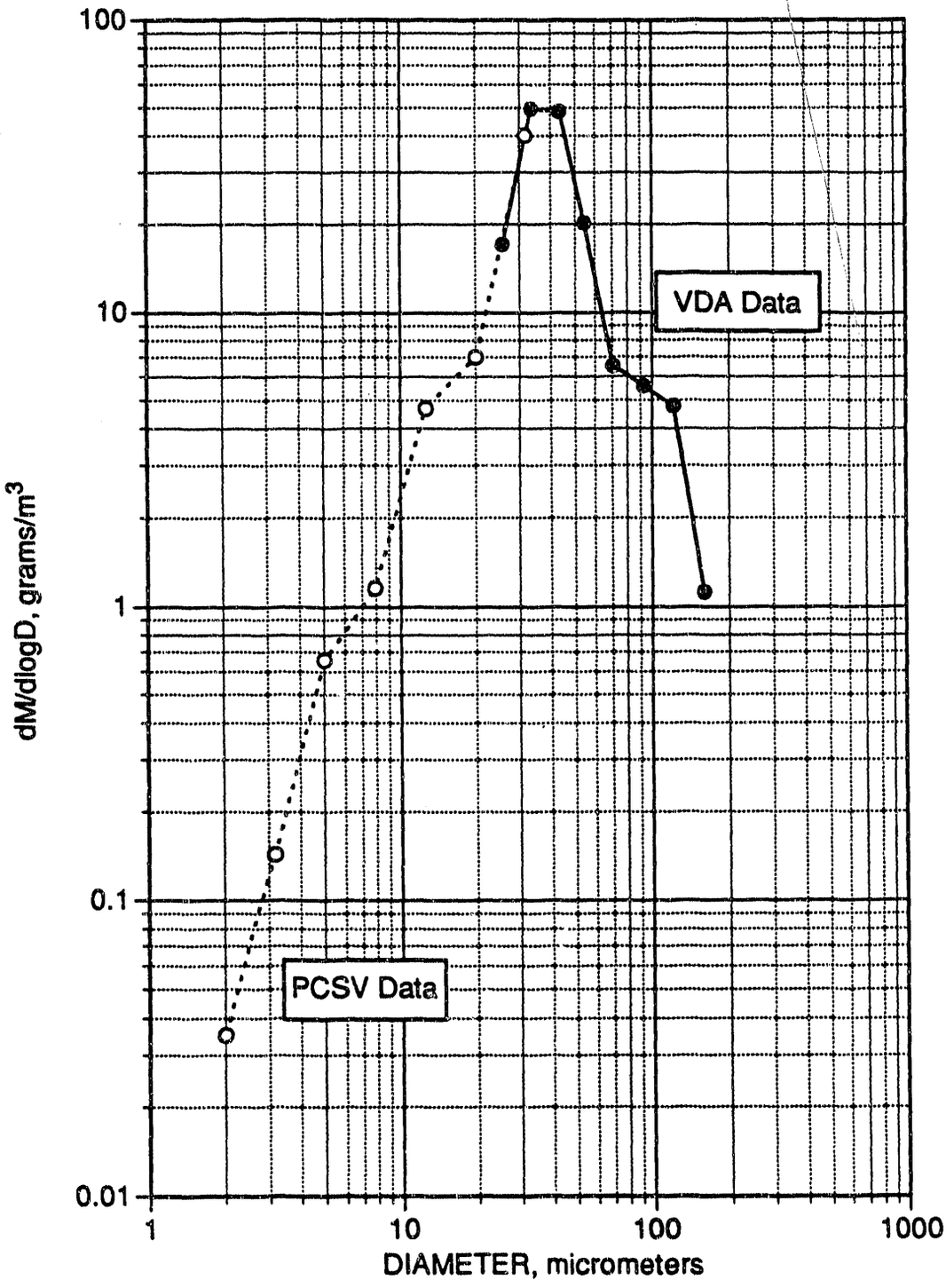

Figure A-2. Differential mass concentration versus particle size for Lechler test #15. PCSV data are shown with dashed lines and open symbols, and VDA data are shown with a solid line and closed symbols.

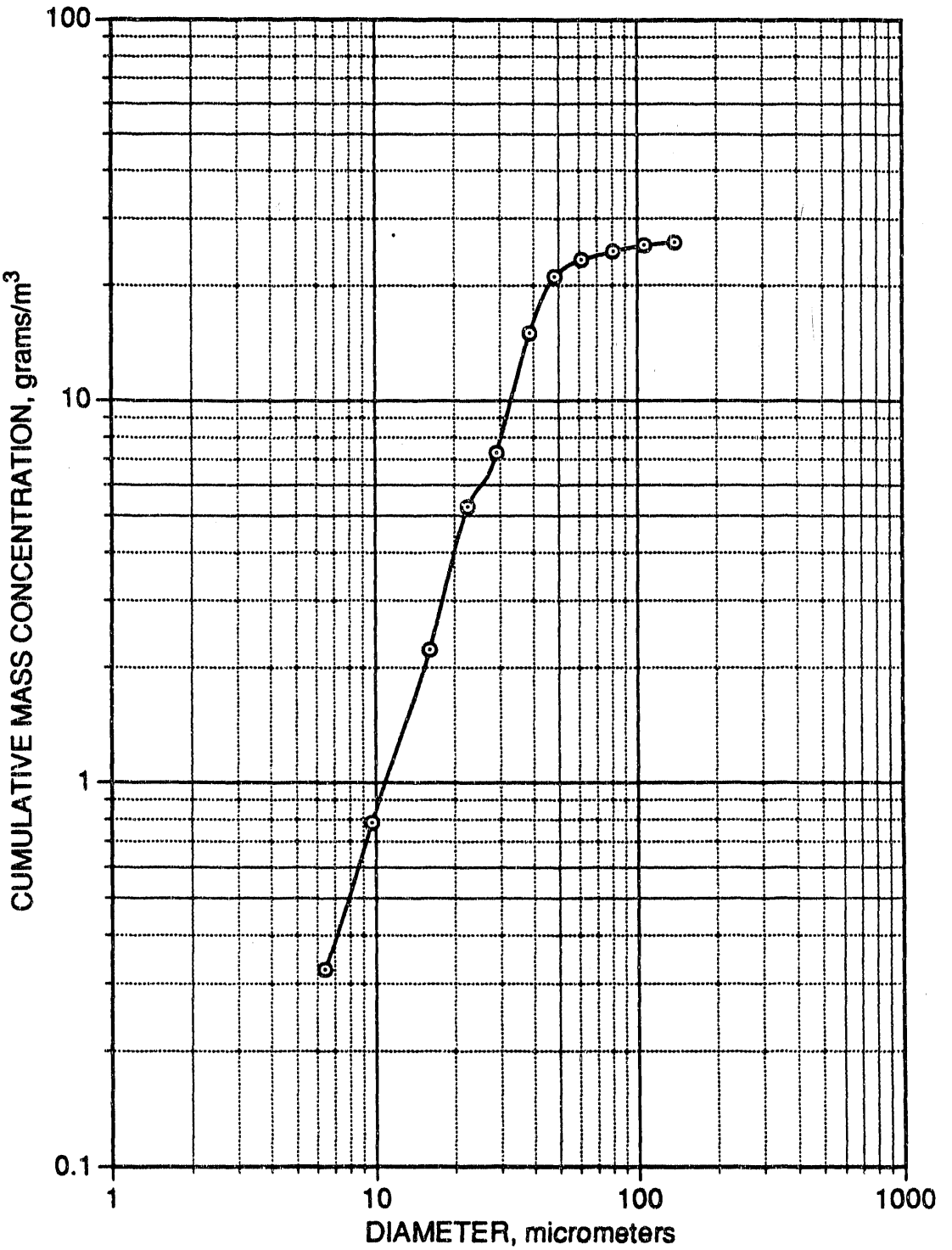

Figure A-3. Cumulative mass concentration versus particle size for Lechler nozzle test #16.

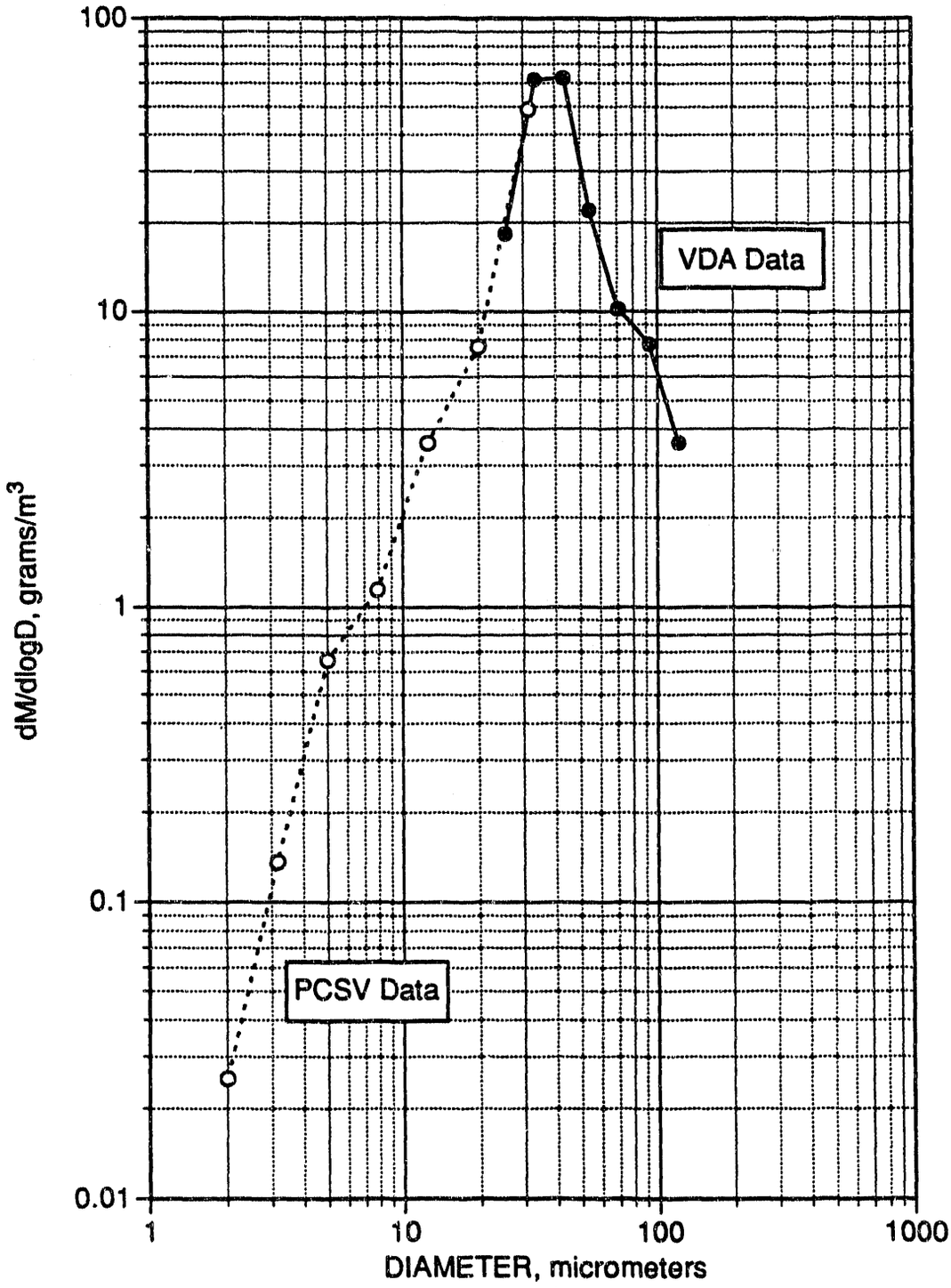

Figure A-4. Differential mass concentration versus particle size for Lechler test #16. PCSV data are shown with dashed lines and open symbols, and VDA data are shown with a solid line and closed symbols.

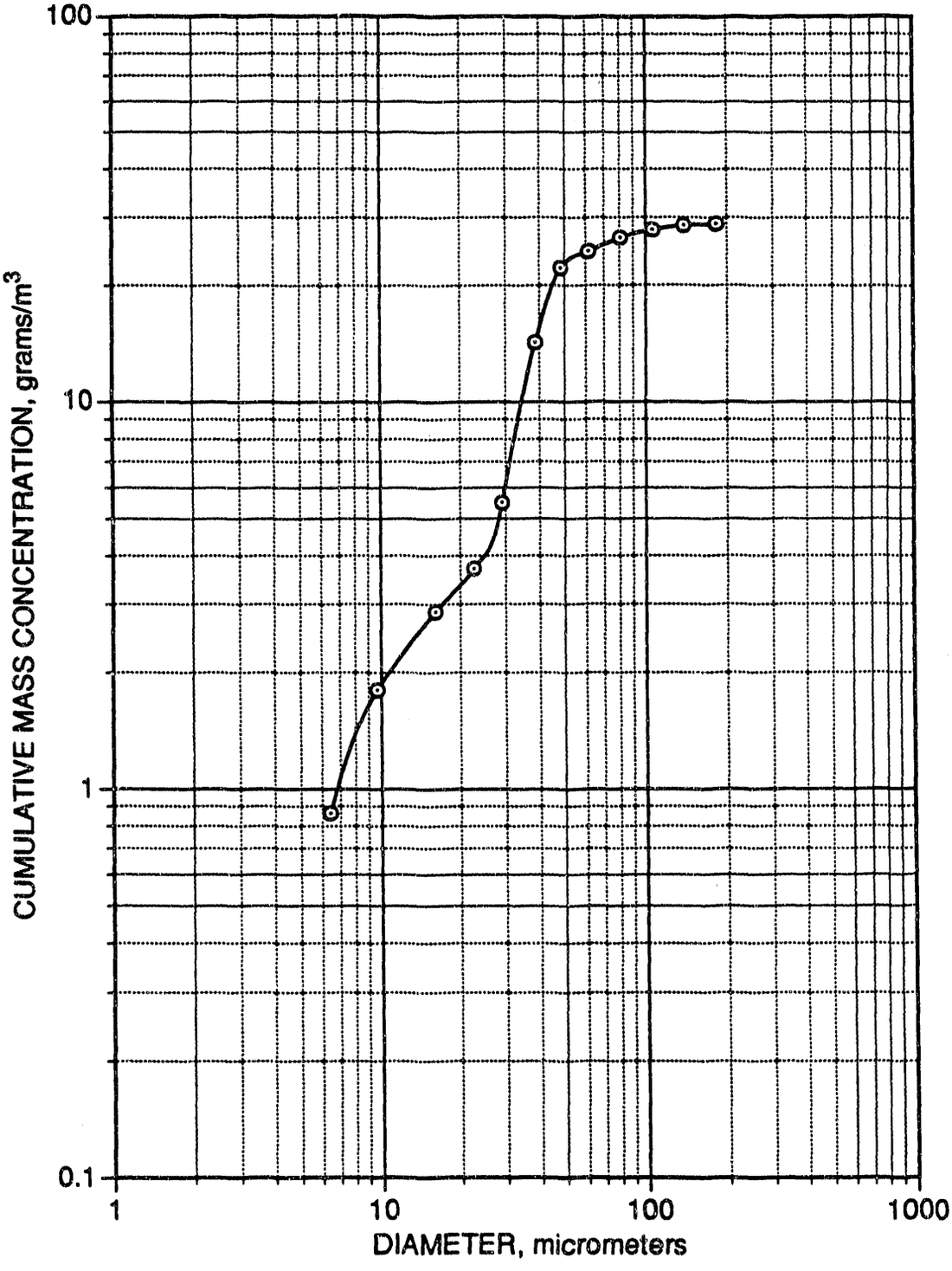

Figure A-5. Cumulative mass concentration versus particle size for Lechler nozzle test #17.

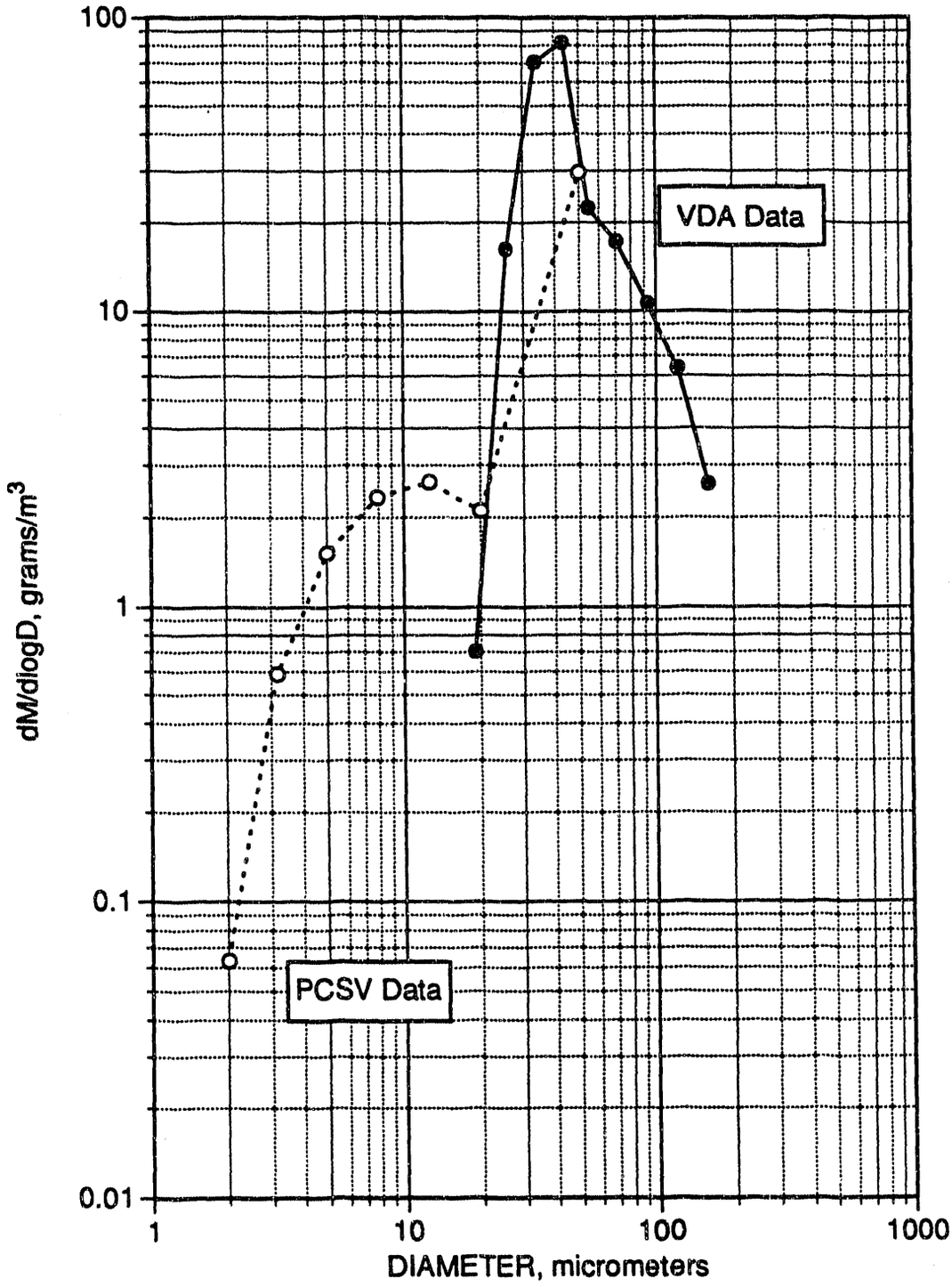

Figure A-6. Differential mass concentration versus particle size for Lechler test #17. PCSV data are shown with dashed lines and open symbols, and VDA data are shown with a solid line and closed symbols.

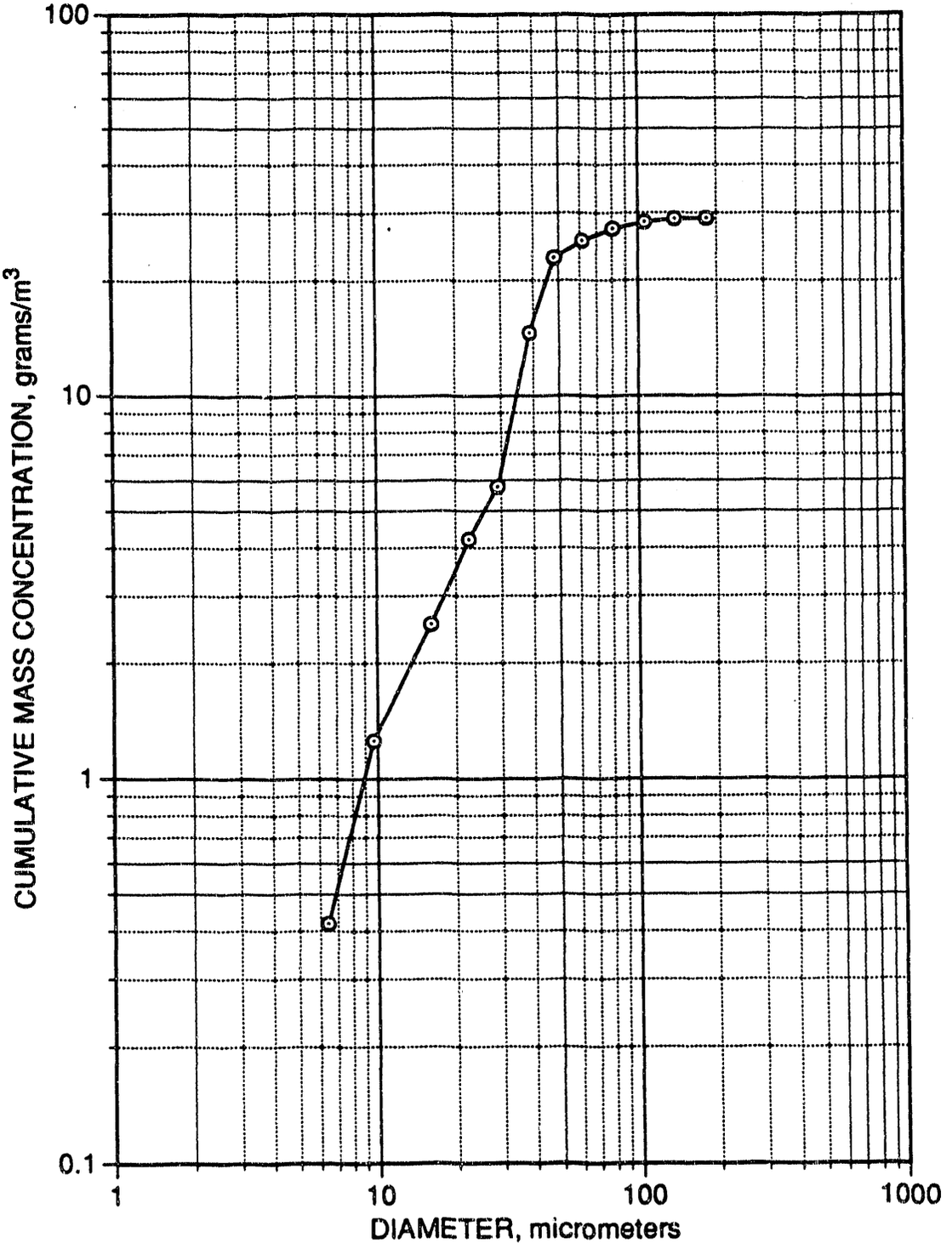

Figure A-7. Cumulative mass concentration versus particle size for Lechler nozzle test #18.

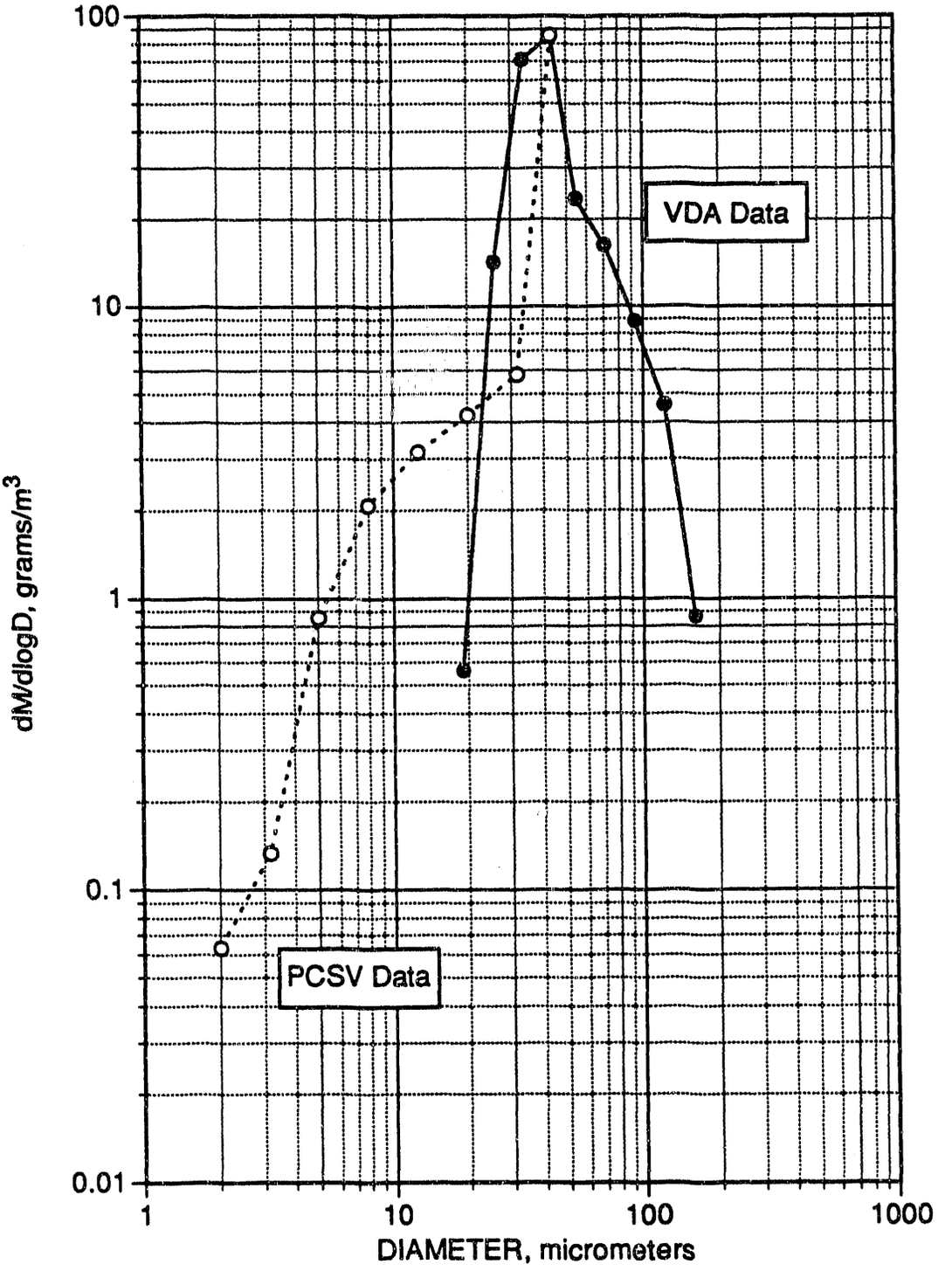

Figure A-8. Differential mass concentration versus particle size for Lechler test #18. PCSV data are shown with dashed lines and open symbols, and VDA data are shown with a solid line and closed symbols.

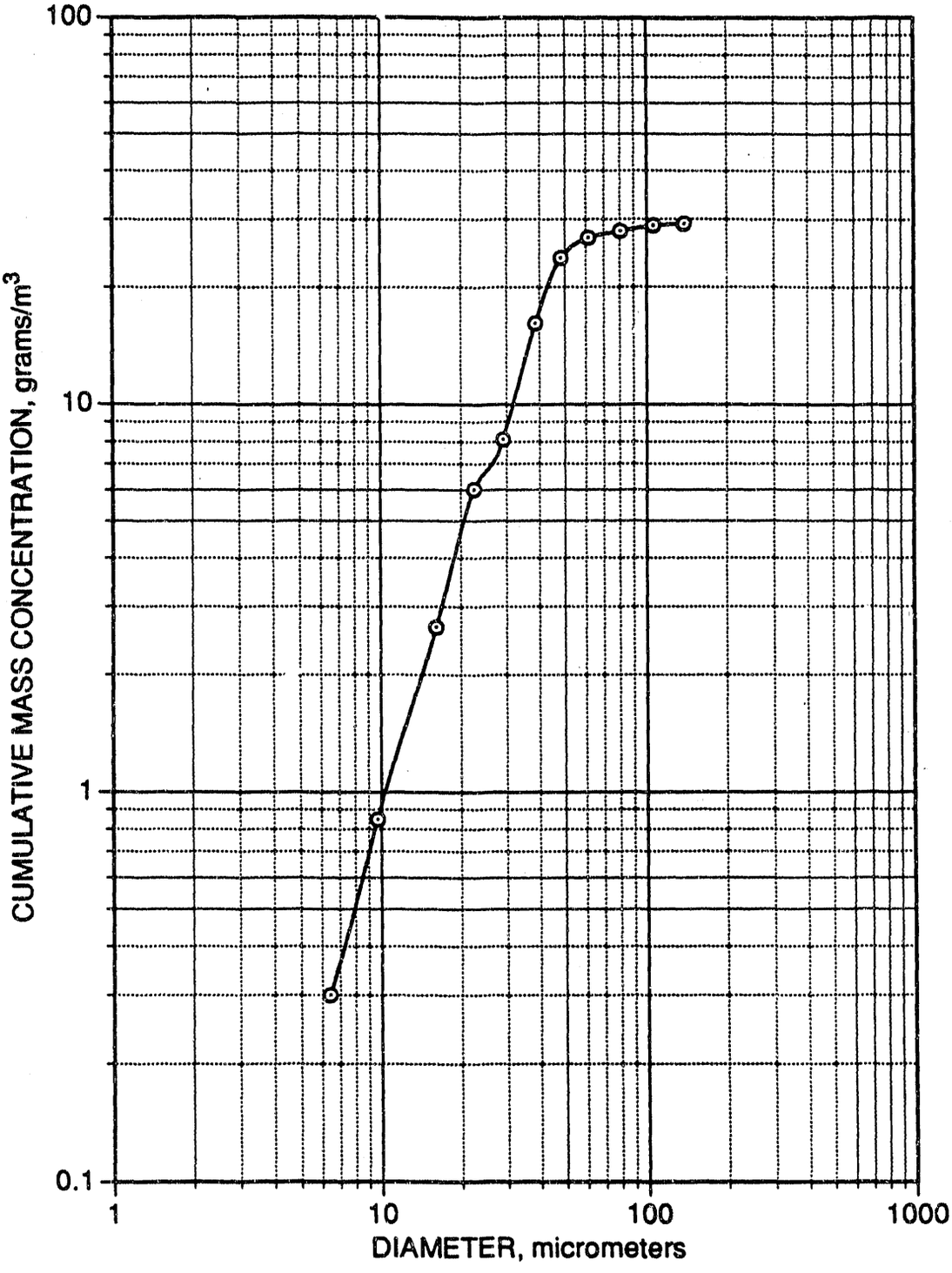

Figure A-9. Cumulative mass concentration versus particle size for Lechler nozzle test #19.

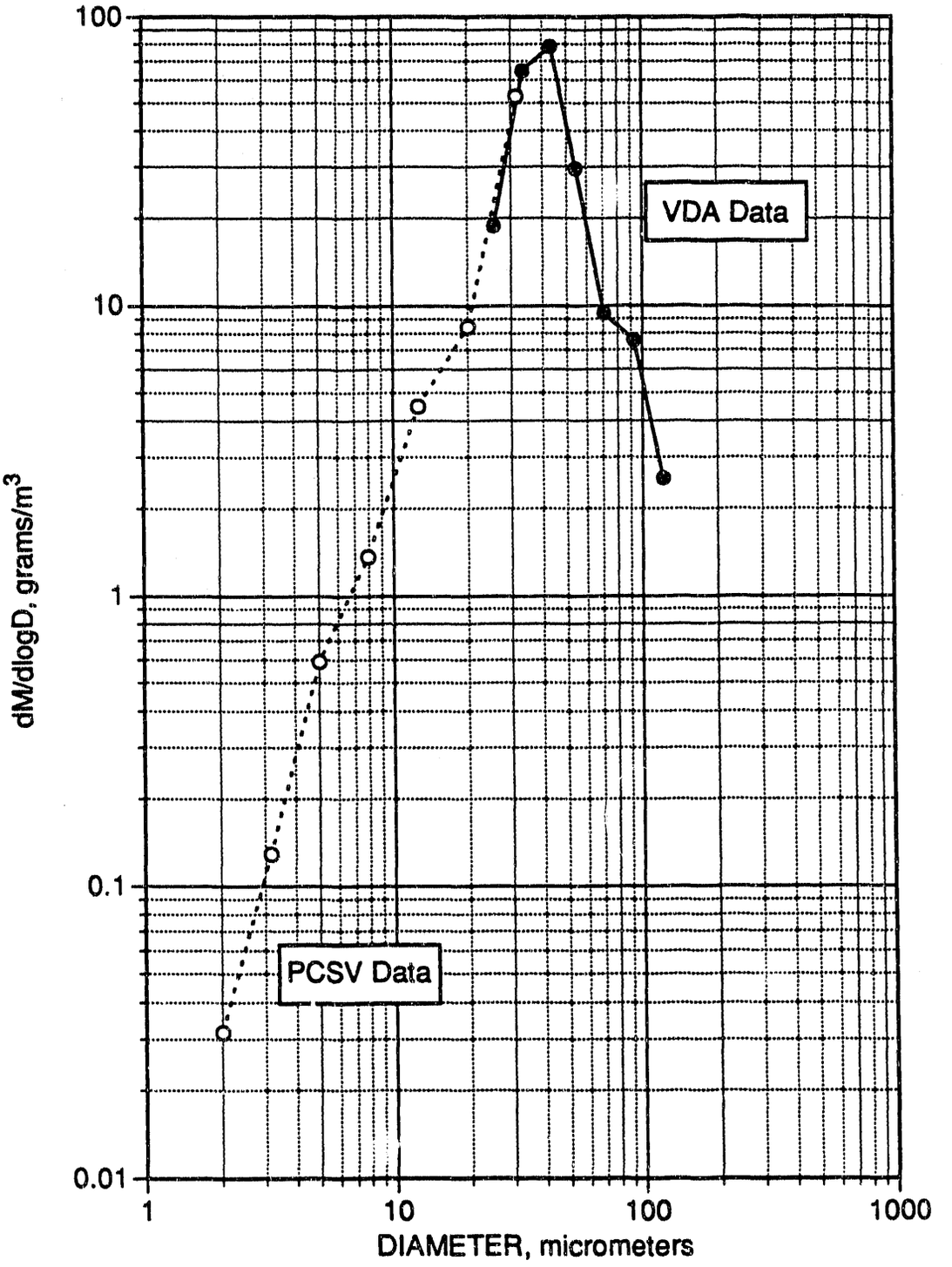

Figure A-10. Differential mass concentration versus particle size for Lechler test #19. PCSV data are shown with dashed lines and open symbols, and VDA data are shown with a solid line and closed symbols.

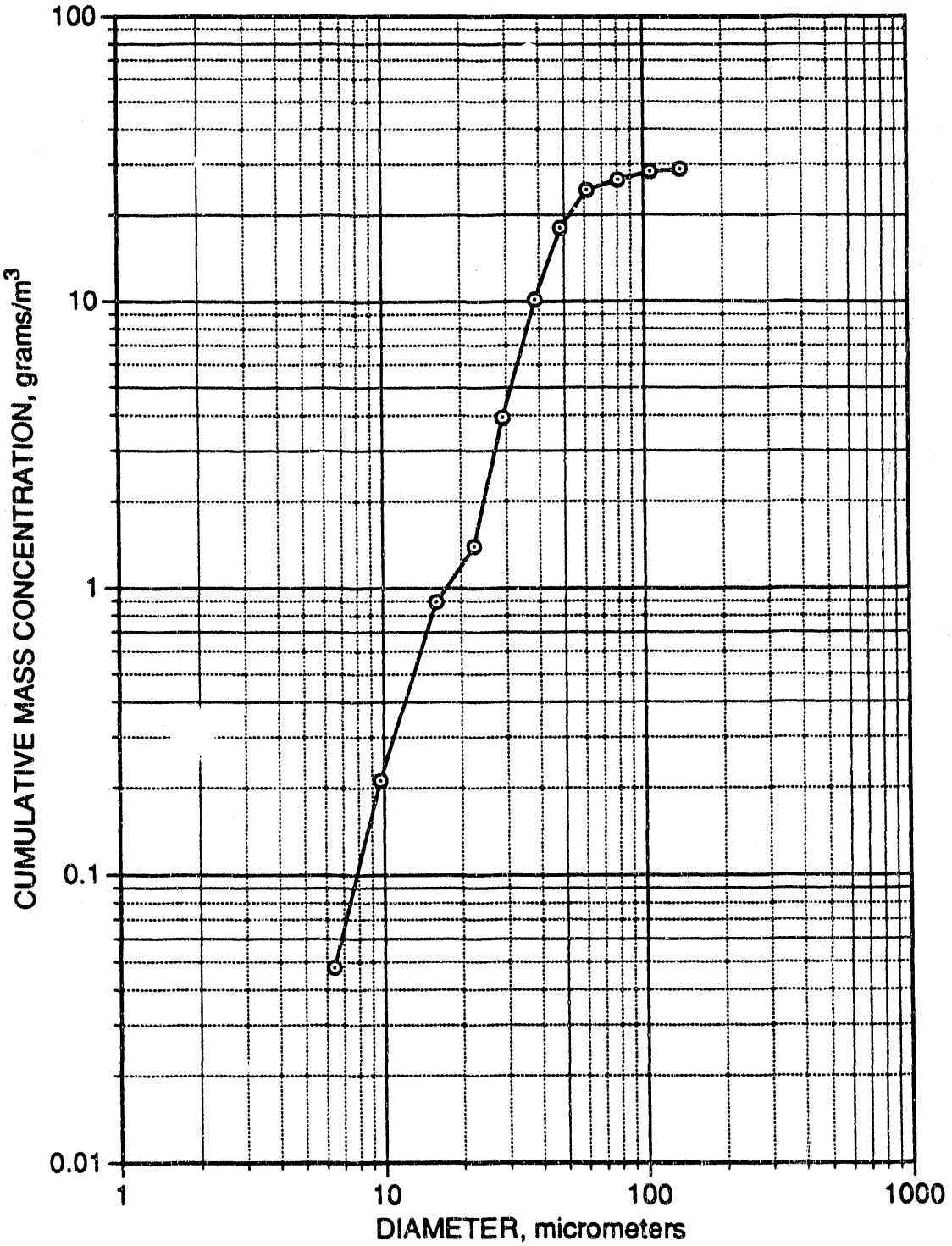

Figure A-11. Cumulative mass concentration versus particle size for Lechler nozzle test #20.

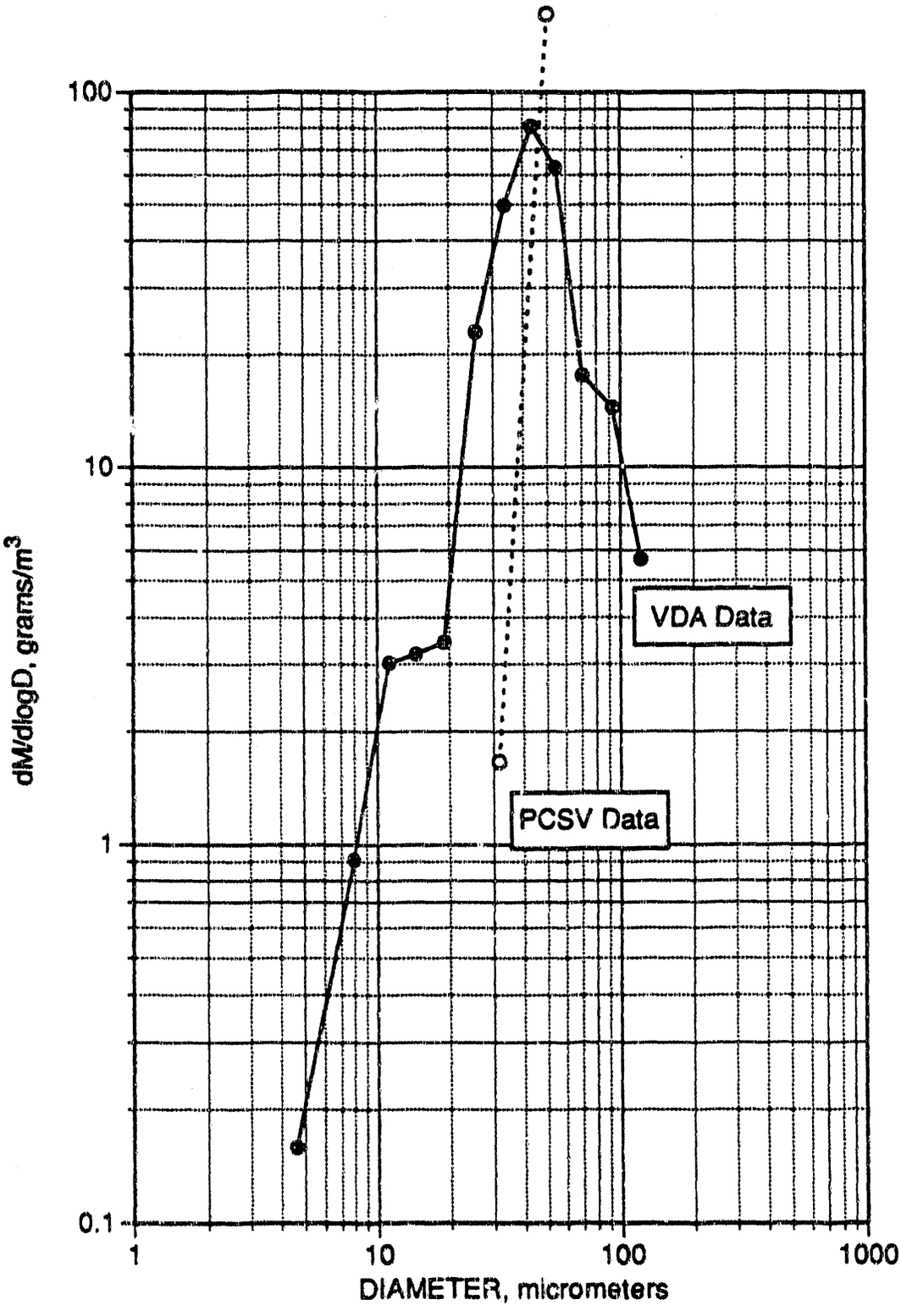

Figure A-12. Differential mass concentration versus particle size for Lechler test #20. PCSV data are shown with dashed lines and open symbols, and VDA data are shown with a solid line and closed symbols.

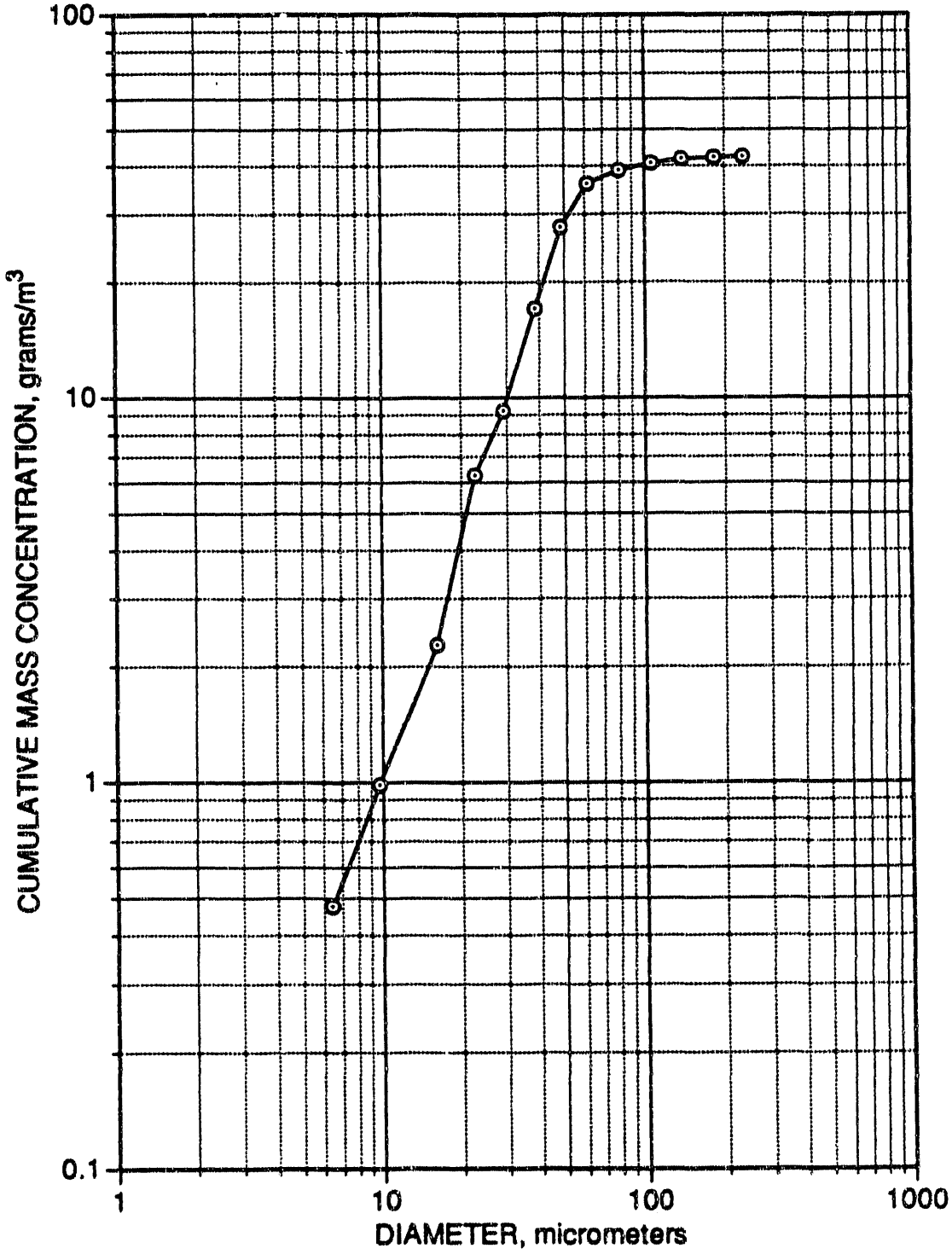

Figure A-13. Cumulative mass concentration versus particle size for Lechler nozzle test #21.

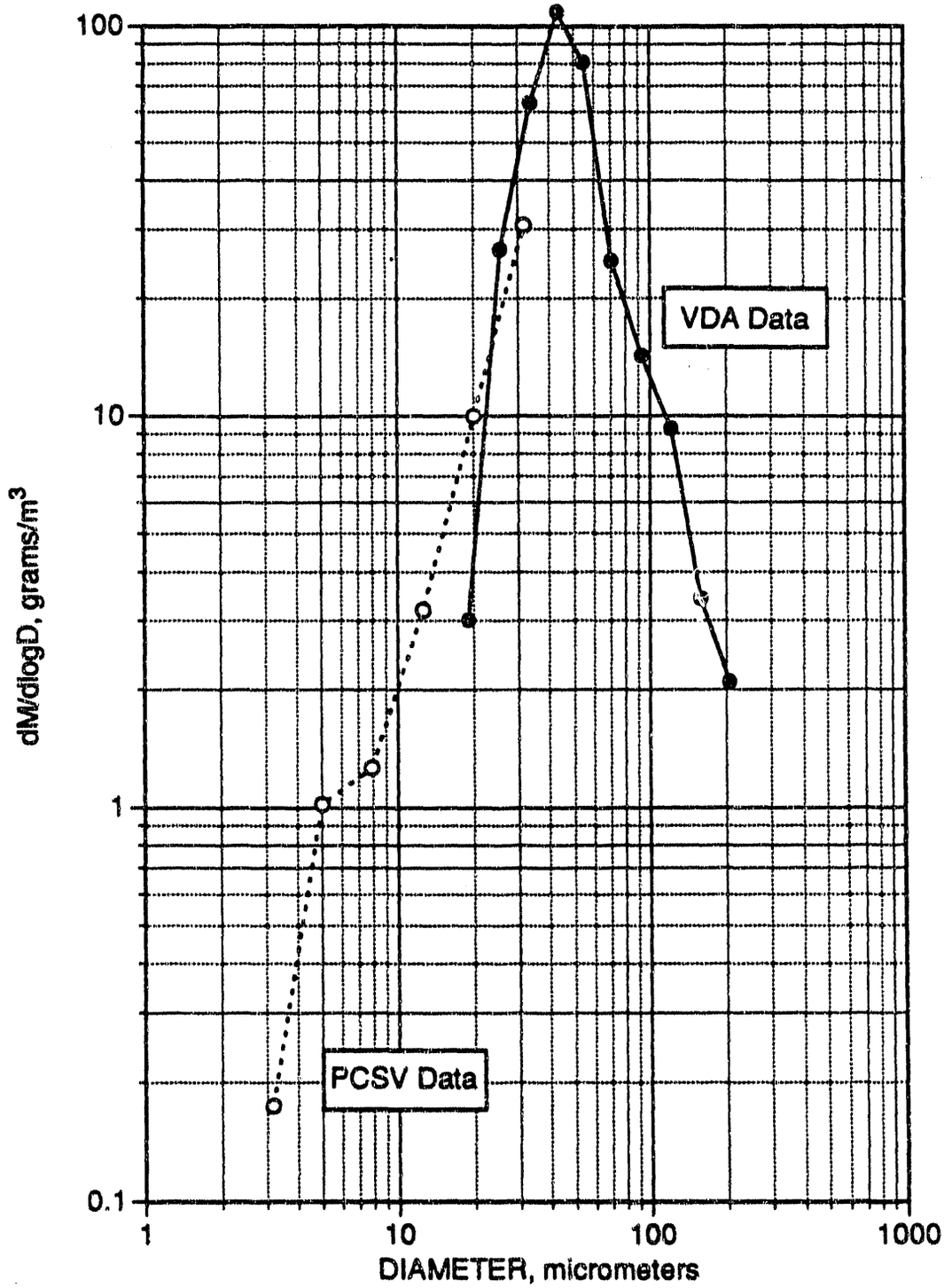

Figure A-14. Differential mass concentration versus particle size for Lechler test #21. PCSV data are shown with dashed lines and open symbols, and VDA data are shown with a solid line and closed symbols.

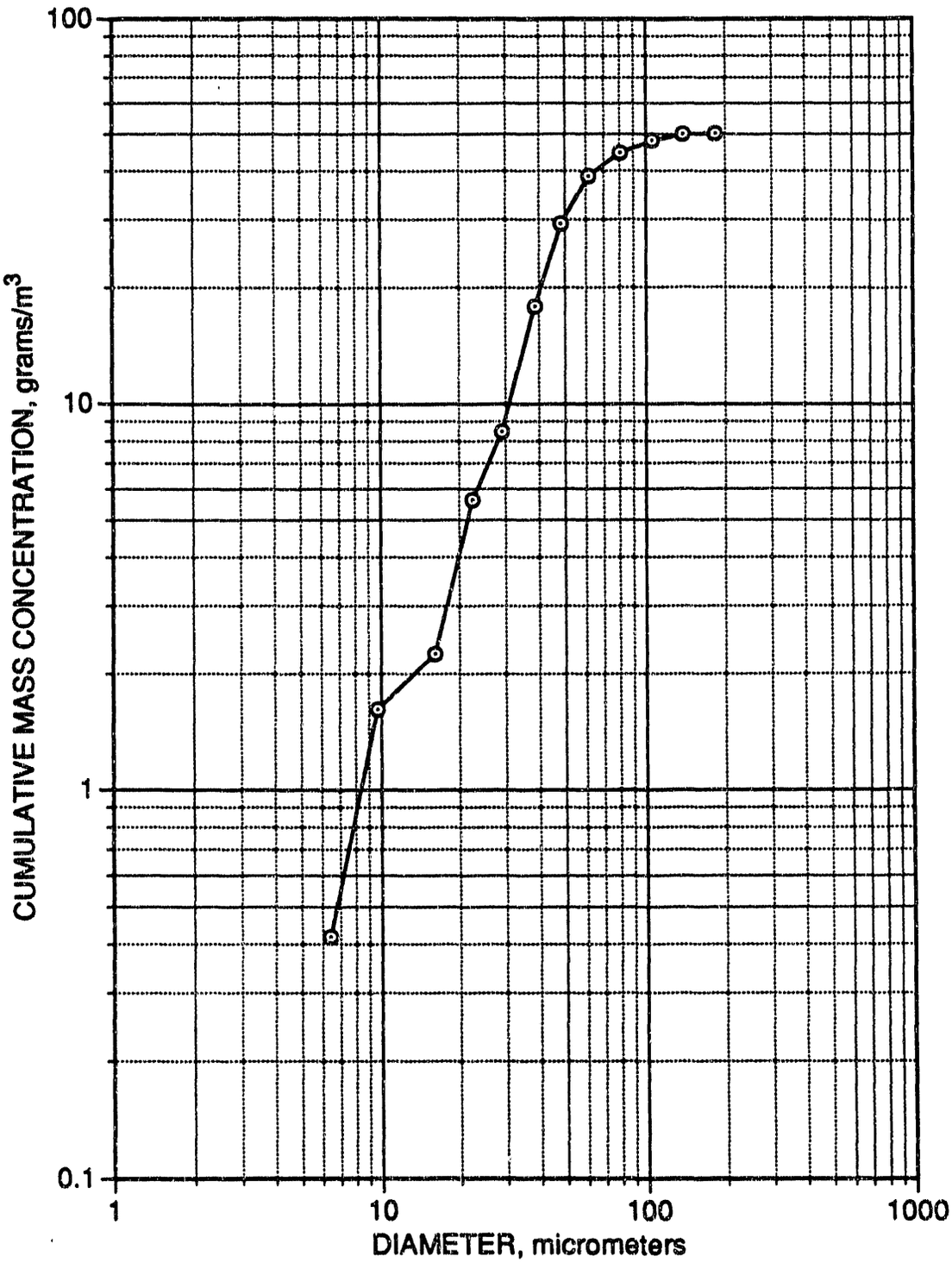

Figure A-15. Cumulative mass concentration versus particle size for Lechler nozzle test #22.

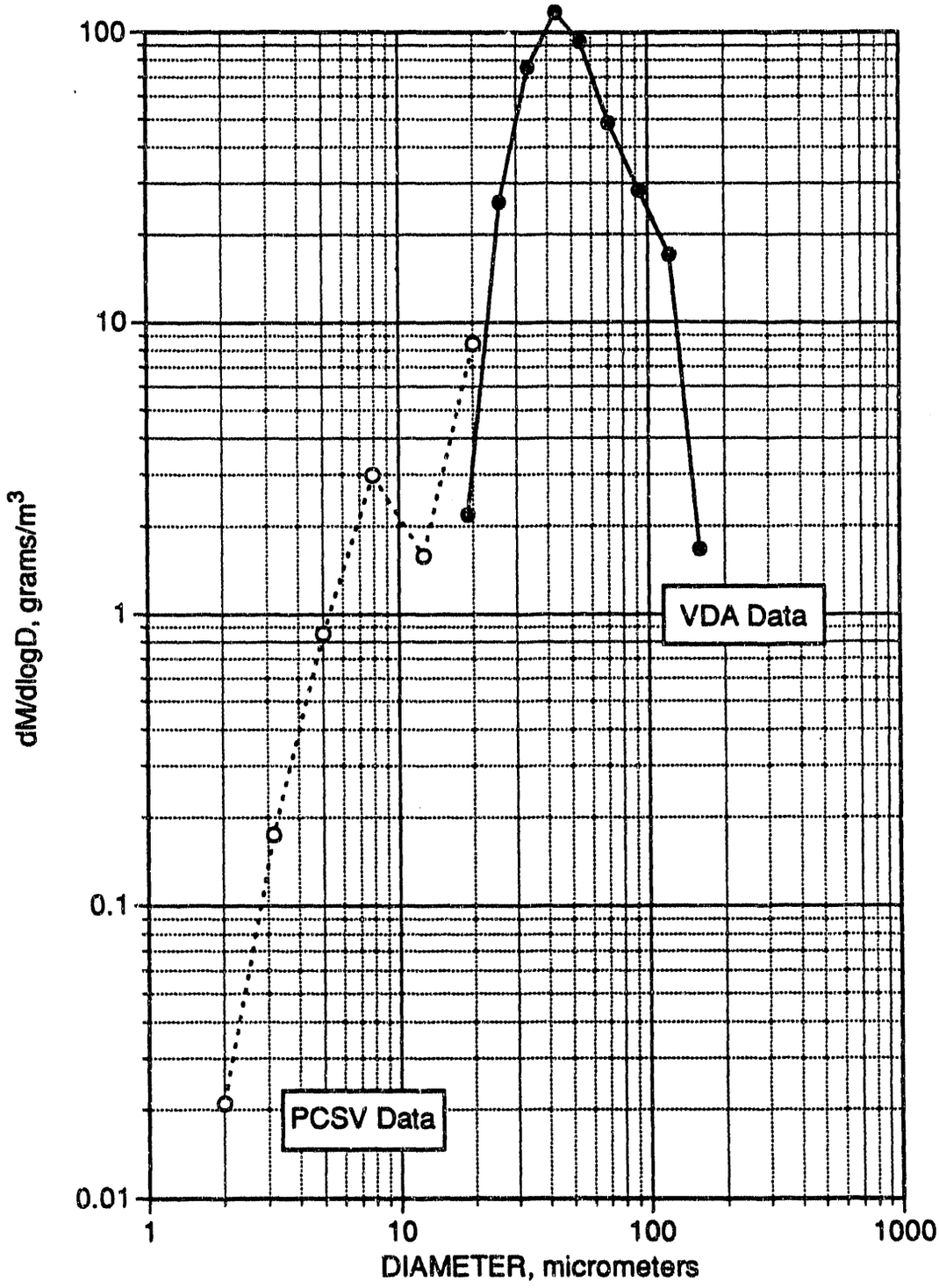

Figure A-16. Differential mass concentration versus particle size for Lechler test #22. PCSV data are shown with dashed lines and open symbols, and VDA data are shown with a solid line and closed symbols.

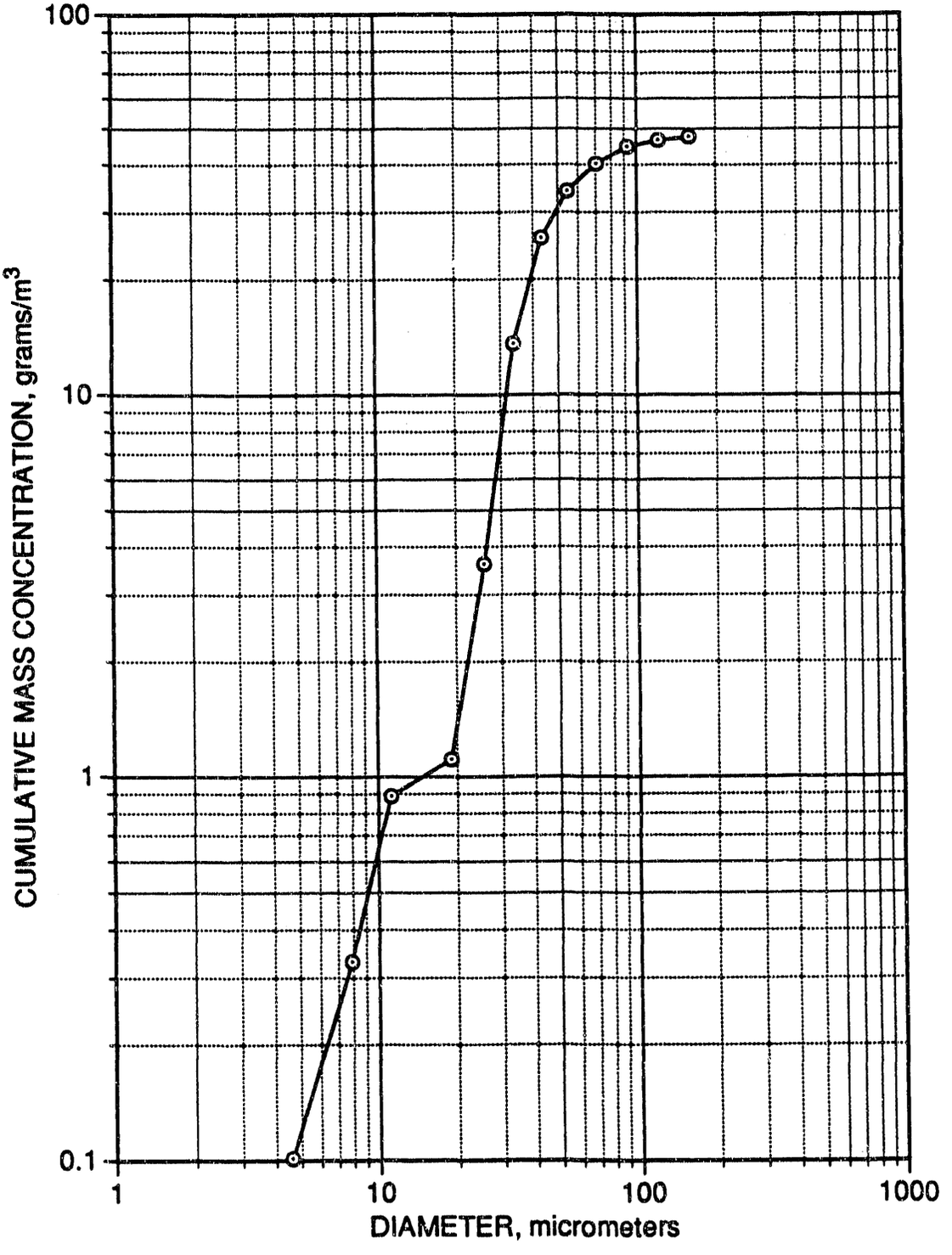

Figure A-17. Cumulative mass concentration versus particle size for Lechler nozzle test #23. VDA data only.

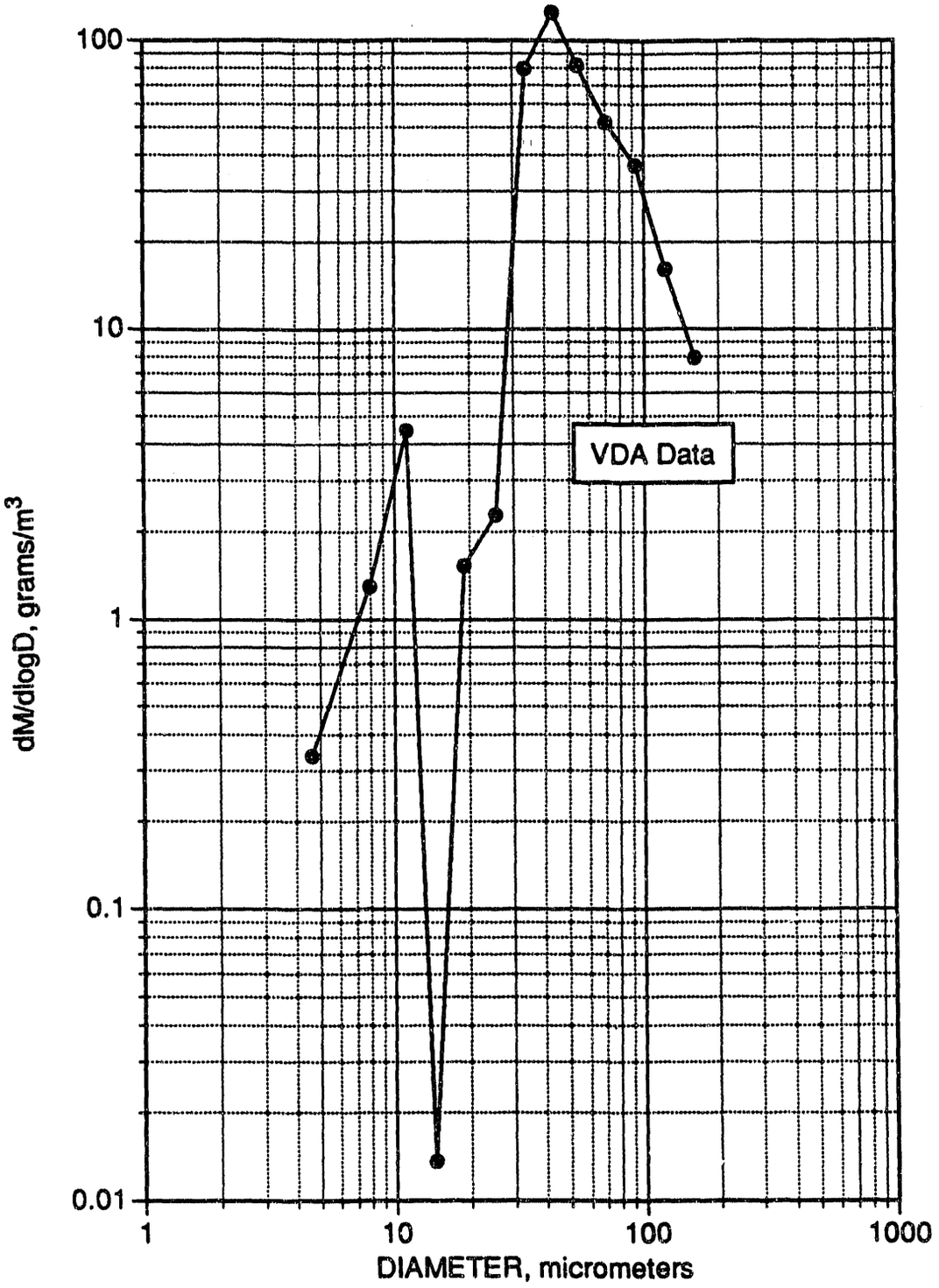

Figure A-18. Differential mass concentration versus particle size for Lechler test #23. VDA data are shown with a solid line and closed symbols. PCSV data were unusable for this test due to fouled windows.

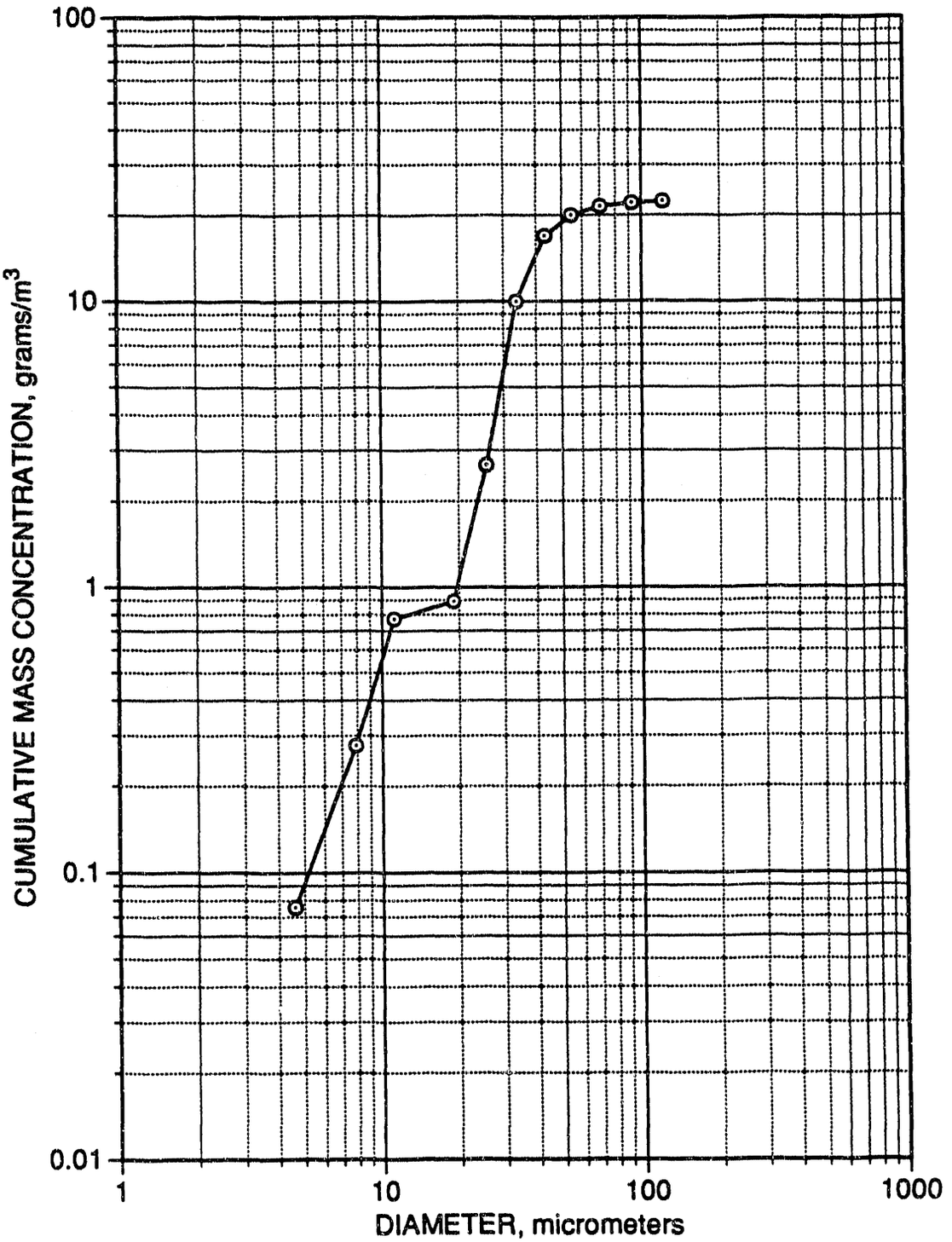

Figure A-19. Cumulative mass concentration versus particle size for Lechler nozzle test #24. VDA data only.

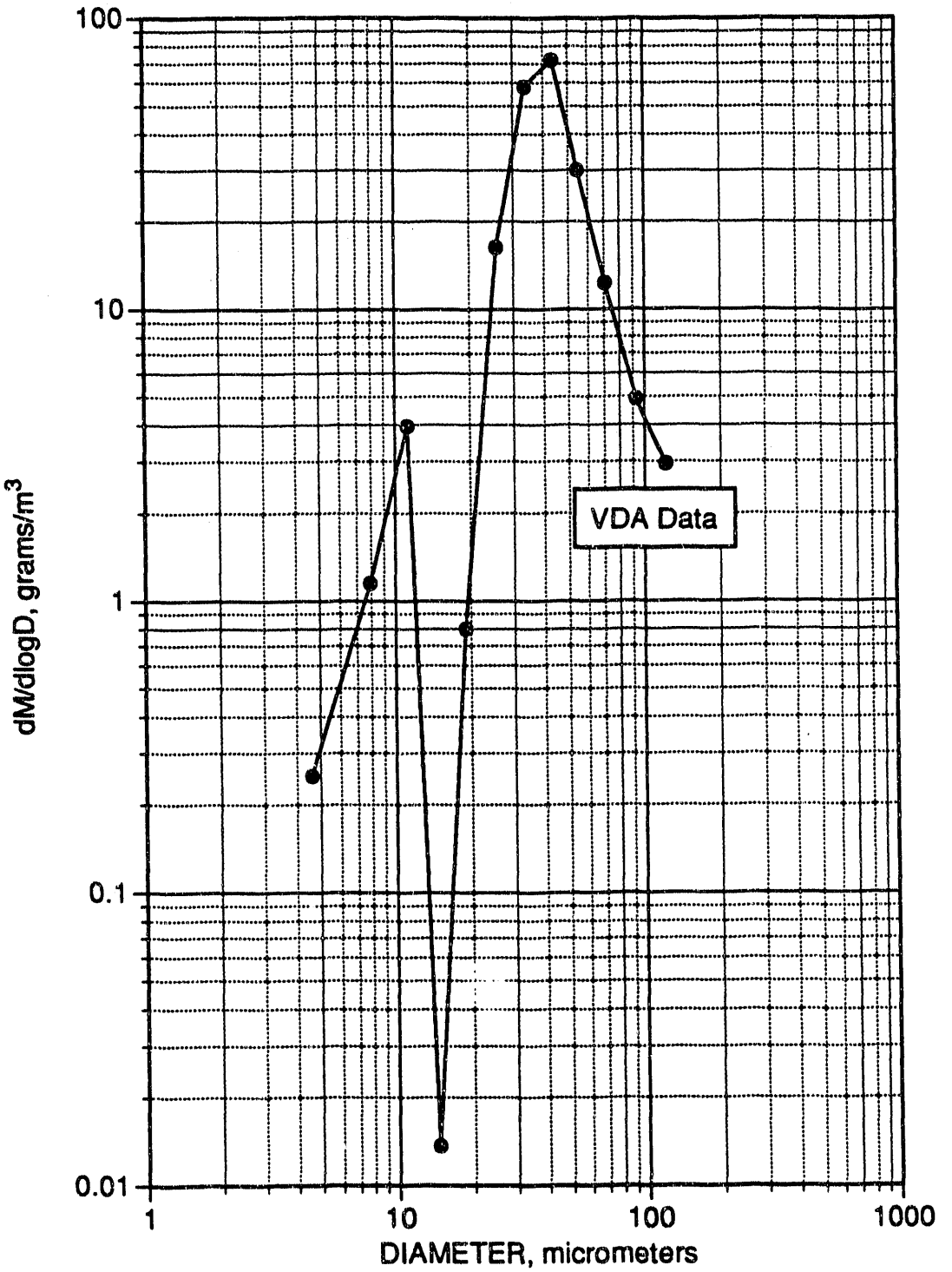

Figure A-20. Differential mass concentration versus particle size for Lechler test #24. VDA data are shown with a solid line and closed symbols. PCSV data were unusable for this test due to fouled windows.

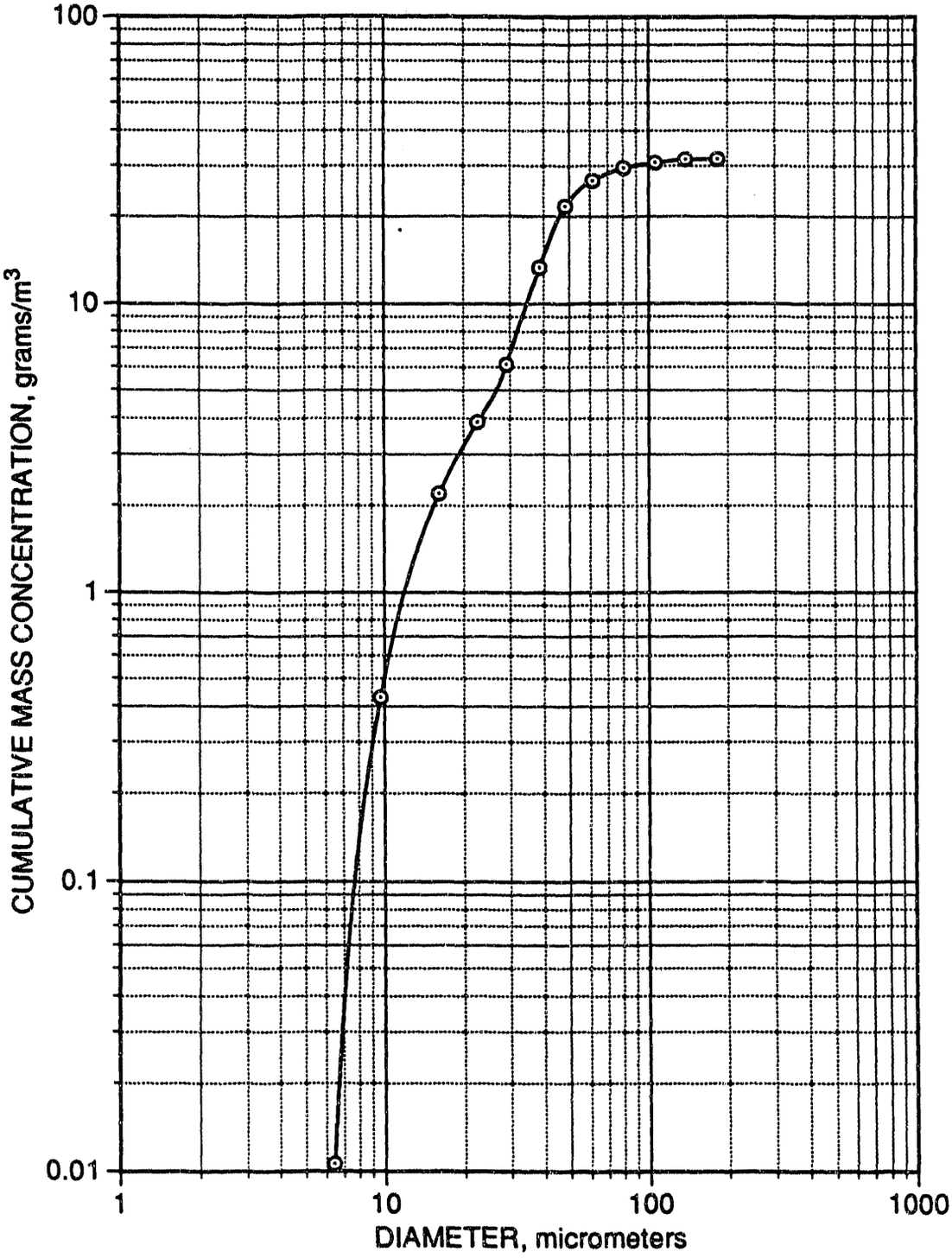

Figure A-21. Cumulative mass concentration versus particle size for Parker-Hannifin nozzle test #18.

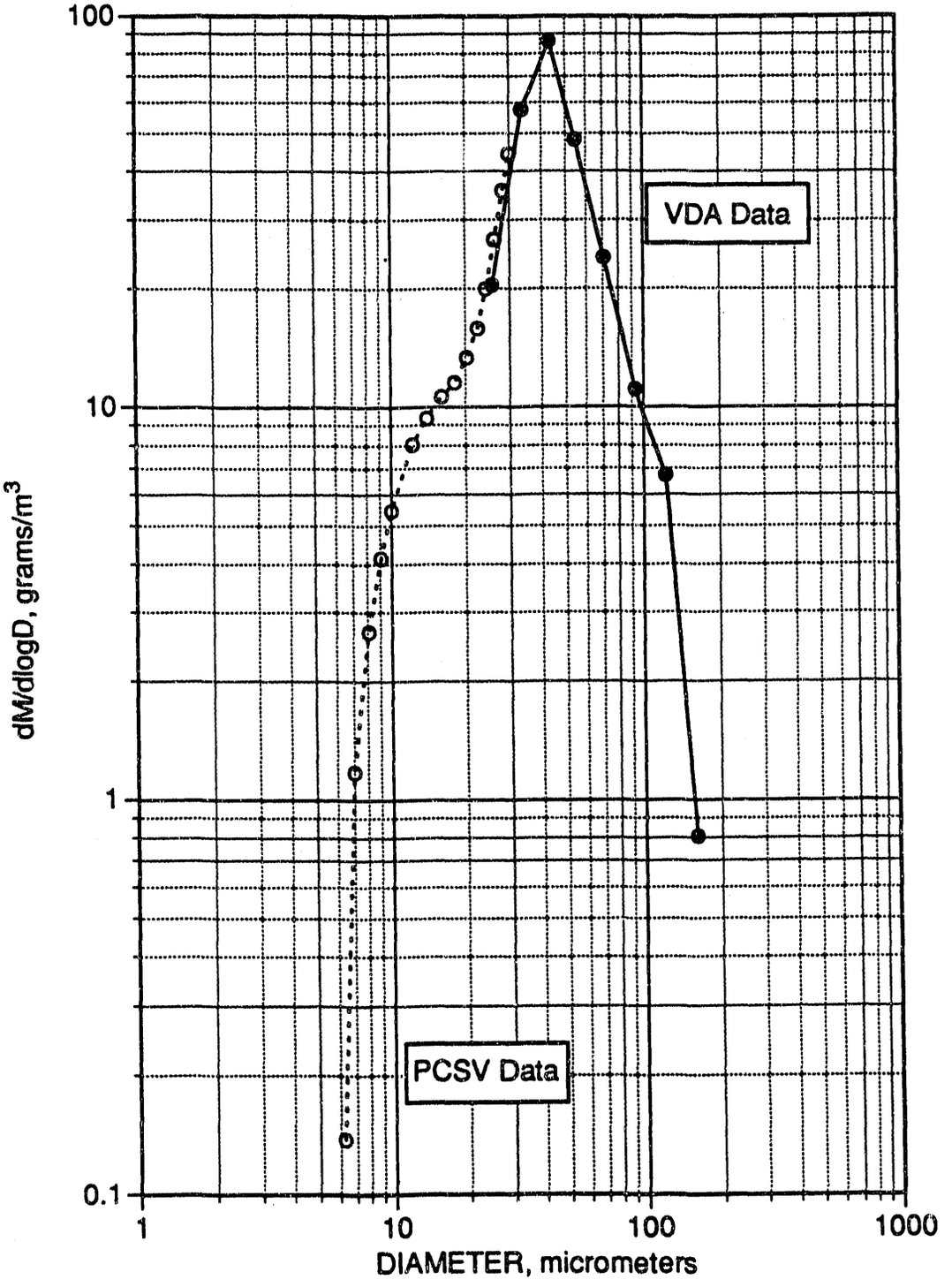

Figure A-22. Differential mass concentration versus particle size for Parker-Hannifin nozzle test #18. PCSV data are shown with a dashed line and open symbols, and discrete VDA data are shown with a solid line and closed symbols.

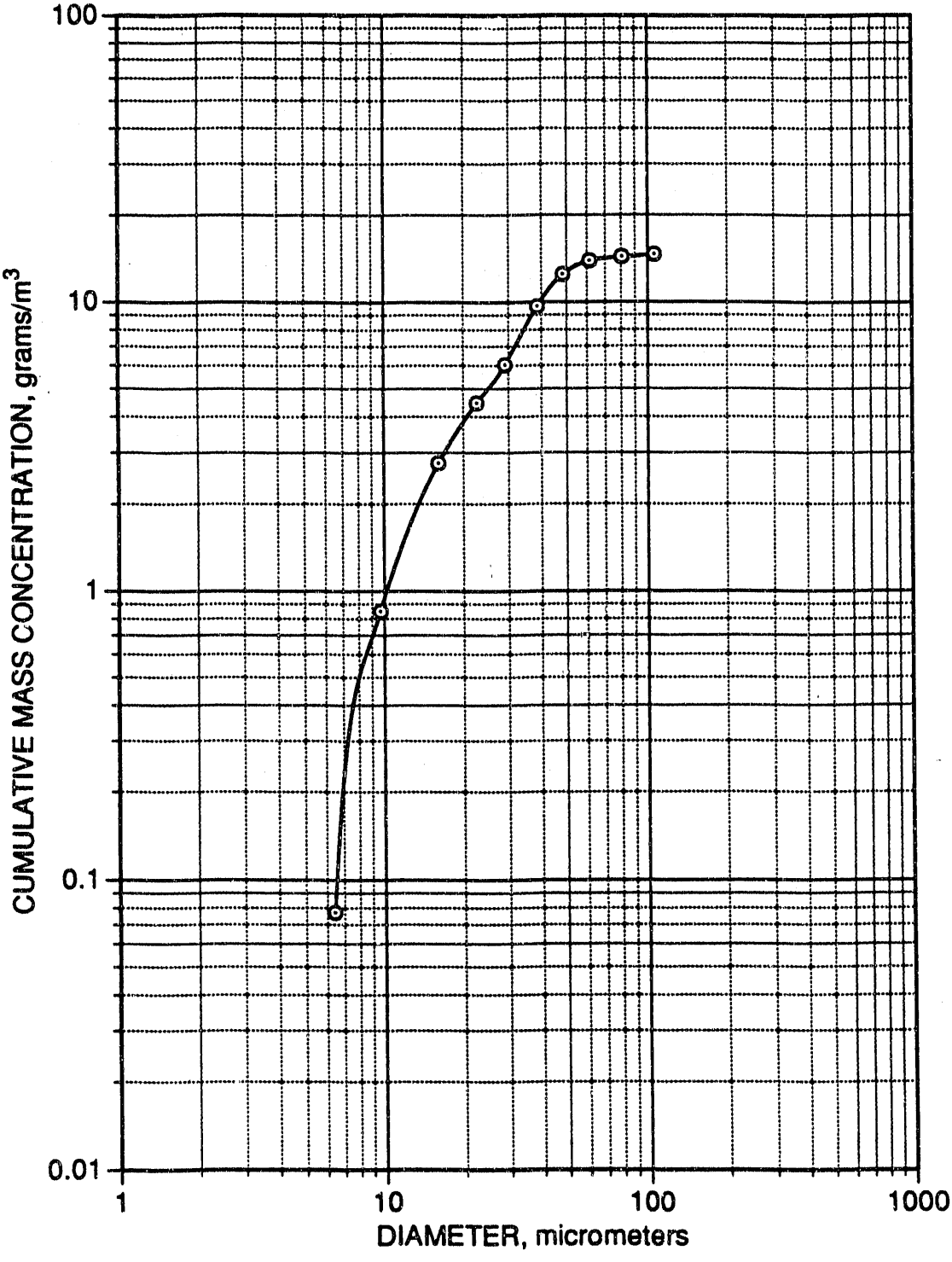

Figure A-23. Cumulative mass concentration versus particle size for Parker-Hannifin nozzle test #19.

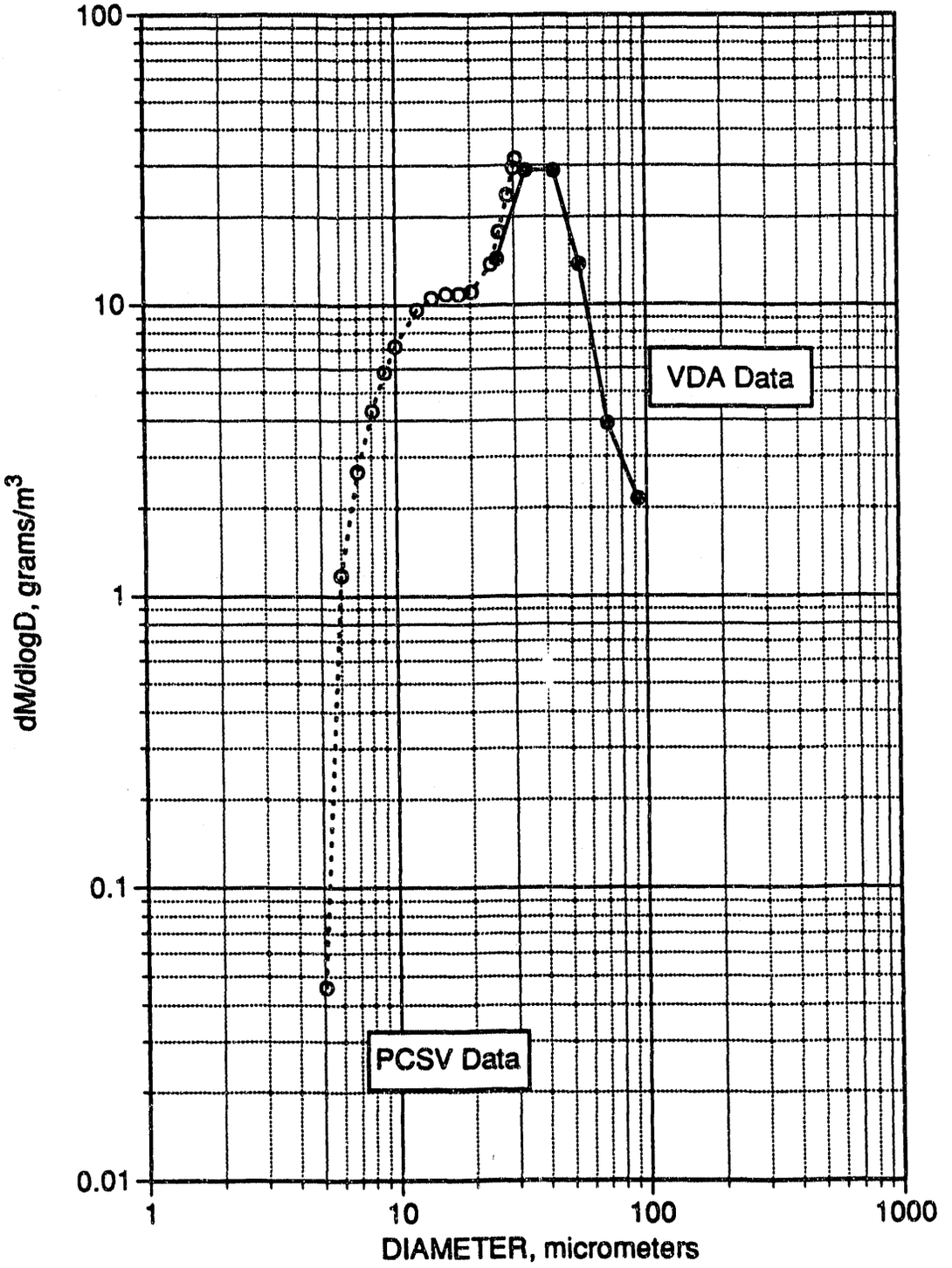

Figure A-24. Differential mass concentration versus particle size for Parker-Hannifin nozzle test #19. PCSV data are shown with a dashed line and open symbols, and discrete VDA data are shown with a solid line and closed symbols.

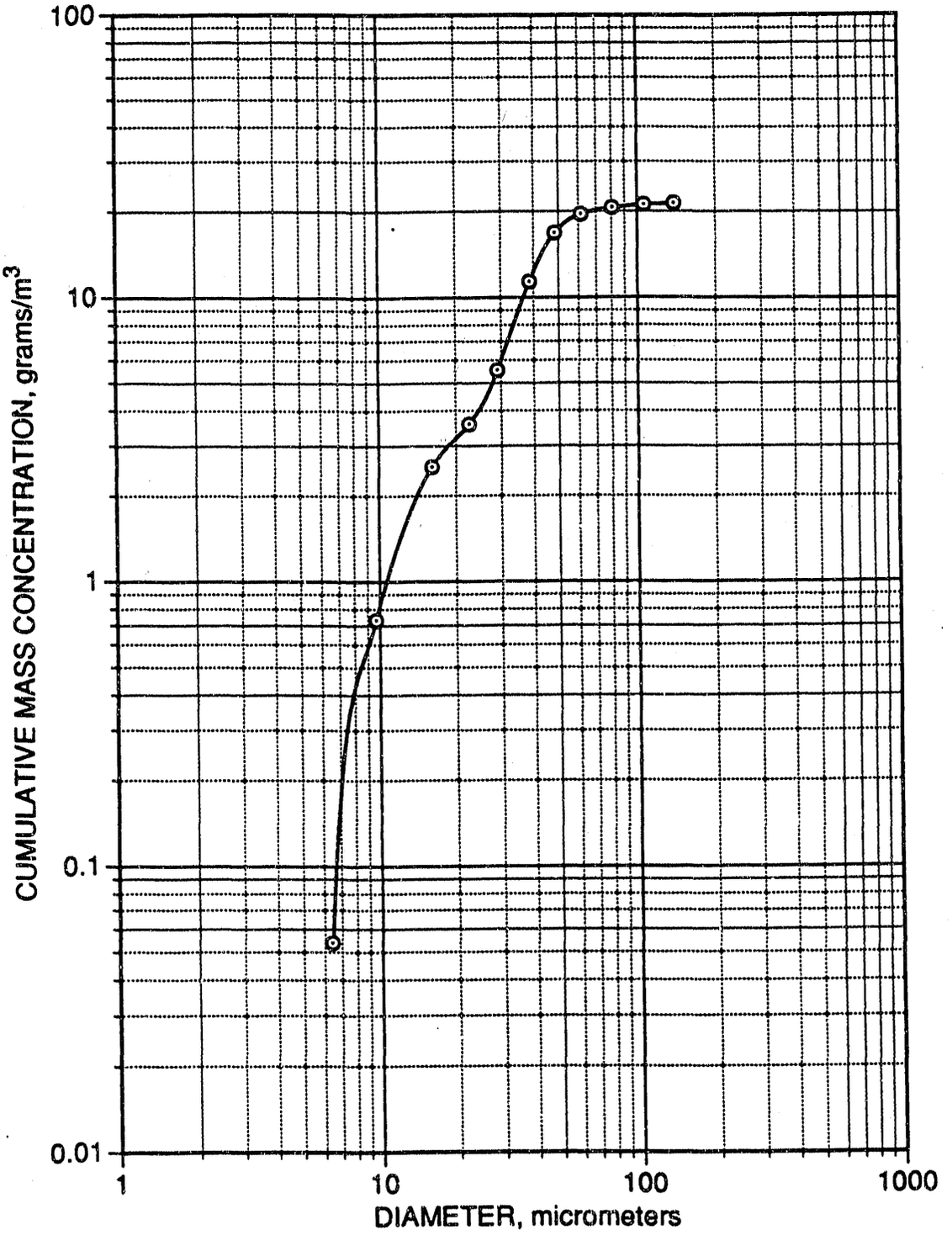

Figure A-25. Cumulative mass concentration versus particle size for Parker-Hannifin nozzle test #20.

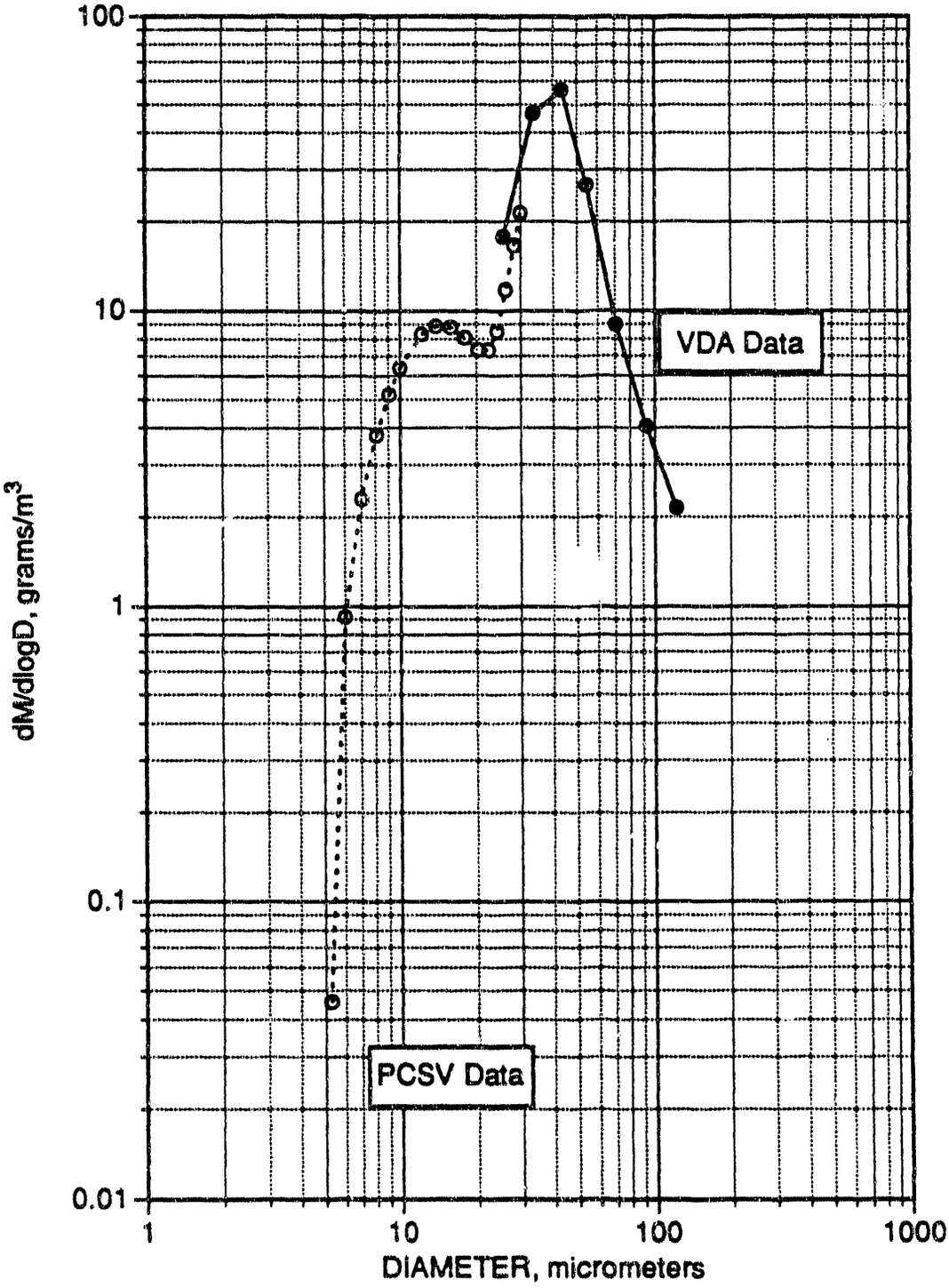

Figure A-26. Differential mass concentration versus particle size for Parker-Hannifin nozzle test #20. PCSV data are shown with a dashed line and open symbols, and discrete VDA data are shown with a solid line and closed symbols.

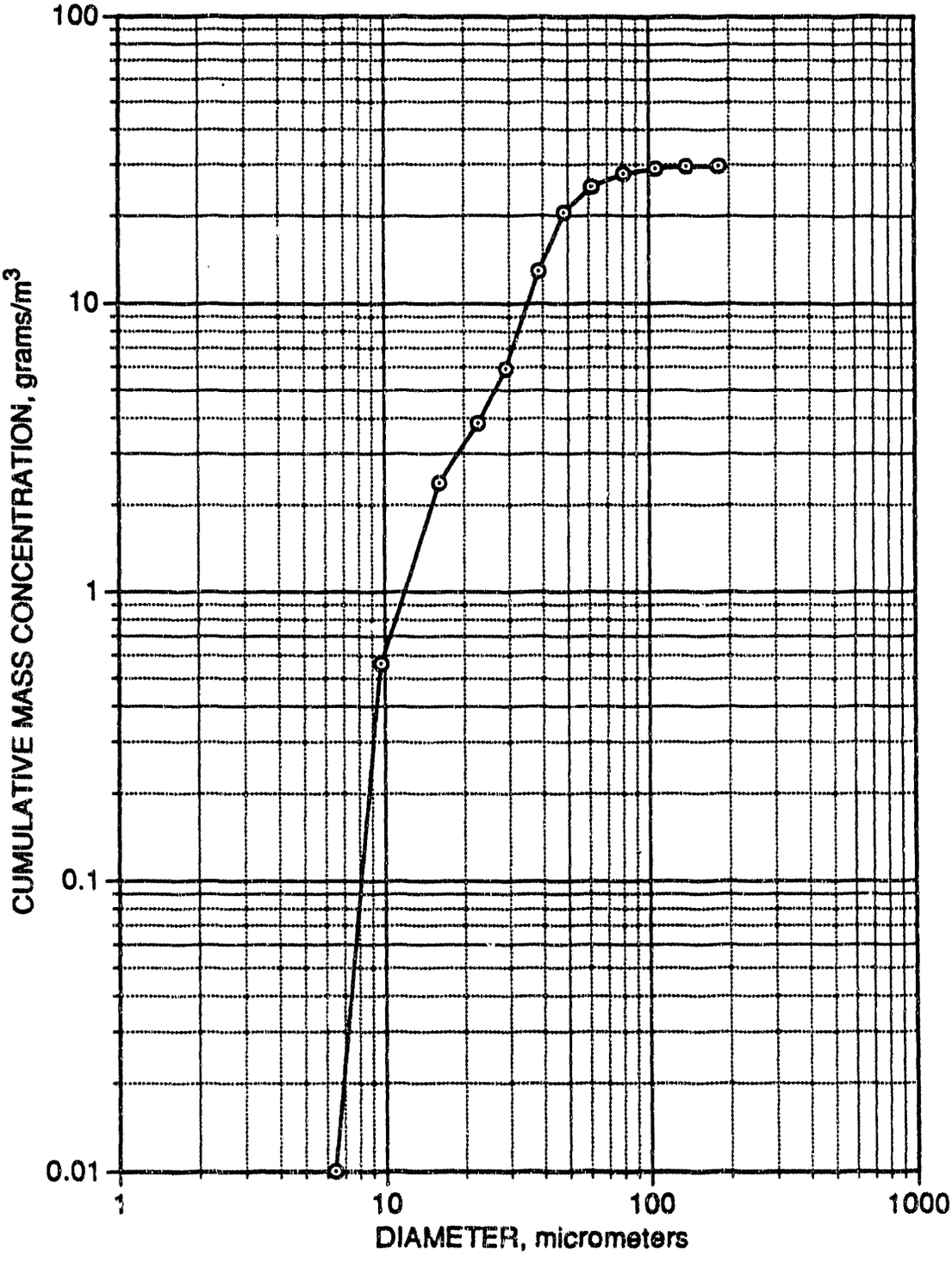

Figure A-27. Cumulative mass concentration versus particle size for Parker-Hannifin nozzle test #21.

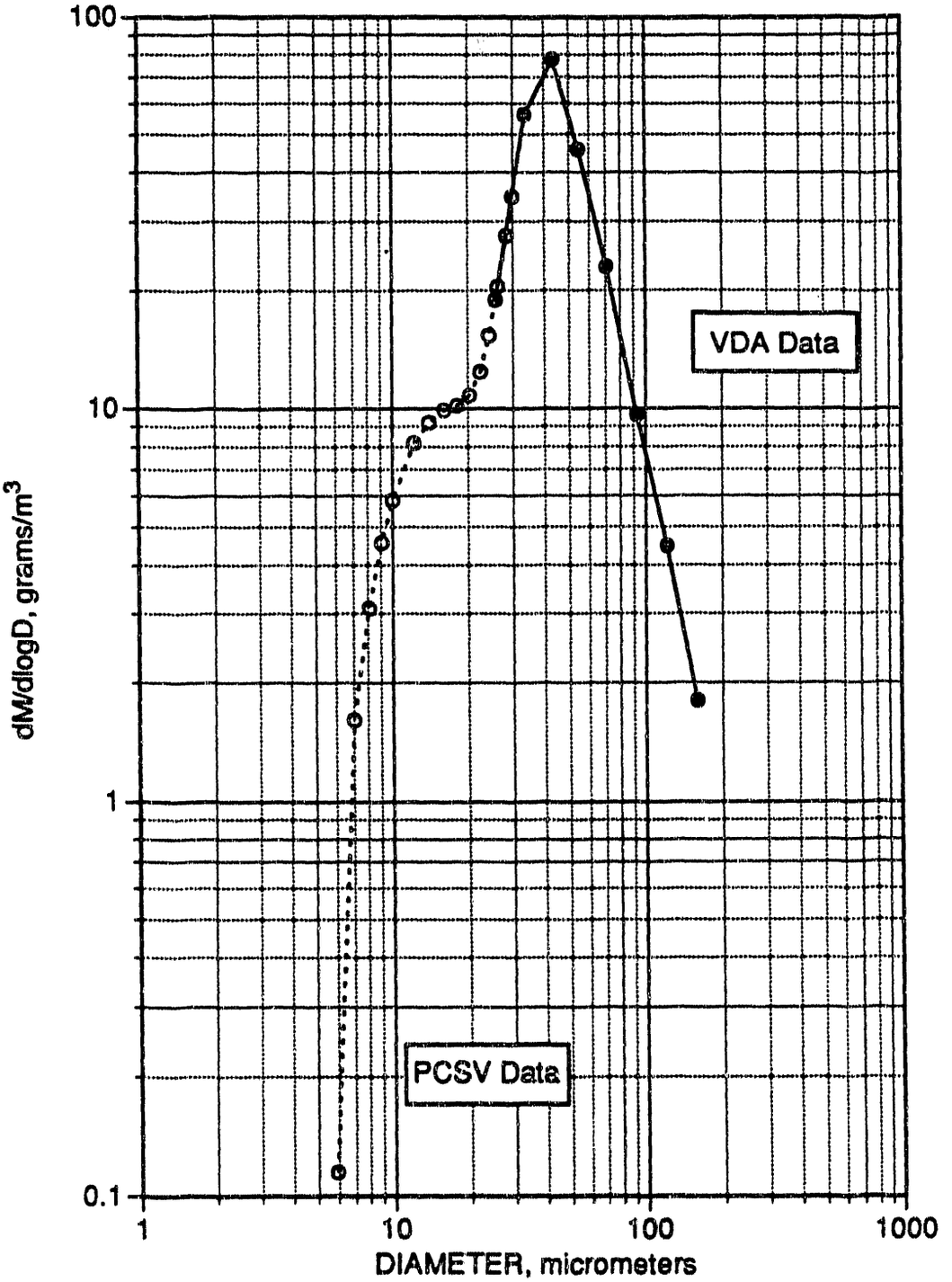

Figure A-28. Differential mass concentration versus particle size for Parker-Hannifin nozzle test #21. PCSV data are shown with a dashed line and open symbols, and discrete VDA data are shown with a solid line and closed symbols.

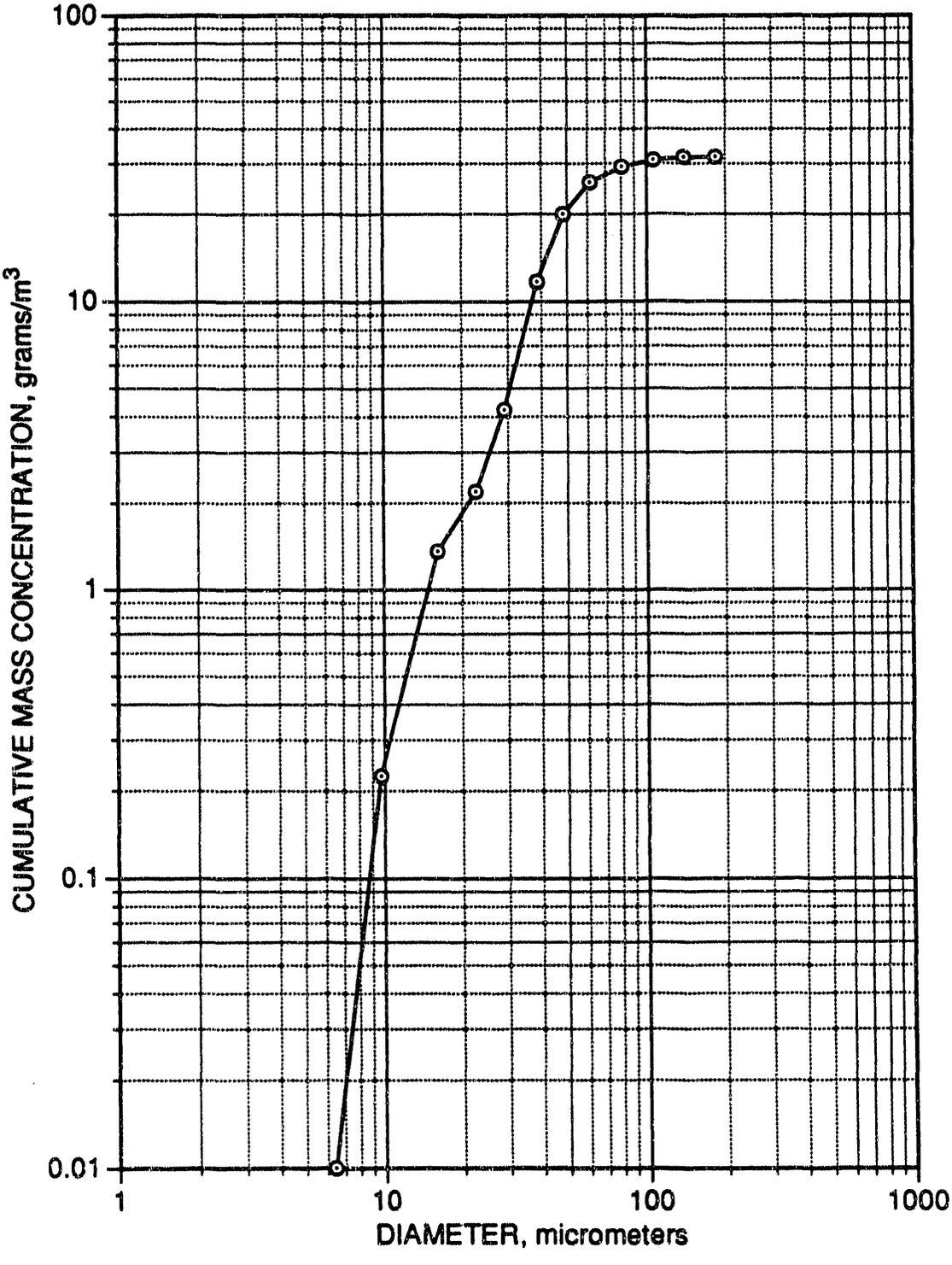

Figure A-29. Cumulative mass concentration versus particle size for Parker-Hannifin nozzle test #22.

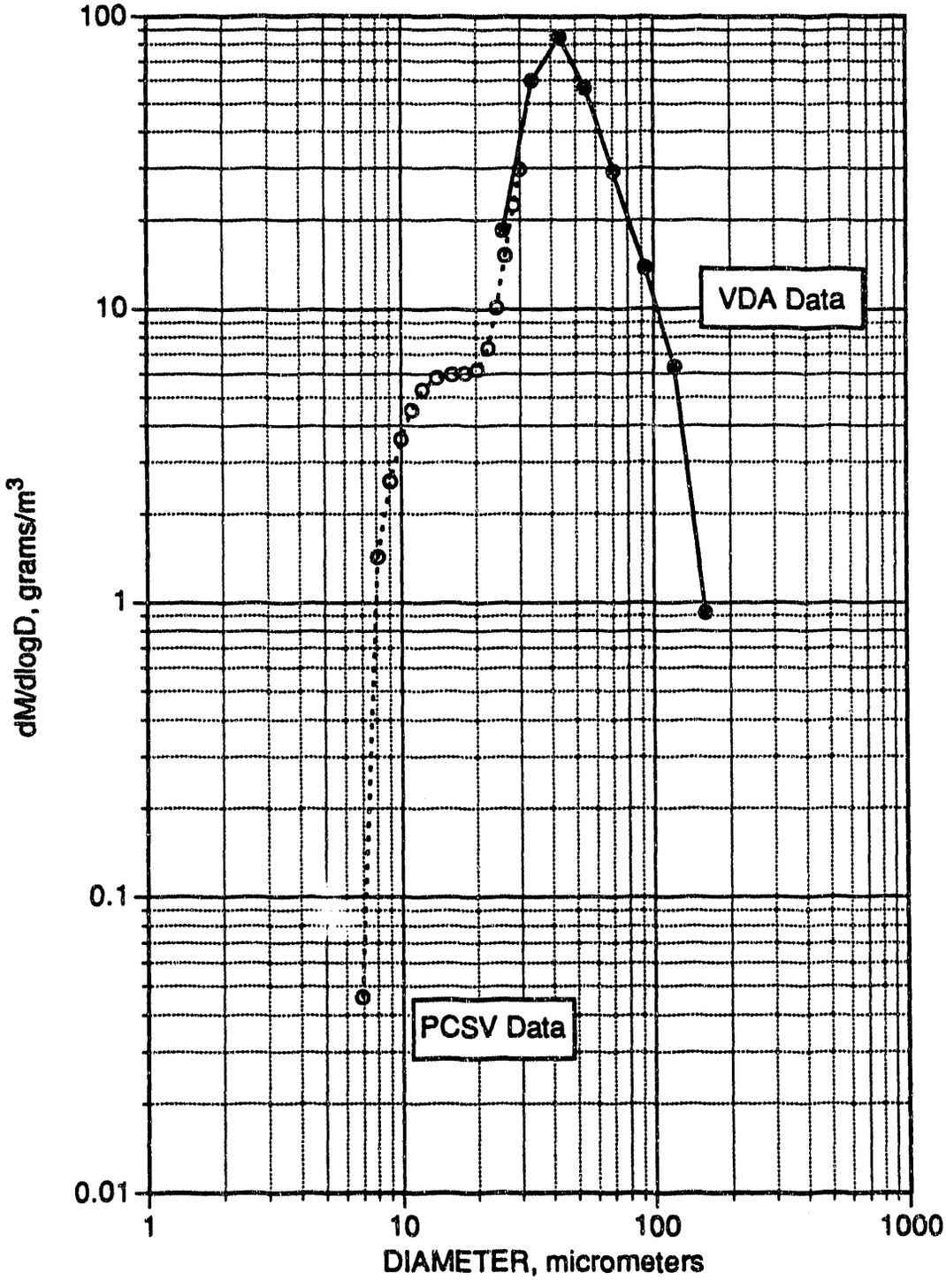

Figure A-30. Differential mass concentration versus particle size for Parker-Hannifin nozzle test #22. PCSV data are shown with a dashed line and open symbols, and discrete VDA data are shown with a solid line and closed symbols.

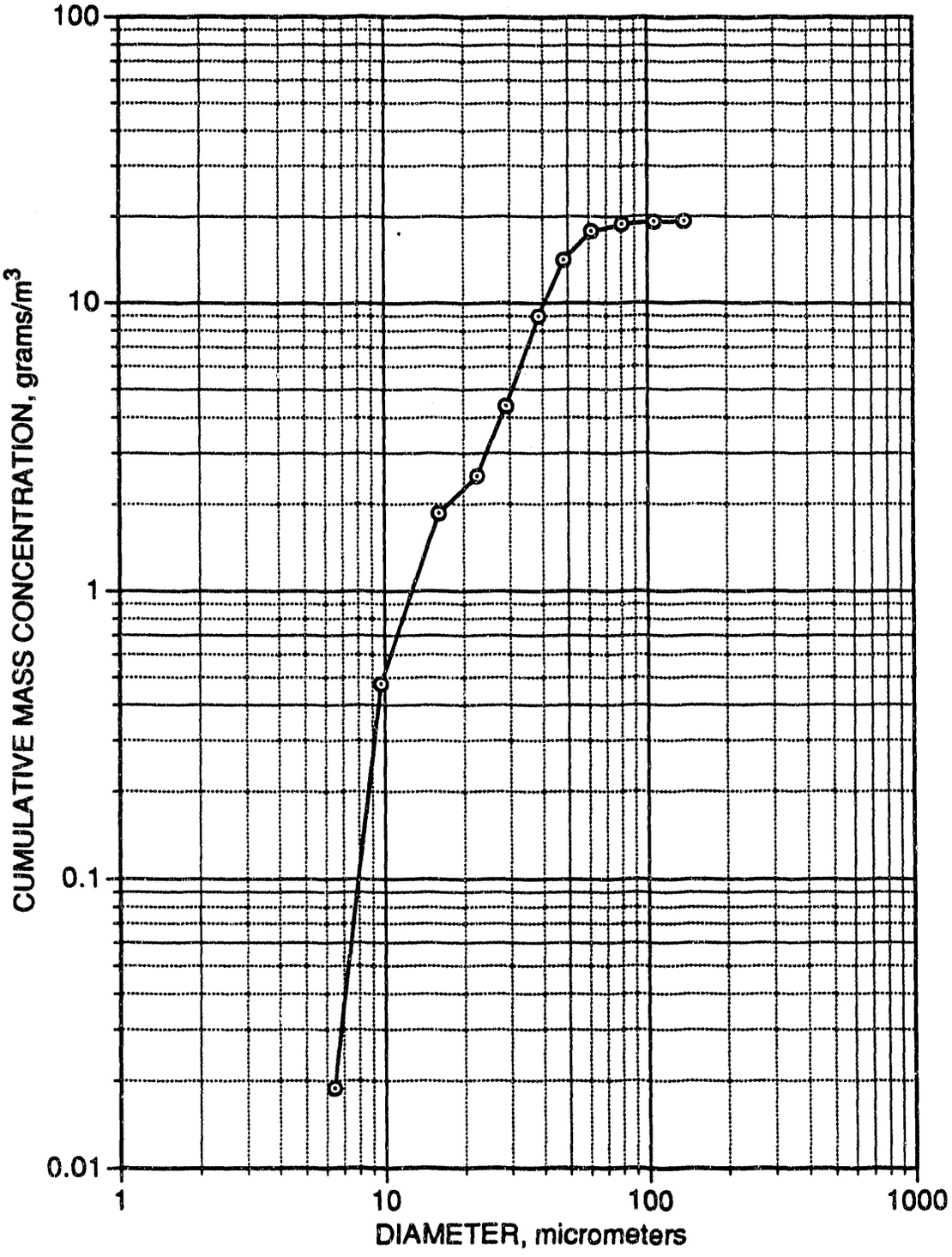

Figure A-31. Cumulative mass concentration versus particle size for Parker-Hannifin nozzle test #23.

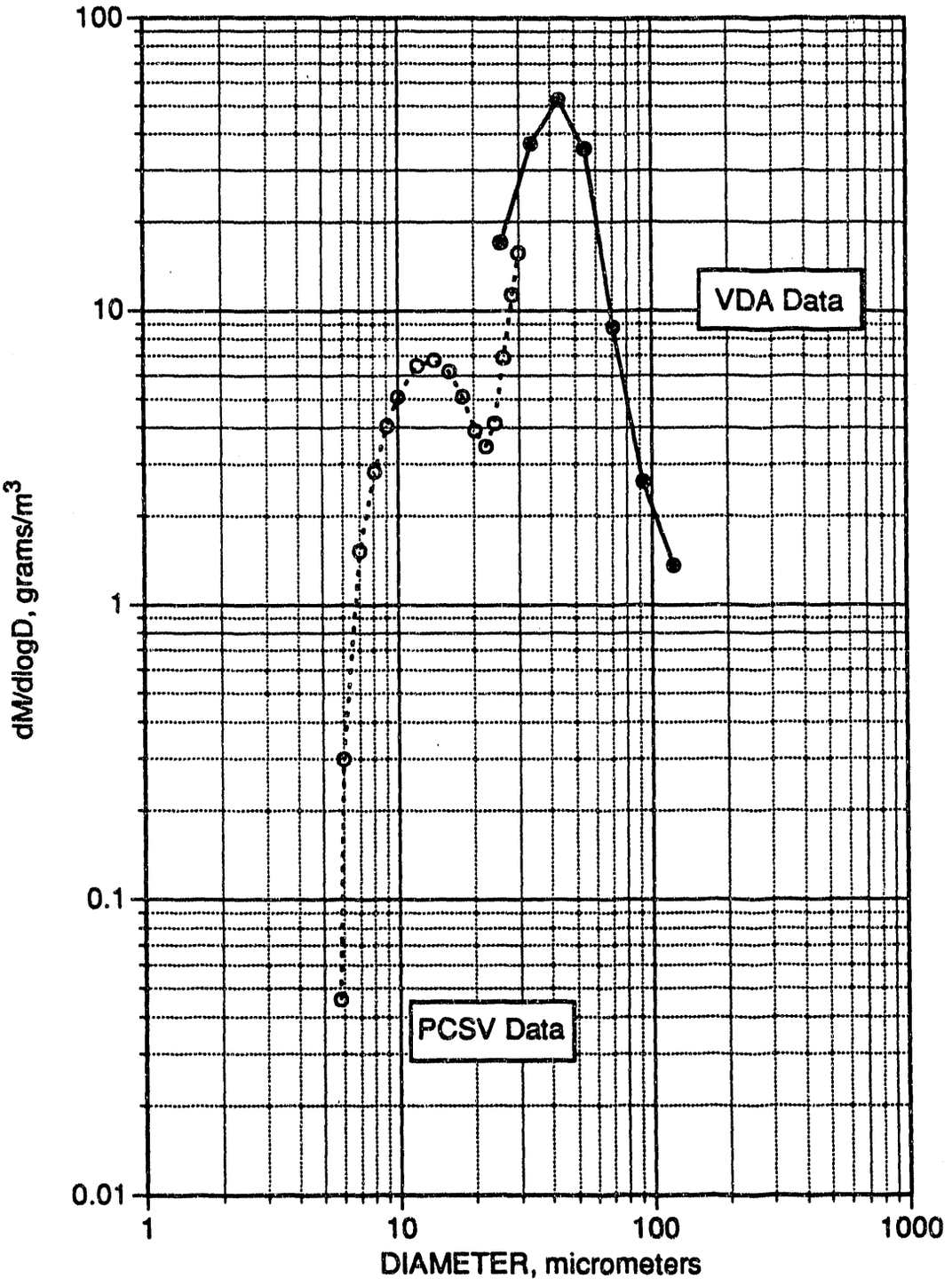

Figure A-32. Differential mass concentration versus particle size for Parker-Hannifin nozzle test #23. PCSV data are shown with a dashed line and open symbols, and discrete VDA data are shown with a solid line and closed symbols.

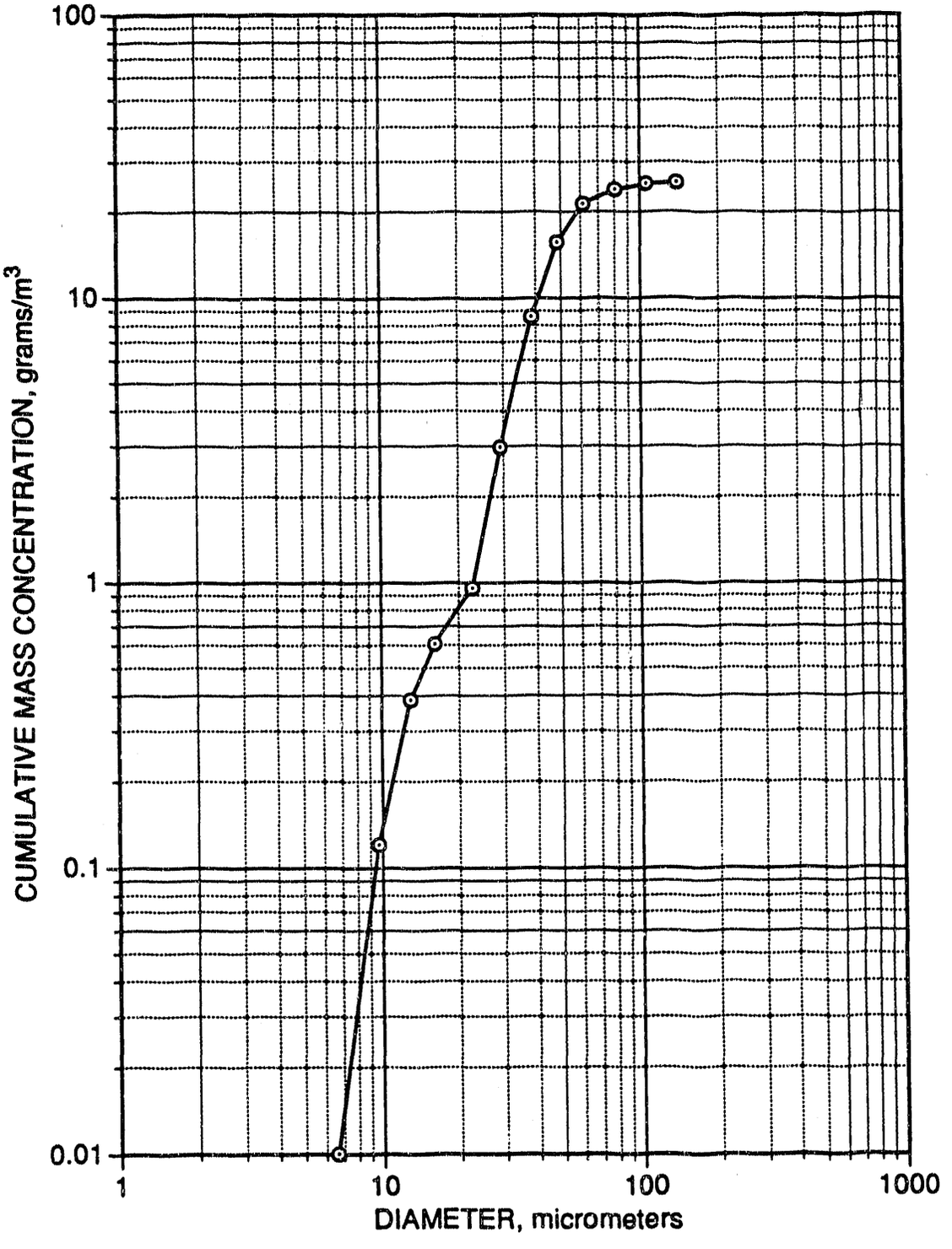

Figure A-33. Cumulative mass concentration versus particle size for Parker-Hannifin nozzle test #24.

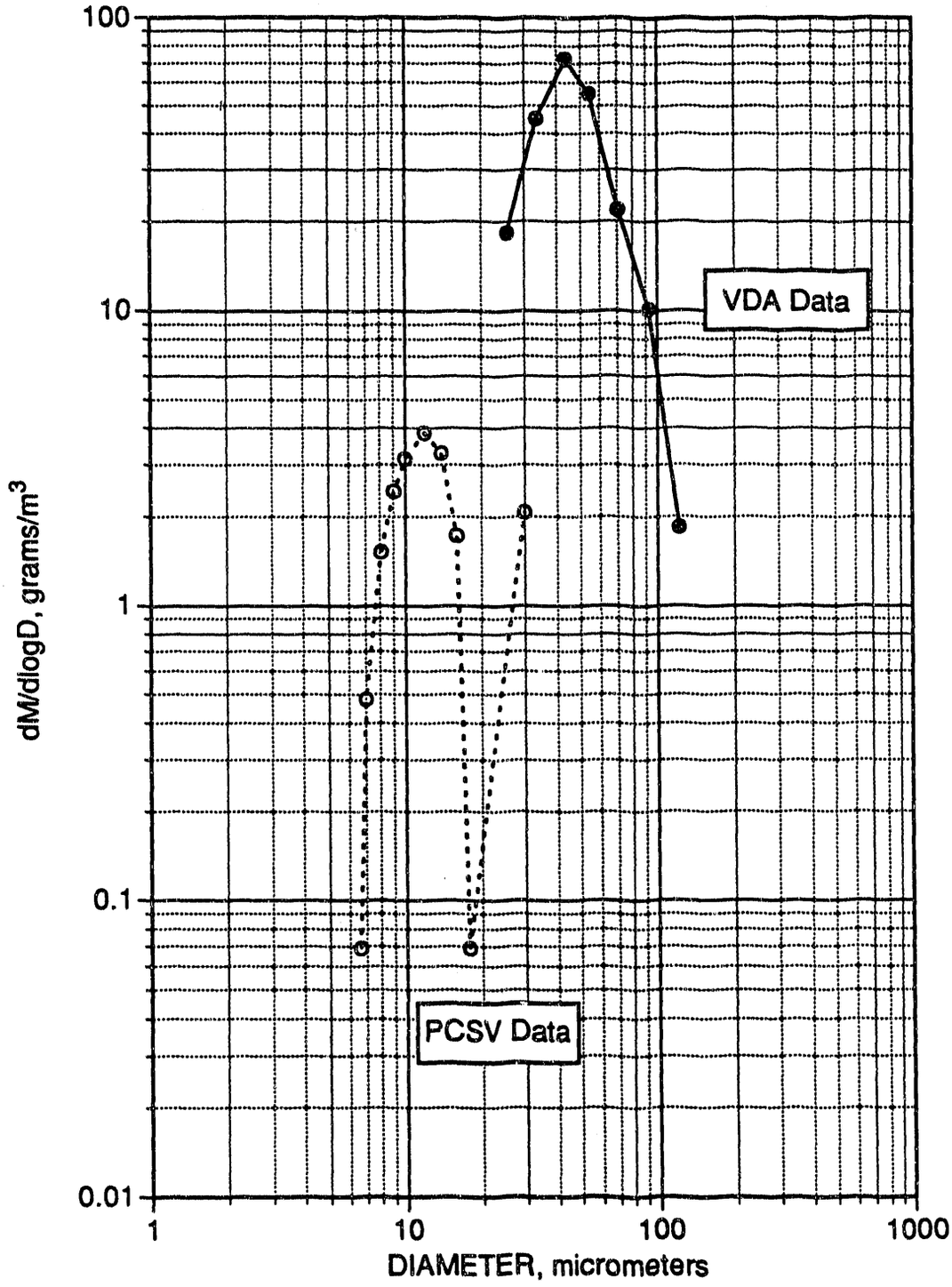

Figure A-34. Differential mass concentration versus particle size for Parker-Hannifin nozzle test #24. PCSV data are shown with a dashed line and open symbols, and discrete VDA data are shown with a solid line and closed symbols.

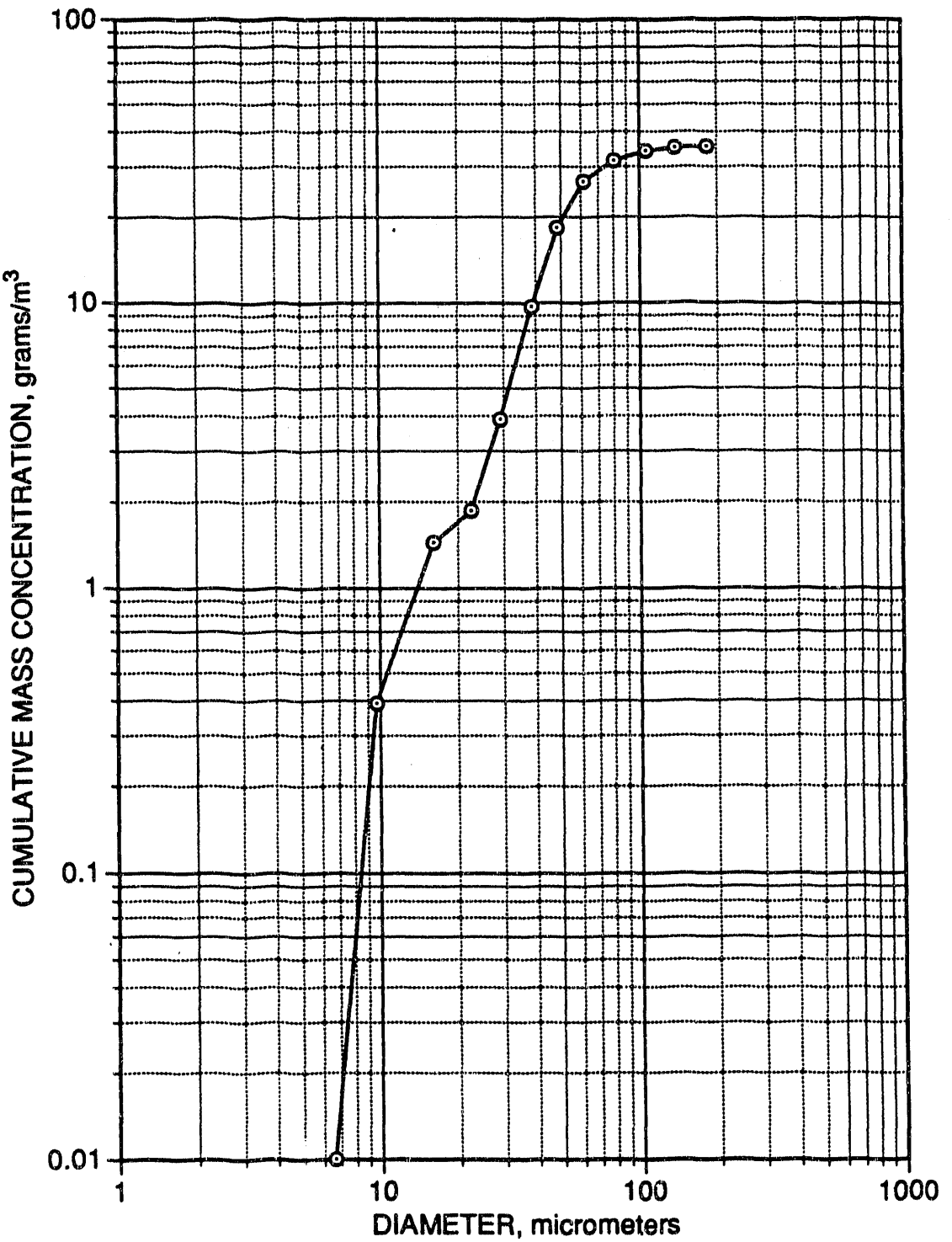

Figure A-35. Cumulative mass concentration versus particle size for Parker-Hannifin nozzle test #25.

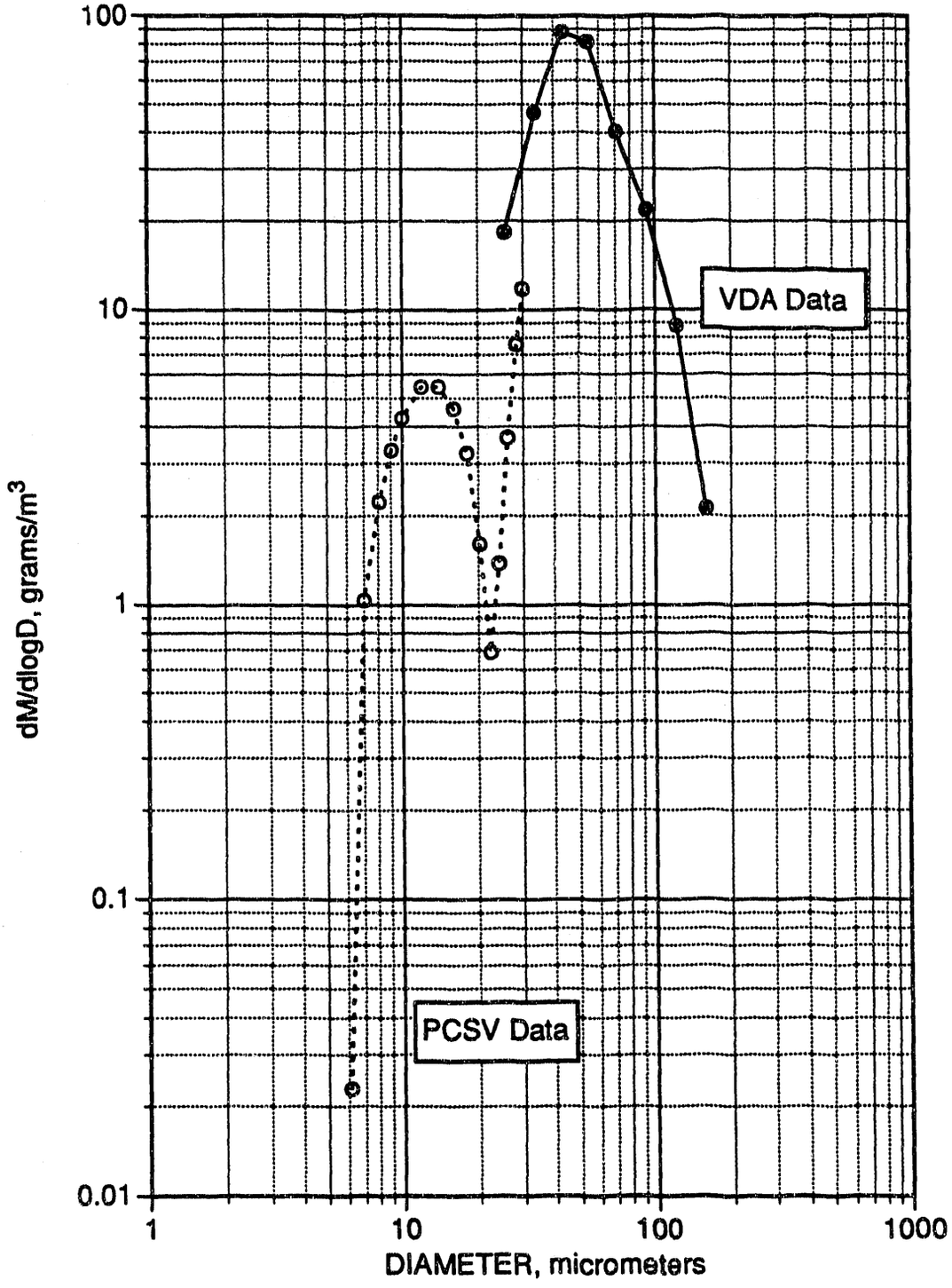

Figure A-36. Differential mass concentration versus particle size for Parker-Hannifin nozzle test #25. PCSV data are shown with a dashed line and open symbols, and discrete VDA data are shown with a solid line and closed symbols.

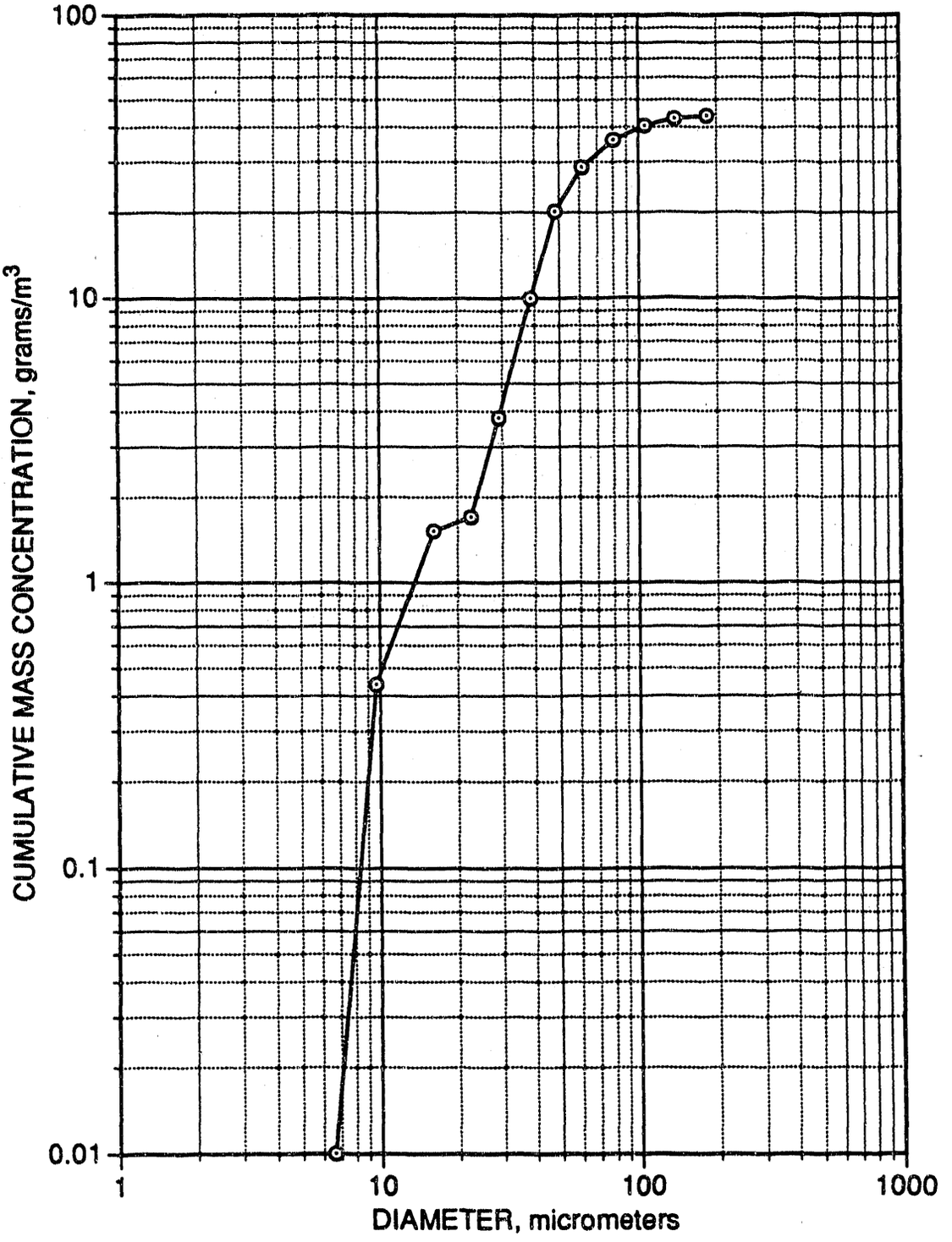

Figure A-37. Cumulative mass concentration versus particle size for Parker-Hannifin nozzle test #26.

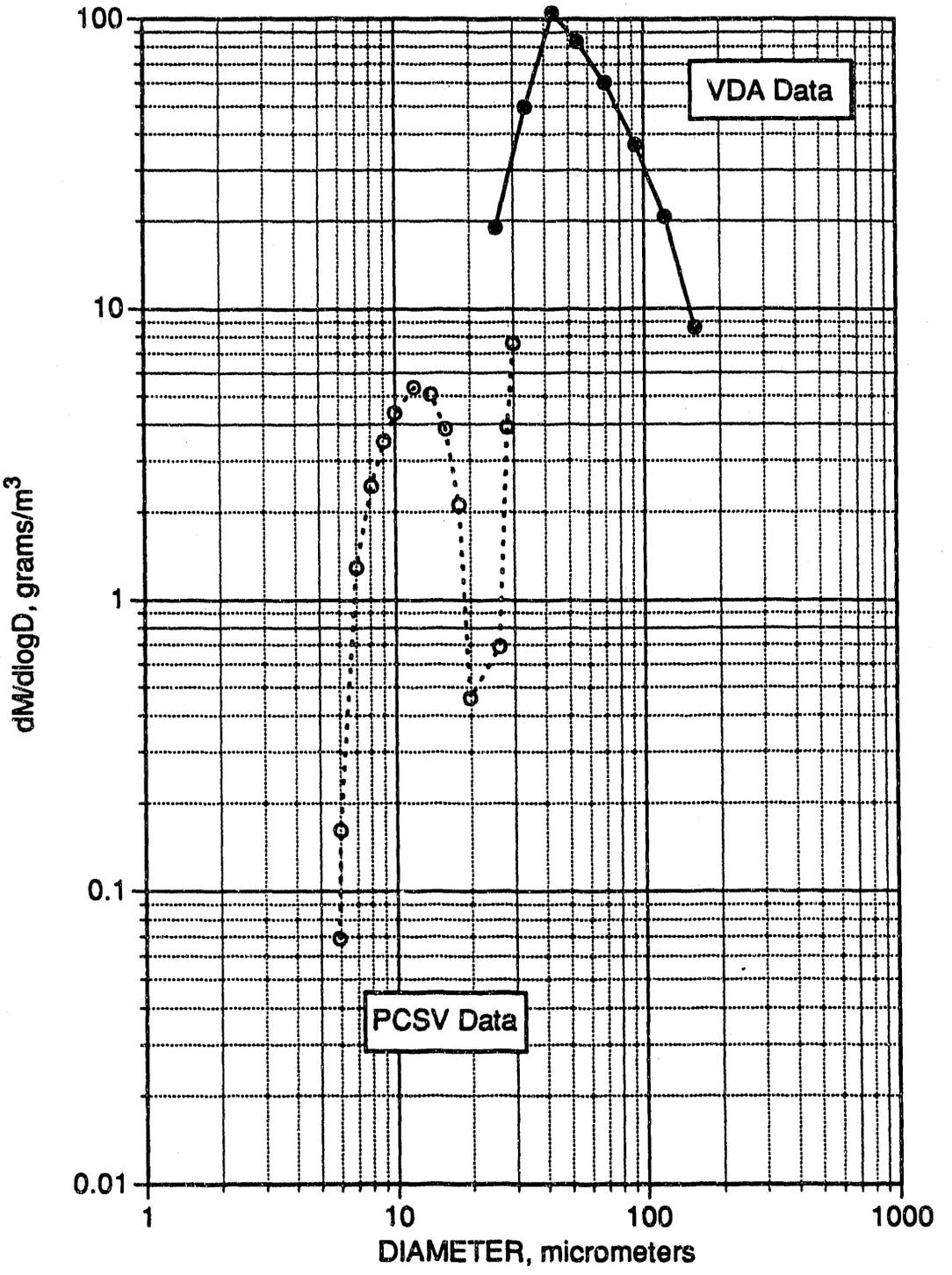

Figure A-38. Differential mass concentration versus particle size for Parker-Hannifin nozzle test #26. PCSV data are shown with a dashed line and open symbols, and discrete VDA data are shown with a solid line and closed symbols.

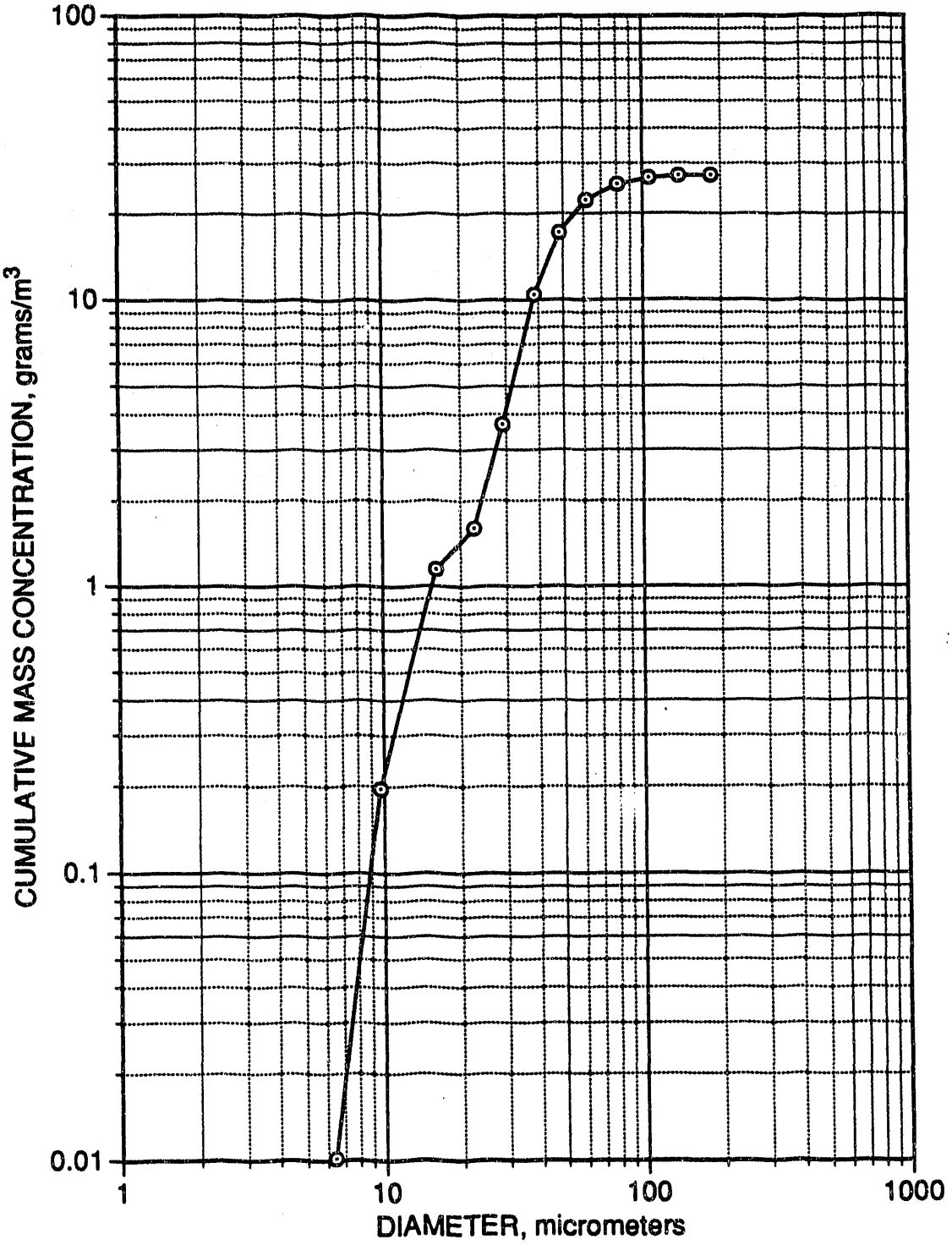

Figure A-39. Cumulative mass concentration versus particle size for Parker-Hannifin nozzle test #27.

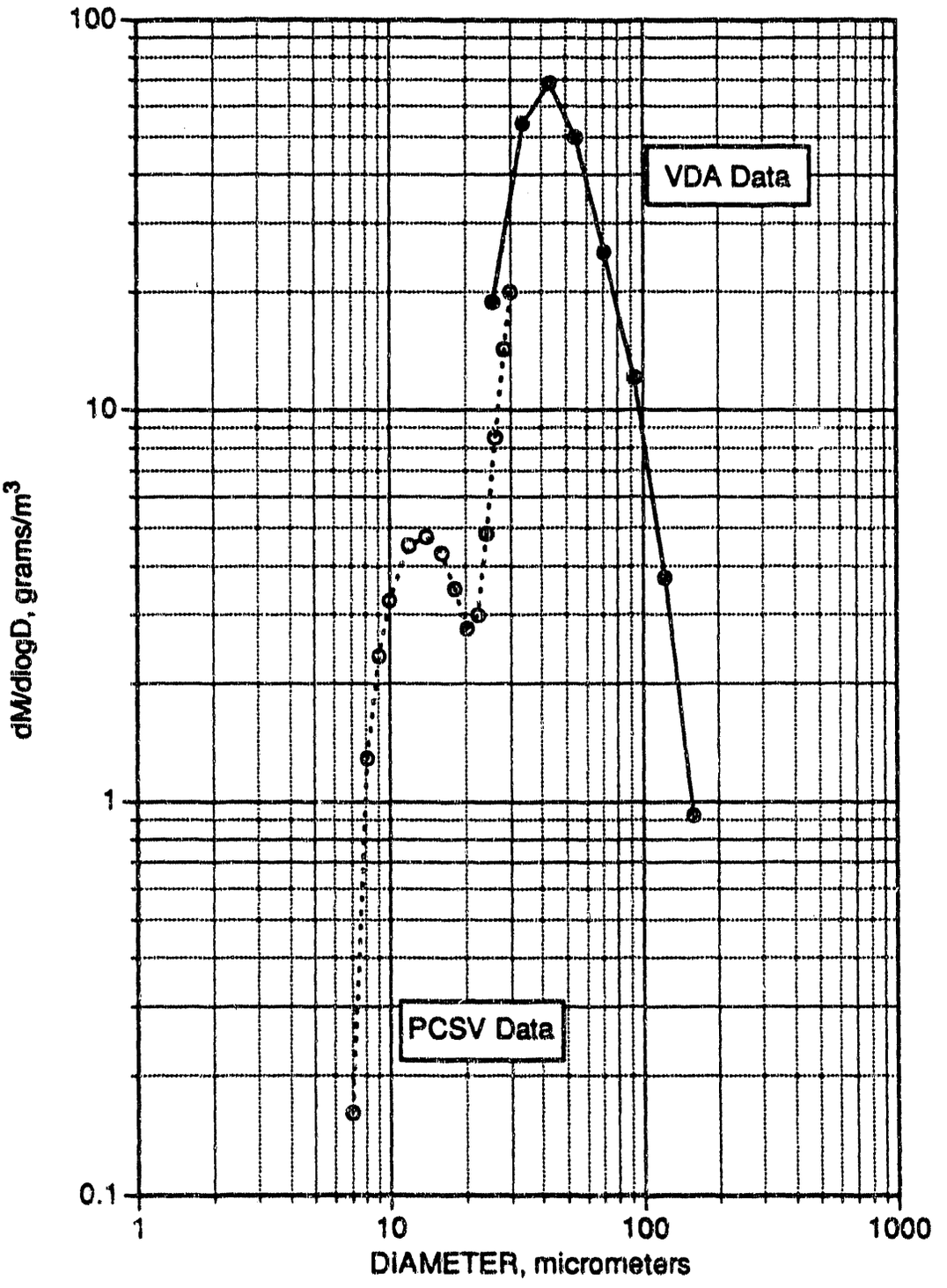

Figure A-40. Differential mass concentration versus particle size for Parker-Hannifin nozzle test #27. PCSV data are shown with a dashed line and open symbols, and discrete VDA data are shown with a solid line and closed symbols.

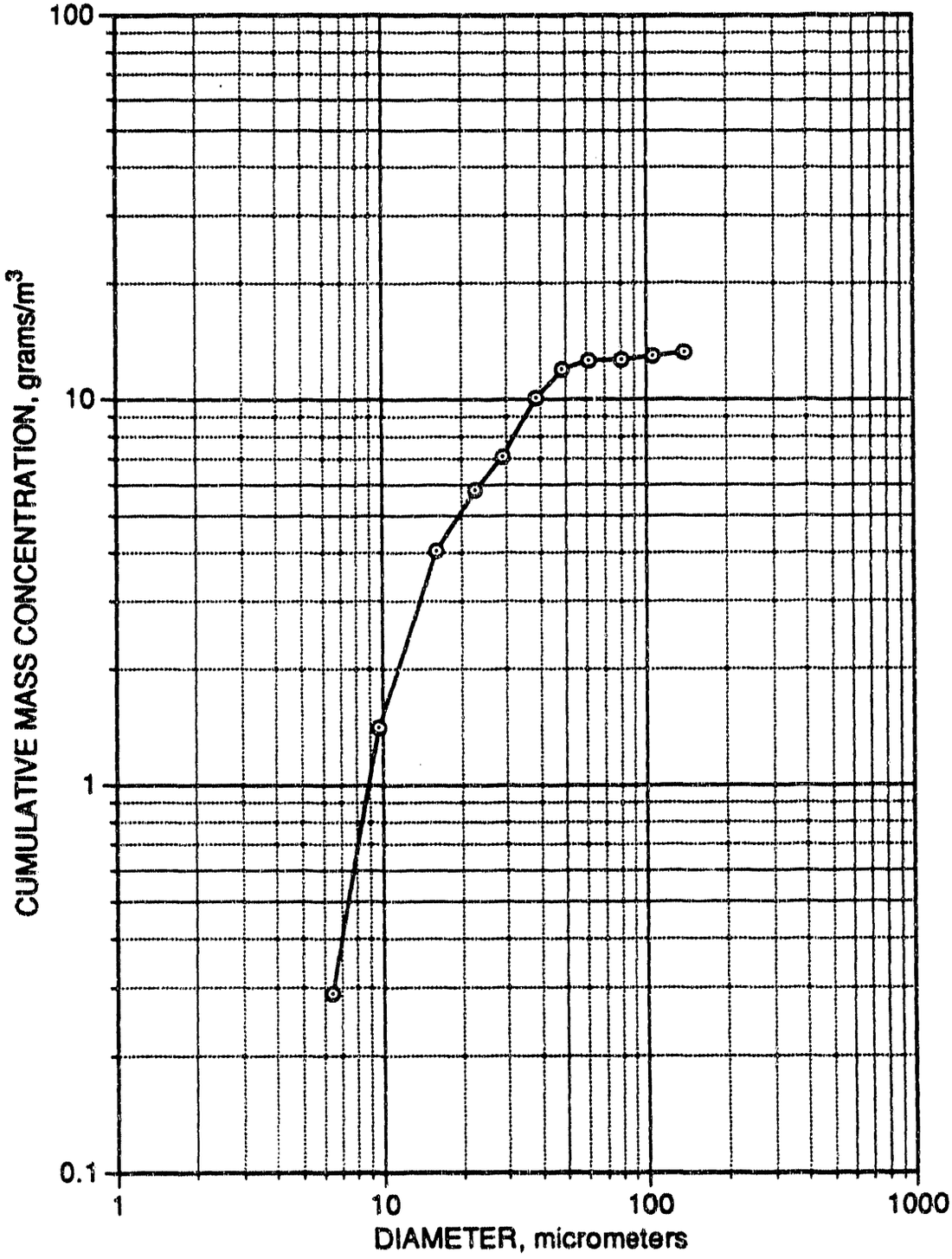

Figure A-41. Cumulative mass concentration versus particle size for Parker-Hannifin nozzle test #28.

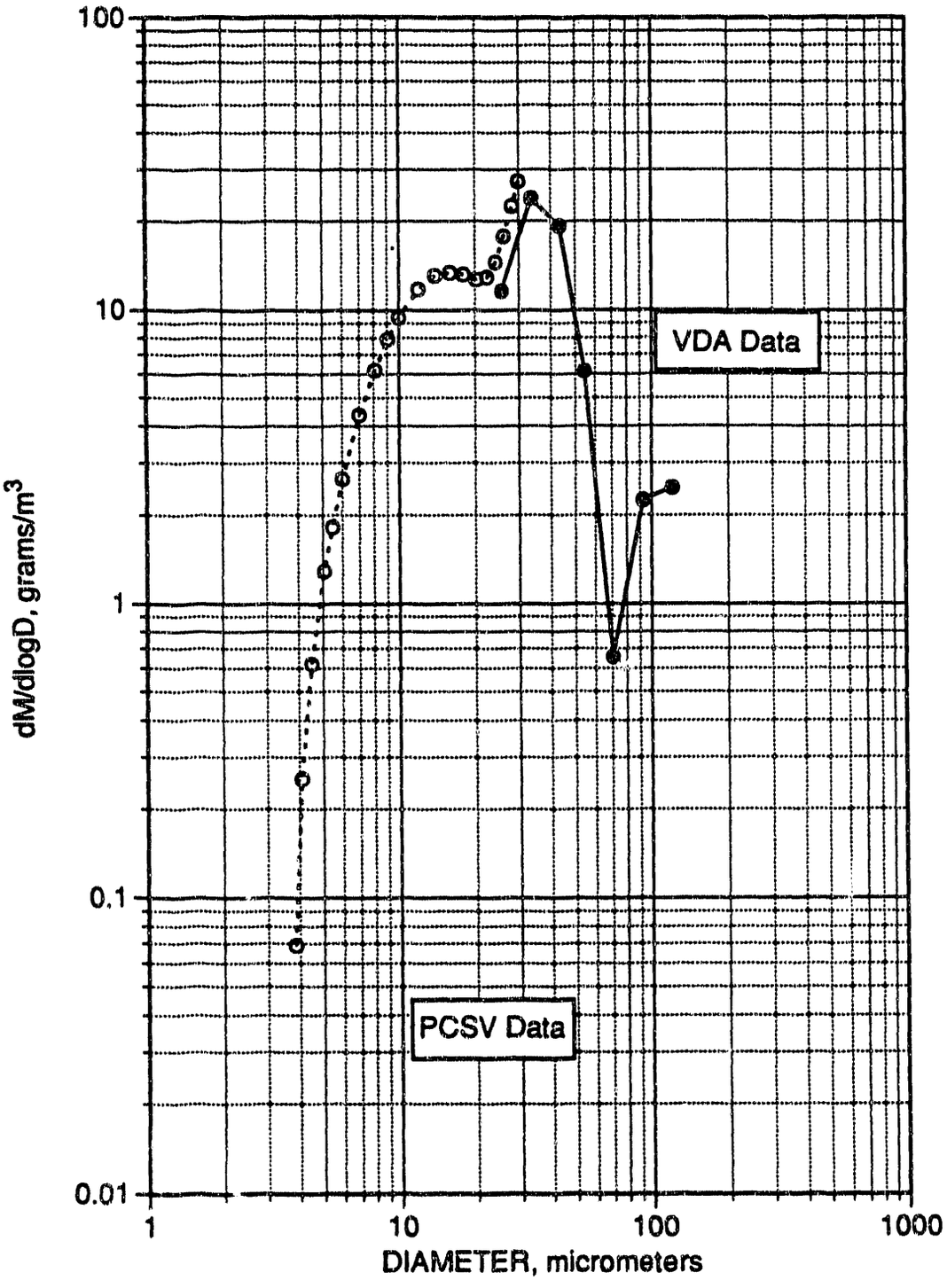

Figure A-42. Differential mass concentration versus particle size for Parker-Hannifin nozzle test #28. PCSV data are shown with a dashed line and open symbols, and discrete VDA data are shown with a solid line and closed symbols.

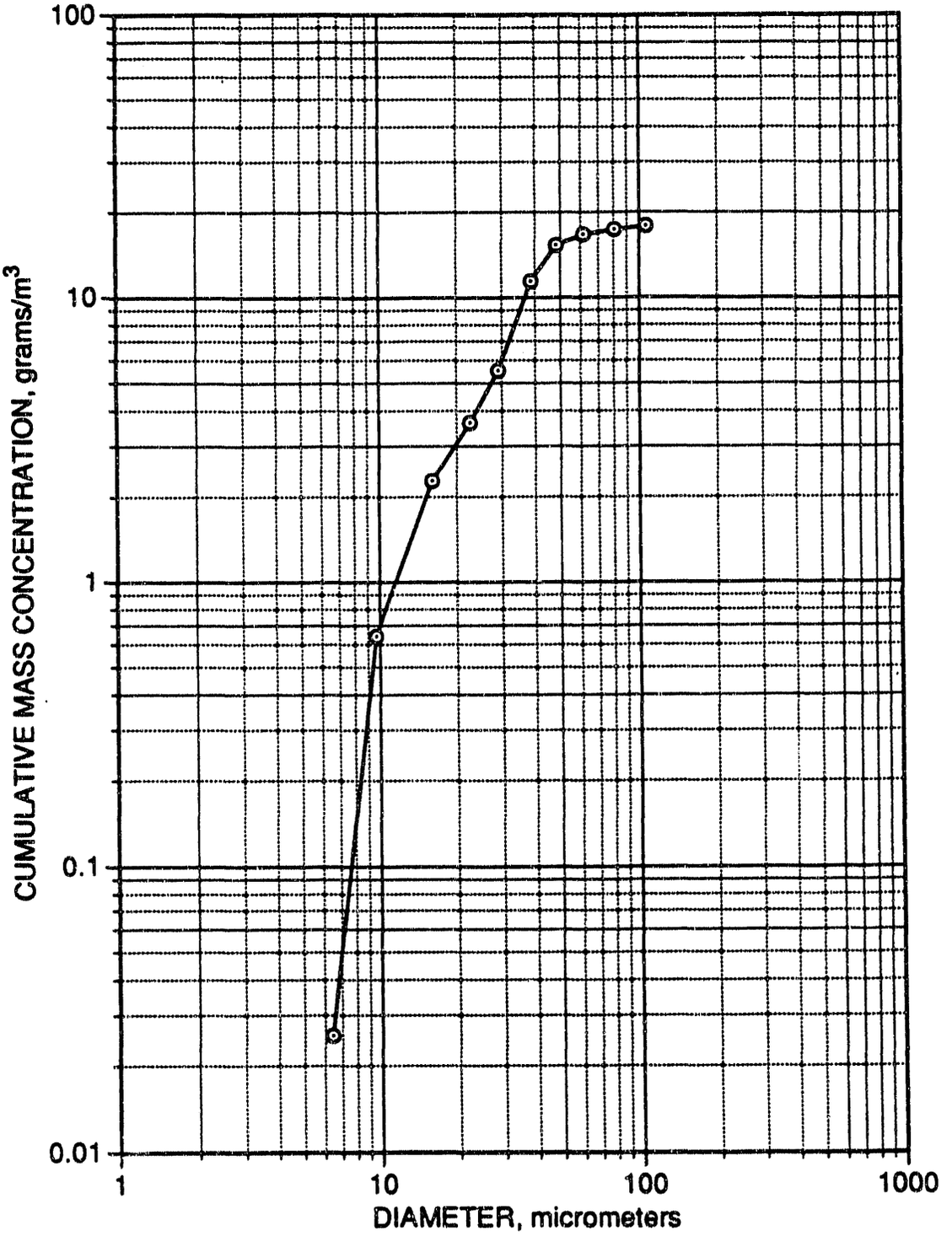

Figure A-43. Cumulative mass concentration versus particle size for Parker-Hannifin nozzle test #29.

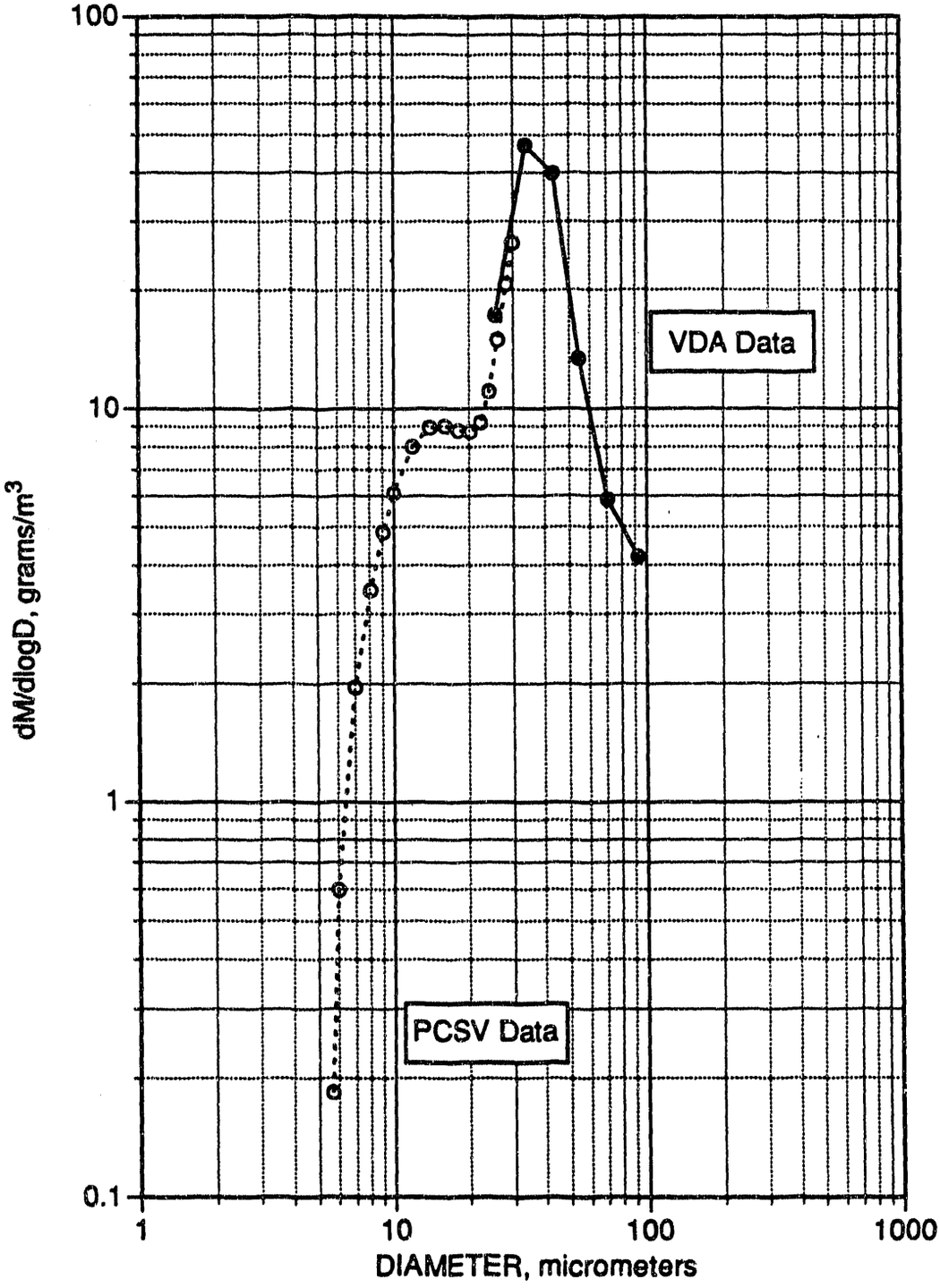

Figure A-44. Differential mass concentration versus particle size for Parker-Hannifin nozzle test #29. PCSV data are shown with a dashed line and open symbols, and discrete VDA data are shown with a solid line and closed symbols.

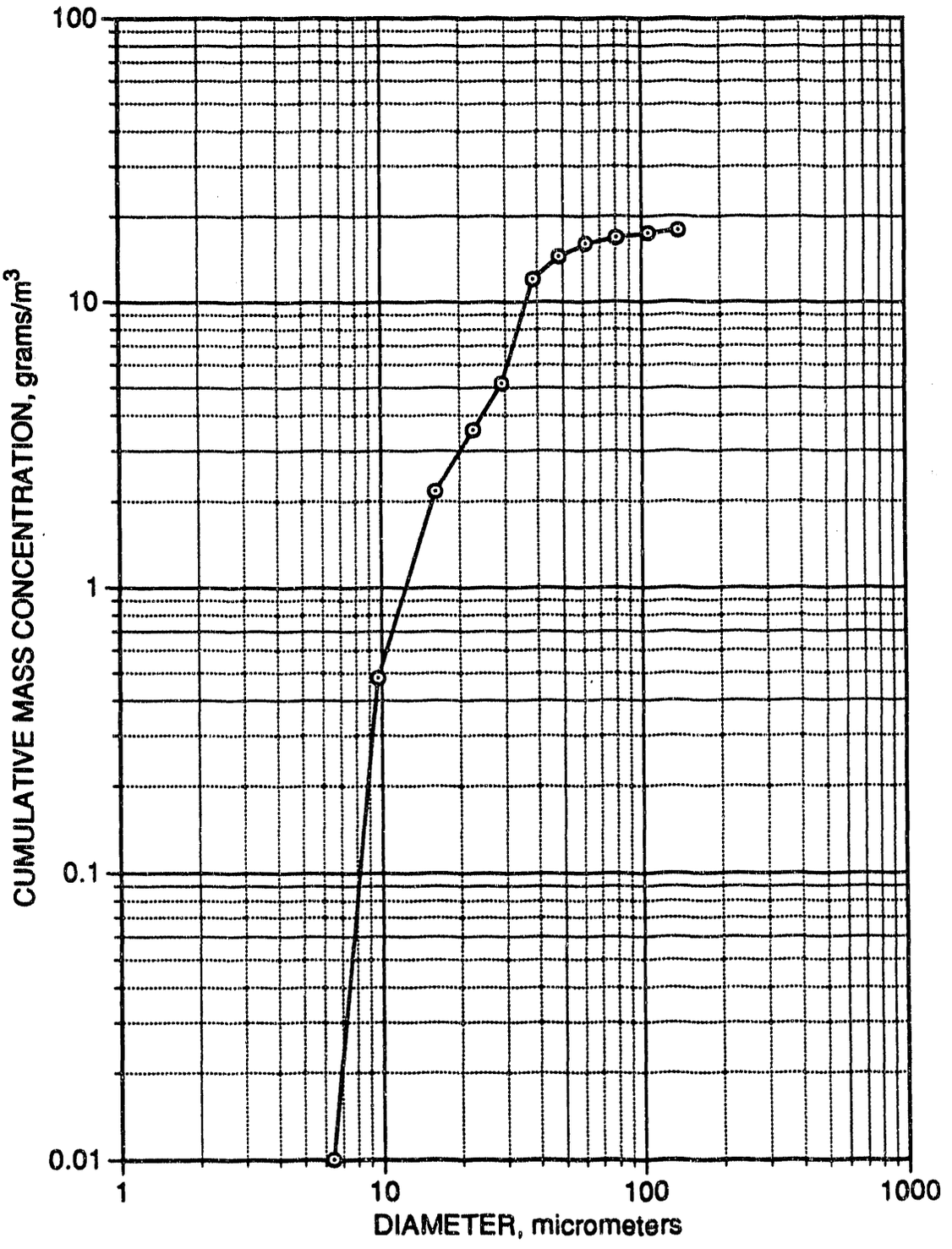

Figure A-45. Cumulative mass concentration versus particle size for Parker-Hannifin nozzle test #30.

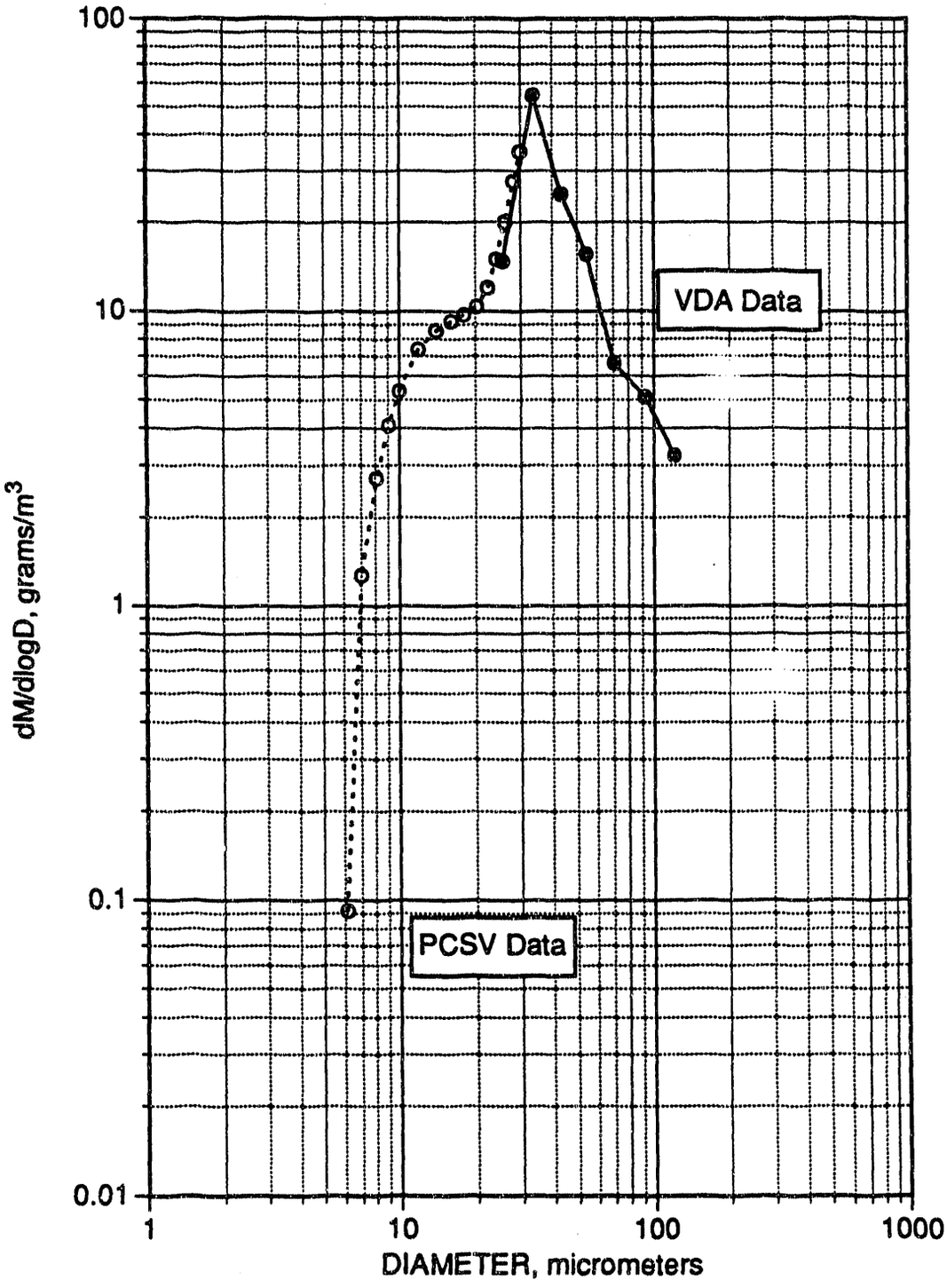

Figure A-46. Differential mass concentration versus particle size for Parker-Hannifin nozzle test #30. PCSV data are shown with a dashed line and open symbols, and discrete VDA data are shown with a solid line and closed symbols.

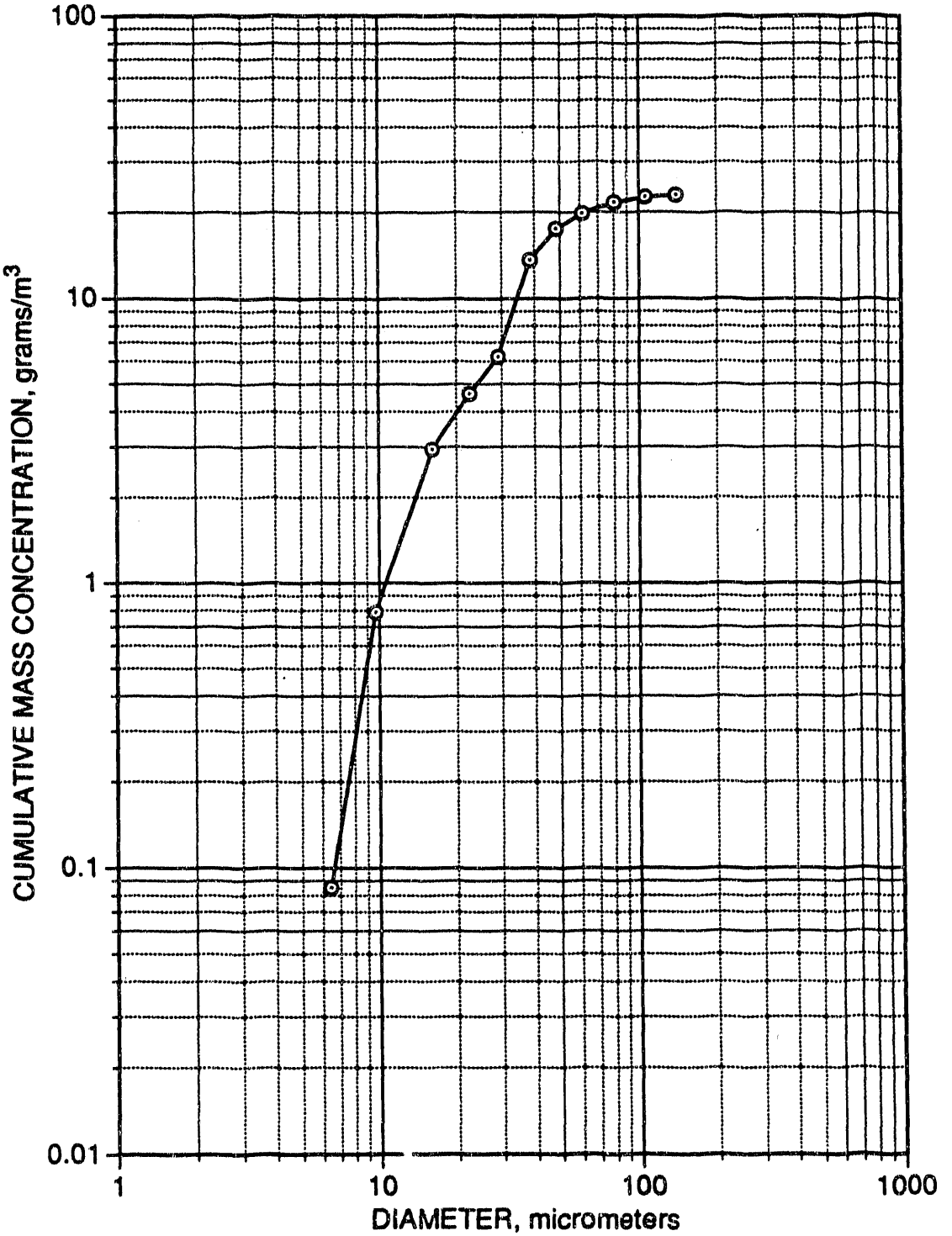

Figure A-47. Cumulative mass concentration versus particle size for Parker-Hannifin nozzle test #31.

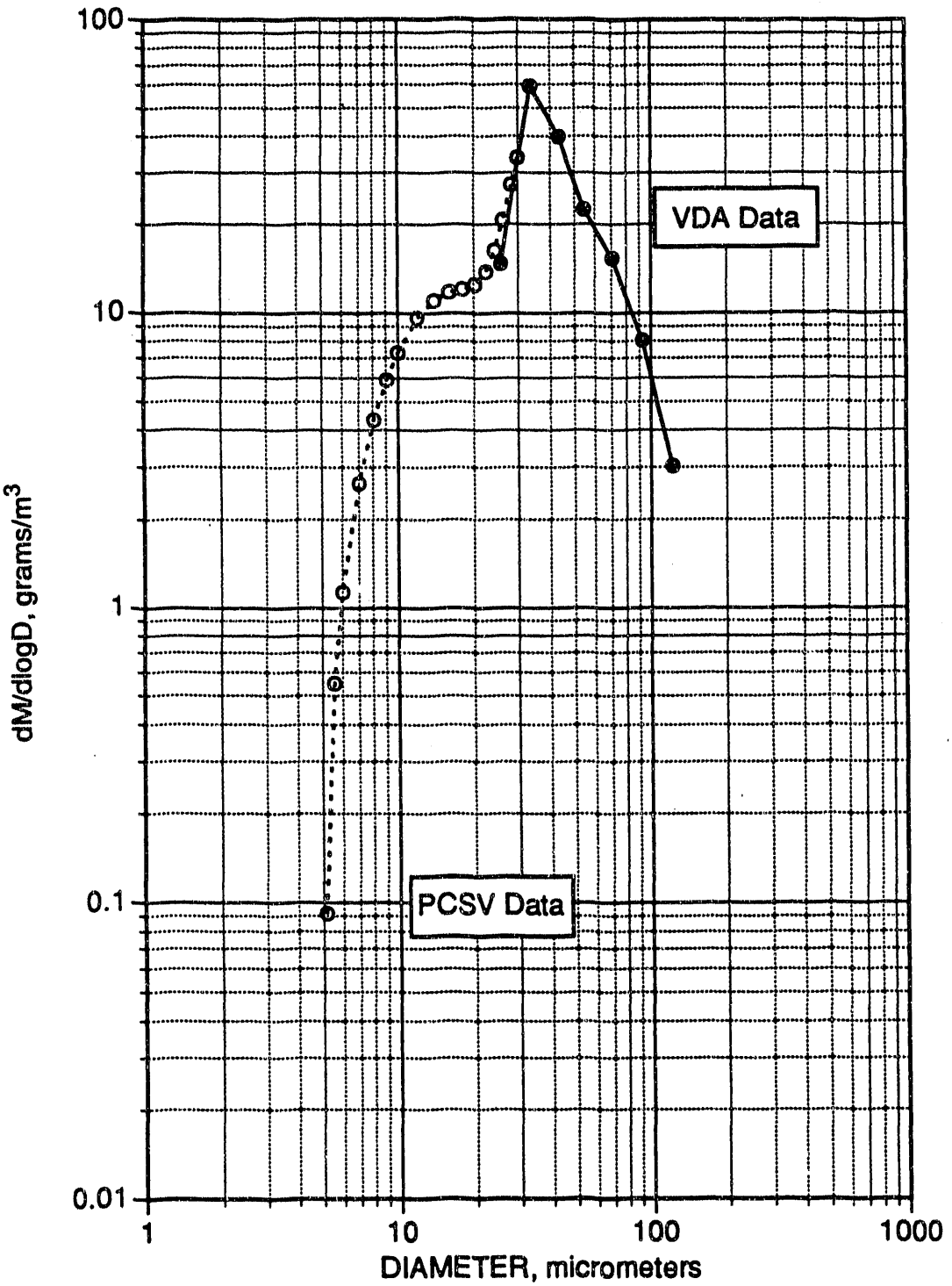

Figure A-48. Differential mass concentration versus particle size for Parker-Hannifin nozzle test #31. PCSV data are shown with a dashed line and open symbols, and discrete VDA data are shown with a solid line and closed symbols.

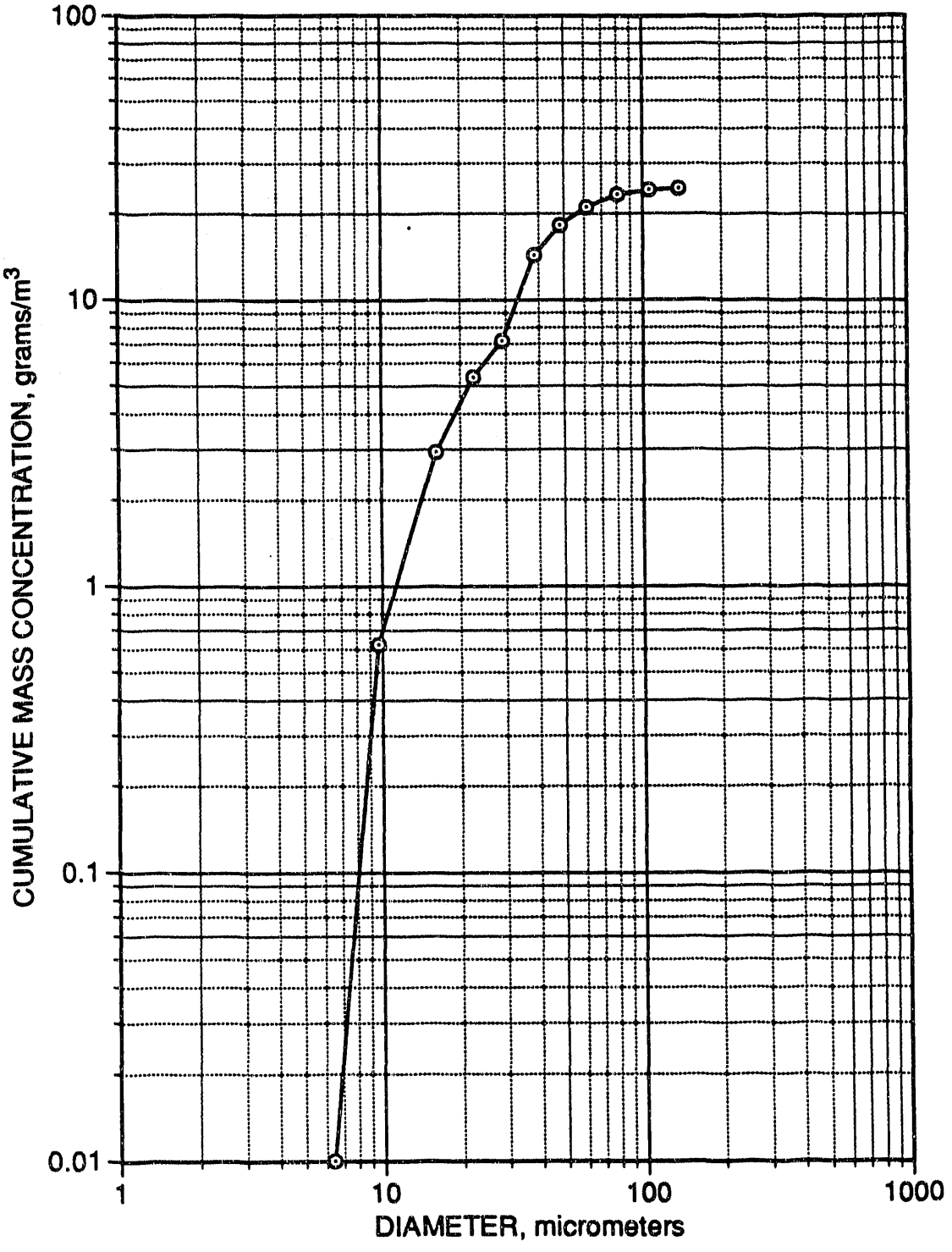

Figure A-49. Cumulative mass concentration versus particle size for Parker-Hannifin nozzle test #32.

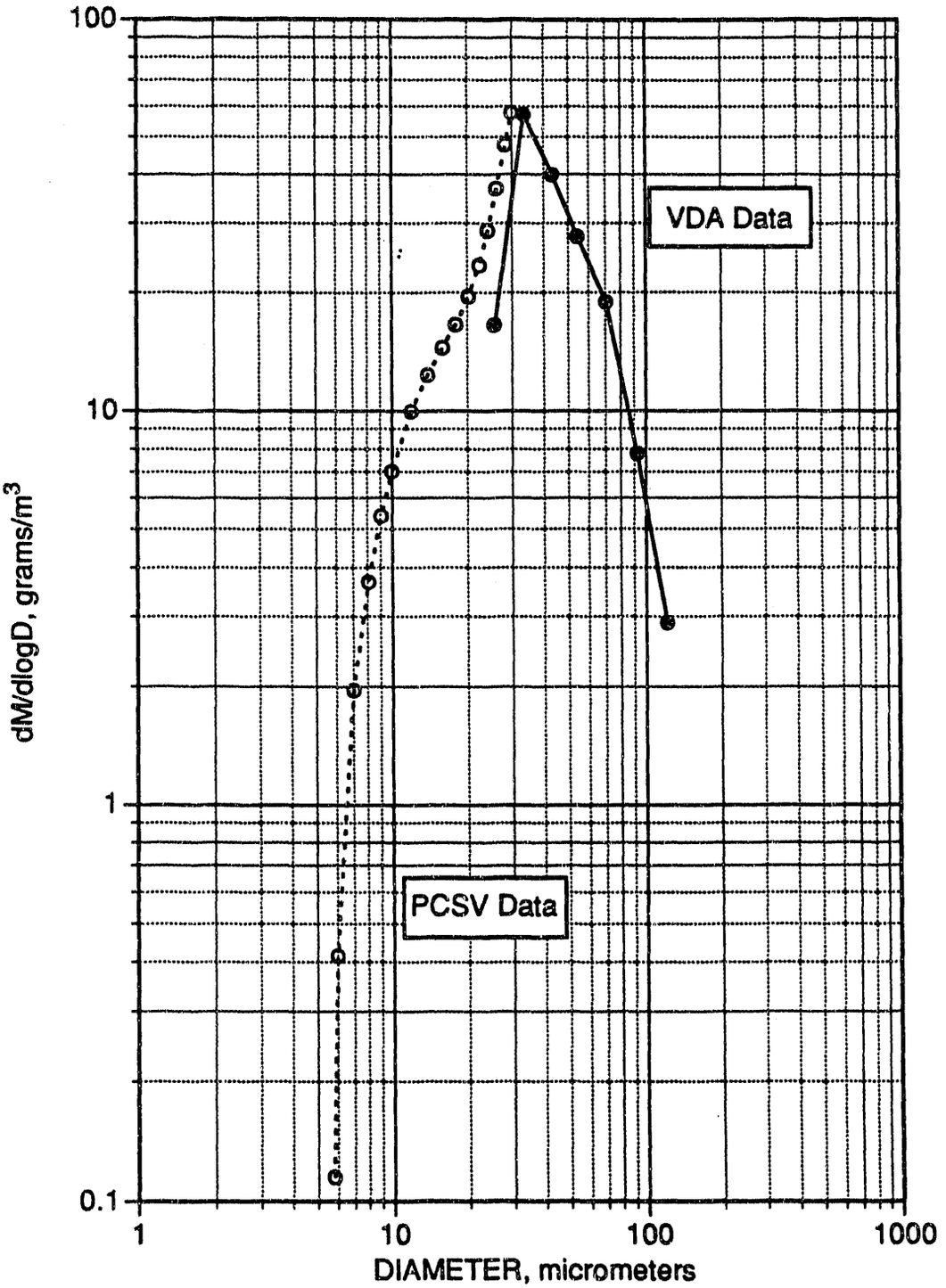

Figure A-50. Differential mass concentration versus particle size for Parker-Hannifin nozzle test #32. PCSV data are shown with a dashed line and open symbols, and discrete VDA data are shown with a solid line and closed symbols.

APPENDIX B

WEEKLY TEST SCHEDULE

WEEKLY TEST SCHEDULE

BEG. DATE	WEEK NO.	TOPIC	TASKS
		3.1--CHARACTERIZE SYSTEM PERFORMANCE	
4/30	1		Begin nozzle characterization and wall wetting evaluations
5/7	2		
5/14	3		
5/21	4		
5/28	5		
6/4	6		
6/11	7		
6/18	8		
6/25	9		Begin lime handling system check-out
7/2	10		Continue lime handling system check-out
7/9	11		Begin non-scavenging mode dry test
7/16	12		Continue non-scavenging; begin scavenging
7/23	13		Continue scavenging mode testing
7/30	14		Continue scavenging mode testing
8/6	15		Long-term scavenging tests
8/13	16		Continue long-term scavenging tests, prepare for slurry tests
8/20	17		Begin slurry testing
OUTAGE			
		3.1--CONTINUED (ACTUAL)	(PLANNED)
11/19	18 (AS PLANNED)		Short week--Slurry system check-out, DAS changes, ESP-P5A & other instrumentation
11/26	19 (NO SLURRY TESTING--EQUIPMENT PROBLEMS)		Parametric slurry testing--compare local & Belmont lime at selected conditions with 1300 ppm SO_2
12/3	20 (LIMITED SLURRY PARAMETRIC TESTS)		Continue parametric slurry tests--additional lime comparisons if needed. Determine mininum air pressure required for nozzles.
12/10	21 (120 HR TEST WITH INTERRUPTIONS)		Perform 120 hr test at selected condition--include some ESP testing
12/17	22 (120 HR TEST CONTINUED)		P-H slurry testing at selected conditions
12/24	23 (DEBUG ESP; NOZZLE PRESSURE TESTS)		Short week--repeat selected conditions

(Continued)

12/31	24 (OUTAGE; LIMITED SLURRY TESTS)	Short week--repeat selected conditions
1/7	25 (SLURRY PARAMETRIC)	Explore short residence time testing at selected conditions with slurry--move nozzles to downstream location
1/14	26 (EQ. PROBLEMS; LIMITED SLURRY TESTS)	Parametric ESP testing at selected slurry injection condition--probably with long residence time
	3.2--SCALE-UP TESTS (3.1 EXTENDED DUE TO EQUIPMENT PROBLEMS)	
1/21	27 (OUTAGE;+FROZEN SLURRY LINES)	Parametric tests--slurry recycle
1/28	28 (PARAMETRIC SLURRY & ESP TESTS)	Parametric tests--slurry recycle
	(BEGIN 3.2--SCALE-UP TESTS)	
2/4	29 (BEGIN SLURRY RECYCLE)	Parametric testing--additive one slurry for SO_2
2/11	30 (CONTINUE SLURRY RECYCLE)	Parametric testing--additive two slurry for SO_2
2/18	31 (OUTAGE--COMPRESSOR FAILURE)	Parametric testing--additive one or two
	3.3--ADVANCED CONCEPTS--moved up due to requirement for review of additives	
2/25	32	Slurry recycle parametric + side stream parametric
3/4	33	Side-stream parametric
3/11	34	Side stream paramtric--SO_2 & permeability
3/18	35	Side stream parametric + slurry recycle
3/25	36	Side stream parametric with slurry + dry recycle
4/1	37	Dry injection--pulse-jet side stream parametric
4/8	38	Dry injection--different nozzle (P-H?) & modified duct cleaning
4/15	39	Dry injection--high surface area hydrate (or different lime source)
4/22	40	Dry injection--different lime source
4/29	41	Dry injection--modified duct cleaning
5/6	42	Slurry injection--modified nozzles & upgraded duct cleaning
5/13	43	Slurry injection--additives parametric testing
5/20	44	Slurry injection--ESP reduced SCA testing
5/27	45	Slurry injection--ESP/SO_2 parametric with one or two additives
6/3	46	Slurry injection--ESP additive one
6/10	47	Slurry injection--ESP additive two

(Continued)

6/17	48	Slurry injection--ESP with modified rapping
6/24	49	Slurry injection--recycle parametric with ESP upgrade
7/1	50	Slurry injection--sidestream parametric with additive
7/8	51	Slurry injection--sidestream parametric with additive
7/15	52	Slurry injection--repeat selected conditions
		3.2--SCALE-UP TESTS
7/22	53	Slurry injection--long term test of optimized configuration
7/29	54	Slurry injection--long term test of optimized configuration
8/5	55	Slurry injection--long term test of optimized configuration
8/12	56	Slurry injection--long term test of optimized configuration
8/19	57	Slurry injection--long term test of optimized configuration
8/26	58	Dry injection--long term test of optimized configuration
9/2	59	Dry injection--long term test of optimized configuration
9/9	60	Dry injection--long term test of optimized configuration
		3.5--FAILURE MODES
9/16	61	Response to process condition upsets--slurry (include changes in SO_2)
9/23	62	Response to process condition upsets--dry (include changes in SO_2)
9/30	63	Response to duct injection equipment upsets--slurry
10/7	64	Response to duct injection equipment upsets--slurry & dry
10/14	65	Response to ESP equipment upsets--dry
10/21	66	Response to ESP equipment upsets--slurry
10/28	67	Response to ash handling system upset--slurry
11/4	68	Response to ash handling system upsets--dry
11/11	69	Optimized failure response strategy
		4.1--MODEL VALIDATION
11/18	70	Validation of droplet evaporation rates--slurry
11/25	71	Validation of droplet-sorbent collision rates
12/2	72	Validation of SO_2 absorption rates--slurry
		Validation of SO_2 absorption rates--dry
12/9	73	Validation of modified ESP model--slurry

(Continued)

12/16	74	Validation of modified ESP model--dry
12/23	75	Overall model parametric evaluation--dry
12/30	76	Overall model parametric evaluation--slurry
1/6	77	Overall model parametric evaluation--slurry
1/13	78	Overall model parametric evaluation--slurry
1/20	79	Overall model parametric evaluation--slurry
1/27	80	Overall model parametric evaluation--slurry

END

DATE FILMED

9/11/92